THIS FILE IS MADE AVAILABLE THROUGH THE DECLASSIFICATION EFFORTS AND RESEARCH OF:

THE BLACK VAULT

THE BLACK VAULT IS THE LARGEST ONLINE FREEDOM OF INFORMATION ACT / GOVERNMENT RECORD CLEARING HOUSE IN THE WORLD. THE RESEARCH EFFORTS HERE ARE RESPONSIBLE FOR THE DECLASSIFICATION OF THOUSANDS OF DOCUMENTS THROUGHOUT THE U.S. GOVERNMENT, AND ALL CAN BE DOWNLOADED BY VISITING:

HTTP://WWW.BLACKVAULT.COM

YOU ARE ENCOURAGED TO FORWARD THIS DOCUMENT TO YOUR FRIENDS, BUT PLEASE KEEP THIS IDENTIFYING IMAGE AT THE TOP OF THE .PDF SO OTHERS CAN DOWNLOAD MORE!

(2)

Report No. CG-D-02-94

AD-A278 796

EVALUATION OF SYNTHETIC APERTURE RADAR FOR OIL-SPILL RESPONSE

G. L. HOVER
U.S. Coast Guard Research and Development Center
1082 Shennecossett Road, Groton, Connecticut 06340-6096

AND

G. A. MASTIN, R. M. AXLINE, and J. D. BRADLEY
Sandia National Laboratories
Albuquerque, New Mexico 87185-0843

DTIC
ELECTE
MAR 02 1994
S B D

FINAL REPORT

OCTOBER 1993

DISTRIBUTION STATEMENT A
Approved for public release
Distribution Unlimited

This document is available to the U.S. public through the National Technical Information Service, Springfield, Virginia 22161.

Prepared for:

216pg 94-12950

U.S. Department of Transportation
United States Coast Guard
Office of Engineering, Logistics, and Development
Washington, D. C. 20593-0001

DTIC QUALITY INSPECTED 3

94 4 28 070

NOTICE

This document is disseminated under the sponsorship of the Department of Transportation in the interest of information exchange. The United States Government assumes no liability for its contents or use thereof.

The United States Government does not endorse products or manufacturers. Trade or manufacturers' names appear herein solely because they are considered essential to the object of this report.

The contents of this report reflect the views of the Coast Guard Research & Development Center. This report does not constitute a standard, specification, or regulation.

D. L. Motherway
Technical Director, Acting
United States Coast Guard
Research & Development Center
1082 Shennecossett Road
Groton, CT 06340-6096

DISCLAIMER NOTICE

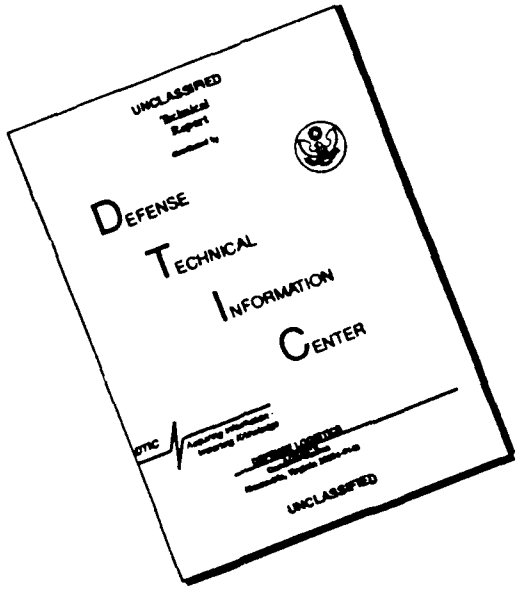

THIS DOCUMENT IS BEST QUALITY AVAILABLE. THE COPY FURNISHED TO DTIC CONTAINED A SIGNIFICANT NUMBER OF PAGES WHICH DO NOT REPRODUCE LEGIBLY.

Technical Report Documentation Page

1. Report No.	2. Government Accession No.	3. Recipient's Catalog No.
CG-D-02-94		

4. Title and Subtitle	5. Report Date
Evaluation of Synthetic Aperture Radar for Oil-Spill Response.	October 1993
	6. Performing Organization Code
7. Author(s)	8. Performing Organization Report No.
G. Hover, G. Mastin, R. Axline, J. Bradley	R&DC 27/93

9. Performing Organization Name and Address		10. Work Unit No. (TRAIS)
USCG Research and Development Center 1082 Shennecossett Road Groton, CT 06340-6096	Sandia National Laboratories P. O. Box 5800 Albuquerque, NM 87185	11. Contract or Grant No. MIPR Z51100-2-E00467
12. Sponsoring Agency Name and Address		13. Type of Report and Period Covered
Department of Transportation U.S. Coast Guard Office of Engineering, Logistics, and Development Washington, D.C. 20593-0001		Final Report June 1992 - Sept. 1993
		14. Sponsoring Agency Code

15. Supplementary Notes

16. Abstract

This report provides a detailed evaluation of synthetic aperture radar (SAR) as a potential technology improvement over the Coast Guard's existing side-looking airborne radar (SLAR) for oil-spill surveillance applications. The U. S. Coast Guard Research and Development Center (R&D Center), Environmental Safety Branch, sponsored a joint experiment including the U. S. Coast Guard, Sandia National Laboratories, and the National Oceanographic and Atmospheric Administration (NOAA), Hazardous Materials Division. Radar imaging missions were flown on six days over the coastal waters off Santa Barbara, CA, where there are constant natural seeps of oil. Both the Coast Guard SLAR and the Sandia National Laboratories SAR were employed to acquire simultaneous images of oil slicks and other natural sea surface features that impact oil-spill interpretation. Surface truth and other environmental data were also recorded during the experiment. The experiment data were processed at Sandia National Laboratories and delivered to the R&D Center on a PC-based computer workstation for analysis by experiment participants.

Upon completion of the experiment, the potential utility of SAR as a replacement for SLAR in Coast Guard oil-spill applications was assessed during two data analysis workshops held at the R&D Center. Workshop participants included U. S. Coast Guard operational personnel and research staff, a NOAA Hazardous Materials Division scientist, and several Sandia radar and image processing experts. SAR and SLAR experiment data were evaluated to determine key parameters and capabilities. Finally, a cost-benefit analysis between the existing Coast Guard SLAR and a conceptual SAR design tailored to Coast Guard requirements was performed.

17. Key Words	18. Distribution Statement
Synthetic Aperture Radar, Side Looking Airborne Radar, Oil Slicks	Document is available to the public through the National Technical Information Service, Springfield, VA 22161

19. Security Classif. (of this report)	20. SECURITY CLASSIF. (of this page)	21. No. of Pages	22. Price
UNCLASSIFIED	UNCLASSIFIED		

Form DOT F 1700.7 (8/72) Reproduction of form and completed page is authorized.

METRIC CONVERSION FACTORS

Approximate Conversions to Metric Measures

Symbol	When You Know	Multiply By	To Find	Symbol
		LENGTH		
in	inches	* 2.5	centimeters	cm
ft	feet	30	centimeters	cm
yd	yards	0.9	meters	m
mi	miles	1.6	kilometers	km
		AREA		
in^2	square inches	6.5	square centimeters	cm^2
ft^2	square feet	0.09	square meters	m^2
yd^2	square yards	0.8	square meters	m^2
mi^2	square miles	2.6	square kilometers	km^2
	acres	0.4	hectares	ha
		MASS (WEIGHT)		
oz	ounces	28	grams	g
lb	pounds	0.45	kilograms	kg
	short tons (2000 lb)	0.9	tonnes	t
		VOLUME		
tsp	teaspoons	5	milliliters	ml
tbsp	tablespoons	15	milliliters	ml
fl oz	fluid ounces	30	milliliters	ml
c	cups	0.24	liters	l
pt	pints	0.47	liters	l
qt	quarts	0.95	liters	l
gal	gallons	3.8	liters	l
ft^3	cubic feet	0.03	cubic meters	m^3
yd^3	cubic yards	0.76	cubic meters	m^3
		TEMPERATURE (EXACT)		
°F	Fahrenheit temperature	5/9 (after subtracting 32)	Celsius temperature	°C

*1 in = 2.54 (exactly).

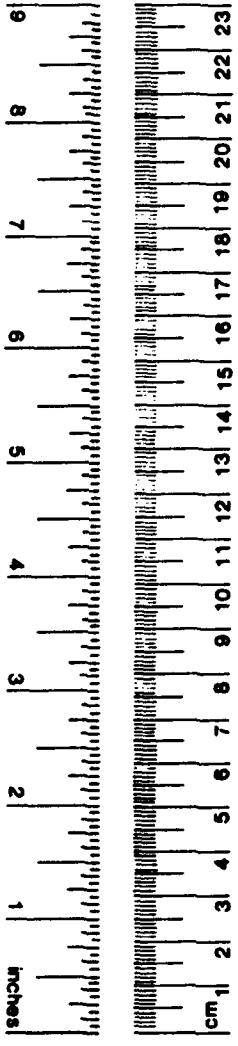

Approximate Conversions from Metric Measures

Symbol	When You Know	Multiply By	To Find	Symbol
		LENGTH		
mm	millimeters	0.04	inches	in
cm	centimeters	0.4	inches	in
m	meters	3.3	feet	ft
m	meters	1.1	yards	yd
km	kilometers	0.6	miles	mi
		AREA		
cm^2	square centimeters	0.16	square inches	in^2
m^2	square meters	1.2	square yards	yd^2
km^2	square kilometers	0.4	square miles	mi^2
ha	hectares (10,000 m^2)	2.5	acres	
		MASS (WEIGHT)		
g	grams	0.035	ounces	oz
kg	kilograms	2.2	pounds	lb
t	tonnes (1000 kg)	1.1	short tons	
		VOLUME		
ml	milliliters	0.03	fluid ounces	fl oz
l	liters	0.125	cups	c
l	liters	2.1	pints	pt
l	liters	1.06	quarts	qt
l	liters	0.26	gallons	gal
m^3	cubic meters	35	cubic feet	ft^3
m^3	cubic meters	1.3	cubic yards	yd^3
		TEMPERATURE (EXACT)		
°C	Celsius temperature	9/5 (then add 32)	Fahrenheit temperature	°F

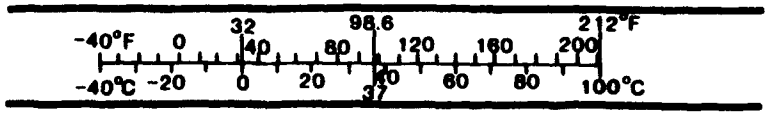

TABLE OF CONTENTS

EVALUATION OF SYNTHETIC APERTURE RADAR FOR OIL-SPILL RESPONSE
LIST OF FIGURES viii
LIST OF TABLES x
EXECUTIVE SUMMARY EX-1
INTRODUCTION EX-1
Background EX-1
Approach EX-1
RESULTS AND CONCLUSIONS EX-1
Image Analysis Results EX-1
Parameters for a Conceptual Coast Guard SAR EX-2
Cost vs. Benefit of SAR EX-3
RECOMMENDATIONS EX-3
ACKNOWLEDGEMENTS EX-5
CHAPTER 1
INTRODUCTION
1.1 PROJECT BACKGROUND 1-1
1.2 PROJECT SCOPE AND OBJECTIVES 1-1
1.3 TECHNICAL BACKGROUND 1-2
1.3.1 Ocean Dynamics and Effects of Oil 1-2
1.3.2 Electromagnetic Scattering from Ocean Waves 1-2
1.3.3 Sensor Descriptions (SAR/SLAR) 1-3
1.3.3.1 The AN/APS-131 SLAR 1-3
1.3.3.2 The SNL SAR 1-5
1.4 EXPERIMENT DESCRIPTION 1-7
1.4.1 Participants 1-7
1.4.1.1 Control 1-7
1.4.1.2 Twin Otter SAR 1-9
1.4.1.3 AIREYE 1-9
1.4.1.4 Surface Truthing 1-9
1.4.2 Summary of Field Test Operations 1-15
1.4.3 Summary of Data Collected 1-17
1.5 ANALYSIS TOOLS AND IMAGE DATA 1-17
1.5.1 Image Data Sets 1-18
1.5.2 Workstation 1-23
1.5.3 Image Manipulation and Processing Software 1-23
1.5.3.1 SNL-Provided Software 1-23
1.5.3.2 Commercial Software 1-28
1.6 DESCRIPTION OF IMAGE ANALYSIS ACTIVITIES 1-29
1.6.1 Measures of Effectiveness Definition 1-29
1.6.2 ROI Selection and Analysis of Image Processing Methods 1-30
1.6.3 Analysis of Required Image Resolutions 1-34
1.6.3.1 Evaluation of Methods for Simulating Degraded Image Resolutions 1-34

Availability Codes
Dist | Avail and/or Special
A-1

1.6.3.2 Method for evaluating Full-Swath Image Resolution Requirements 1-49
1.6.3.3 Method for Evaluating Maximum System Resolution Requirements 1-49
1.7 DESCRIPTION OF SAR PARAMETERS ANALYSIS ACTIVITIES 1-50
1.7.1 Development of Requirements 1-50
1.7.2 Calculations and System Specifications 1-50
1.7.3 Trade-off Studies 1-50
1.7.4 SAR Capabilities Survey 1-50
CHAPTER 2
EVALUATION RESULTS
2.1 INTRODUCTION 2-1
2.2 IMAGE DATABASE 2-1
2.3 IMAGE ANALYSIS RESULTS 2-1
2.3.1 Results of Speckle Smoothing Evaluation 2-4
2.3.2 Results of SAR Resolution Study 2-33
2.3.2.1 Single-look vs. Multi-look Processing 2-33
2.3.2.2 Maximum System Resolution Requirement 2-34
2.3.2.3 Other Resolution Issues 2-34
2.3.2.4 Full-Swath Image Resolution Requirements 2-45
2.4 SAR vs. SLAR: DISCUSSION OF TECHNICAL ISSUES 2-45
2.4.1 Attributes That Need Not Be Used in the Comparison 2-45
2.4.2 Attributes for Which SAR and SLAR Differ Significantly 2-51
2.5 SAR PARAMETERS ANALYSIS RESULTS 2-55
2.5.1 Development of Requirements 2-55
2.5.2 Calculations and System Specifications 2-56
2.5.2.1 General Description of Recommended Design 2-57
2.5.2.2 System Specifications 2-58
2.5.2.3 System Block Diagrams and Related Discussion 2-63
2.5.3 Trade-Off Studies 2-74
2.5.3.1 Squinted Operation Versus Antenna Steering 2-74
2.5.3.2 Number of Bits Per Image Pixel 2-74
2.5.3.3 Slant-Range Resolution 2-75
2.5.3.4 Azimuth Resolution 2-75
2.5.3.5 Minimum σ^{o} of Noise Required 2-75
2.5.3.6 Choice of Operating Frequency 2-75
2.5.3.7 Multi-look Processing 2-76
2.5.3.8 Image-Formation Algorithm/Signal-Processing Approach 2-76
2.5.3.9 Pulse-Compression Issues 2-77
2.5.4 SAR Capabilities Survey Results 2-78
2.5.4.1 Listing of Responding Vendors 2-78
2.5.4.2 Overview of Vendor-Supplied Materials 2-80
2.5.4.3 Summary of System Functional Performance Characteristics 2-81
2.5.4.4 Interpretation of Data Provided on SAR Systems 2-85

2.6 DISCUSSION OF COST VS. BENEFIT OF SAR 2-87
2.6.1 Image Quality Benefits, SAR vs. SLAR 2-87
2.6.2 Identified Technical Benefits of SAR 2-101
2.6.3 Rough Estimates of Coast Guard SAR Size, Power, and Cost 2-111
2.6.4 Discussion of Other Identified Costs of SAR 2-114
CHAPTER 3
CONCLUSIONS AND RECOMMENDATIONS
3.1 CONCLUSIONS 3-1
3.1.1 Benefits and Cost Effectiveness Offered by SAR and SLAR 3-2
3.1.2 Critical SAR Parameters 3-2
3.1.3 Benefits of Image Processing Techniques 3-4
3.1.4 Comments on "Off-the-Shelf" SAR Technology 3-5
3.1.4.1 New SAR Design 3-5
3.1.4.2 Existing SARs 3-5
3.2 RECOMMENDATIONS 3-5
3.2.1 If SAR, What SAR 3-5
3.2.1.1 New SAR Design 3-5
3.2.1.2 Modification of an Existing SAR 3-6
3.2.2 Image Presentation, Manipulation, and Exploitation Algorithms 3-7
3.2.3 Recommended Follow-On SAR Testing 3-8
REFERENCES R-1
APPENDIX A
SLAR SENSITIVITY A-1
APPENDIX B
SAR CONCEPTUAL REQUIREMENTS B-1
APPENDIX C
SAR INFORMATION SURVEY C-1
APPENDIX D
SAR DESIGN CALCULATIONS D-1
APPENDIX E
MOVING-TARGET-INDICATOR MODE E-1
APPENDIX F
REAL APERTURE RADAR MODE F-1
APPENDIX G
ADDITIONAL SAR DESIGN CALCULATIONS G-1
APPENDIX H
INTERIM RESPONSE H-1
APPENDIX I
REGION-OF-INTEREST INFORMATION I-1

LIST OF FIGURES

Figure 1-1 The SLAR imaging process. 1-4
Figure 1-2 The SAR imaging process. 1-6
Figure 1-3 Multi-look imaging process. 1-8
Figure 1-4 Photograph of the DOE DeHavilland DHC-6 Twin Otter aircraft. 1-11
Figure 1-5 Photograph of the Coast Guard Dassault-Breguet Falcon 20 jet aircraft 1-13
Figure 1-6 The experimental test areas. 1-16
Figure 1-7 A 4-pass mosaic, downsampled by a factor of 5 for display. 1-21
Figure 1-8 Coast Guard SAR image viewing station. 1-24
Figure 1-9 Relationship between the key image and region-of-interest (ROI) image. . . . 1-26
Figure 1-10 SAR data processing flow for images selected for analysis. 1-27
Figure 1-11 Schematic for sliding window averaging. 1-32
Figure 1-12 The subsampling process. 1-35
Figure 1-13 Full-resolution ROI. Each pixel represents 2 m. 1-37
Figure 1-14 ROI downsampled to 10-m pixel resolution by phase history interpolation. 1-39
Figure 1-15 ROI subsampled to 10-m pixel resolution to simulate phase history downsampling. 1-41
Figure 1-16 Schematic for adjacent window averaging ("boxcar" filtering). 1-44
Figure 1-17 Multi-look version of the ROI, downsampled in the phase history domain before noncoherent averaging to 20-m pixel resolution. 1-45
Figure 1-18 Simulated multi-look image of ROI at 20-m pixel resolution. 1-47
Figure 1-19 Flow of SAR Parameters Analysis Activities. 1-51
Figure 2-1 Photograph of oil entrained in the current off of Coal Oil Point, during a Nov. 15, 1992, SAR imaging pass. 2-5
Figure 2-2 Small photomosaic created from several KS-87 frames captured by the AIREYE off of Coal Oil Point, on Nov. 15, 1992. 2-7
Figure 2-3 2-m pixel resolution SAR region-of-interest (ROI) image off of Coal Oil Point, captured by the SNL SAR on Nov. 15, 1992. 2-9
Figure 2-4 SLAR ROI just off of Coal Oil Point, captured by the AIREYE SLAR on Nov. 15, 1992. 2-11
Figure 2-5 Oil slick extending from below the Holly platform diagonally toward Coal Oil Point, Nov. 14, 1992. 2-13
Figure 2-6 SAR image of oil slick seen in Figure 2-5. 2-15
Figure 2-7 SLAR image of oil slick seen in Figure 2-5. 2-17
Figuer 2-8 Photograph captured from the SNL Twin Otter on Nov. 15, 1992, showing an oil slick just east of the Holly platform and just south of Naples, CA. 2-19
Figure 2-9 SAR mosaic of oil slick seen in Figure 2-8, but imaged 30 min. after the photograph. 2-21
Figure 2-10 Full-resolution ROI from the Nov. 12, 1992, south-looking data set. 2-25
Figure 2-11 Result of 5 x 5 sliding window average on original ROI. 2-27
Figure 2-12 Result of 5 x 5 sliding window median on original ROI. 2-29

Figure 2-13 Result of 3 iterations of the Crimmins morphological filter on original ROI. 2-31
Figure 2-14 Single-look ROI at full resolution (2-m pixels). 2-35
Figure 2-15 Simulated 10-m pixel resolution multi-look ROI created from the image in Figure 2-14. 2-37
Figure 2-16 Simulated 14-m pixel resolution multi-look ROI created from the image in Figure 2-14. 2-39
Figure 2-17 Simulated 20-m pixel resolution multi-look ROI created from the image in Figure 2-14. 2-41
Figure 2-18 Example of a SAR image where the antenna is looking across the wave crests (up-wind or down-wind). 2-43
Figure 2-19 Example of 20-m and 40-m full-swath display images from the Nov. 12, 1992, data set. 2-47
Figure 2-20 Example of 20-m and 40-m full-swath display image from the Nov. 15, 1992, data set. 2-49
Figure 2-21 High-level block diagram of the SAR system. 2-64
Figure 2-22 Block diagram of the SAR rf front-end assembly. 2-66
Figure 2-23 Block diagram of the phase history collector. 2-67
Figure 2-24 Recommended parallel processing architecture for the image former. 2-70
Figure 2-25 Data recorder assembly. 2-71
Figure 2-26 Image buffer for holding full-resolution images for ROI extraction and operational display of downsampled, full-swath images. 2-72
Figure 2-27 Full-swath SAR image from the Nov. 12, 1992, experiment. 2-89
Figure 2-28 ROI extracted from the full-swath SAR image. 2-91
Figure 2-29 Wide-swath SLAR image from the Nov. 12, 1992, experiment. 2-93
Figure 2-30 ROI extracted from the wide-swath SLAR image. 2-95
Figure 2-31 Full-swath SAR image from the Nov. 12, 1992, experiment. 2-97
Figure 2-32 ROI extracted from the full-swath SAR image. 2-99
Figure 2-33 Wide-swath SLAR image from the Nov. 12, 1992, experiment. 2-103
Figure 2-34 ROI extracted from the wide-swath SLAR image. 2-105
Figure 2-35 South-looking SLAR image from Nov. 12, 1992. 2-107
Figure 2-36 West-looking SLAR image from Nov. 12, 1992. 2-109

LIST OF TABLES

Table 2-1 SAR Data Summary 2-2

Table 2-2 SLAR Data Summary 2-3

Table 2-3 SAR System Specifications 2-59

Table 2-4 Functional Performance Characteristics 2-82

Table 2-5 Rough Estimates for New Coast Guard SAR. 2-112

Table 3-1 Advantages and Disadvantages of SAR and SLAR 3-3

Table I-1 Regions-of-Interest I-2

EXECUTIVE SUMMARY

INTRODUCTION

Background

This report provides a detailed evaluation of synthetic aperture radar (SAR) as a potential technological improvement over the Coast Guard's existing side-looking airborne radar (SLAR) for oil-spill surveillance applications. The U. S. Coast Guard Research and Development Center (R&D Center), Environmental Safety Branch, sponsored a joint experiment including the U. S. Coast Guard, Sandia National Laboratories, and the National Oceanographic and Atmospheric Administration (NOAA), Hazardous Materials Division. Radar imaging missions were flown on six days over the coastal waters off Santa Barbara, CA, where there are constant natural seeps of oil. Both the Coast Guard SLAR and the Sandia National Laboratories SAR were employed to acquire simultaneous images of oil slicks and other natural sea surface features that impact oil-spill interpretation. Surface truth and other environmental data were also recorded during the experiment. The experiment data were processed at Sandia National Laboratories and delivered to the R&D Center on a PC-based computer workstation for analysis by experiment participants.

Approach

Upon completion of the experiment, the potential utility of SAR as a replacement for SLAR in Coast Guard oil-spill applications was assessed during two data analysis workshops held at the R&D Center. Workshop participants included U. S. Coast Guard operational personnel and research staff, a NOAA Hazardous Materials Division scientist, and several Sandia radar and image processing experts. The methods of evaluation provided a systematic framework for evaluating SAR experiment data to determine key parameters and capabilities. These included:

1. The optimal resolution for oil-spill image analysis.
2. The feasibility of locating oil-slick boundaries.
3. Sensitivities to environmental conditions and oil slick thickness.
4. Radar design parameters that impact Coast Guard applications.

Furthermore, the methods of evaluation provided a framework for assessing cost/benefit trade-offs between the existing Coast Guard SLAR and a conceptual SAR whose design is tailored to U.S. Coast Guard oil spill surveillance requirements. The cost effectiveness of such a system was evaluated by considering the availability and applicability of commercial systems or components; size, power, and weight constraints; operational requirements, and the expected quality and utility of the image products. This was a concept feasibility study. No attempt was made to identify a final point design, a specific manufacturer, or detailed costs for integrating a specific system into the existing Coast Guard HU-25B aircraft.

RESULTS AND CONCLUSIONS

Image Analysis Results

Participants in the two data analysis workshops identified an optimal spatial resolution for oil-spill image interpretation and recommended a specific method for acquiring, cueing, and analyzing SAR images in an operational scenario. The optimal spatial resolution for detailed

image analysis is 10 m (pixel spacing and impulse response width). This resolution is coarser than the resolution acquired by the Sandia SAR, but significantly finer than the resolution of the existing Coast Guard SLAR. Wide-swath coverage (25 nautical miles) at 10-m pixel resolution provides more data to an operator than can realistically be displayed and interpreted. The workshop participants, therefore, recommended:

1. A wide-swath mode where images are displayed to the operator at 20-m to 30-m resolution for cueing regions-of-interest.

2. A 10-m resolution display capability for detailed analysis, and potential down-linking of region-of-interest images that depict probable oil-spill sites.

Analysts agreed that several SAR capabilities were superior to the existing SLAR, and that SAR introduced some difficulties that are not inherent in SLAR. The benefits of SAR are:

1. Finer resolution and better image acuity for identifying oil-slick boundaries.

2. Sensitivity to surface features with minimal radar scattering cross section is better than that of the existing Coast Guard SLAR.

3. Spatial resolution that does not degrade with increasing range to the surface, as is the case with SLAR. This improves the interpretability of radar data by presenting a uniform acuity over the entire area being imaged.

SAR difficulties are:

1. Single-look SAR images at 10-m resolution have adequate resolution, but speckle can reduce acquity. Multi-look SAR imaging at 10-m resolution, however, alleviates this problem.

2. Ocean waves whose motion includes a significant directional component oriented toward (or away from) the radar antenna cause acuity degradation in the SAR image. Using higher aircraft speeds and transmitting perpendicular to the direction of dominant wave motion can mitigate this effect.

3. Images of rigid moving targets (such as ships or boats) can show the targets displaced from their actual locations. The amount of displacement depends upon target speed and radar parameters. This can affect a SAR image of, for example, moving ships dumping waste. A dual-mode (real and synthetic aperture) radar design or special doppler processing of the SAR data could alleviate this problem.

Analysts saw no significant difference in the sensitivity of SAR and SLAR to low-wind conditions or to oil slick thickness.

Parameters for a Conceptual Coast Guard SAR

Results of the SAR image analysis; including optimal resolutions for region-of-interest and wide-swath images, benefits of multi-look imaging, dual-image display strategies, and

requirements for imaging rigid moving targets, were used to set some basic design parameters for a conceptual Coast Guard SAR. Should the U. S. Coast Guard decide at a future date that its existing oil-spill surveillance capabilities should be upgraded to include SAR systems, the parameters defined in this report should provide a foundation for the acquisition. Topics such as antenna size, transmitter power, image formation processor architecture, special methods to address the rigid moving target issue, and image display buffering are addressed in detail. In summary, the parameters required for a SAR to meet Coast Guard mission requirements:

1. Define a system that might be purchased commercially and slightly modified.

2. Define a new product that can be assembled from a combination of commercially-available subsystems and commercially-available components integrated into subsystems by a SAR vendor.

A vendor survey of commercially-available systems, subsystems, and components was performed to substantiate these alternatives.

Cost vs. Benefit of SAR

SAR offers a distinct benefit in image quality when compared to SLAR. SAR provides finer resolution, constant (not a function of range to the surface) resolution, excellent acquity in multi-look mode, better sensitivity in terms of the minimum-detectable target-cell radar cross section, and a smaller, steerable (if desired) antenna. All but the last of these quality benefits are generic to SAR and cannot be achieved by replacing the existing Coast Guard SLAR with a newer technology SLAR. There are several areas where SAR and SLAR are similar. These include size, weight, power consumption, maintenance time, and operator training. SAR, however, incurs some costs that are not encountered in SLAR. A SAR requires a high-accuracy inertial navigation unit, precise aircraft motion compensation of acquired data to prevent image blurring, antenna gimbals with multiple degrees of freedom and control for image acquisition (if a steerable antenna is desired), and a sophisticated image formation computer. These subsystems add complexity and additional hardware and software costs above and beyond the cost of a SLAR. These costs could be as high as an additional $2 to $3 million for developing a new system configured from commercially available subsystems and components. Even if a new SAR development were not pursued and an existing commercial SAR system were procured, an additional cost of $400 thousand to $500 thousand per installed unit would be expended for a SAR vs. a SLAR.

RECOMMENDATIONS

1. Based on the analysis performed during this study, the U.S. Coast Guard should seriously consider moving to SAR as a future replacement for the AN/APS-131 SLAR. This recommendation is made on the basis of the superior image acuity and uniformity that SAR technology can provide. This should not be construed as a endorsement of SAR over SLAR at any cost; the cost of upgrading to SAR technology would be significant. The balance among mission priorities, anticipated useage, and budgetary constraints could sway the decision toward either technology.

2. Should the Coast Guard choose to procure a SAR capability, the system should include the following characteristics:

- 10-m pixel resolution and a 25-nmi image swath.
- X-band radar.
- Real-time motion compensation.
- Real-time multi-look image formation.
- Image and auxiliary radar data recording.
- Full-swath and region-of-interest displays.
- Moving target indication.

3. The recently-initiated AIREYE upgrade program which will likely provide the APS-131 SLAR with digital image storage, digital image enhancement/display, and an image downlink capability, should be monitored closely to determine if a modernized SLAR can adequately meet spill surveillance requirements without incurring the additional costs of SAR.

4. The Coast Guard should explore the possibility of simultaneously imaging a series of oil slicks with the modernized APS-131 SLAR and an available contractor SAR whose capabilities approximate those of the conceptual system defined in this study. The resultant SAR and SLAR images should be compared directly to evaluate the potential benefits of replacing SLAR with SAR when the APS-131 system reaches the end of its supportable life early in the next century.

ACKNOWLEDGEMENTS

The authors wish to express appreciation for the project contributions made by numerous individuals from the Coast Guard, Sandia National Laboratories, NOAA, and the private sector. Special thanks to the Coast Guard and contractor aircrews for safely and successfully flying the data collection missions in Santa Barbara. The pilots of Ross Aviation (Sandia Twin Otter); numerous Coast Guardsmen from Air Stations Cape Cod (AIREYE) and Los Angeles (HH-65 helicopter); and pilots from ERA Aviation (NOAA helicopter flights) all provided outstanding support to the experiment. Dr. Jerry Galt of the NOAA Hazardous Materials Response Division and numerous members of the HAZMAT staff provided invaluable advice, data collection support, and analysis insights throughout the course of this project. CDR Ross Tuxhorn and MST1 Chris Weiller of the USCG National Strike Force provided essential perspective as operational Coast Guard users in addition to their surface truth data and analysis inputs. Special thanks are extended to several groups at Sandia; the radar operations crew, the data formation and reformatting team, the Radar Viewing Workstation integration and testing team, and the other individuals who created special image products for analysts. Mr. Jeff Mason, in particular, contributed significantly to all of the Sandia activities. Finally, thanks to Mr. Jeff Plourde of Analysis & Technology, Inc. for his efforts in producing the hundreds of processed SAR and SLAR images required for the analysis workshops.

(This page intentionally left blank.)

CHAPTER 1
INTRODUCTION

1.1 PROJECT BACKGROUND

The Coast Guard Research and Development Center (USCG R&D Center) is evaluating sensor technologies that could significantly enhance the Coast Guard's oil-spill remote sensing capabilities by the mid-1990's. Part of this evaluation is specifically aimed at identifying sensors that could replace elements of, or be added to, the existing HU-25B AIREYE spill reconnaissance aircraft suite. Sensor technologies that could supplement the AIREYE capability on different aircraft (Coast Guard or otherwise) are also being examined.

In January of 1991, the R&D Center hosted a multi-agency workshop to discuss oil-spill surveillance requirements, to identify sensor technologies that could meet those requirements, and to identify potential research and development initiatives. Synthetic aperture radar (SAR) technology was identified by workshop participants as holding promise for reducing the number of "false positives", or non-petroleum slicks, reported by sensor operators during spill surveillance missions. SAR images can provide finer and more uniform spatial resolution within the radar image of an oil slick than can the current AIREYE side-looking airborne radar (SLAR). Workshop participants postulated that image interpreters might be able to exploit finer-resolution SAR images to distinguish features that are characteristic of petroleum oil slicks. The workshop proceedings are listed in reference [1].

In May of 1992, Sandia National Laboratories (SNL), as an internal effort and in cooperation with the Coast Guard, applied its resources and expertise in SAR technology and image processing toward an exploratory imaging exercise over the Santa Barbara Channel. Results of this exercise confirmed that Sandia's SAR was capable of successfully imaging the naturally-occurring oil seeps in that area.

In June of 1992, the Department of Energy (DOE) accepted a Military Interdepartmental Purchase Request (MIPR) from the Coast Guard funding SNL to conduct the research and analysis work reported in this document. SNL was tasked to conduct literature research on the application of SAR and SLAR sensor technologies to the oil-spill surveillance mission; to plan, conduct, and analyze a joint SAR/SLAR sensor evaluation over the Santa Barbara oil seeps; to determine the system requirements for a conceptual Coast Guard SAR; and to conduct a cost/benefit analysis of the two sensor technologies relative to the Coast Guard's oil-spill surveillance mission.

1.2 PROJECT SCOPE AND OBJECTIVES

The primary objective of this project was to evaluate, relative to oil-spill remote sensing requirements, the cost-effectiveness of supplementing or replacing the AIREYE system's real-aperture, AN/APS-131 side-looking airborne radar (SLAR) with a lightweight, state-of-the-art, fine-resolution SAR that is capable of producing imagery in near real-time.

The first step was to determine whether a fine-resolution SAR offered an oil-spill detection performance comparable or superior to that of the existing AIREYE SLAR. A coordinated oil-spill reconnaissance experiment involving the Coast Guard AIREYE SLAR and the SNL SAR was conducted over the Santa Barbara Channel in November of 1992 to address this issue. Analysis of the experimental data led to basic performance and preliminary design specifications for a future Coast Guard SAR system. The cost-effectiveness of such a system was evaluated by considering the availability and applicability of commercial systems or components; size, power, and weight constraints; operational requirements, and the expected quality and utility of the image products. This was a concept feasibility study. No attempt was made to identify a final point design, a specific manufacturer, or detailed costs for integrating a specific system into the existing Coast Guard HU-25B aircraft.

1.3 TECHNICAL BACKGROUND

The effectiveness of radar as a sensor for monitoring oils spills depends on 1) ocean wave dynamics and effects of oil on those dynamics; 2) interaction of electromagnetic waves with the moving ocean surface; and 3) the particular design of the sensor.

1.3.1 Ocean Dynamics and Effects of Oil

Ocean waves are caused by the conversion of energy, primarily from the wind, into water motion. Significant energy inputs include gravitational forces of celestial bodies, distant winds, and local winds. Primary wave components of interest for radar imaging of the ocean are so-called long waves and capillary waves [2]. Long waves have wavelengths of the order of tens of meters or longer and are produced by energy sources other than local winds. Capillary waves, which have shorter wavelengths, are produced by local winds and can appear and disappear in short periods of time. Capillaries comprise a spectrum of wavelengths; however, they have significant energy in wavelengths of the order of cm. The capillary waves ride atop the longer-wave motion; therefore, the long waves are said to modulate the movement of the capillary waves.

Oil on the surface of the ocean damps, or attenuates the capillary waves, thereby smoothing the surface of the long waves. It is this damping that allows oil to be discriminated from open ocean in radar images. Oil-covered areas, because they are smoother, scatter back less energy to an illuminating radar than do the areas of open water. Of course, in order for discrimination to be possible, there must be local winds present to generate the capillary waves.

1.3.2 Electromagnetic Scattering from Ocean Waves

Radars operate by illuminating the target area with radiated electromagnetic energy and receiving and processing the resulting echoes. Most radars designed to image the ocean's surface operate at cm wavelengths (C, X, or Ku bands). A perfectly smooth ocean will act like a mirror, scattering no energy back to radar, except at nadir (the radar looks straight down). Presence of long waves causes echo from the ocean's surface at look angles off of nadir. Generally, the maximum slope of the surface will determine the angular width of the scattering response curve. This type of return is sometimes called quasi-specular. Significant echo out to 10° (of incidence angle) or more would be typical. Presence of capillaries on the surface greatly extends the width of the scattering response curve. The scattering response is expressed in terms of σ^o, the scattering coefficient. σ^o is a normalized quantity, being equal to the surface's radar cross section

per square meter of surface area. σ^o for ocean typically varies from around +10 dB at nadir to -40 or -50 dB at incidence angles greater than 80^o [3]. Although σ^o decreases monotonically with increasing incidence angle, echoes from capillary waves at very large incidence angles (or small depression angles) can be detected. Therefore, in the presence of local winds, it is possible to perform wide-swath imaging of the ocean's surface.

Other factors affect the amount of echo scattered back to the radar. VV polarization provides better return at small grazing angles than HH. Returns are also somewhat stronger when the radar looks either up- or down-wind, as opposed to cross-wind. Finally, the long-wave structure tends to be more easily seen in radar images when the radar look direction is normal to the wavefronts.

The contrast, at VV polarization, of returns from oil-covered ocean and open ocean varies with look angle and frequency. Contrast appears to be best near 60^o of incidence and decreases somewhat with increasing incidence. Contrast is better at X band than at lower frequencies. Contrast at Ku band appears to be at least as good as at X band [4,5].

The fact that the ocean is moving complicates target/sensor interactions. When a radar images a stationary scene, the Doppler spectrum of the echo arises only due to the motion of the sensor platform. When a radar images the ocean, the Doppler spectrum is determined partly by ocean movement and partly by sensor-platform movement. Effects of the Doppler spectrum tend to be relatively unimportant when the sensor is a SLAR. However, because a SAR forms its image via Doppler filtering, significant target motion can affect the quality of the image.

1.3.3 Sensor Descriptions (SAR/SLAR)

Two sensors have been analyzed and flown as part of this study: the Coast Guard AN/APS-131 SLAR and the SNL Ku-band SAR.

1.3.3.1 The AN/APS-131 SLAR

This SLAR is a component of the Coast Guard's AIREYE sensor suite that is carried aboard the HU-25B aircraft. A detailed description of the AN/APS-131 is given in [6]. The SLAR provides broad-swath imaging to a maximum range of 80 nmi to either or both sides of the aircraft. The radar achieves 30-m range resolution via a 200-ns real pulse. Azimuth resolution is controlled by the SLAR antenna's azimuth beamwidth (0.8^o), which is about equal to the electrical wavelength divided by the physical width of the antenna (λ/W_A). Therefore, azimuth resolution is coarse, being about 50 m at 2 nmi range and about 500 m at 20 nmi range, and only the near-range portion of the broad swath is normally useful for oil-spill monitoring. See Figure 1-1, which depicts the SLAR imaging process.

The radar is a noncoherent-pulse real-aperture radar. Current AN/APS-131 image products are photographic film hardcopy; however, a capability for digital output to 4-mm magnetic tape was implemented for the joint sensor evaluation conducted as a part of this project. These modifications were made by Motorola Government Electronics Group in Scottsdale, Arizona, under contract to SNL. In this digital-output version, echo pulse amplitudes are averaged in each range bin for the amount of time taken for the AIREYE to travel about 30 m along-track. This

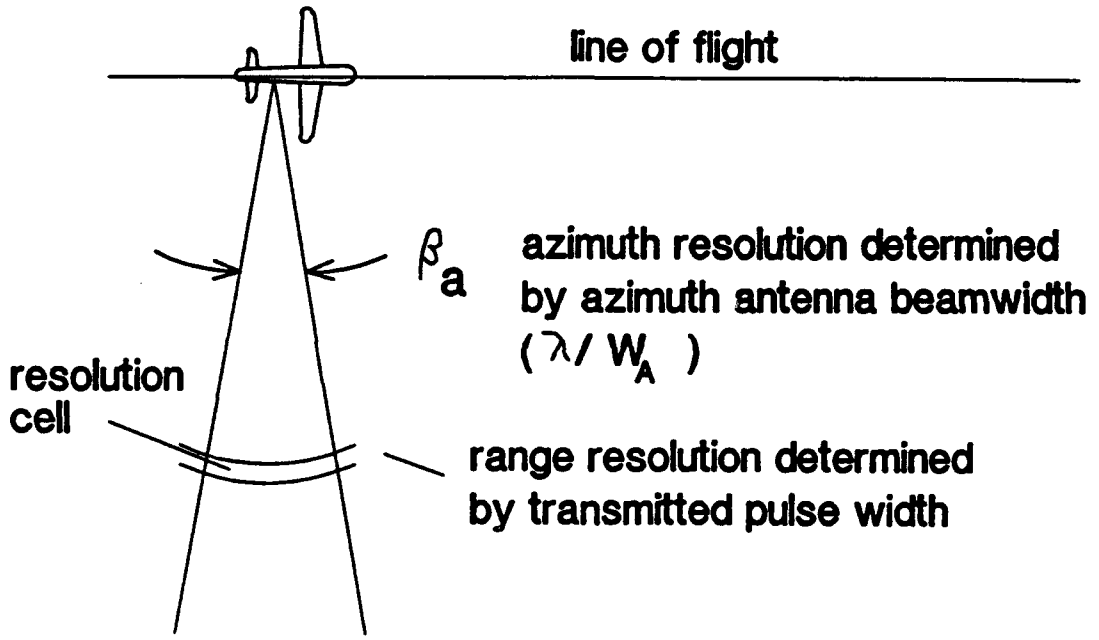

Figure 1-1. The SLAR imaging process.

improves signal-to-noise ratio in the image and degrades azimuth resolution only slightly at near-range.

The SLAR operates in the X band (9.315 GHz). The transmitter is a 200-kW magnetron. The antenna is steered only over very small azimuth angles to account for short-term yaw variations. Image corrections for radar beam squint (due to aircraft drift angles of up to ±15 degrees) are accomplished by manipulation of the CRT trace. The sensitivity (minimum detectable scattering coefficient) of the AIREYE SLAR has been estimated to be about -41.9 dB at a range of about 29 nmi [7](Appendix A).

1.3.3.2 The SNL SAR

The SNL SAR is a state-of-the-art imaging SAR carried aboard a DeHavilland DHC-6 Twin-Otter aircraft. The SAR provides relatively narrow-swath imaging capability (about 2 km swath) at modest ranges (typically, about 7 km to the scene center-line). Achievable resolution is much finer than that of the AIREYE SLAR. Resolution settings used for the November 1992 joint flight tests were 3 m in slant range and 3 m in azimuth[1]. Resolution in range is achieved by transmission of a frequency-chirped, long pulse of appropriate bandwidth, dechirping the pulse on receive, and digitally compressing the pulse using FFT processing. Azimuth resolution is achieved using fully-focused, coherent, SAR processing of echo pulses.

The SAR operates in the Ku band (15 GHz). The transmitter is an 80-W traveling wave tube. This low peak power is possible because of the relatively long uncompressed pulse (24 μs) used by the SAR. The antenna is gimbaled and can move over a wide range of pointing angles. The antenna is always pointed at a right angle to the aircraft's desired flight path and along a direction so that the center of the antenna's beam lies on the desired scene center-line. The estimated sensitivity of the SNL SAR at a range of 6400 m (as configured for the November 1992 tests) was estimated at about -45 dB [8].

To form its image, the SAR collects echoes over a "synthetic" aperture, typically tens of meters long. The complex computational procedure by which distinct pulses are combined (to achieve finer azimuth resolution than can be obtained using a SLAR) is the distinguishing strength of the SAR technique. In the azimuth processing, target cells are resolved based upon their Doppler frequency. Cells in front of the aircraft yield positive Doppler; cells behind the aircraft exhibit negative Doppler. By combining pulses over the aperture, the SAR synthesizes the equivalent of a very narrow virtual antenna beamwidth (typically a few hundredths of one degree), which is about equal to $\lambda/(2L_{SA})$, where L_{SA} is the length of the synthetic aperture. See Figure 1-2, which depicts the SAR processing scheme.

Digital image products are recorded, during flight, on a high-speed magnetic tape recorder. Raw, unprocessed radar echoes, called "phase histories", are also recorded, along with motion-compensation and other auxiliary data. Because phase histories are recorded, images can be

1. The term "resolution" has different meanings in different contexts. In this experiment, the radar was configured to produce 2-m pixels in the ground-plane in both the range and azimuth dimensions. The impulse response width in the ground-plane is 3.5 m in range and 3.0 m in azimuth. Unless otherwise specified, from this point on, resolution will refer to the ground-plane pixel spacing which is 2 m..

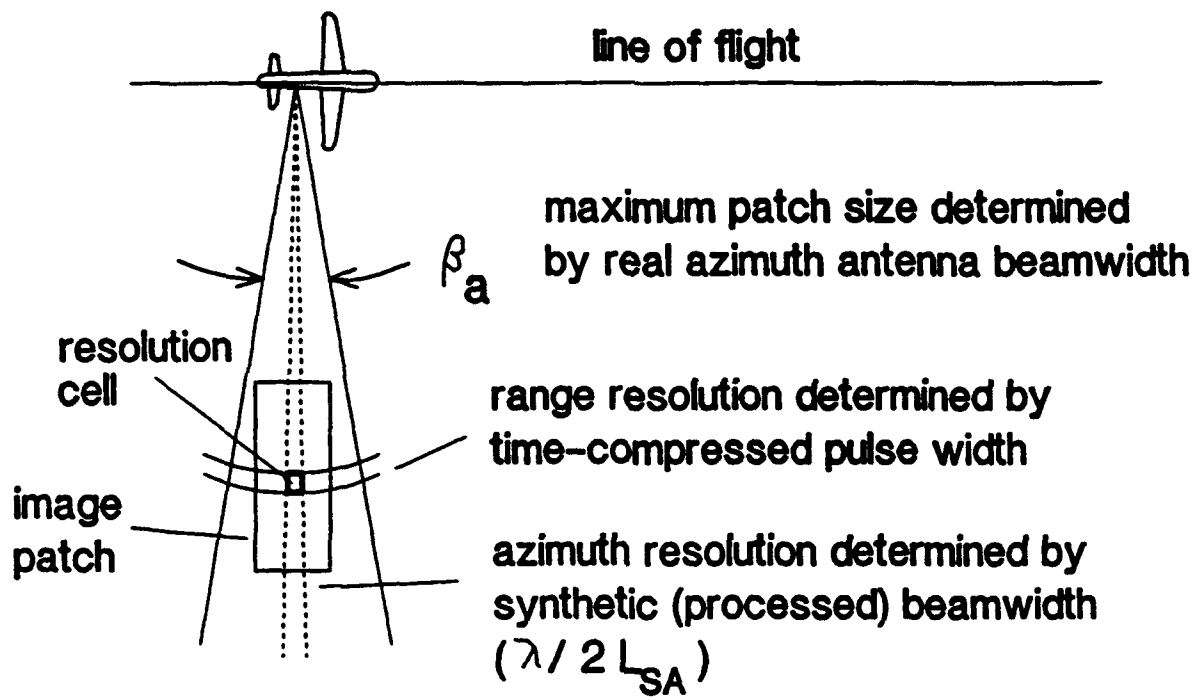

Figure 1-2. The SAR imaging process.

reformed, using ground-based image-formation software, either to vary resolution or to perform multi-look processing.

SAR processing of a single synthetic aperture of echoes results in a "single-look" patch. For the SNL SAR, patches are 1200 to 1800 pixels in slant range (this is selectable) and several hundred pixels in the azimuth (along-track dimension). In order for the SAR to form an image patch, all scattering cells in the patch must remain in the antenna beam over the entire synthetic aperture. In the event that the antenna's beam is much wider than necessary to meet this requirement, the SAR can use several closely-spaced apertures to form multiple "looks" at the target area. Each look is an image patch. Patches resulting from adjacent apertures can be formed in such a way that there is a significant amount of overlap in the patches. In this way, any particular target pixel can be seen in several overlapping looks (see Figure 1-3). The number of achievable looks depends on the antenna's azimuth beamwidth, the patch size, and the desired azimuth resolution.

Multi-look imagery is created by summing amplitudes or squared amplitudes of pixel voltages (for a given pixel location) across all available looks. The effect of this averaging is to increase signal-to-noise ratio in the image and to reduce speckle in the image.

A possible disadvantage of the multi-look technique for imaging of the ocean is the fact that total integration time over all looks may be so long that the ocean's movement during that time will degrade the resulting multi-looked images [9]. Although this may be a factor when the imagery is to be used to study details of wave structure, experience with flight-test data indicates that integration times of the order of seconds do not cause a problem when the images are to be used for oil-spill discrimination.

1.4 EXPERIMENT DESCRIPTION

In support of the comparative analysis of SAR and SLAR capabilities, an at-sea experiment was conducted during November 10-16, 1992. SNL's SAR and the Coast Guard's AIREYE SLAR systems were used to collect data simultaneously over naturally occurring oil seeps off the coast near Santa Barbara, CA. The purpose of the exercise was to collect a comprehensive enough data set to:

1. Evaluate the suitability of high-resolution SAR for oil-spill surveillance and

2. Support a cost/benefit comparison of SAR and SLAR sensor technology relative to USCG oil-spill surveillance mission requirements.

1.4.1 Participants

Several organizations participated in the data collection. Participants and resources have been grouped in four categories: Control, Twin Otter SAR, AIREYE, and Surface Truth.

1.4.1.1 Control

The USCG R&D Center, Environmental Safety Branch, served as the overall controller of the experiment. The R&D Center arranged for participating USCG aircraft and personnel,

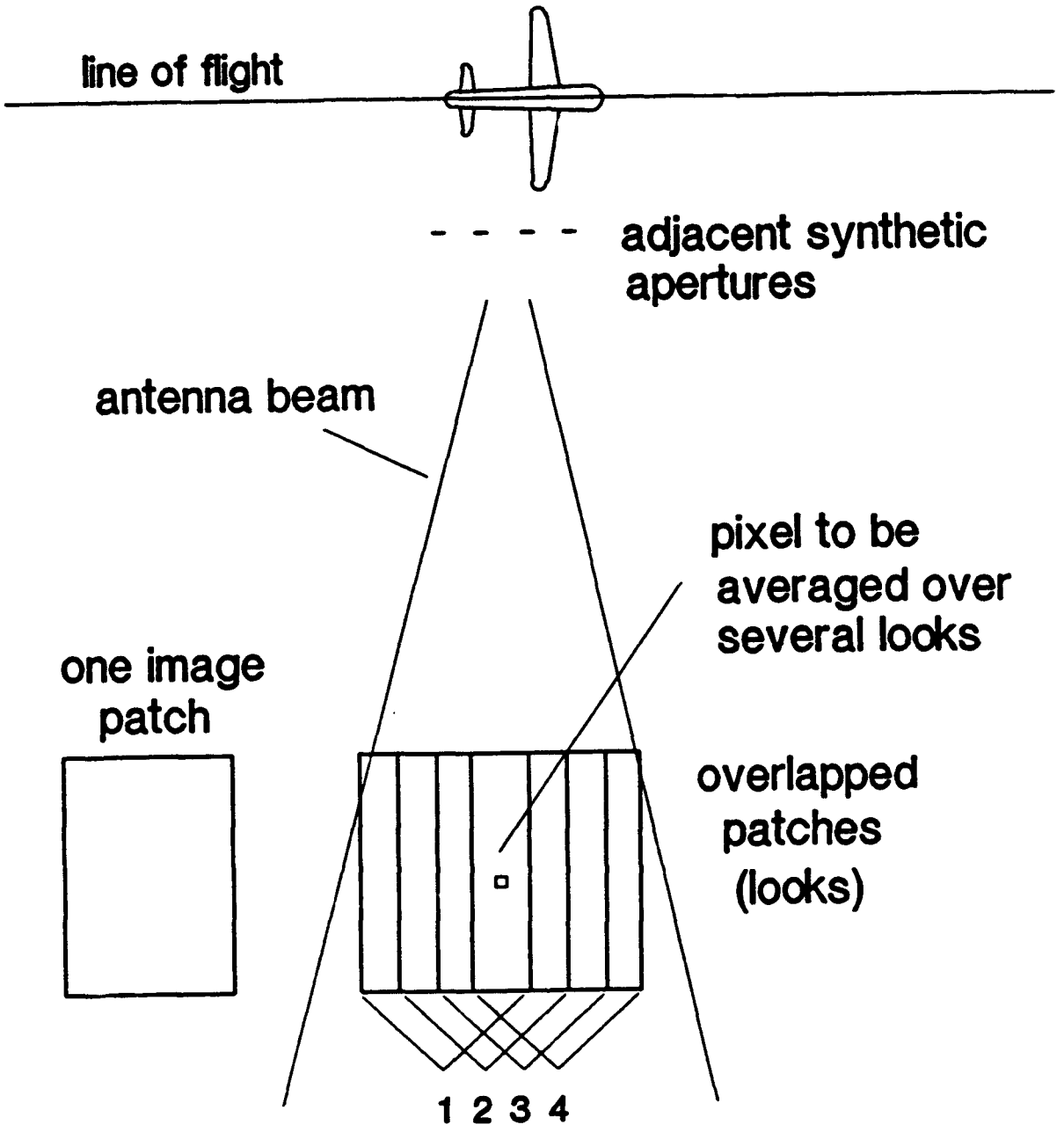

Figure 1-3. Multi-look imaging process.

obtained support from NOAA oil-spill response specialists, and provided a Test Director on-site in Santa Barbara, CA, during the data collection. The R&D Center Test Director was responsible for coordinating the daily activities of the various Coast Guard, NOAA, and SNL participants during the test and for collating the USCG and NOAA data inputs to SNL.

SNL provided a Project Manager to coordinate SNL resources and activities with those of the USCG, NOAA, and Motorola. In Santa Barbara, the SNL Project Manager served as a single point of contact for the SNL test team to communicate with the other test participants.

1.4.1.2 Twin Otter SAR

SNL provided personnel, an aircraft and a SAR system for the experiment. Sandia used their internally developed DCS (Data Collection System) radar. The SNL participants included the Sandia Project Manager, two pilots, two logistics and aircraft support personnel, one differential GPS ground station operator, three sensor operators, and several data analysts. The radar system is an R & D oriented, Ku-band SAR with built-in image formation capability. A differential GPS system is used for precise motion compensation. For this experiment, data were collected at 2 m resolution (ground-plane range and azimuth); images were formed by the on-board processor. The antenna polarization was VV. For a near optimum depression angle of 30°, the swath width was on the order of 2.5 km. The testbed aircraft was a DOE owned DeHavilland DHC-6 Twin Otter. It is shown in Figure 1-4.

1.4.1.3 AIREYE

USCG Air Station Cape Cod provided a seven-person aircrew and an HU-25B AIREYE surveillance jet for the Santa Barbara data collection. The AIREYE platform, a specially-modified Dassault-Breguet Falcon 20 jet, is a multi-mission remote sensing aircraft designed to detect, identify, verify, and document oil slicks in the marine environment. The AIREYE avionics package includes the AN/APS-131 SLAR (described in Section 1.3.2), an RS-18C infrared/ ultraviolet (IR/UV) line scanner, and a KS-87 aerial reconnaissance camera. A hand-held, 70-mm Agiflite camera is also used on board the AIREYE aircraft to photograph features of interest. The aircrew included two pilots, three sensor system operators, and two maintenance/support personnel. Five crewmembers, including two sensor operators, flew on each data collection sortie. Figure 1-5 shows the Coast Guard Falcon aircraft.

The AIREYE platform was responsible for obtaining SLAR images of the test area and for producing a geo-registered, KS-87 photo-mosaic of the test area each day.

1.4.1.4 Surface Truthing

NOAA HAZMAT, (Seattle, WA), USCG Gulf Strike Team, (Mobile, AL), and USCG Pacific Strike Team, (Novato, CA) provided personnel for the surface truth function. USCG Air Station Los Angeles provided helicopter support for surface truth operations. NOAA also leased a commercial helicopter operator for this task.

(This page intentionally left blank.)

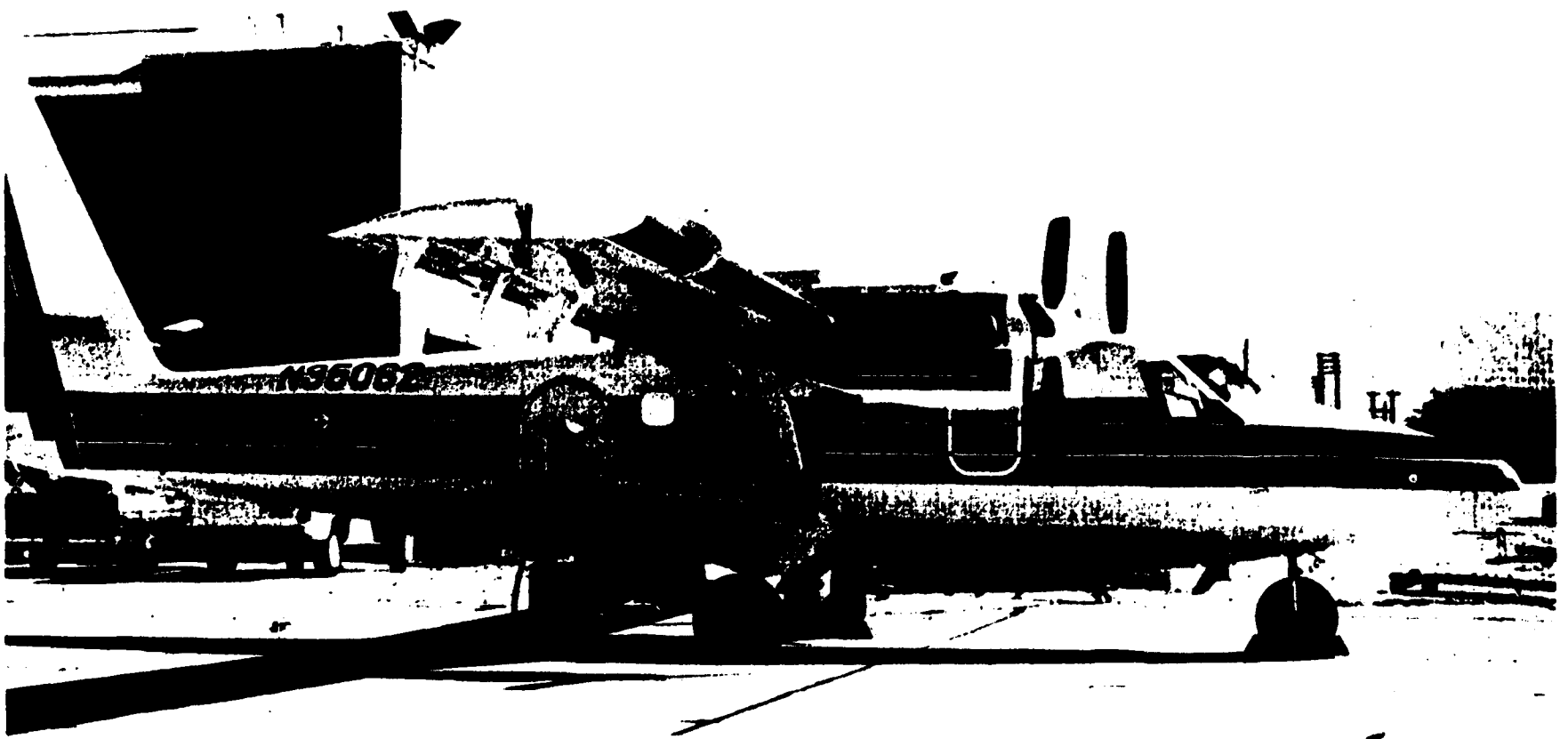

Figure 1-4. Photograph of the DOE DeHavilland DHC-6 Twin Otter aircraft carrying the Ku-band SAR. The antenna radome is visible just below the aft cargo door.

Figure 1-5. Photograph of the Coast Guard Dassault-Breguet Falcon 20 jet aircraft containing an AN/APS-131 SLAR, a RS-18C IR/UV line scanner, and a KS-87 reconnaissance camera. The SLAR antenna is mounted on the forward starboard fuselage. The IR/UV pod is mounted on the starboard wing.

1.4.2 Summary of Field Test Operations

Coordination among the various USCG organizations, Sandia, NOAA, Motorola, and the FAA began in July. These activities included temporarily upgrading the SLAR, obtaining frequency clearances, locating a differential GPS base station site, defining mission parameters and test areas, taking care of aircraft and crew logistics, and briefing local control tower authorities on the experiment. A detailed test plan containing all pertinent information on the experiment was also written [10].

Four adjacent test areas were defined for use in the experiment, as shown in Figure 1-6. Each test area measured 5 by 10 nmi. Area 1 was to be used if the slicks were drifting westward. It contained a main source of oil (and natural gas) and the Holly Platform. Area 2 was to be used if the main slick was drifting eastward, for imaging of kelp (false positives), or for other slicks of opportunity. Area 3 was to be used for slicks of opportunity. It contained the Hondo Platform. Area 4 was to be used as an alternate to Areas 1 and 2.

In-field activities began on November 7th-8th, with the arrival on-site of the Twin Otter SAR, AIREYE, and all crews. The SAR was flown in the area to verify proper operation. November 9th was also used for an equipment checkout day and for the pre-experiment briefing for all participants, which was delivered by the Test Director.

Data collections began on November 10th. The SAR and SLAR crews began this day, and all other mission days, with a 0700 hours briefing. Based on information from the NOAA surface truth observers, who had flown a "dawn patrol", Test Area 4 was chosen for this day's mission. Surface winds over the test area were 2-8 knots from the west at the Holly Platform; look directions were chosen to be north, east, and west. The sorties were flown between 0845 and 1200 hours. The Twin Otter SAR was able to collect data over the entire test area from the north and west look directions before having to terminate the sortie due to lack of fuel. The AIREYE was able to complete patterns for all required look directions; however, the tape used to record the SLAR data was corrupted and the data were lost.

Test Area 4 was again selected for the November 11th mission. Surface winds were 5-10 knots from the west at the Holly Platform; look directions were chosen to be south and east. The sorties were flown between 0900 and 1200 hours. Both the Twin Otter SAR and the AIREYE completed all patterns. Surface truth sorties were flown by both NOAA and USCG personnel in the charter helicopter and the Coast Guard HH-65A. The water in the test area was so calm that the reflection from the bright orange HH-65A could be seen from the Twin Otter flying 10,500 ft above. The test area contained windrows of rough, weathered oil (which trapped flotsam) and rafts of sea birds.

For the November 12th mission, Test Area 1 was selected. The dawn patrol sortie indicated winds from the west, so look directions were chosen to be south and west. Wind speeds were 1-10 knots at the Holly Platform. All aircraft departed for their sorties at about 1100 hours and completed their patterns. The USCG HH-65A was used for surface truthing; a Coast Guard observer was also carried on the Twin Otter.

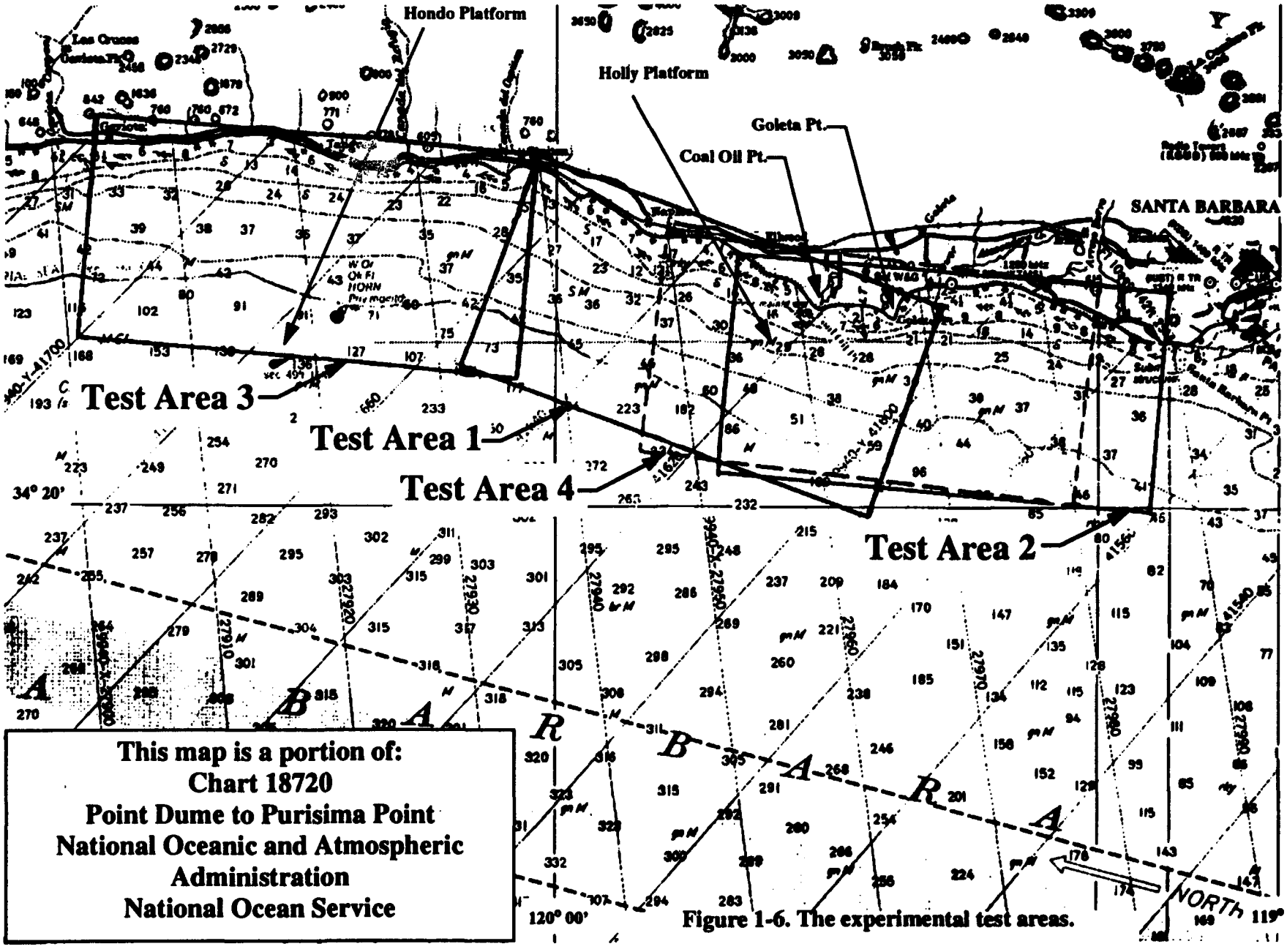

This map is a portion of:
Chart 18720
Point Dume to Purisima Point
National Oceanic and Atmospheric Administration
National Ocean Service

Figure 1-6. The experimental test areas.

After a day off, data collection missions were resumed on November 14th. Test Area 1 was chosen. Winds were calm; east, south, and west look directions were selected. Sorties were flown between 1300 - 1600 hours. The Twin Otter / SAR completed its south and west looking patterns before having to terminate the sortie due to lack of fuel. The AIREYE completed all its patterns. The USCG HH-65A was used for surface truthing. A Coast Guard surface truth observer was carried on the Twin Otter.

Test Area 1 was again selected for the November 15th mission. Surface winds were calm, blowing between 0 and 2 knots at the Holly Platform. North and east look directions were chosen. The sorties were flown between 1300 and 1600 hours. The Twin Otter / SAR and AIREYE completed all their patterns over the test area without incident. The USCG HH-65A and a commercial helicopter were used for surface truthing.

November 16th marked the last data collection day. Due to poor forecast data collection conditions, (calm seas and windless), this day was to be used for training and for imaging targets of opportunity. Sorties began at 0900 hours. However, once the aircraft got over the test areas, it was observed that the conditions for imaging oil on the water might be better than anticipated. A new plan was coordinated over the radio; Test Area 1 and south and west look directions were selected. The AIREYE completed its patterns without incident. Unfortunately, the SAR data recorder on the Twin Otter malfunctioned and could not be repaired in the air. No SAR data were collected. AIREYE and its crew departed for home after the November 16th mission was completed. The Twin Otter and crew departed the next day.

1.4.3 Summary of Data Collected

A detailed summary of the collected SAR and SLAR image data will be presented in Chapter 2. Besides the SAR and SLAR data, several other types of data were collected during the experiment. AIREYE was used to collect IR and UV data over selected areas. Its KS-87 camera was also used to photo-map the selected test area once each day. In addition, both the SAR and SLAR crews kept log sheets and mission notes during each data collection sortie. Surface truth and weather data were obtained from a number of sources. The primary source was helicopter-borne NOAA and Coast Guard observers who were on-scene during each data collection mission to document surface conditions within the test area. Wind speed estimates and sketches of surface features and oil slick positions were made by these NOAA and Coast Guard observers. Black and white 70-mm and color 35-mm photographs of noteworthy features within the test area were also taken by the observers during most of the missions. In addition, the USCG R&D Center obtained recorded wind conditions at the Holly platform (which resides in the middle of the experiment area) from ARCO Oil and Gas Co. Information from the pilot's weather briefings were also recorded for each mission.

1.5 ANALYSIS TOOLS AND IMAGE DATA

SNL was tasked to provide the Coast Guard with SAR and SLAR image data from the experiment and to deliver appropriate hardware and software tools for its analysis. These deliverables included a computer workstation, customized and commercial software, SAR and SLAR image files, and auxiliary data files. Sections 1.5.1 through 1.5.3 will describe these deliverables in detail.

In developing these deliverables, certain data characteristics and analysis goals had to be considered. Key analysis goals were to establish whether SAR has benefits over SLAR for imaging oil on water and to evaluate the effectiveness of various image processing techniques. To accomplish this, side-by-side comparisons of full-resolution SAR and SLAR images showing common regions had to be made. It was not sufficient to simply lay prints of SAR and SLAR images side-by-side. The sheer size of the SAR mosaics at full resolution (up to 9400 by 4900 pixels) would make image printing extremely difficult. Differences in the printed size of SAR and SLAR images depicting the full test area would make feature-to-feature comparisons difficult. Differences in contrast between SAR and SLAR prints could bias interpretations. These limitations were addressed by providing a capability to extract full-resolution regions-of-interest (ROIs) from the raw SAR and SLAR images. These smaller ROI images were sized to fit on the workstation display monitor and on a single-page hardcopy from the Kodak high-resolution dye-sublimation printer. The ROIs could then be processed using techniques such as contrast stretching, speckle smoothing, enlarging/reducing, simulated multi-look processing, and simulations of various resolutions. These techniques enabled analysts to evaluate the information content of the images in detail and to evaluate the effectiveness of the processing techniques themselves.

Another analysis goal was to determine the spatial resolutions required for SAR imagery to retain features of interest at the acuity desired by sensor operators and analysts. The best technique for evaluating SAR resolution is to resample the raw phase history data and form new images from the resampled data. This is a very expensive post-processing task and was beyond the scope of this study. Past SNL comparisons between reformed images made by resampling the phase history and simple subsampling of existing full-resolution images (followed by pixel replication) indicated that this simpler method is a valid simulation of reduced resolution SAR imaging. This simulation could be easily performed on the workstation and large volumes of data could be processed by the USCG R&D Center at low cost when compared to phase history resampling. Sandia developed software to support this reduced resolution simulation so that analysts could evaluate SAR resolution trade-offs. A validation of this simulation method was performed specifically for this project. This validation will be described in Section 1.6.3.1.

1.5.1 Image Data Sets

SAR data deliverables were in two formats: full-resolution mosaics and down-sampled mosaics. These products could be post-processed on the workstation supplied for data analysis (described below). Full resolution mosaics were required for detailed region-of-interest analysis, but they were too large to be displayed on the workstation monitor or printed as hardcopy. Down-sampled mosaics were supplied to give analysts full scene views that could be displayed on the workstation monitor and used to locate regions-of interest. More will be said about the use of the full resolution mosaics and down-sampled mosaics later in this section.

The SAR image data were processed at SNL to form detected image mosaics for distribution and analysis. Mosaics were required because the Twin Otter SAR images range swaths that are smaller than the range swaths normally produced by the AIREYE. Comparable range coverage could only be attained by mosaicking multiple strips of imagery. Each strip represented an imaging pass by the aircraft, hence, each strip is called a "pass". Mosaics created from a south-looking or a north-looking antenna were composed of 4 "passes", while those created from an

east-looking or a west-looking antenna were composed of roughly 8 "passes". To conserve aircraft fuel, the Twin Otter flew a serpentine path, the antenna imaging on the left of the aircraft for one pass, imaging on the right of the aircraft for the next pass, etc., until all passes for the mosaic were completed.

The normal SAR processing creates linearly scaled image intensities, each pixel in the detected image having 16 bits of dynamic range. The full 16-bit dynamic range of the detected image was not required since the sea return was faint compared to land return. To conserve memory and to facilitate easy image display, the 16-bit data were rescaled to 8 bits of dynamic range. The rescaling, a simple multiplication by a constant, was performed to enhance faint sea returns at the expense of saturating land returns from the coast. The same rescaling was performed on all passes from all days of the experiment. The noisy sea return in passes that included land, such as the one shown in Figure 1-7, is due to two factors: decreased receiver gain (to avoid saturation of sea returns by land returns), followed by a compensating increase in signal processor gain. This technique amplified the thermal noise across all passes that intercepted land.

The 16-bit raw SAR image passes that were processed to create the 8-bit image mosaics were also provided as a backup. Should there be a future interest in reprocessing the raw data and forming new mosaics, these data are available to the Coast Guard for processing with Sandia's "Imview" software (provided with the computer workstation).

SLAR data were also processed at SNL and delivered for exploitation on the workstation. This processing amounted to editing the SLAR data that were recorded on Digital Audio Tape (DAT). Scenes that corresponded to SAR mosaics were extracted from the DAT. These scenes were also geometrically rectified so that land always appeared at the top of the image (north is upward) and so that all SLAR scenes had the same size (total number of bytes). Aside from this geometric registration, no additional processing was performed on the SLAR data. Data samples were kept at their original 8-bit dynamic range and no rescaling of intensities was performed.

Auxiliary files were supplied that contain information about imaging times, modes, environmental states, and mosaic identification. This information was included for the creation of key image and region-of-interest text banners, as will be discussed in Section 1.5.3. SAR and SLAR auxiliary files contained the following information:

1. Image or mosaic size, in pixels.

2. Downsampling factor for creating a key image (SAR only).

3. Flight date.

4. Flight times.

5. Antenna look direction.

6. Mosaic size, in meters (SAR only).

7. Wind direction, in degrees.

(This page intentionally left blank.)

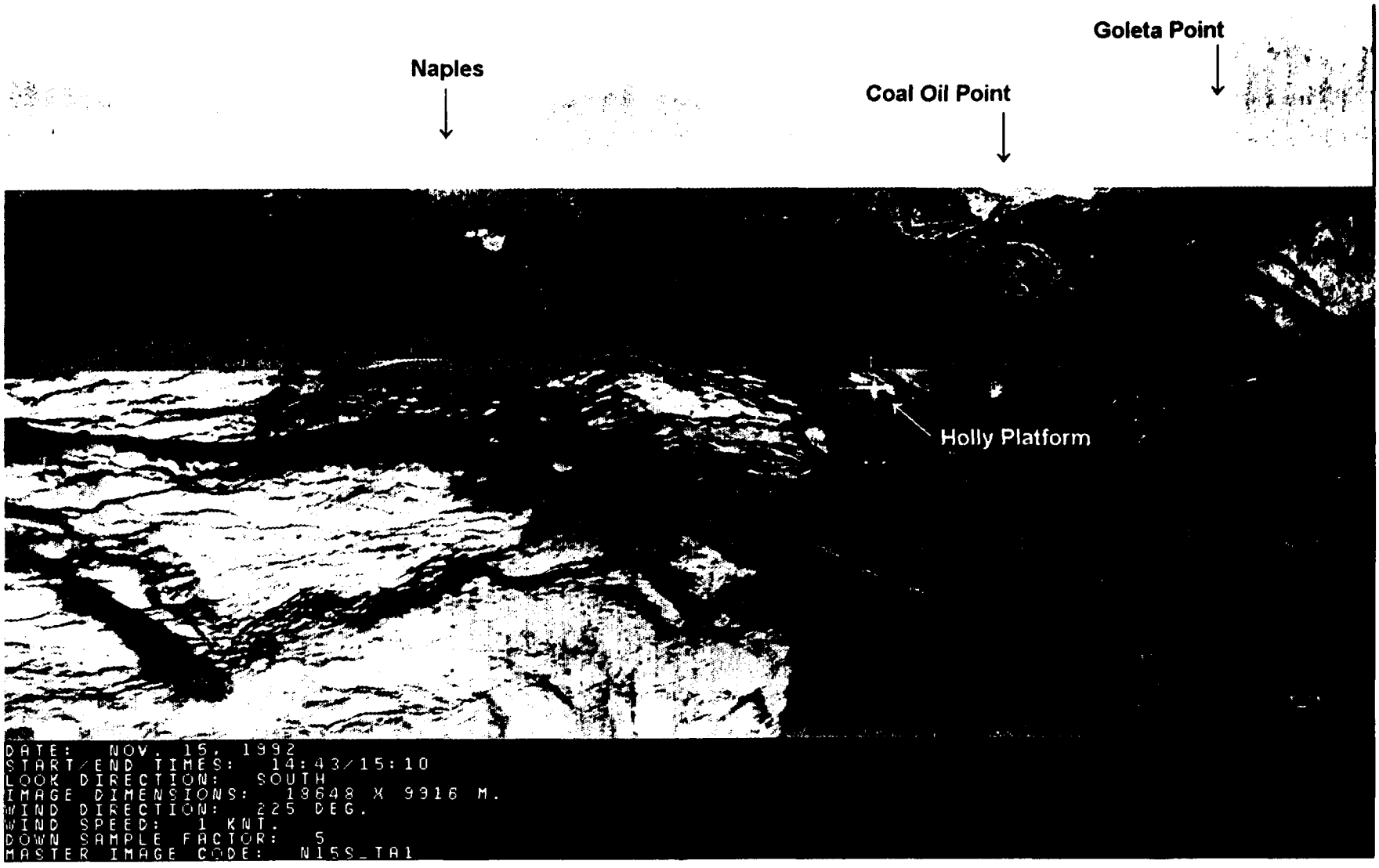

Figure 1-7. A 4-pass mosaic, downsampled by a factor of 5 for display. Notice the increased noise in the first (top-most) pass. *See Section 1.5.1 for details.*

8. Wind speed, in knots.

9. Master image identifier.

10. Pixel resolution, in meters (SAR only).

All data were supplied on computer-compatible laser disks.

1.5.2 Workstation

SNL delivered to the Coast Guard a 486/66 PC-based workstation that enabled viewing, manipulation, processing, annotation, and printing of SAR and SLAR images from the November 1992 joint flight test. The workstation (see Figure 1-8) included a fine-resolution (1280 x 1024 pixels) graphics monitor, high-capacity magnetic and magneto-optical read/write storage media, and a fine-resolution (2048 by 1536 pixels) color graphics printer. Delivered software included both commercial (DOS, Windows, Photostyler) and SNL-designed products (to be described in Section 1.5.3.1).

The fine-resolution, 20-inch monitor allowed high-fidelity display of large images in multiple windows. Test data were transferred to the Coast Guard on 1-Gbyte optical cartridges. The 650-Mbyte fixed disk contained all system and application software and was used for temporary storage of processed data. Memory for the system was sized to allow adequate RAM storage for processing and simultaneous display of multiple SAR or SLAR images. This hardware and software provided the USCG R&D Center with the processing power and software tools necessary to analyze the SAR and SLAR flight-test data.

1.5.3 Image Manipulation and Processing Software

Software was developed at SNL to present the SAR and SLAR data in standardized formats for analysis, to display the SAR imagery at full and degraded resolutions, and to filter any undesireable speckle that might degrade interpretability. This software was complimented by commercial software providing standard image display and printing capabilities. Both the SNL software and the commercial software were installed on the PC-based workstation discussed in Section 1.5.2.

1.5.3.1 SNL-Provided Software

SNL provided the USCG R&D Center with a general-purpose computer program and three customized computer programs for formatting, processing, and analyzing the SAR and SLAR image data. These programs and their capabilities are as follows.

IMVIEW - IMVIEW is a general purpose software package developed by SNL for manipulation of raw, 16-bit SAR strip-image data. It was provided to the USCG to facilitate manipulation of the raw SAR image data, should the need arise. This software also provides a wide array of general-purpose image processing capabilities that were not required for this analysis. A detailed description of these capabilities is provided in reference [11] (the IMVIEW User's Guide).

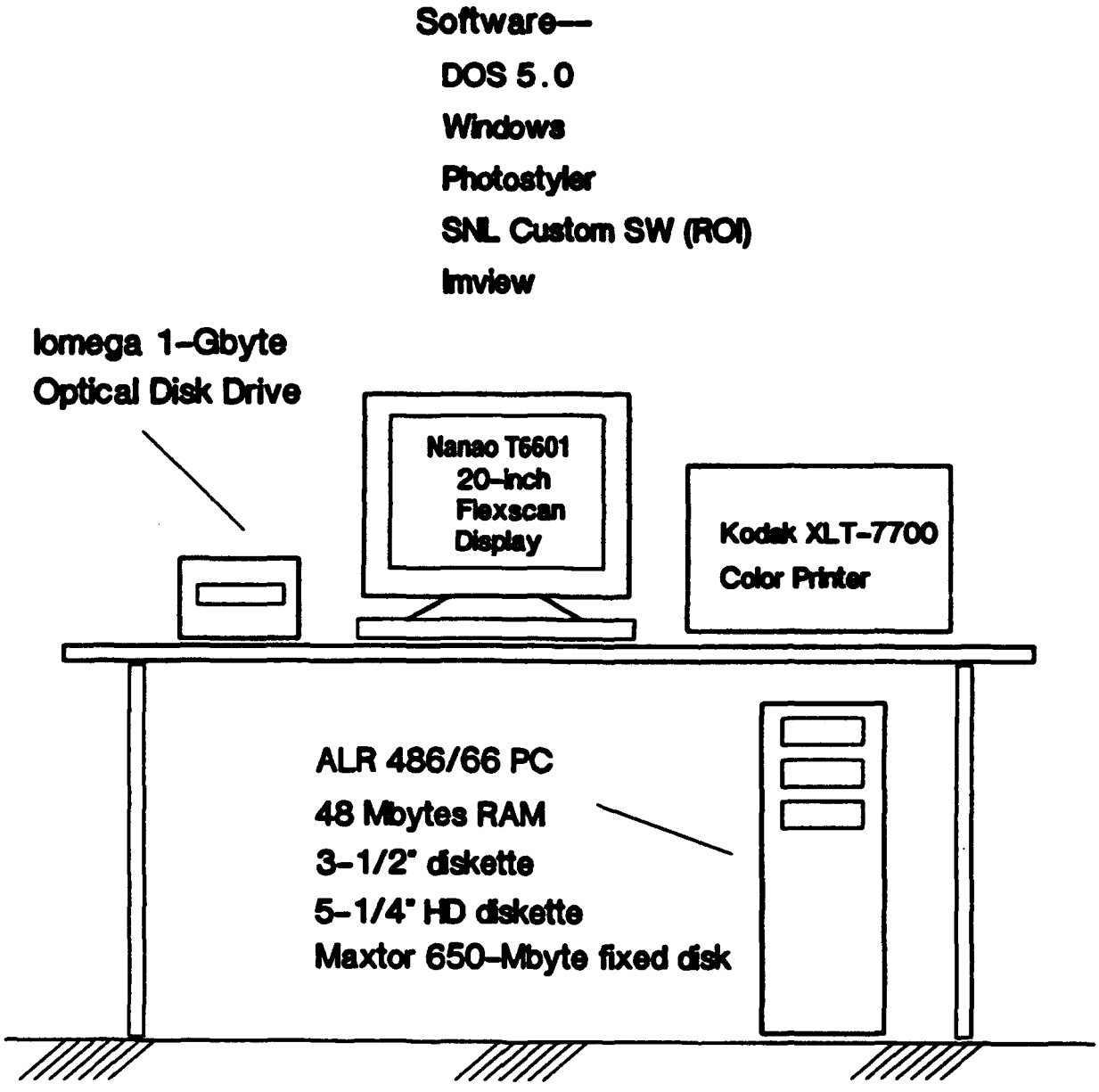

Figure 1-8. Coast Guard SAR image viewing station.

Swath_vu - Swath_vu enables analysts to vary the spatial resolution of a SAR image containing the full 5- to 10-nmi test area from 2-meter, square-pixel ground projection to lower resolutions that are more practical for real-time display. This software was used to simulate various levels of full-swath SAR image resolution that a sensor operator might use for real-time viewing/printing and ROI selection. The object of creating full-swath imagery at multiple resolutions was to allow an evaluation of trade-offs among the image resolution, the geographic dimensions of an image, and the pixel capacities of available video displays and printers. A banner detailing the image processing accomplished is appended to the bottom of each output image.

ROI - The region-of-interest (ROI) software extracts image data, bounded by user-specified pixel coordinates, from a full-swath SAR mosaic and creates a new ROI image file. The maximum ROI size was set to be a 3- by 4-km rectangle. This size was dictated by the number of pixels that can be printed by the Kodak XLT 7720 printer (1536 by 2048 pixels) and the 2-m maximum ground pixel resolution of the SAR images. Because knowledge of the location where regions have been extracted is important for analysis, a key image capability was included in the software. A key image is a reduced resolution (subsampled) version of the full mosaic with a region of interest border superimposed. A text banner is also included at the bottom of the subsampled image that uniquely identifies the ROI and lists pertinent environmental information. A region-of-interest image, in conjunction with a key image, provides a mechanism for linking detailed features in a specific region with the full-swath image.

This process is depicted in Figure 1-9. When the ROI file is extracted, the user has the option of performing the following operation.

1. Any of three speckle smoothing routines (described below).

2. Down-sampling the image to a user-defined spatial resolution.

3. Down-sampling the image, then executing one of the speckle smoothing algorithms.

4. Down-sampling the image with a sliding window averaging ("boxcar") algorithm.

5. Simply extracting a full-resolution ROI without any additional processing.

Figure 1-10 provides a pictorial representation of the options provided in the ROI software. Sections 1.6.2 and 1.6.3 describe these options in more detail. Each of the options that down-samples an image reduces the number of pixels in the image (and therefore its size). The ROI software restores the image to its original size through pixel replication to permit comparisons of printed images that are the same physical dimensions. After executing any of the image processing algorithms, the user is asked to enter a file name and the processed image is saved. The user can then execute several image processing algorithms on the original image, select another ROI, or exit the ROI program. A text banner detailing the source of the image and any image processing performed is appended to the bottom of each output image.

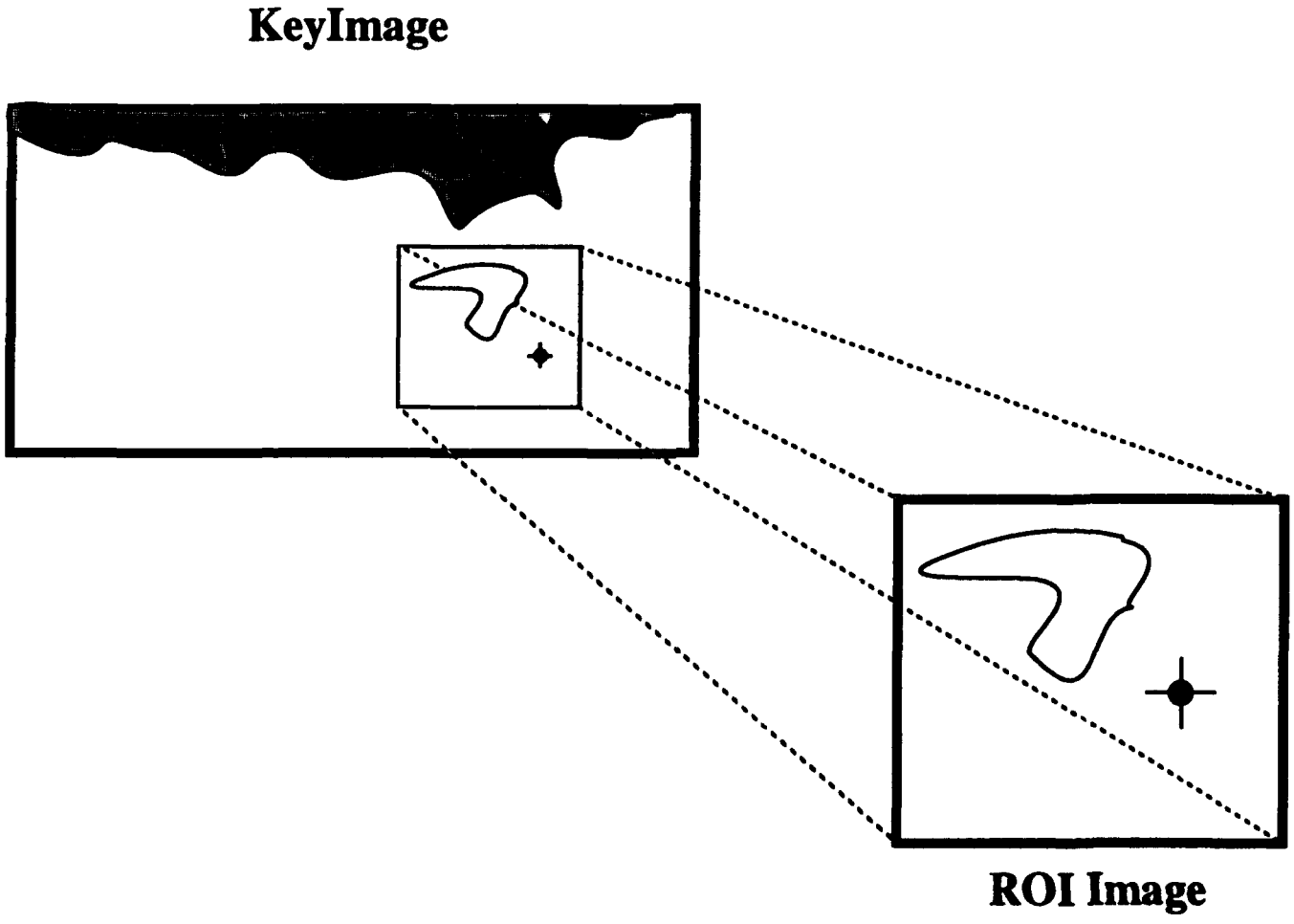

Figure 1-9. Relationship between the key image and region-of-interest (ROI) image.

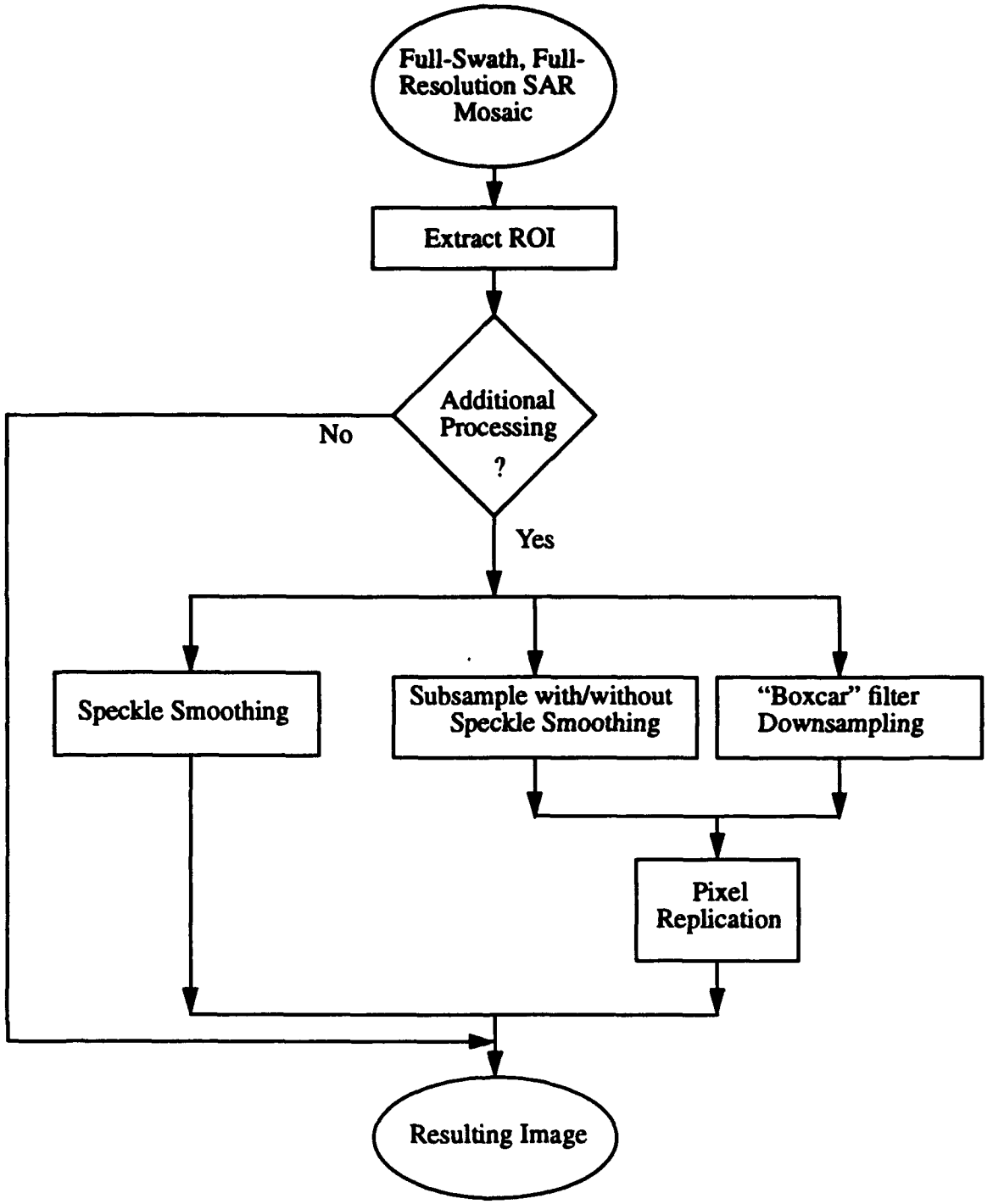

Figure 1-10. SAR data processing flow for images selected for analysis.

LUT - The look-up table (LUT) software operates on an existing ROI file and provides standard brightness and contrast remapping functions. Adjustments for moderate and extreme contrast stretching and darker-than-average, average, and brighter-than-average brightness control are provided. The purpose of this software was to evaluate whether a small number of preset contrast functions could reasonably be established to minimize the burden on an operator of an operational radar. During the analysis, USCG R&D Center project staff found that they preferred to have available the full range of brightness and contrast control provided by the Photostyler software described in the following section. A text banner detailing the source of the image and any image processing performed is appended to the bottom of each output image.

1.5.3.2 Commercial Software

SNL purchased and installed a commercial software package on the workstation to facilitate image display and printing. A summary of this package follows.

ALDUS Photostyler® - The ALDUS Photostyler® software is a commercially-available product that provides a wide array of image import/export, image processing, and image enhancement capabilities. The capabilities used during the SAR/SLAR data analysis include the following:

1. Import/Export - Raw format images created by the ROI and Swath_vu software were imported into Photostyler®. When all image processing functions were completed, the image was exported to the Kodak XLT 7720 printer.

2. Area selection tools - The rectangular region selection tool was primarily used to mark and bound a region of interest from a full-swath image. The pixel coordinates of the upper left and lower right corners were obtained for input to the ROI software. This tool was also used for selecting features from different images to compare.

3. Tuning (brightness and contrast) - This function provided the ability to adjust the image brightness and contrast to enhance image features. It replaced the LUT software functionality by providing the USCG R&D Center analysts a wider range of brightness and contrast adjustments.

4. Resampling - The ability to alter the size and resolution of an original image permitted USCG R&D Center analysts to compare enlarged SLAR images with processed SAR ROI images of the same area. Both pixel replication and pixel interpolation enlargements were supported.

5. Negative - The ability to tune an image to its negative permitted SAR and SLAR imagery to be viewed in the same format that SLAR imagery is currently recorded on the AIREYE system's dry-silver film.

6. Zoom - The capability to increase and/or decrease image size permitted analysts to view the entire test area mosaic down-sampled or to magnify small windows of the

image to full resolution. The ability to magnify and scroll through parts of the image facilitated the selection of some ROIs.

1.6 DESCRIPTION OF IMAGE ANALYSIS ACTIVITIES

Five scheduled tasks were performed as a part of the image analysis activities. The first was a meeting in August of 1992 between the representatives from the USCG, NOAA, and SNL to identify Measures of Effectiveness (MOEs). The role of the MOEs was to outline quantitative and qualitative techniques for answering specific questions about the oil-slick imaging capabilities of SAR and SLAR. All analysis activities were to address the MOEs. The second task was to deliver the computer workstation, with software and data, to the USCG R&D Center. The third task was a workshop involving the Coast Guard, NOAA, and Sandia representatives in March of 1993. The purpose of this workshop was to compare SAR, SLAR, and photographic data from the experiment, and select a number of regions-of-interest for analysis. These regions-of-interest were then contrast enhanced, noise smoothed, and downsampled by USCG R & D staff in preparation for the final task, a data analysis workshop. The final workshop was attended by Coast Guard, NOAA, and SNL representatives and was held at the end of June, 1993. Results from this final workshop form the basis for Chapters 2 and 3.

1.6.1 Measures of Effectiveness Definition

In order to provide a structured method for evaluating SAR for oil-spill response, several Measures of Effectiveness (MOEs) were identified. Representatives from the USCG, NOAA, and SNL participated in the development of these MOEs. The meeting was held at NOAA-HAZMAT in Seattle, WA, on August 20, 1992, and the participants were:

Gary Hover (USCG R&D Center - Environmental Safety Branch)

Jerry Galt (NOAA-HAZMAT Division)

Deborah Simicek-Beatty (NOAA-HAZMAT Division)

Jeff Bradley (SNL, Remote Sensing Field Test Organizer)

Bob Axline (SNL, Radar System Analyst)

At this meeting, the following questions were identified as being central to evaluating the oil-spill imaging capabilities of SAR and SLAR.

1. Do finer resolutions make it easier for image interpreters to differentiate false positives from oil slicks?

2. At what resolution is the optimum benefit gained?

3. How well does SAR bring out edge details for the interpreter, relative to SLAR?

4. How is this "acuity" affected by wind speed, look direction, and apparent slick thickness/oil state?

5. How well does the SAR differentiate between ocean clutter and oil slicks?

6. How sensitive is the SAR to slick thickness?

7. What are the wind speed cutoffs for the SAR, relative to the SLAR?

Due to the nature of the oil-slick image interpretation problem, the MOEs developed to address these questions were more qualitative than quantitative, as follows:

1. Compare the slick edge details that are visible at several SAR resolutions (i.e. the originally collected 2-m resolution as well as several artificially degraded resolutions) with that available on the SLAR system. Acuity is the key parameter: how well does each system bring out edge details for the interpreter, and how is the acuity affected by wind speed, look direction, and apparent slick thickness / oil state?

2. Examine the contrast adjustments required to bring out slick edge details and gradients in slick thickness, as a function of wind speed, look direction, and apparent slick thickness / oil state. Sensitivity is the key parameter.

3. Compare the high- and low-wind speed thresholds (cutoffs) at which each system is capable of discriminating the full outline of a visible oil slick.

The "quantitative" approach to evaluating the MOEs was to select several slick features of interest from the surface truth data collected during the experiment and then to evaluate the ability of each radar system to discriminate those features as a function of the parameters discussed above. Quantitative wind, sea, and oil-slick information (described in Section 1.5.1) was used to help evaluate the MOEs.

1.6.2 ROI Selection and Analysis of Image Processing Methods

The first data analysis workshop was held at the USCG R&D Center in Groton, CT, March 22-25, 1993. The purpose of the workshop was to review the SAR, SLAR, and surface truth data acquired during the Santa Barbara experiment. The participants were:

Gary Hover (USCG R&D Center - Environmental Safety Branch)

Jerry Galt (NOAA-HAZMAT Division)

CDR Ross Tuxhorn (USCG Gulf Strike Team)

Jeff Plourde (contractor to USCG R&D Center)

Gary Mastin (SNL, Digital Image Processing Engineer)

Following the initial data overview, the participants examined SAR and SLAR scenes, in chronological order, to identify oil features of scientific interest that appeared in both the SAR and SLAR images for each day. Factors such as wind speed, wind direction, antenna look direction, and time difference between SAR and SLAR imaging passes were considered. Regions were

identified in the SAR and SLAR images that contained data of primary interest. The coordinates of these regions were recorded for extraction and further analysis at a later time. Photographic images were then reviewed that might show the same features that appeared in the SAR and SLAR scenes. Photographic images included KS-87 reconnaissance photos from the AIREYE, Agiflite photos captured out the window of the AIREYE, 35-mm slides captured out the door of the NOAA surface truth helicopter, and miscellaneous photographs taken by crew members of the Twin Otter. Surface truth maps drawn by NOAA observers during the experiment were also used to help identify features of interest.

After this first workshop, USCG R&D Center analysts used the ROI software to extract full-resolution ROI images from their "parent" mosaic images. Each ROI image was then saved to disk as a raw data file suitable for further processing. As described in Section 1.5.3.1, companion key images were also formed to depict the location of each ROI within the test area. These key images were imported into Photostyler® and printed on the Kodak XLT 7720. Each ROI image was imported into Photostyler®. ROI images that were simple data extractions from the "parent" images were exported directly to the Kodak printer, as were negatives of these images (after tuning for brightness and contrast to highlight ocean surface features).

The next step was to evaluate three image processing filters for their ability to reduce image speckle. SAR images can be corrupted by coherent speckle that obscures the interpreter's ability to discern subtle detail. This speckle often looks like salt-and-pepper has been superimposed on the underlying image, and its effect is to draw attention away from the fundamental underlying features of the image. Noise and speckle smoothing are common techniques employed in the field of digital image processing. Fine image detail is usually sacrificed in order create images that are easier to interpret.

The three speckle filters used in this evaluation were the sliding window average [12], the sliding window median [13], and the Crimmins morphological filter [14]. The concept of the sliding window is simple. For a selected square window size of n x n pixels, the center pixel of the window is changed as a function of the pixels in the window. The sliding window average replaces the center pixel with the average value of the window pixels. The sliding window median replaces the center pixel with the median value in the window. The window is moved pixel-by-pixel to average the entire image. Only the original pixel values are used in the averaging or median calculations. (See Figure 1-11.) The sliding window average is one type of low-pass filter that will smooth speckle, but it has the disadvantage of smoothing edge detail. The sliding window median smoothes speckle by eliminating abrupt noise spikes, resulting in better retention of edge detail than in the sliding window average. The Crimmins filter is an iterative, nonlinear morphological filter specfically designed to smooth speckle in SAR images. It was designed by Tom Crimmins [14] to suppress speckle while retaining edge detail. The number of iterations must be specified. For the Santa Barbara images, one to three iterations were commonly applied. Too many iterations can destroy an image.

The sliding window average, sliding window median, and Crimmins morphological filters were applied to the ROIs selected by participants of the first data analysis workshop. The complete processing for each ROI included 3 x 3 pixel and 5 x 5 pixel sliding window averages and medians (4 processed output ROIs) plus outputs from 1-, 2-, and 3-iteration Crimmins filters (3 processed output ROIs). The extracted, but unprocessed, ROI was also preserved, as was a key

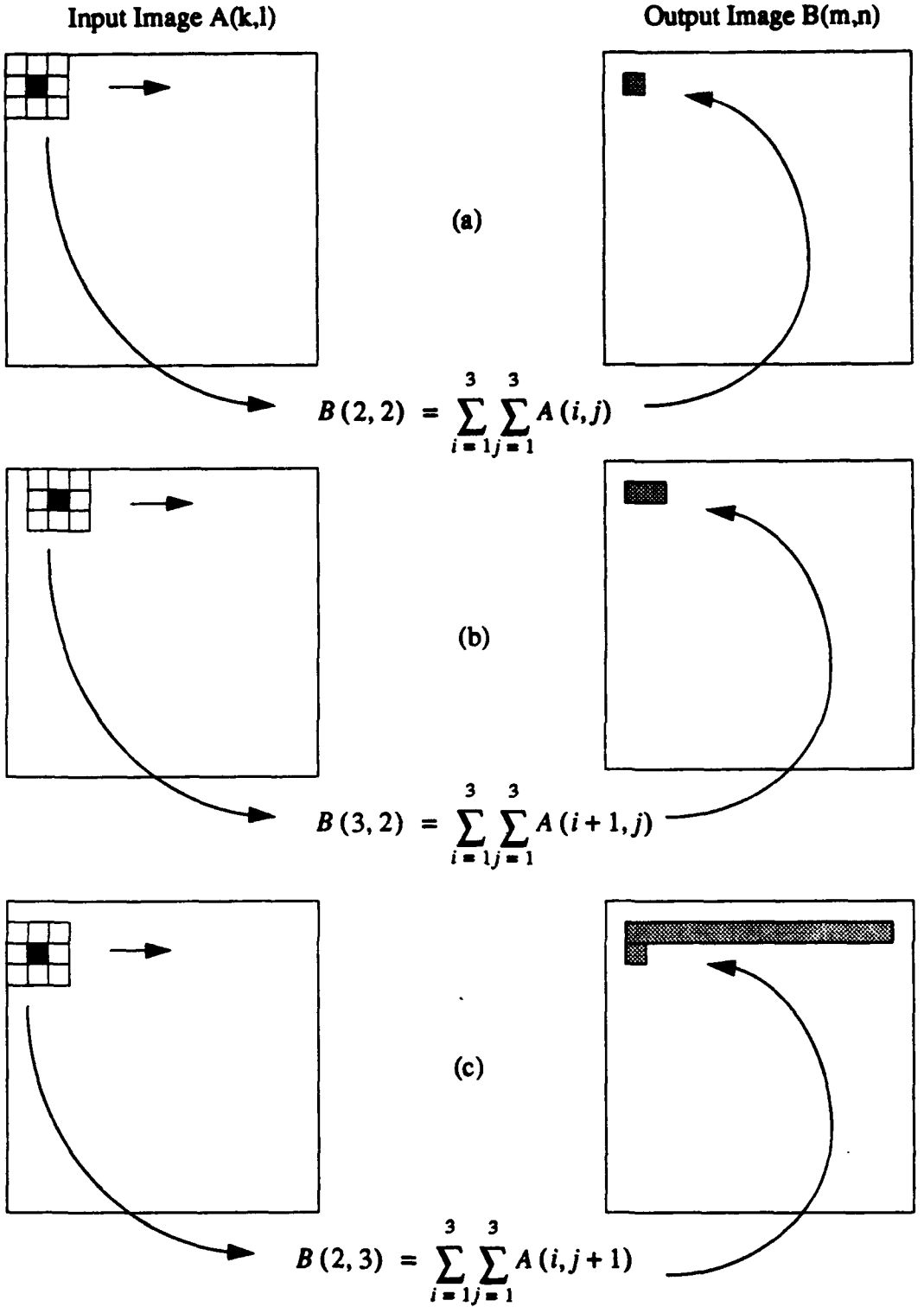

Figure 1-11. Schematic for sliding window averaging. (a) Starting in upper-left corner, computing an output pixel, then moving right one pixel (b) until the entire row is processed. (c) Beginning the process again on the next row.

image for the ROI. This resulted in a total of 8 ROI files and a key image file for each of the selected regions-of-interest. Each image file was imported by Photostyler®, tuned for creating a brightness- and contrast-balanced image (or negative), and exported to the Kodak printer. These prints were then assembled in order (key image, unprocessed ROI, unprocessed ROI negative, 3 x 3 average, 5 x 5 average, 3 x 3 median, 5 x 5 median, then 1-, 2-, and 3-iteration Crimmins) and augmented with a brief listing of the processing history and pertinent scene information. The sets of ROIs for each radar antenna look direction on each day were compiled, then the daily image sets were assembled in chronological order and sent to each participant in the workshop. Companion SLAR imagery was also printed and sent to workshop participants for direct comparison of equivalent areas.

The USCG R&D Center prepared for the second workshop by exploring the effects of resolution degradation on selected SAR ROIs. The Center prepared example images for consideration by the workshop participants where resolutions were degraded by two simulation methods; subsampling and adjacent window averaging. (These techniques will be discussed further in Section 1.6.3.1.) In a related effort, SNL developed a sample set of SAR images to validate the simulation techniques. SNL down-sampled a SAR image in the "optimal" way by reprocessing the phase history returns to form reduced-resolution images. This reprocessing was performed for single-look SAR imagery and multi-look SAR imagery. The results were then compared to the simulated down-sampled SAR images produced with the SNL software at the USCG R&D Center to verify that the simulations were valid.

The second workshop was held at the USCG R&D Center in Groton, CT, June 28 - July 1, 1993. The purpose of this workshop was to examine processed and unprocessed region-of-interest images that were identified at the first workshop, assess the utility of speckle smoothing algorithms for SAR images, determine SAR resolution requirements for identifying features of interest with acceptable acuity, consider whether SAR imagery exhibited clear advantages over SLAR imagery for oil-spill monitoring, and discuss system trade-offs and design issues for a possible oil-spill SAR. The participants were:

Gary Hover (USCG R&D Center - Environmental Safety Branch)

Jerry Galt (NOAA-HAZMAT Division)

AT2 Bruce Verfailie (USCG Air Station Cape Cod)

Jeff Plourde (contractor to USCG R&D Center)

Bob Axline (SNL, Radar System Analyst)

Gary Mastin (SNL, Digital Image Processing Engineer)

Results from the second workshop appear in Chapters 2 and 3 of this report. At the conclusion of the second workshop, several of the most interesting ROIs were selected for a final detailed analysis of required SAR spatial resolution. These ROIs depicted features that could be identified in the SAR, SLAR, and photographic surface truth images. The analysis of these images will be discussed in the next section.

1.6.3 Analysis of Required Image Resolutions

The question of the spatial resolution at which a SAR should image in order to resolve oil-spill features with adequate acuity was central to the study. Too fine a resolution results in unnecessarily large volumes of data being acquired, stored, and managed. Too coarse a resolution results in the loss of information necessary to identify the oil and monitor its movement. SNL's SAR acquired images for this study with 2-m pixel resolution. This resolution was judged to be finer than ultimately required for the oil-spill monitoring task.

The first resolution question, then, was to determine how fine a SAR resolution is necessary for detailed oil-spill image analysis. This determination would define the acuity level of full-resolution imaging that a Coast Guard oil-spill surveillance radar would be required to provide. The best evaluation of resolution would entail reprocessing the raw radar phase returns to form new detected images. This method was beyond the scope of the project; however, validated simulations of resolution degradations (described below) were performed to aid in determining the necessary SAR resolution for oil-spill analysis. Both single-look and multi-look resolution degradations were performed for the data analysis workshops.

A second resolution question related to the real-time presentation of full-swath data to an airborne SAR operator. Analysts at the final workshop needed to determine how to downsample a full-swath SAR image that would be too large to display on a monitor, and to judge how much downsampling should be performed without losing important visual cues that could help the operator identify regions-of-interest for further analysis at full resolution.

1.6.3.1 Evaluation of Methods for Simulating Degraded Image Resolutions

A key issue for this part of the evaluation was the question of how to cost-effectively simulate SAR images at lower resolutions. As mentioned earlier, reprocessing the phase history data to form new images is costly and not feasible given the volume of imagery and the range of resolutions to be evaluated. The overriding goal was to simulate what an operational SAR system (not the SNL research system) could present to the operator and image analyst in near-real time.

The evaluation of degraded resolution imagery began by examining single-look SAR ROI images that were produced at various resolutions by simple subsampling. Subsampling uniformly reduces the number of pixels in an image by retaining only one of every n pixels (both vertically and horizontally) from the original image, where n is the subsampling factor. This concept is illustrated in Figure 1-12. Experience at SNL has shown that simply subsampling pixels in this fashion is a good approximation to phase history downsampling that one would ideally perform on the raw radar returns. Unlike a smoothing or interpolation algorithm, subsampling retains the speckled appearance of the downsampled image and preserves the edge detail in features.

A validation experiment was performed for workshop participants to confirm the integrity of this simulation technique. One single-look ROI was "optimally" downsampled in the phase history domain and a new image was created. This result was then compared with the simulated (subsampled) resolution-degraded image. Figure 1-13 shows the full (2-m pixel) resolution, single-look ROI used in the validation simulation test. Figure 1-14 shows the result of downsampling the phase history and creating a new 10-m pixel resolution image. Figure 1-15 shows the result of simulating 10-m pixel resolution by subsampling the ROI shown in Figure 1-13 by a factor of 5.

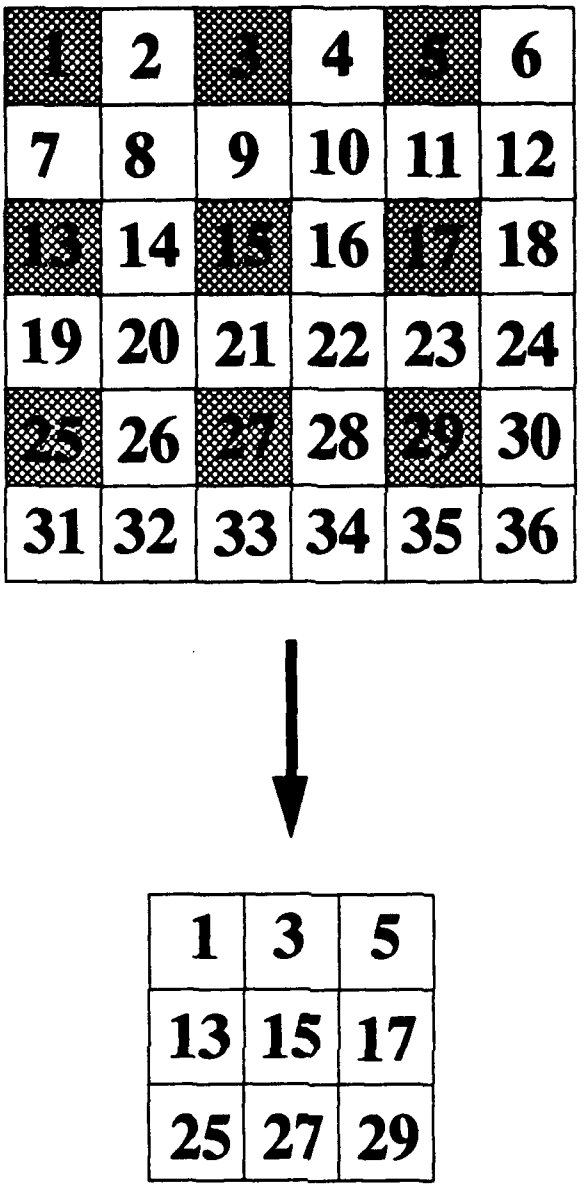

Figure 1-12. The subsampling process. (a) Example of a full-resolution image. Pixel numbers represent locations in the image matrix. (b) Example of downsampled image created by subsampling, in this case by a factor of 2.

(This page intentionally left blank.)

Figure 1-13. Full-resolution ROI. Each pixel represents 2 m.

Figure 1-14. ROI downsampled to 10-m pixel resolution by phase history interpolation.

Figure 1-15. ROI subsampled to 10-m pixel resolution to simulate phase history downsampling.

Note that the principal difference is in the character of the radar speckle, not in the ability to discern features. This simulation was performed by subsampling the full-resolution image, then replicating (repeating) pixels so that the features in the subsampled image are the same size as the full resolution image. Pixel replication allows downsampled images from different resolutions to be compared side-by-side. Pixel replication can result in "blocky" images, but it is a more faithful representation of image content than magnification techniques that invoke smoothing.

After comparing these images, analysts agreed that although the characteristics of the speckle were slightly different, the ability to discern features of interest was similar in both Figure 1-14 and Figure 1-15.

While single-look SAR imagery at a fixed spatial resolution can resolve specific features, the speckled nature of SAR imagery can be distracting to analysts. One could say that the desired acuity is missing. One way of creating a reduced resolution image with better feature definition is to create multi-look images. Multi-look images are created by averaging multiple detected images, all of which were created during one aperture synthesis period. They have a smoother and less speckled appearance, and the improvement is not made at the expense of degrading fine image detail. As with the single-look imagery, a true evaluation of spatial resolution reduction would entail downsampling the multiple raw radar phase histories, forming multiple images, and averaging the images. This was outside the scope of the project. A technique for simulating multi-look, phase history-downsampled images was implemented in the SNL software, but only after a validity check was performed on the same region-of-interest as previously mentioned.

Again, a brief description of how the simulation of reduced resolution multi-look imagery is accomplished is instructive. The concept of adjacent window processing is exploited here. As shown in Figure 1-16, a window of a specific size, say 3 x 3 pixels, is visualized to overlay the upper left 3 x 3 pixel region of an image (input image). The mean (average) intensity of the image within the window is computed and the central pixel of the window is assigned this mean intensity. This intensity is written into the upper-left pixel location in a new image (output image), then the window is moved one *window* (3-pixels in this example) to the right, the mean value computation is repeated, and the result is written to the pixel just right of the previous one in the new image (output image). When an entire row of an image has been processed, the box is moved down one window (3 rows in this example) and the same processing is performed, from left to right. The output pixels will be written to the second row of the new image. This process is continued until all of the input image has been processed. This technique is sometimes called "boxcar" filtering. The resulting output image will be smaller than the input image. In this example, it will be 1/3 the size of the input image. If an output image having features the same size as the input image is required, the output image can be pixel-replicated (by a factor of 3 in our example) to form the desired size output image.

To validate this simulation method for degrading resolution, two new images were created for the same ROI shown previously. These are shown in Figure 1-17 and Figure 1-18. Figure 1-17 shows the 20-meter pixel resolution ROI image formed by phase history downsampling in the "optimal" way to create multiple images that were averaged to form a true multi-look product. Figure 1-18 shows the result of simulating 20-m resolution by "boxcar" filtering the raw image in Figure 1-13 using a 10 x 10 pixel window. As before, pixel replication was performed so that features in the simulated image have the same size as in the full-resolution image. Note that the

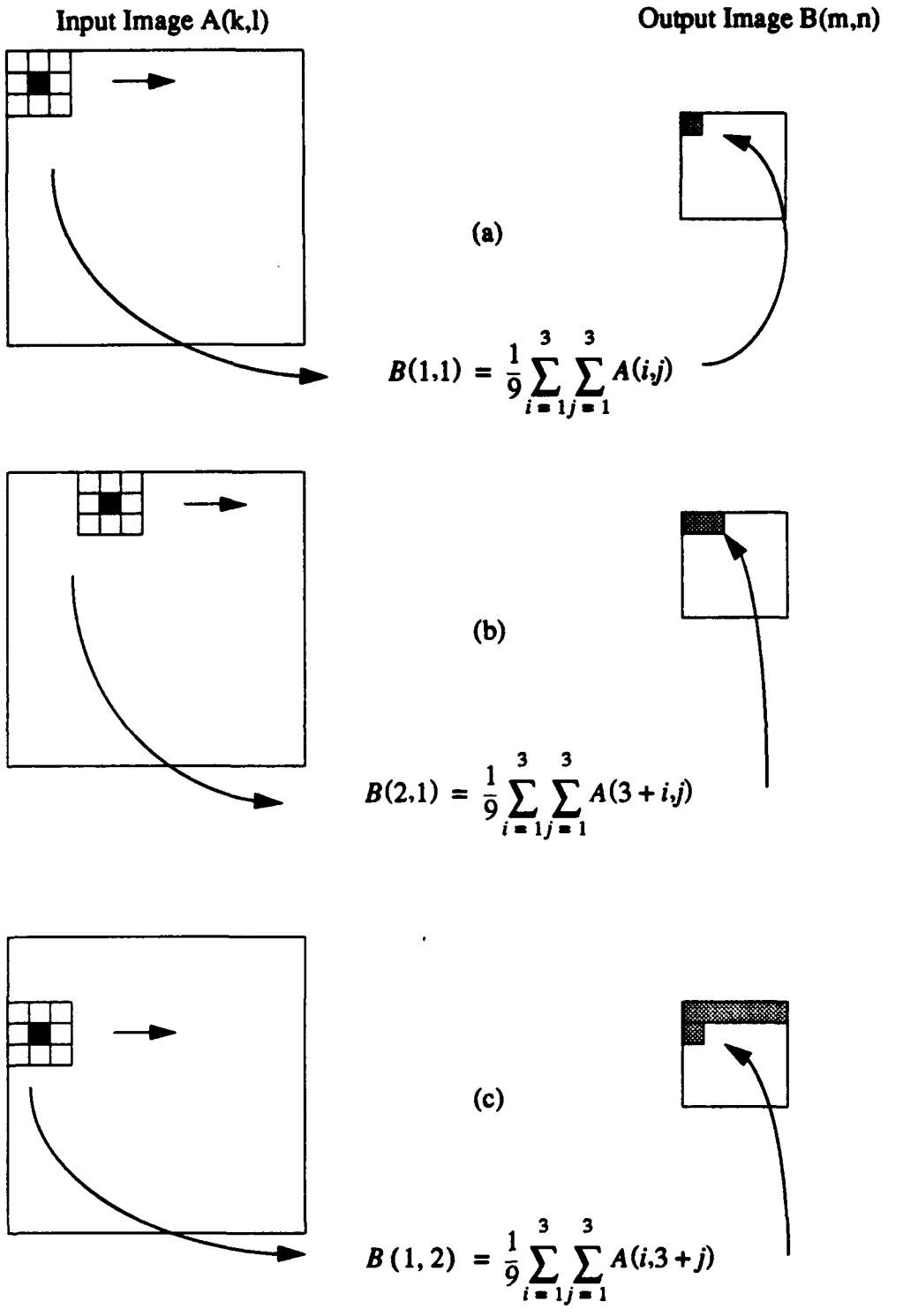

Figure 1-16. Schematic for adjacent window averaging ("boxcar" filtering). (a) Starting in the upper-left corner, computing an output pixel, writing the output pixel. (b) Moving right one window, computing an output pixel, and writing the output pixel. (c) Beginning the process again for the next row of output pixels.

Figure 1-17. Multi-look version of the ROI, downsampled in the phase history domain before noncoherent averaging to 20-m pixel resolution.

Figure 1-18. Simulated multi-look image of ROI at 20-m pixel resolution. Created by adjacent window averaging ("boxcar" filtering) followed by pixel replication.

principal difference is that isolated point scatterers in Figure 1-17 appear slightly dimmer in the Figure 1-18 simulation. Workshop participants agreed that the simulated result portrayed important image features in a manner similar to the optimally-created product. After examining the data processing requirements for a real-time SAR imaging system, SNL determined that simulating the multi-look images would provide a realistic representation of what could be produced in real-time by an operational SAR if not better than 10-m pixel resolution was required. To support the analysis of maximum required SAR resolution, the ROI program was adapted to include an option for performing "boxcar" averaging. The program Swath_vu was also created to permit "boxcar" averaging of full-swath images to support the analysis of full-swath operator display resolution requirements.

1.6.3.2 Method for evaluating Full-Swath Image Resolution Requirements

A SAR with the necessary swath width for oil-spill monitoring could conceivably create full-resolution images that are too large to display on an airborne video monitor. One means of dealing with this problem is to provide to the operator two monitors, or two independent image windows on a single monitor, one showing the full swath at a reduced resolution and one showing a selected ROI at full resolution. A faithful representation of the full scene at a reduced resolution could be used to cue the operator to oil-spill returns, prompting the operator to downlink the surface image to command centers, while a full-resolution view of an ROI could be used for detailed analysis. What is the best means of presenting a faithful representation of the full swath at a reduced resolution?

Experience in other SAR activities at SNL has shown that an adjacent window-averaged, logarithmically-scaled detected image protrays full-swath data at a reduced resolution very well. The oil-spill application of SAR is primarily concerned with imaging ocean scenes as opposed to cultural scenes on land. The range of detected image intensities should be much lower over water than over land; therefore, adjacent window averaging ("boxcar" filtering) of the linearly-scaled (as opposed to logarithmically-scaled) intensities in image mosaics provides an excellent overview of the full-swath data, as demonstrated in the preceding section.

To support the evaluation of full-swath resolution requirements, selected mosaics of the full test area were downsampled to 10-m, 20-m, and 40-m pixel resolutions using the "boxcar" filtering simulation, and were printed for further analysis. These images were not magnified by pixel replication because the objective of the full-swath downsampling was to fit a large-swath SAR image on the operator's monitor. This produced the added benefit of eliminating the adverse effects of pixel replication (i.e. blockiness). Results of the analysis of these images are documented in Section 2.3.2.4 of this report.

1.6.3.3 Method for Evaluating Maximum System Resolution Requirements

The purpose of this evaluation was to determine a design point for the maximum SAR system resolution required to support Coast Guard oil-spill surveillance missions. The resolution of the system should facilitate discrimination of oil slicks from false positivies based on slick edge detail and drift patterns.

To support this analysis, images were produced at 10-, 14- and 20-m pixel resolutions for selected ROIs. ROI images were provided with pixel replication and without pixel replication. The images without pixel replication resulted in smaller images, but the adverse effects of pixel replication did not appear. These images sere sent to the participants of the second working group for review and comment. Results obtained as a result of the analysis by the working group appear in Section 2.3.2 of this report.

1.7 DESCRIPTION OF SAR PARAMETERS ANALYSIS ACTIVITIES

The objective of this part of the project was to arrive at a set of specifications and a design approach for a conceptual Coast Guard SAR for oil-spill monitoring and with an added capability for imaging moving ships in a target area. The approach taken in this study is shown in the flow diagram of Figure 1-19.

1.7.1 Development of Requirements

Using Coast Guard and NOAA inputs, SNL collected and documented conceptual requirements for a Coast Guard SAR capability. Results of this portion of the study are documented in Reference [15](Appendix B).

1.7.2 Calculations and System Specifications

Using (principally) the above-mentioned requirements as input, SNL developed preliminary system specifications for the Coast Guard SAR. This was done using both manual and SAR-design spread-sheet calculations to arrive at numerical values for key radar parameters (pulse length, prf, transmitter power, and so on). When appropriate, calculations were performed parametrically so that the impact on system performance and complexity of changing certain parameters could be determined. For example, design calculations were performed at a number of assumed range/azimuth resolution settings and various assumed antenna sizes.

Results of an early literature search and more recent analyses of November 1992 flight-test data also helped in the development and refinement of system specifications.

1.7.3 Trade-off Studies

For a number of the system parameters (e.g., resolution and antenna size), trade-off studies were conducted to examine options, costs, and benefits. Results of these studies were then fed back to the system definitions.

1.7.4 SAR Capabilities Survey

In order to determine current state-of-the-art capabilities of SAR vendors, SNL conducted a "SAR Capabilities Survey" [16](Appendix C). The survey was sent to twelve vendors, along with a copy of the conceptual requirements document [15](Appendix B). The survey consisted of two parts: a) a request for specific numerical tabulated data on vendor systems, and b) a request for a more free-form textual discussion of the vendor's capabilities as they might relate to meeting Coast Guard requirements. Seven of the twelve vendors responded, each at varying levels of detail. Results of the survey are summarized in Section 2.5.4 of this report.

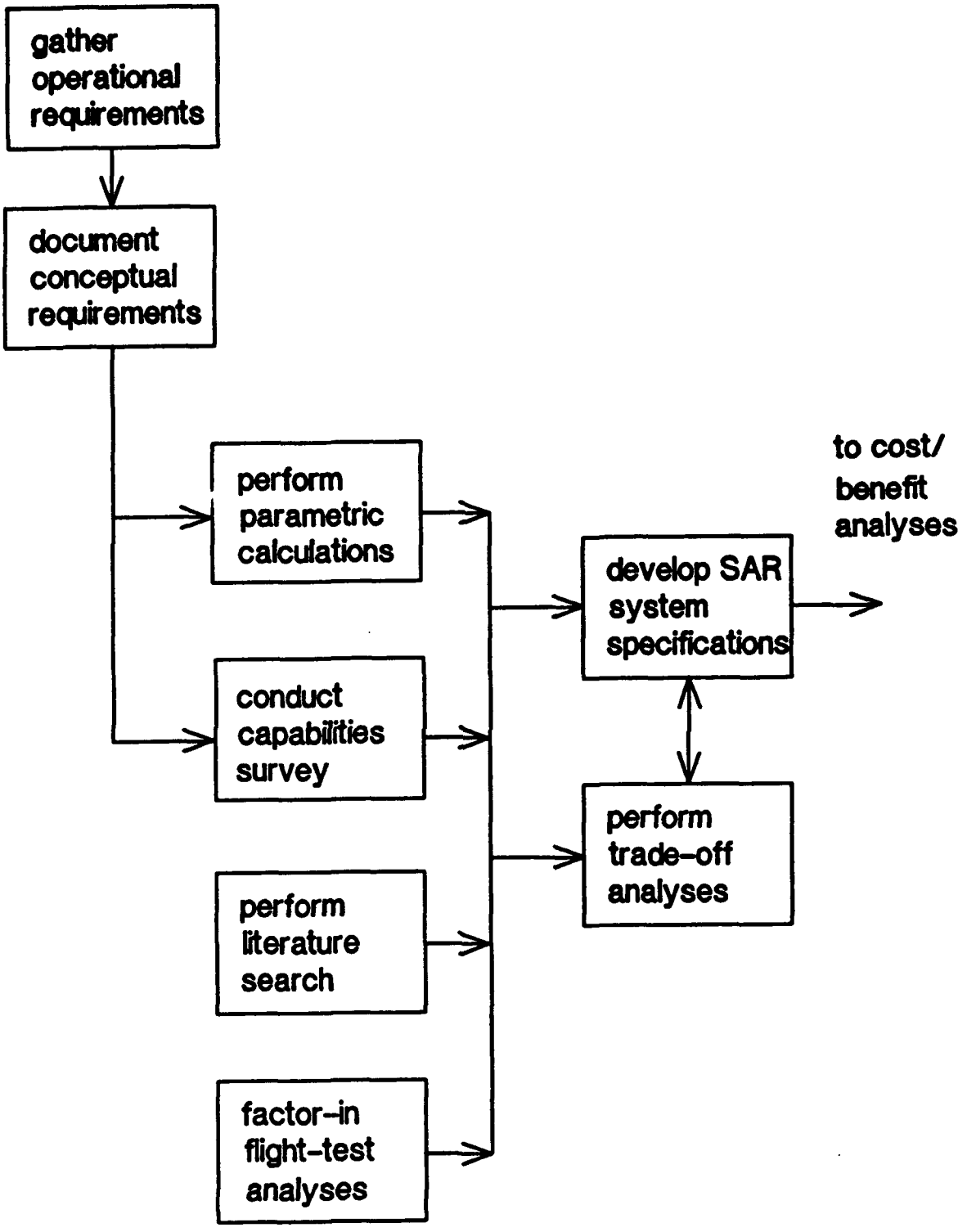

Figure 1-19. Flow of SAR Parameters Analysis Activities.

(This page intentionally left blank.)

CHAPTER 2
EVALUATION RESULTS

2.1 INTRODUCTION

This chapter presents the results of evaluating the SAR and SLAR data obtained during the November 1992, Santa Barbara experiment, identifies important SAR parameters that could affect a Coast Guard-specific SAR design, and discusses the costs and benefits of a SAR system relative to the existing Coast Guard AIREYE SLAR system. The information presented here provides the cornerstone for a mission-tailored system design should the Coast Guard determine that a SAR capability would benefit its operations. The image analysis activities have been performed by a team of experts representing operational and scientific interests in order to assure as unbiased an assessment as possible. Likewise, the expertise of a variety of SAR design and manufacturing firms has been solicited in identifying SAR capabilities that are currently available to be integrated into operational systems. The knowledge obtained from this diverse pool of expertise has been evaluated to objectively identify cost/benefit trade-offs for a SAR system vs. the existing, or slightly modified, Coast Guard SLAR system.

2.2 IMAGE DATABASE

The image data acquired by both the USCG AIREYE SLAR and the SNL SAR are summarized in Table 2-1 and Table 2-2. The test area number listed in the tables can be referenced to the chart shown in Figure 1-6. Any problems in data acquisition are cited, as are the general environmental conditions.

As will be mentioned in the next section, the database was pruned to identify subsets of particular interest for specific analysis tasks. One subset of the data was identified for region-of-interest study by participants during the first data analysis workshop. Table I-1(Appendix I) lists these images. A further subset of this data was identified by participants in the second data analysis workshop to be used in a detailed SAR spatial resolution study. These images are highlighted in Table I-1 with an "*" in the "Date" column heading. Note that in several cases the region-of-interest dimensions were expanded for the resolution study. The expanded dimensions are also marked with an "*".

2.3 IMAGE ANALYSIS RESULTS

The image analysis task began with an image-by-image review of all the SAR and SLAR data acquired during the November flight tests. Participants at the first data analysis workshop (see Section 1.6.2) compared and contrasted SAR and SLAR images with each other and with KS-87 aerial reconnaissance photographs, Agiflite, and other available photographs. The comparison of SAR and SLAR data showed that the best oil and sea returns occurred on the Nov. 12 and Nov. 15 tests. The majority of the analysis activities concentrated on regions-of-interest extracted from data acquired on these days. When features that were of interest to the analysts appeared in both SAR and SLAR scenes, an attempt was made to identify the same features in the available photographs. The USCG R&D Center created very large photomosaics from the KS-87 frames and these mosaics were the primary source of photographic comparison. Voids between

Table 2-1. SAR Data Summary

Date	Test Area[1]	Passes Flown	Comments
Nov. 10	4	north-looking	low wind, some contrast
Nov. 10	4	west-looking	low wind, some contrast
Nov. 11	4	east-looking	calm, low contrast
Nov. 11	4	south-looking	calm, low contrast
Nov. 12	1	west-looking	low wind, good contrast
Nov. 12	1	south-looking	low wind, good contrast, waves visible
Nov. 14	1	south-looking	very, very calm one pass
Nov. 14	1	west-looking	very, very calm
Nov. 15	1	north-looking	calm, some contrast
Nov. 15	1	east-looking	calm, some contrast
Nov. 15	1	south-looking	calm, variable contrast
Nov. 16	1	south-looking	no data
Nov. 16	1	west-looking	no data

1. All SAR passes were flown at an altitude of 10,500 ft.

Table 2-2. SLAR Data Summary

Date	Test Area	Passes Flown	Comments
Nov. 10	4, altitude - 5500 ft	east-looking north-looking west-looking	Low wind, some contrast. Technical problem, data were unrecoverable.
Nov. 10	4, altitude - 9500 ft	east-looking north-looking west-looking	Technical problem, data were unrecoverable.
Nov. 11	4, altitude - 5500 ft	east-looking north-looking west-looking	Calm, low contrast. West-looking data very good.
Nov. 11	4, altitude - 9500 ft	east-looking north-looking west-looking	West-looking shows linear emulsified oil feature.
Nov. 12	1, altitude - 5500 ft	south-looking east-looking west-looking	Low wind. Good contrast. West-looking and south-looking data very good.
Nov. 12	1, altitude - 9500 ft	south-looking east-looking west-looking	South-looking and west-looking data very good.
Nov. 14	1, altitude - 5500 ft	south-looking east-looking west-looking	Very, very calm.
Nov. 14	1, altitude - 9500 ft	south-looking east-looking west-looking	
Nov. 15	1, altitude - 5500 ft	north-looking east-looking west-looking	Calm, but increasing contrast with time. North-looking and west-looking data very good.
Nov. 15	1, altitude - 9500 ft	north-looking east-looking west-looking	North-looking data very good.
Nov. 16	1, altitude - 5500 ft	south-looking east-looking west-looking	Medium wind, very [illegible] contrast. Very good data.
Nov. 16	1, altitude - 9500 ft	south-looking east-looking west-looking	Very good data.

frames and sun glint made some feature identification difficult, but workshop participants were able to correlate many features in both radar and optical images.

Before beginning a discussion of specific issues investigated by the workshop participants, such as speckle smoothing techniques, single-look and multi-look resolution, and operational data presentations, it is helpful to present a brief synopsis of the SAR, SLAR, and photographic data reviewed by the participants. This will give the reader a sense of what can be seen in SAR, SLAR, and photographic data and how differently similar features are portrayed by the various sensors.

A representative set of images (Figure 2-1 through Figure 2-4) comes from the Nov. 15 tests. These images concentrate on the region just offshore (south) from Coal Oil Point where oil is entrained in the near-shore current. Kelp beds are also visible in the SAR and SLAR images. Figure 2-1 is a photograph of the region taken by a crew member aboard the SNL Twin Otter aircraft. Figure 2-2 is a small photomosaic created from several frames of the KS-87 reconnaissance camera aboard the AIREYE. Figure 2-3 is a SAR region-of-interest corresponding to the area of the photographs. Figure 2-4 is a region-of-interest extracted from a SLAR image of the same area. Pixels have been replicated to create this image. All of these images were captured within roughly 30 minutes of each other. Despite differences in illumination wavelength and spatial resolution between the radars and between radar and optical sensors, the same basic structure of the oil can be perceived. In particular, note the ability of the radars to identify the edges of the slicks.

Surface oil can, after a period of time, take on physical properties similar to partially dried latex paint and can entrap flotsam. This drastically changes the radar signature of the oil from being a flat, mirror-like reflector (deflecting the radar signal away from the receiver) to becoming a roughened surface reflector, many parts of which return a significant portion of the incident signal directly back to the antenna. In these cases, the edge of the oil slick appears bright in radar images. Figure 2-5 is a photograph of this type of oil slick extending from below the Holly platform diagonally upward toward Goleta Point. The same feature is visible in both the SAR (see Figure 2-6) and SLAR (see Figure 2-7) images of this area.

The final example shows an extensive oil slick just east of the Holly platform. Figure 2-8 is a photograph of the slick taken from the SNL Twin Otter. Figure 2-9 is a SAR mosaic of the same area. During the final two imaging passes (bottom two mosaic strips), the surface wind picked up enough to provide excellent sea return where the water surface was not damped by oil. The photograph was captured 30 min. before the SAR image, so there is some difference in the oil boundaries.

2.3.1 Results of Speckle Smoothing Evaluation

The three speckle smoothing algorithms described in Section 1.6.2 were applied to the 2-m resolution ROI images listed in Appendix I. The resulting images were analyzed during the second data analysis workshop held June 28 through July 1, 1993, at the USCG R&D Center. The workshop participants, representing the USCG R&D Center, the USCG Air Station Cape Cod, NOAA-HAZMAT, and SNL, examined roughly 250 raw and processed images selected from 32 ROIs. A typical set of data for a region-of-interest included the following:

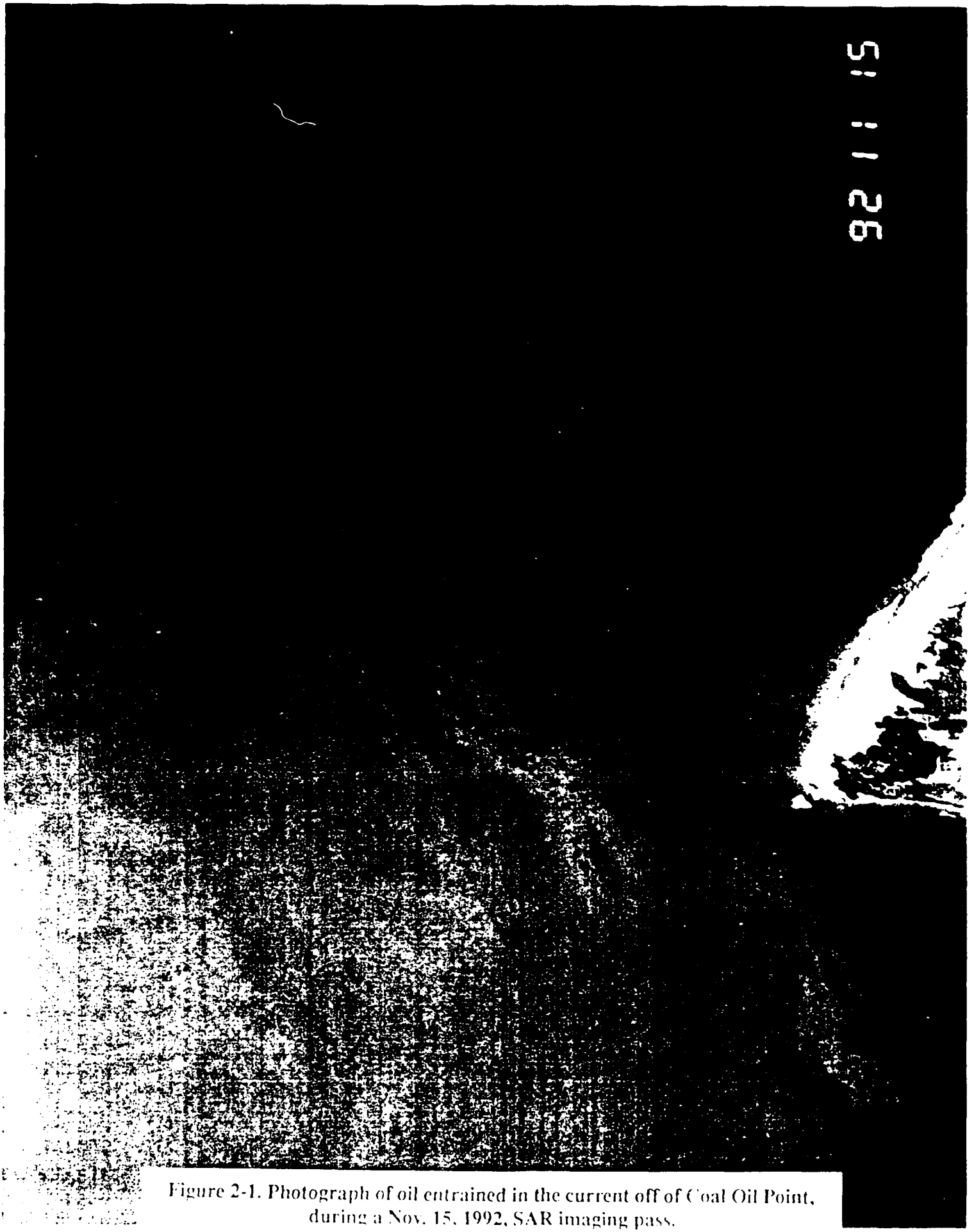

Figure 2-1. Photograph of oil entrained in the current off of Coal Oil Point, during a Nov. 15, 1992, SAR imaging pass.

Figure 2-2. Small photomosaic created from several KS-87 frames captured by the AIREYE off of Coal Oil Point, on Nov. 15, 1992.

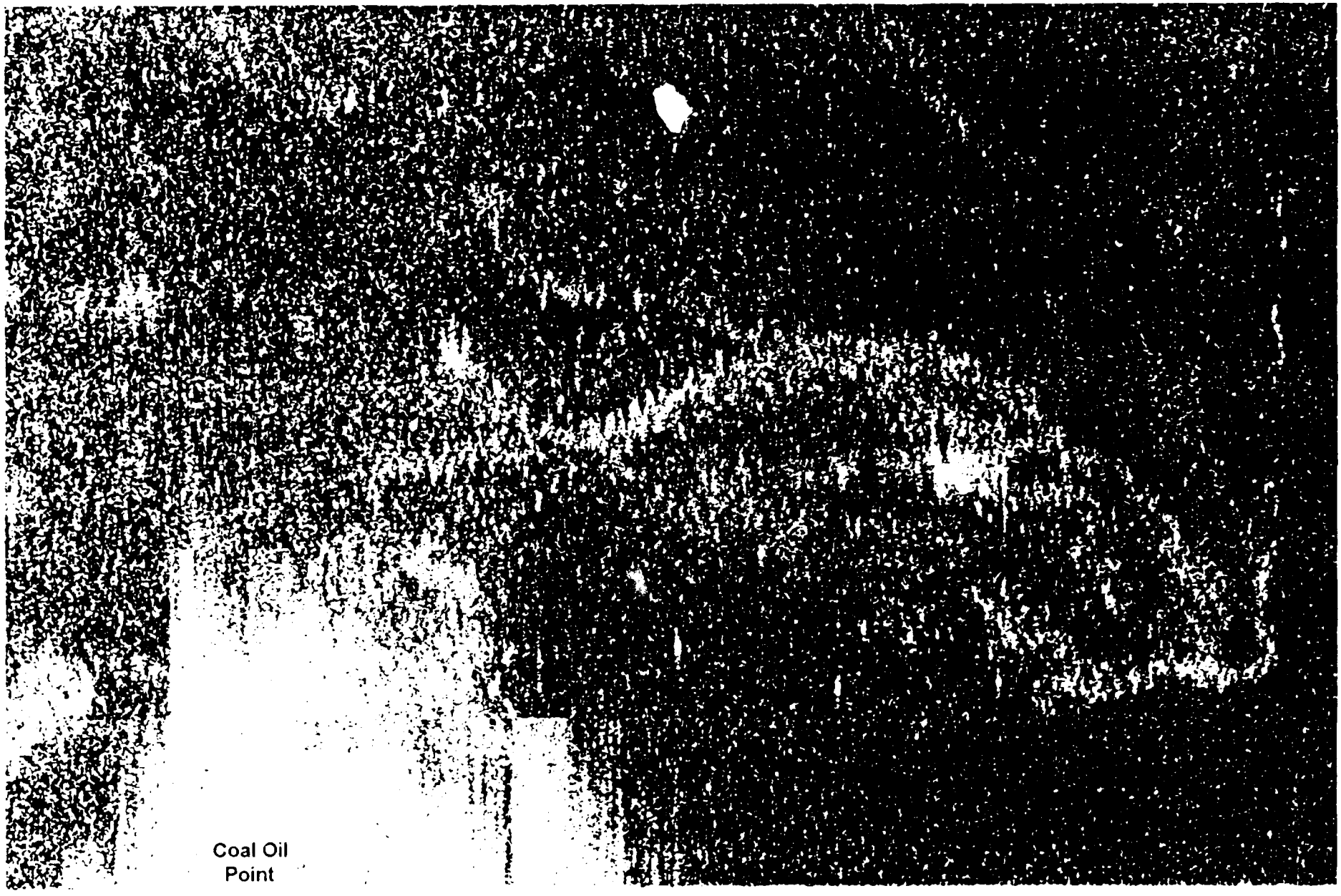

Figure 2-3. 2-m pixel resolution SAR region-of-interest (ROI) image off of Coal Oil Point, captured by the SNL SAR on Nov. 15, 1992.

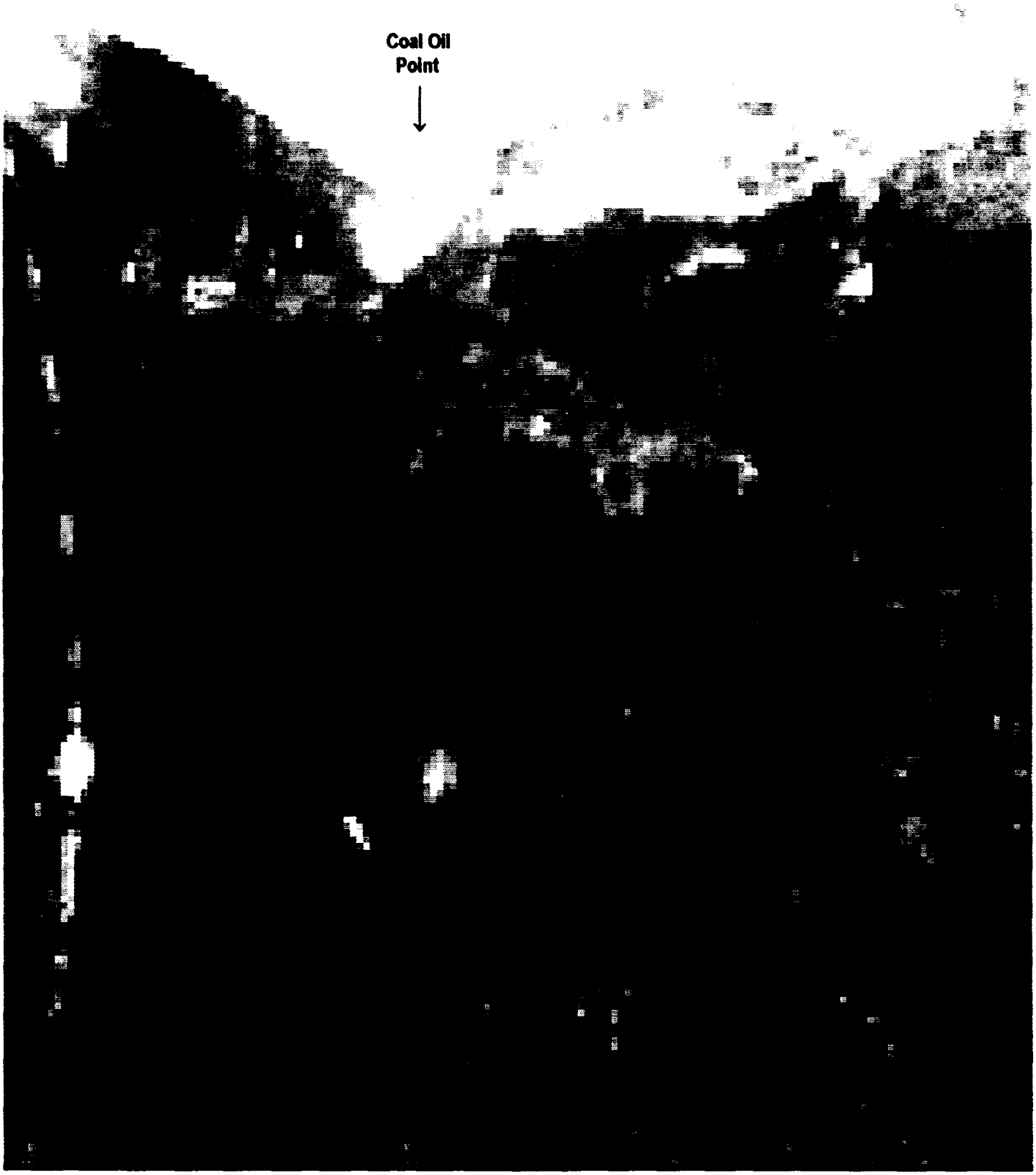

Figure 2-4. SLAR ROI just off of Coal Oil Point, captured by the AIREYE SLAR on Nov. 15, 1992.

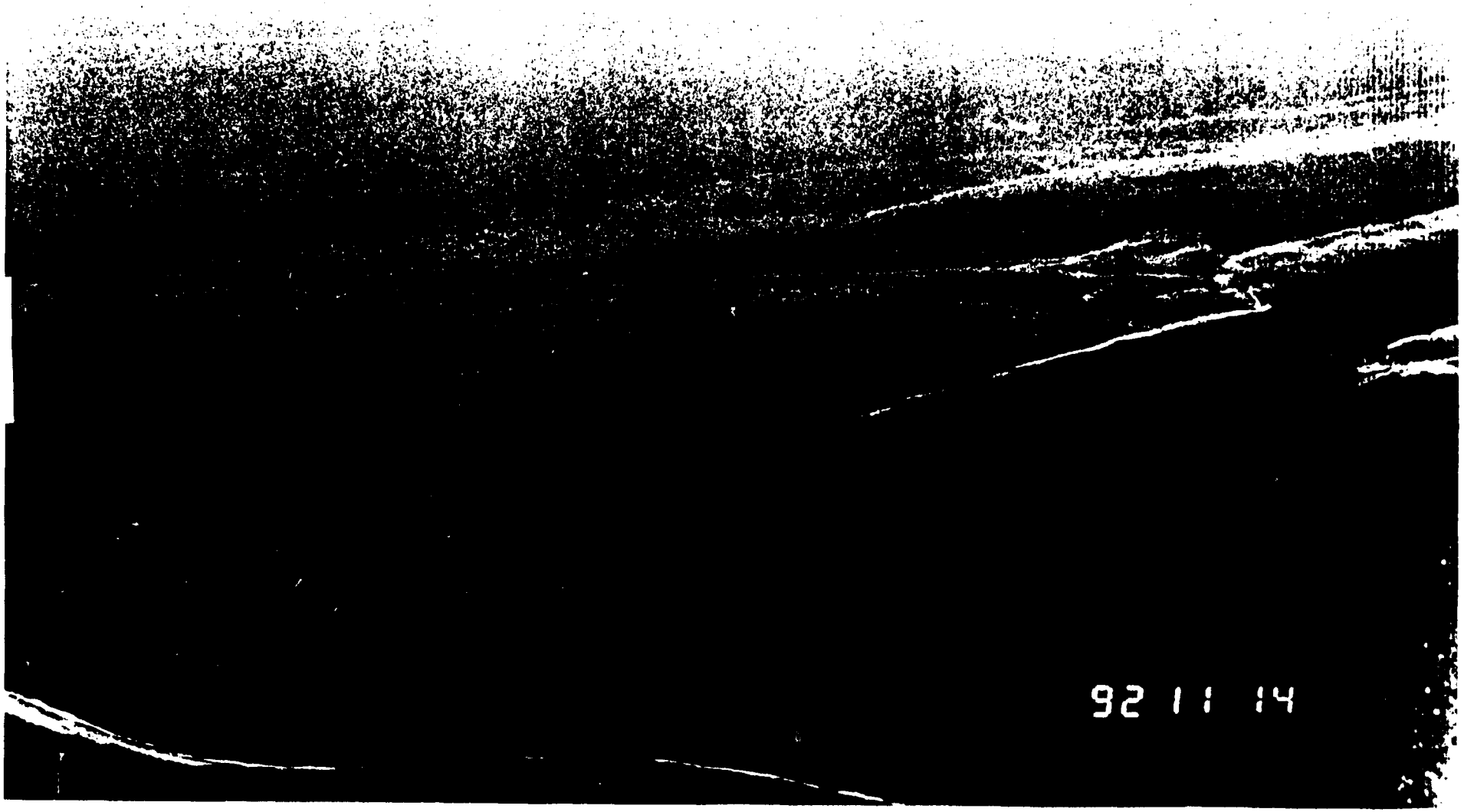

Figure 2-5. Photograph of oil slick extending from below the Holly platform diagonally toward Coal Oil Point, Nov. 14, 1992.

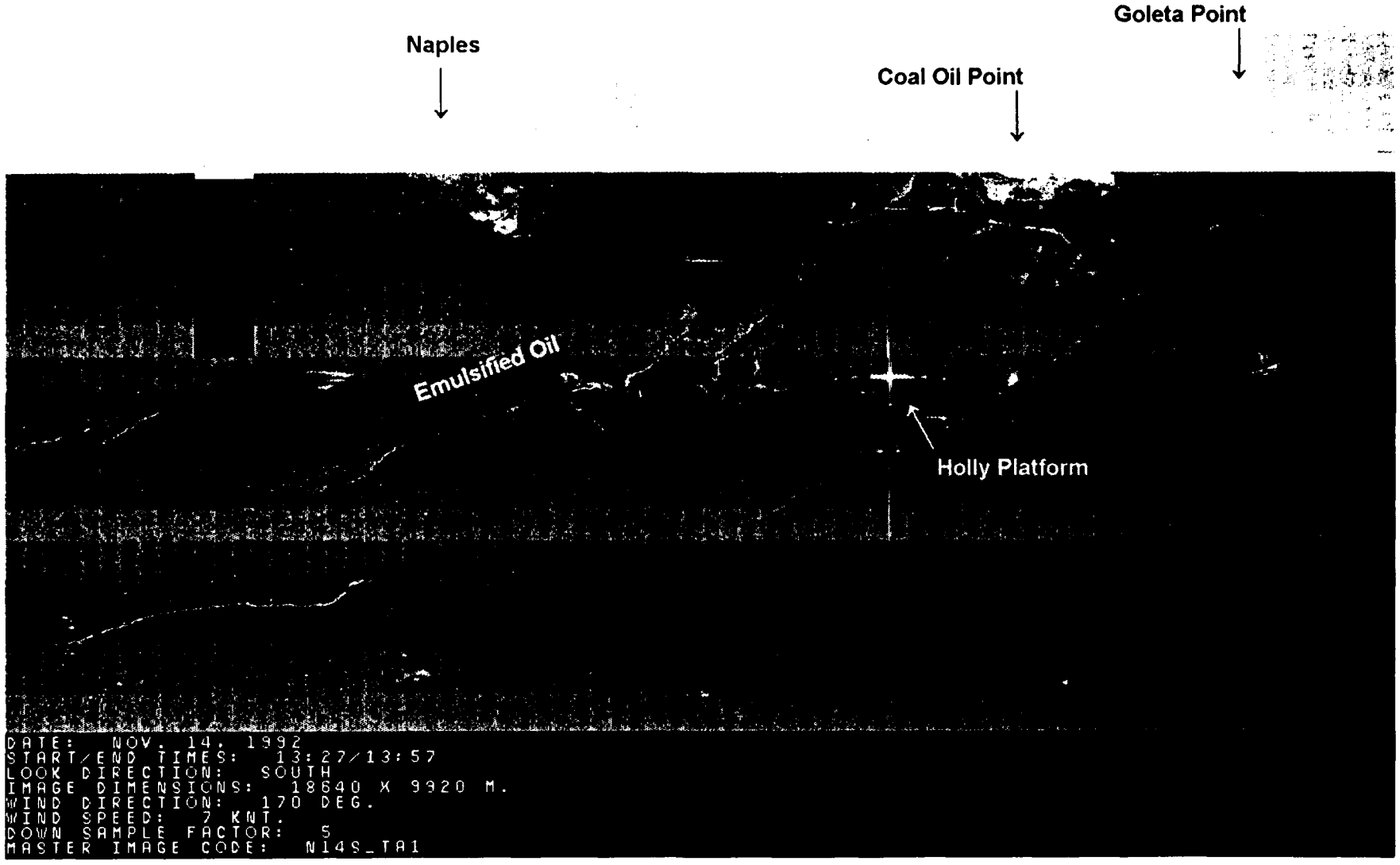

Figure 2-6. SAR image of oil slick seen in Figure 2-5.

Figure 2-7. *SLAR image of oil slick seen in Figure 2-5. Magnified by* **pixel replication. The contrast has been stretched to highlight the slick.**

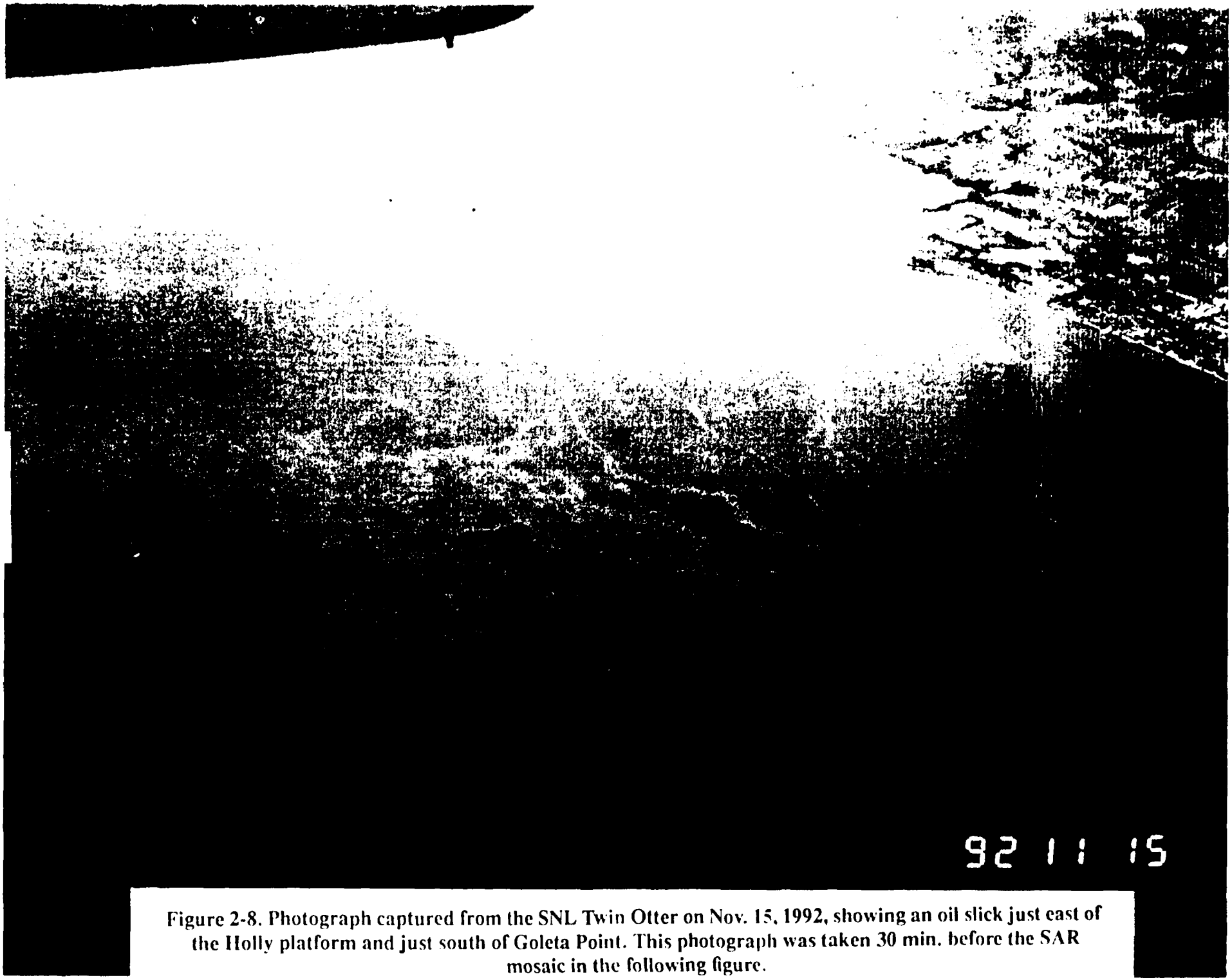

Figure 2-8. Photograph captured from the SNL Twin Otter on Nov. 15, 1992, showing an oil slick just east of the Holly platform and just south of Goleta Point. This photograph was taken 30 min. before the SAR mosaic in the following figure.

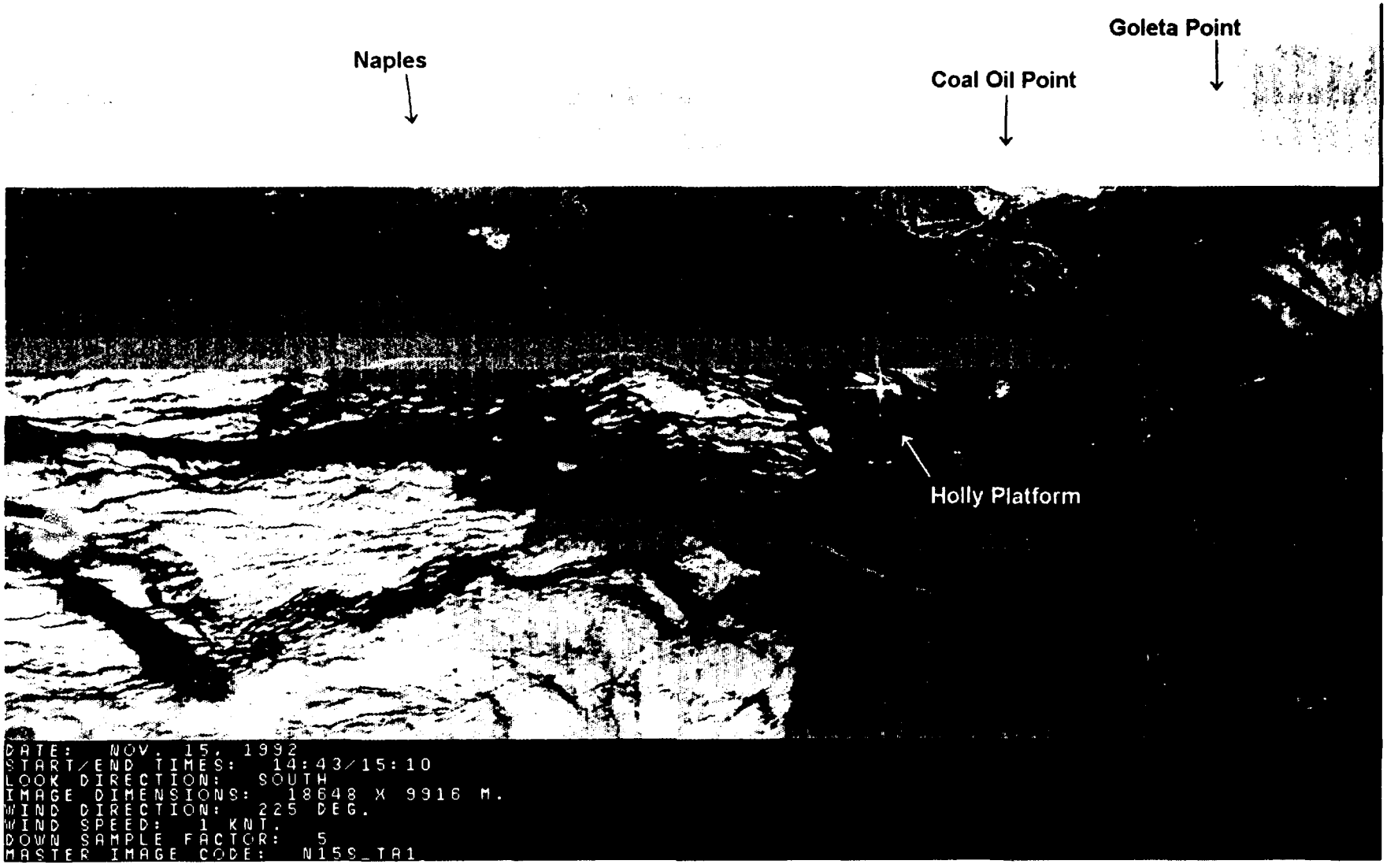

Figure 2-9. SAR mosaic of oil slick seen in Figure 2-8, but imaged 30 min. after the photograph. The oil has moved. Surface winds increased during the final two passes of this mosaic to give good oil/water boundaries.

1. Raw image file.

2. Sliding window average, 3 x 3 pixel window.

3. Sliding window average, 5 x 5 pixel window.

4. Sliding window median, 3 x 3 pixel window.

5. Sliding window median, 5 x 5 window.

6. Crimmins morphological filter, 1 iteration of 3 x 3 pixel window.

7. Crimmins morphological filter, 2 successive iterations of 3 x 3 pixel window.

8. Crimmins morphological filter, 3 successive iterations of 3 x 3 pixel window.

Figure 2-10 through Figure 2-14 show some of the results selected from the list above for one region-of-interest.

Speckle smoothing reduces the objectionable effect of coherent speckle in radar images, but it does so at the expense of visual acuity. This is most obvious in the sliding window average example, Figure 2-11. The averaging process not only smooths speckle, it also smooths edges. The edges at the oil/water interface in Figure 2-11 (central box) are smoothed to such a degree that workshop participants felt important detail that can occasionally be used to characterize petroleum oil, as opposed to plant or animal oils, were lost. Notice also that point-like specular reflectors (upper box in Figure 2-11) appear to be smeared as a result of sliding window averaging. Median filtering is an alternative to the edge-smoothing criticism of average filtering. By replacing the central pixel of the sliding window with the median, speckle is reduced since speckle is characterized by exceedingly bright or dark single pixels within the window. The advantage of the median over the average is that edge contrast is better maintained. Edge intensities tend to have gray s[illegible] closer to median intensities within the window than do speckle intensities, hence, edge [illegible]reserved. This benefit is easily observed by comparing the oil/water interfaces in Figure 2-[illegible] and Figure 2-12 (central boxes). A radical departure from either average or median filtering is the Crimmins morphological filter. The Crimmins filter attempts to find and reduce the intensity of isolated bright scatterers (or, alternately, to find and increase the intensity of isolated dark pixels). By attempting to alter only speckle pixels, edges are preserved. A comparison of the Crimmins-filtered image (Figure 2-13) with the average- and median-filtered results (Figure 2-11 and Figure 2-12) shows that sea returns are smoothed less (central box) and isolated scatterers retain their structure (upper box).

Any type of speckle filtering has the distinct disadvantage of destroying information. No matter how the filtering algorithm is tailored, it is impossible to distinguish speckle pixels from other pixels. As a result, potentially important information is lost at the same time that speckle is reduced. It is generally not a good idea to incorporate a process that destroys information into the data acquisition and image formation process. It is better to reserve speckle smoothing as a post-processing step to be invoked only when required.

(This page intentionally left blank.)

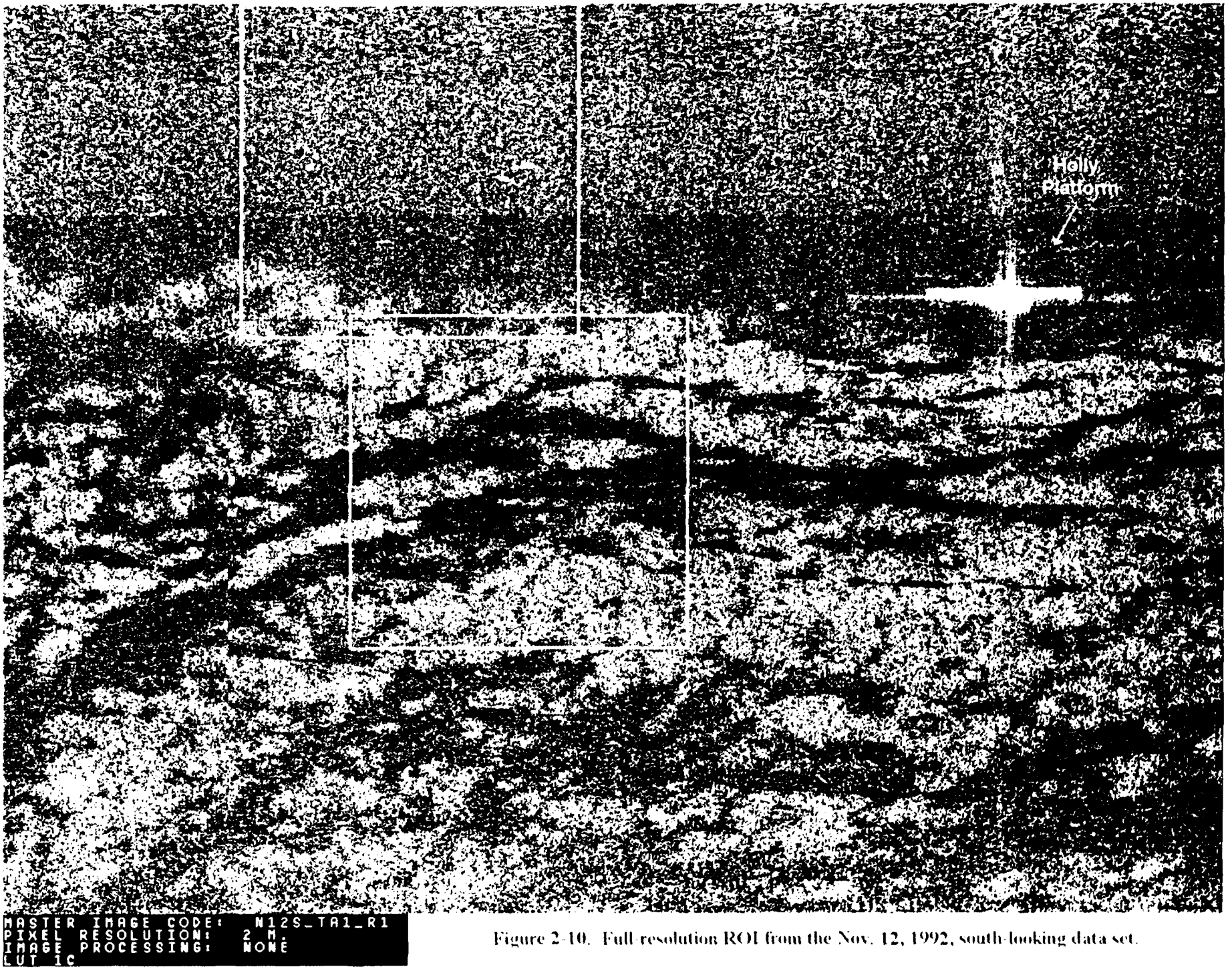

Figure 2-10. Full-resolution ROI from the Nov. 12, 1992, south-looking data set.

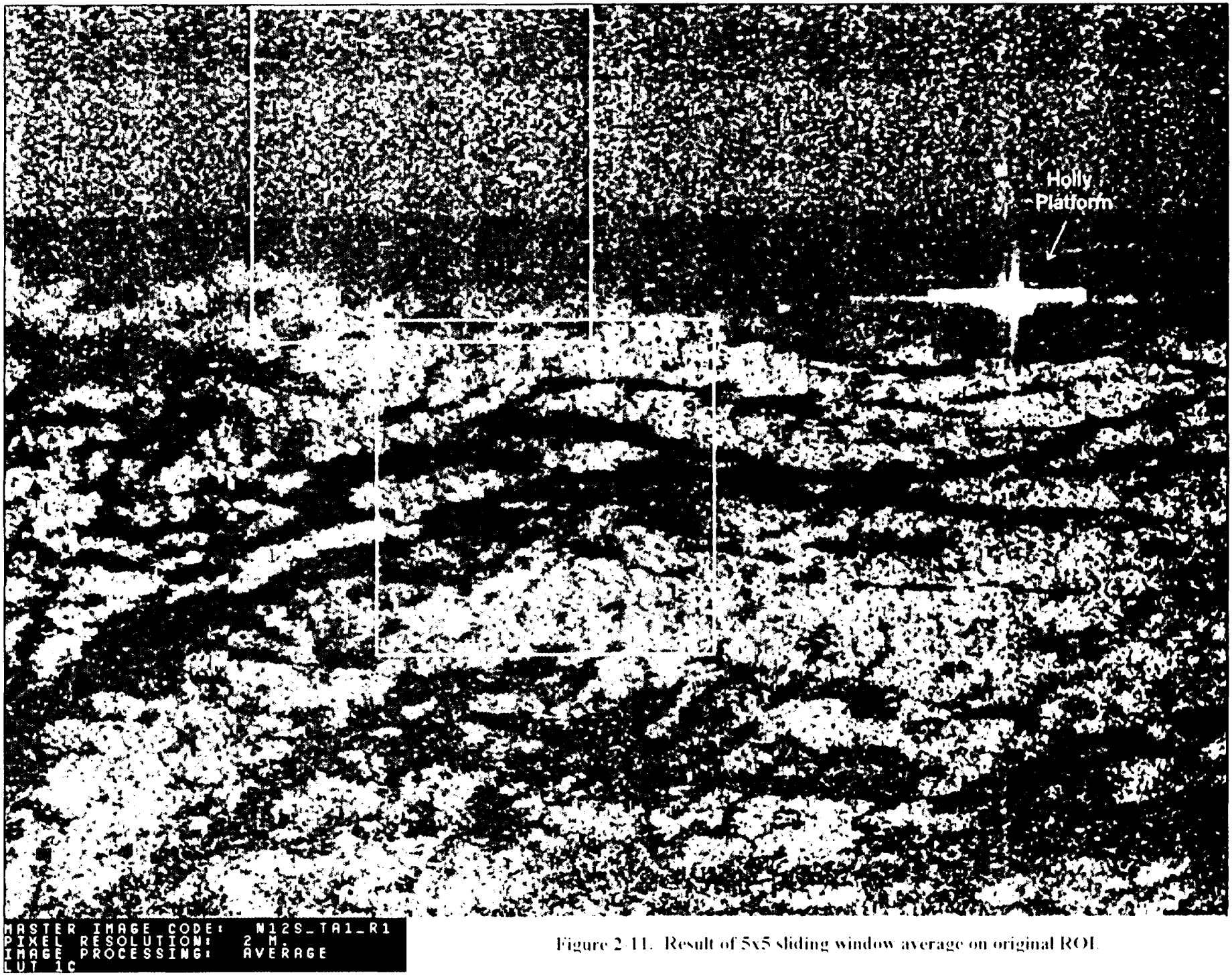

Figure 2-11. Result of 5x5 sliding window average on original ROI.

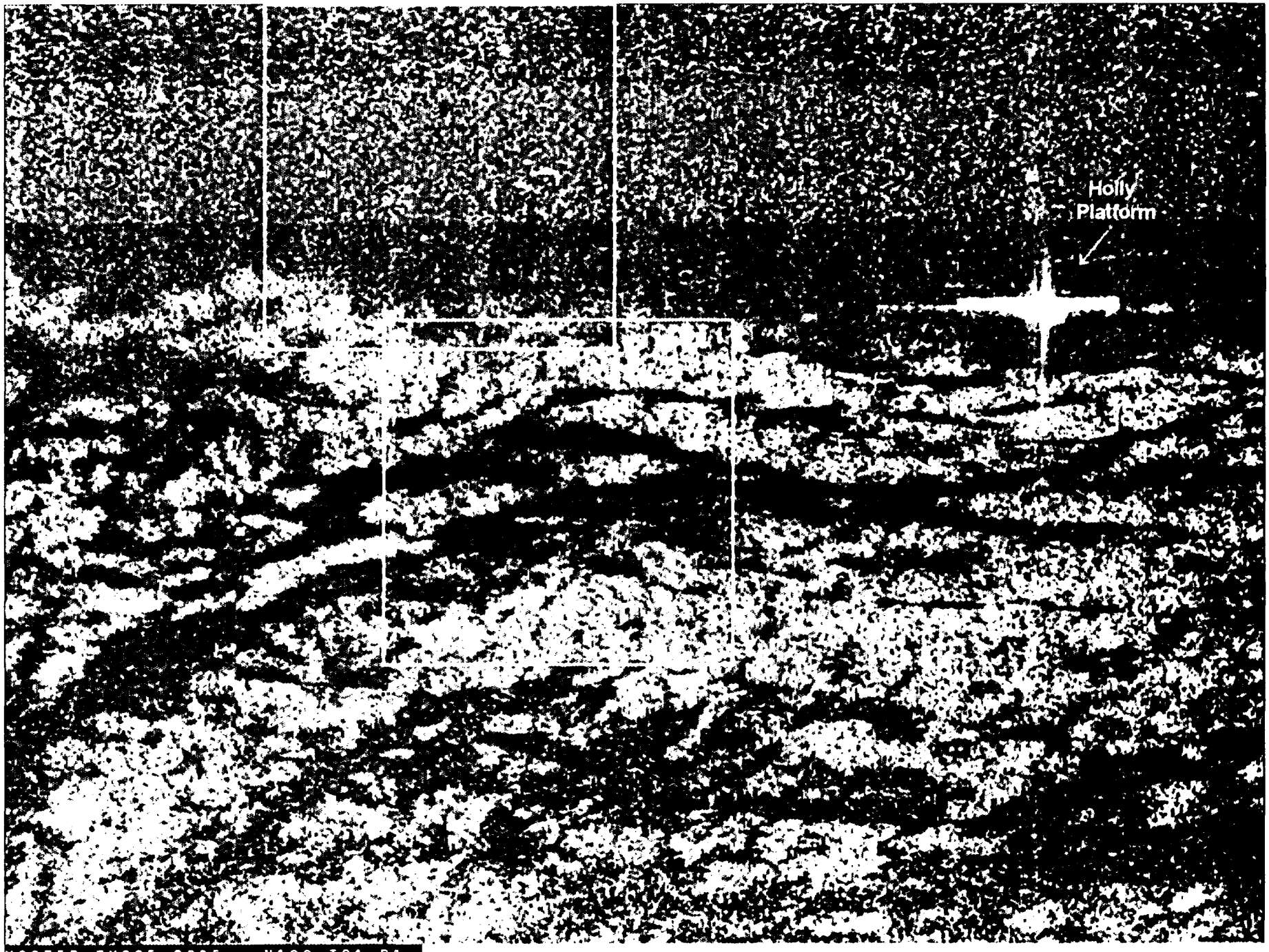

Figure 2-12. Result of 5x5 sliding window median on original ROI.

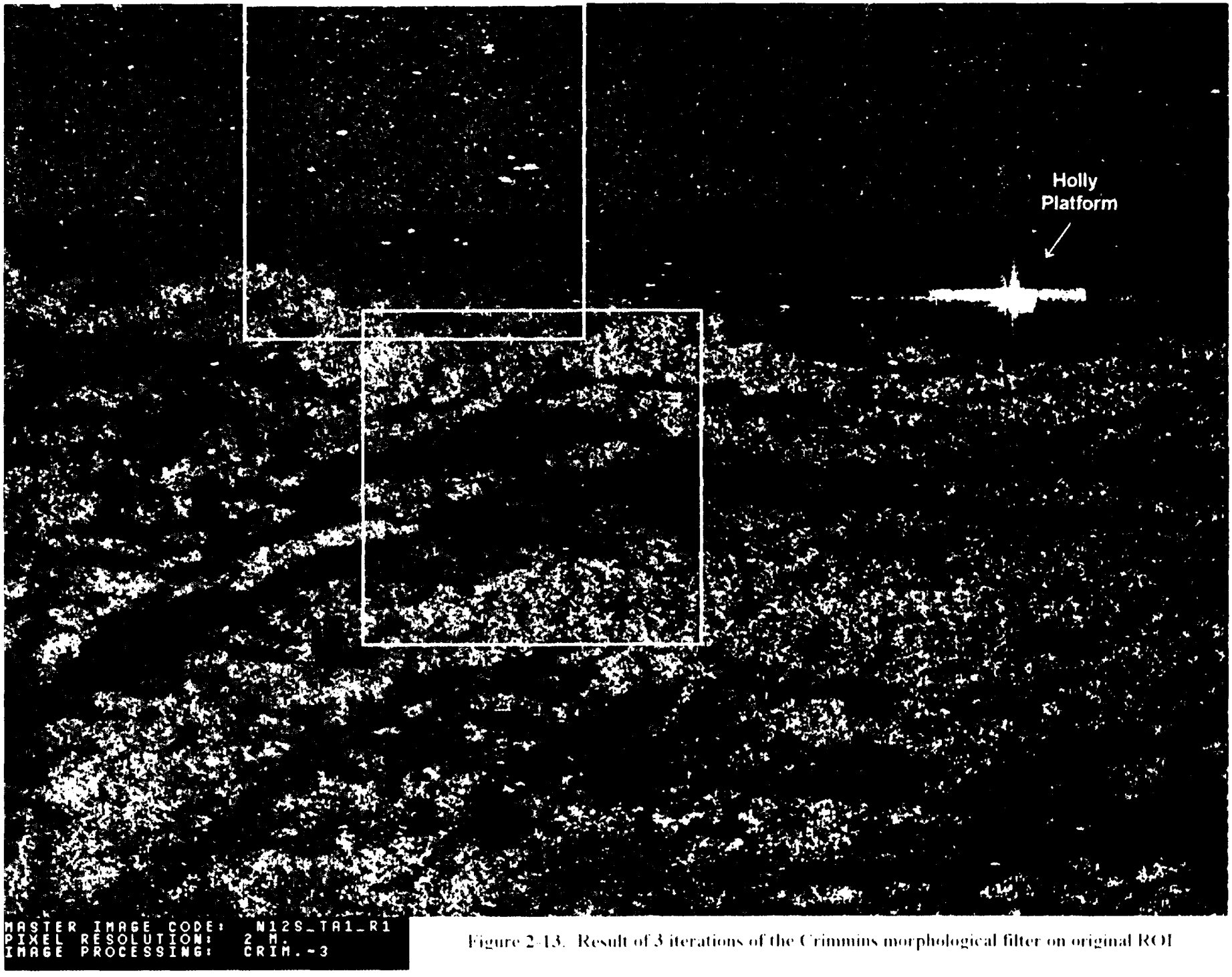

Figure 2-13. Result of 3 iterations of the Crimmins morphological filter on original ROI

The consensus of the workshop participants was that speckle smoothing should not be included as a part of an on-board SAR processor. The majority of the SAR images resulting from the Santa Barbara experiment were of a high enough quality that any type of speckle smoothing resulted in a poorer quality product than the original. A similar performance is expected in an operational SAR for oil-spill reconnaissance. The workshop participants did, however, recognize that there could be situations where ground-based post-processing of regions-of-interest would be appropriate. Any ground-based exploitation system for detailed analysis of images should include speckle smoothing capabilities. The participants recommend the median or the Crimmins morphological filter (or both). The mean filter smooths edge detail to too great a degree.

2.3.2 Results of SAR Resolution Study

The same workshop participants that evaluated the speckle smoothing filters also investigated the selection of the "optimal" SAR resolution. As explained in Chapter 1, the analysis of required SAR resolution addressed three issues:

1. Single-look versus multi-look processing
2. Required maximum system resolution
3. Required full-swath display resolution.

The maximum system resolution study determined the finest spatial resolution required for discerning subtle image features within an ROI that are necessary for identifying oil spills. This was the primary study. The full-swath resolution study attempted to identify the amount and type of downsampling necessary to reasonably present full swath imagery to the system operator. This study was necessary because the display hardware cannot present a full swath of data that was originally acquired with the same resolution required for ROI analysis. Because the operational data presentation study depended upon the results of the ROI study, the data presentation study was secondary.

2.3.2.1 Single-look vs. Multi-look Processing

A subset of the 32 raw regions-of-interest used in the speckle smoothing study was used in the resolution study. Simulated resolution degradation was performed by subsampling and pixel replicating some of the 32 single-look ROI images to create 10-m, 20-m, and 40-m pixel resolution products. While examining the region-of-interest shown in Figure 2-14 through Figure 2-17, several participants commented that 10-m pixel resolution was quite adequate for identifying subtle image features, but that fine detail was obscured by image speckle. (See oval-shaped return in center of image that is crossed by thin oil streaks.) Rather than sacrifice acuity by performing a speckle smoothing operation, the participants investigated the possibility of exploiting multi-look processing. As explained in Section 1.6.3.1, multi-look processing results from averaging multiple independent looks at a common scene which were gathered at the same time. The averaging process reduces the effect of speckle (improves acuity) while preserving the pixel resolution of single-look imagery. Workshop participants judged the multi-look imagery to be superior to single-look imagery at the same spatial resolution. The decision was made to recommend multi-look imaging for any future Coast Guard SAR.

2.3.2.2 Maximum System Resolution Requirement

As stated in Chapter 1, reprocessing all of the raw SAR data from the experiment to create multi-look images was beyond the scope of the project, so a high-quality simulation of multi-look images was performed by post-processing the existing single-look data. A reduced set of ROIs was identified by the participants for this processing to support a detailed analysis of the required Coast Guard system maximum resolution. These regions are listed with a "*" in Appendix I. Downsampled pixel resolutions of 10-m, 14-m, and 20-m were presented for the regions in Appendix I marked with an "*".

A representative set of simulated multi-look ROIs is presented in Figure 2-14 through Figure 2-17. Figure 2-14 shows the ROI at full resolution (2-m pixel). Figure 2-15 shows the same ROI after a 5 x 5 "boxcar" filtering followed by pixel replication, as discussed in Section 1.6.2. This figure simulates 10-m multi-look imagery. Figure 2-16 shows the result of 7 x 7 "boxcar" filtering to simulate 14-m multi-look imagery. Finally, Figure 2-17 shows the result of 10 x 10 "boxcar" filtering to simulate 20-m multi-look imagery. When comparing the images, attention is directed to detail in the emulsified oil (brightened linear return) entrained near the kelp bed below and left of the point of land. Attention is also directed to the water/oil interface near the bright point scatterer in the lower left of the image, which is the Holly oil platform, and to the natural gas upwelling in the lower right corner of the image. The loss of fine detail with degradation in resolution is obvious.

Pixel replication was used to create downsampled images having the same size as the full resolution image, but this can create an objectionable "blocky" appearance in the downsampled images. This is especially true for the 20-m pixel images. Several workshop participants were concerned about this artifact, so some of the ROIs were downsampled and printed without pixel replication. This resulted in substantially smaller images. These smaller images were examined with optical loupes to verify that important features could be visualized at reduced resolutions.

Workshop participants studied the reduced resolution multi-look simulated images independently and reported their conclusions. A few of the participants were willing to accept 14-m pixel resolution, but all agreed that 10-m resolution was preferred. The consensus of the group was that 10-m multi-look images were preferred for ROI analysis.

2.3.2.3 Other Resolution Issues

An important issue arose during the resolution study regarding SAR imaging look directions. There can be a distinct difference in perceived resolution of SAR images of the same scene when looking across wave crests (up-wind or down-wind) and along wave crests (cross-wind). This difference is evident when comparing Figure 2-18 (looking across the wave crests, up-wind/down-wind) and Figure 1-13 (looking along the wave crests, cross-wind). The poorer acuity in Figure 2-18 is due to the radial motion of waves along the antenna look direction. This creates a doppler signal that is interpreted by the SAR as a change in the horizontal location of the waves in the image. (See Section 1.3.2 and Section 2.4.2 for further discussions.) This look direction anomaly is not tied to resolution. Higher spatial resolutions, however, provide more information and higher acuity to the analyst even in the presence of motion degradation.

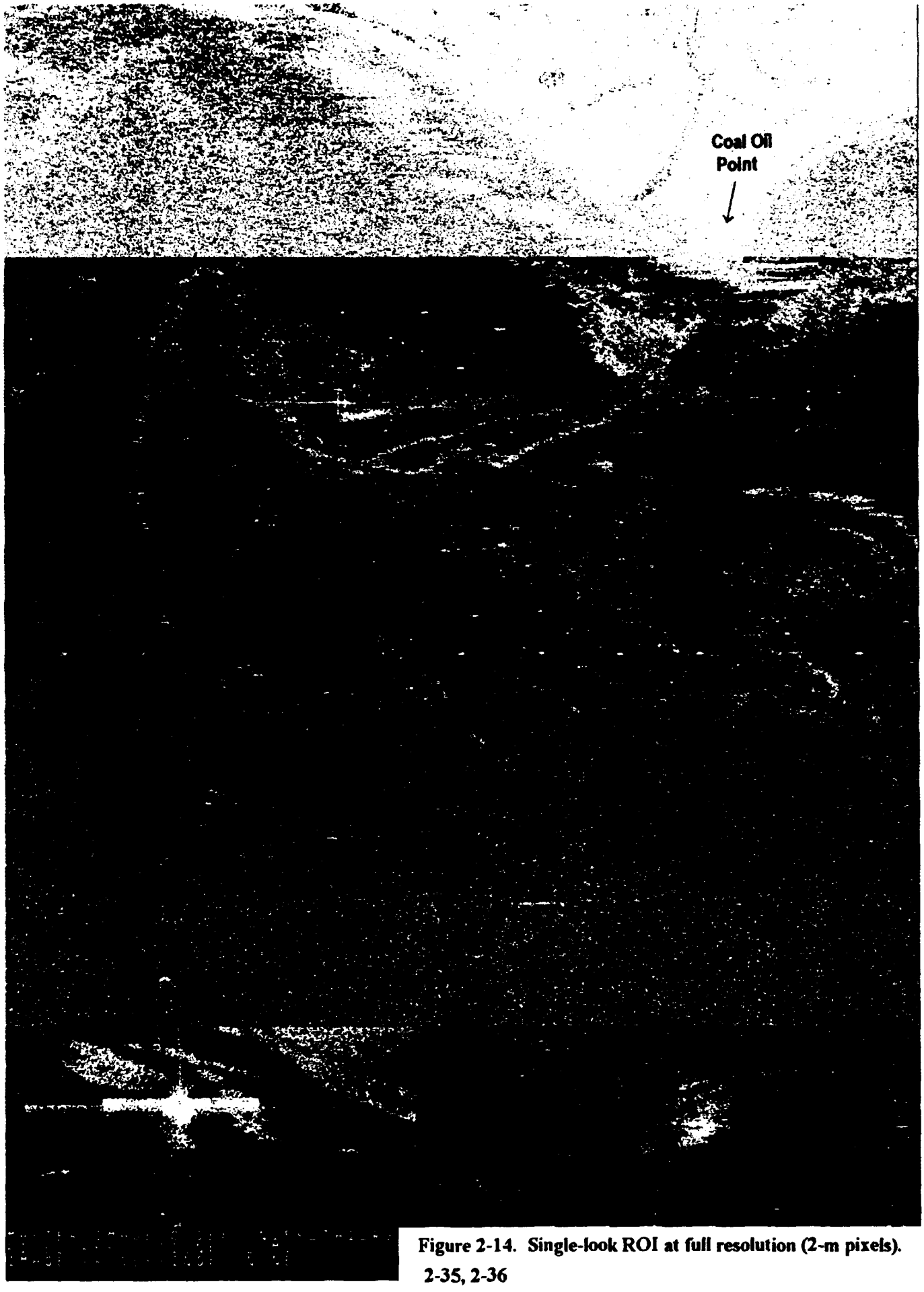

Figure 2-14. Single-look ROI at full resolution (2-m pixels).

2-35, 2-36

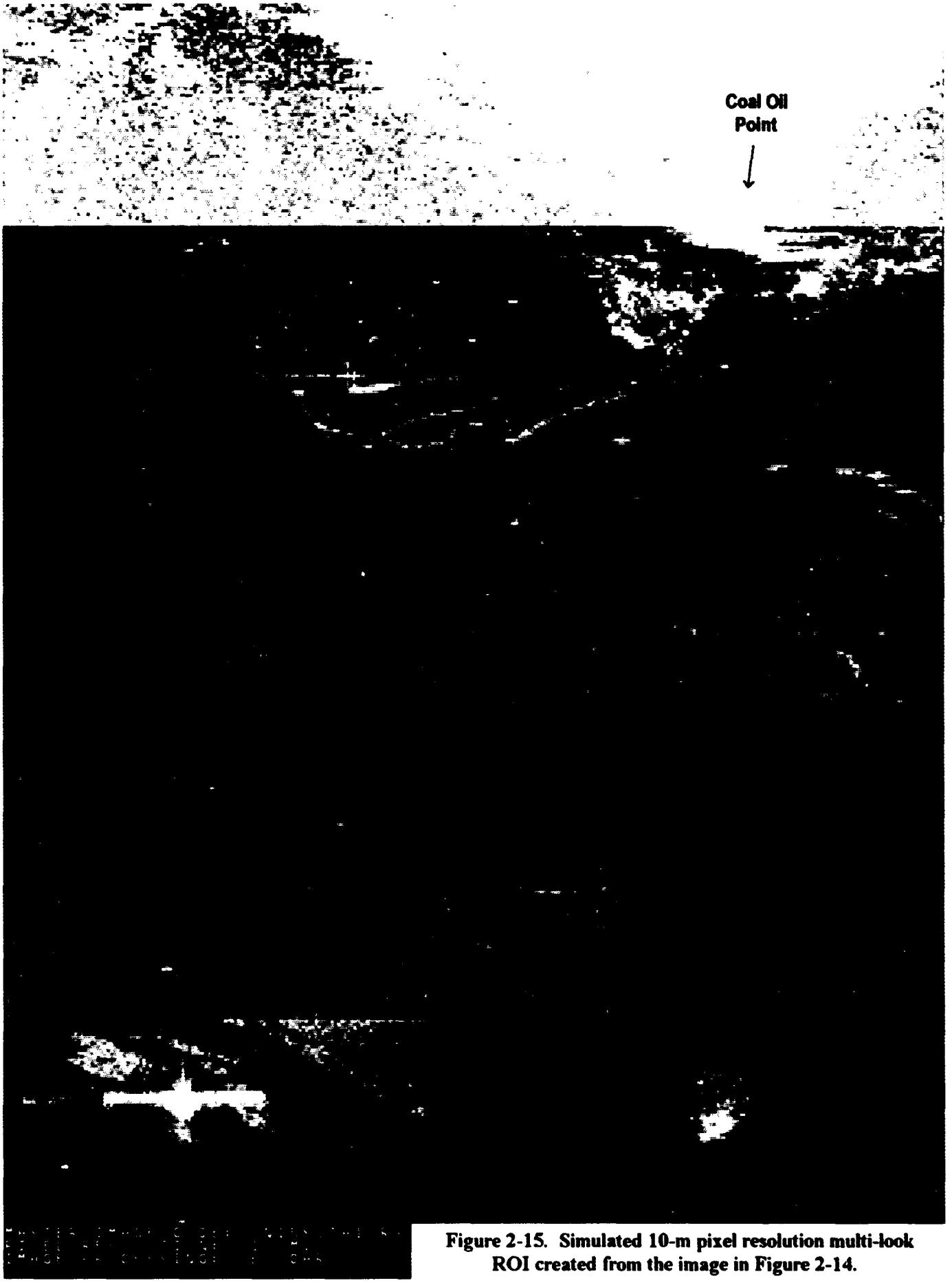

Figure 2-15. Simulated 10-m pixel resolution multi-look ROI created from the image in Figure 2-14.

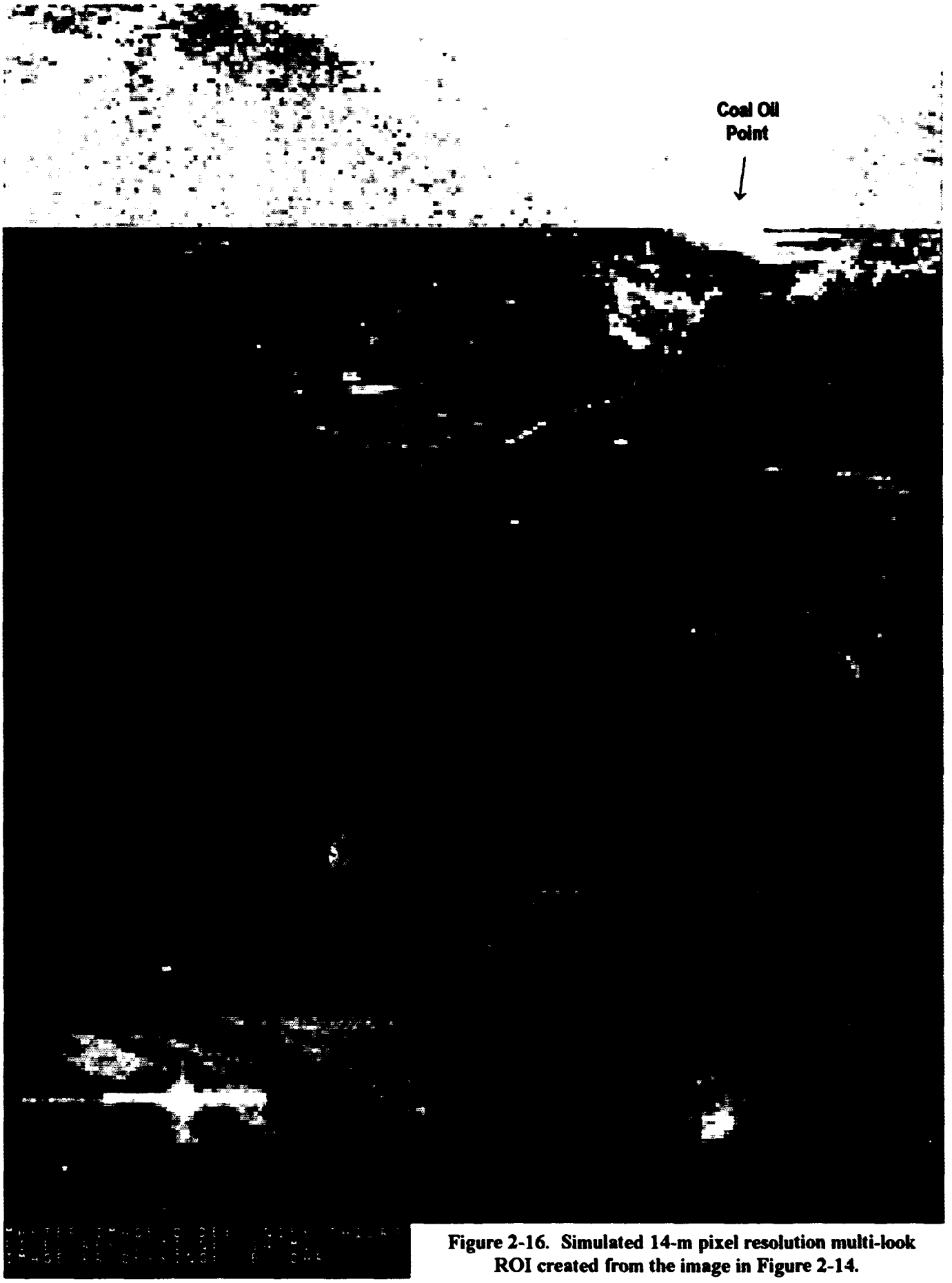

Figure 2-16. Simulated 14-m pixel resolution multi-look ROI created from the image in Figure 2-14.

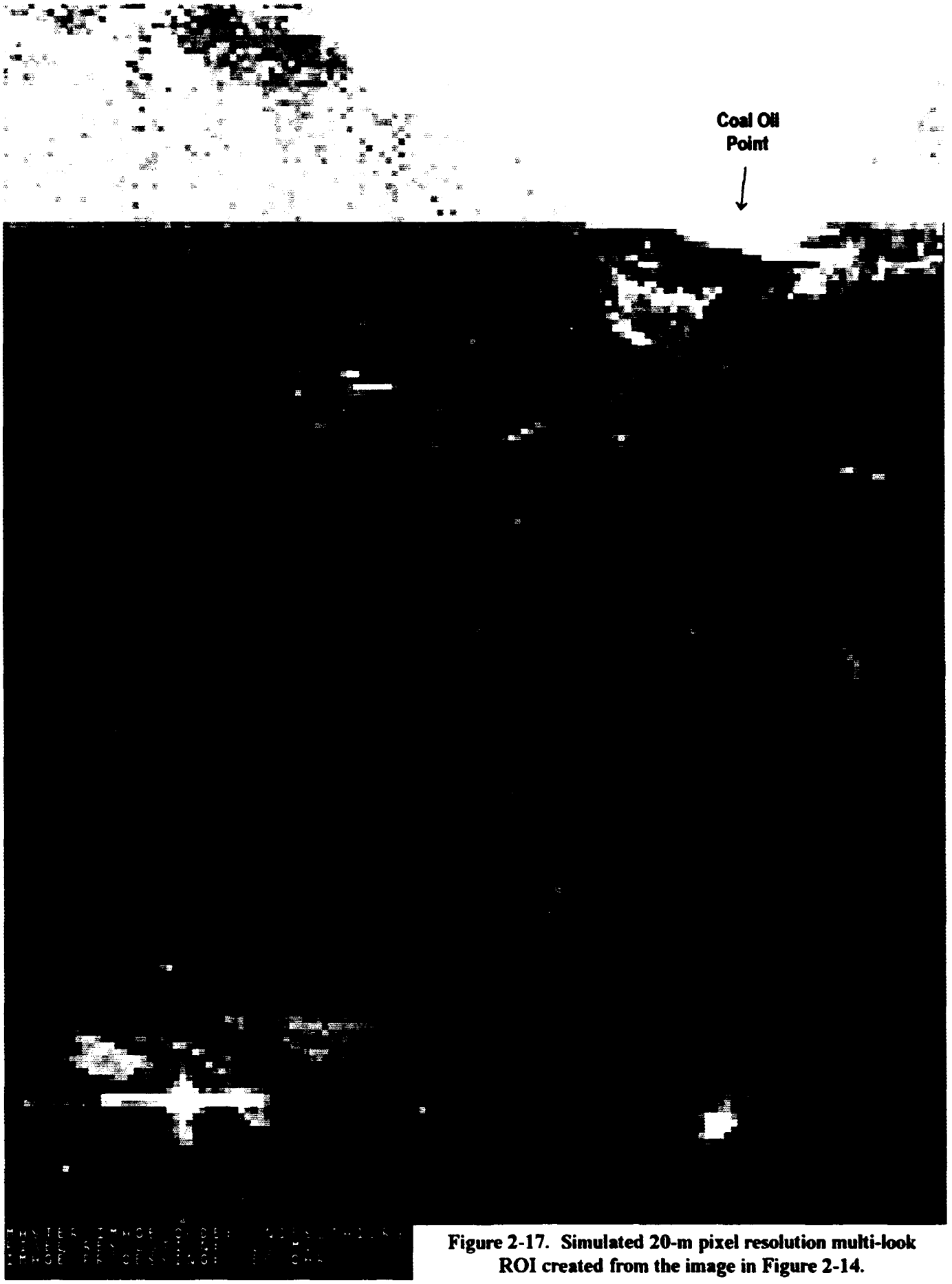

Figure 2-17. Simulated 20-m pixel resolution multi-look ROI created from the image in Figure 2-14.

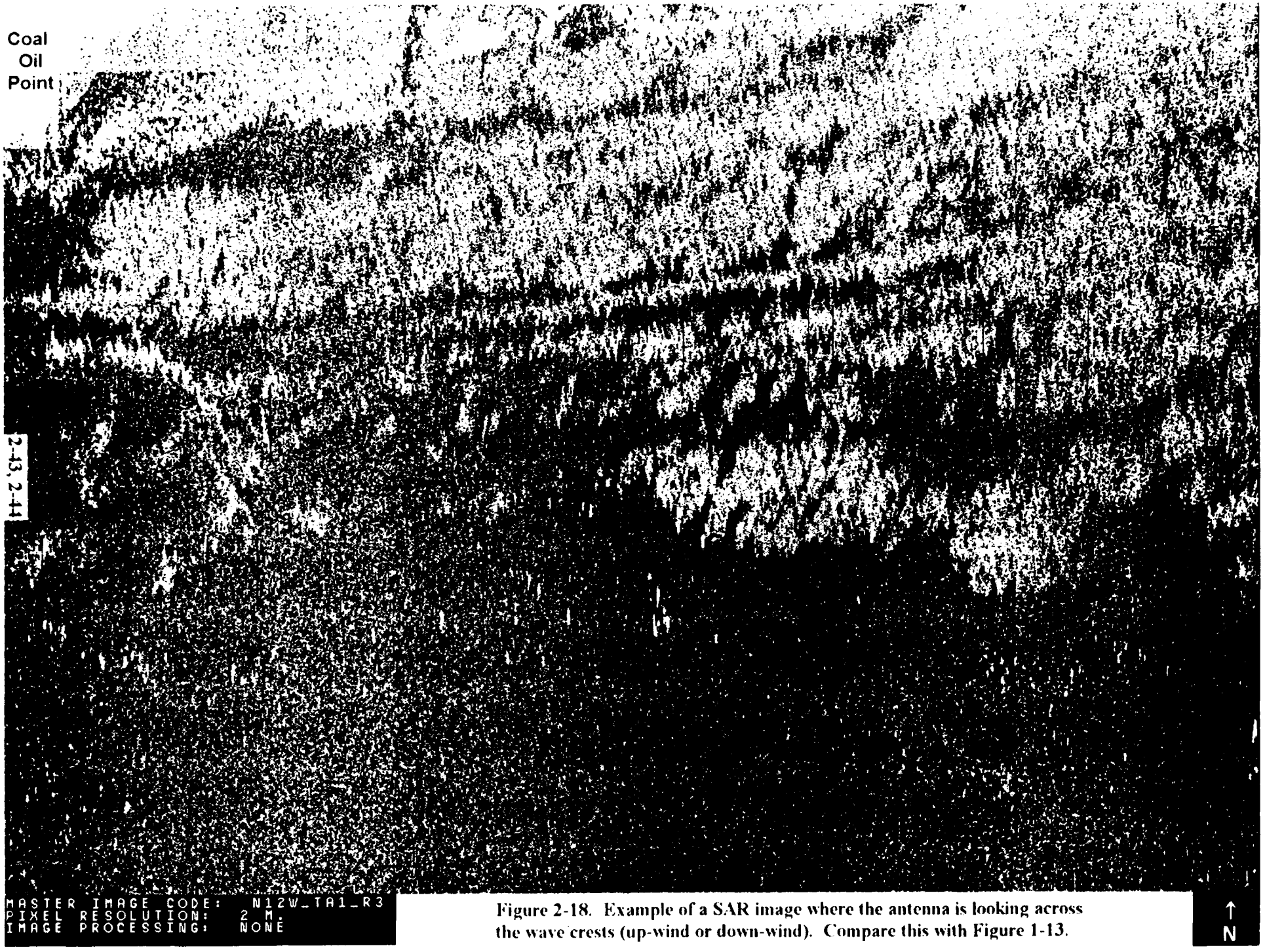

Figure 2-18. Example of a SAR image where the antenna is looking across the wave crests (up-wind or down-wind). Compare this with Figure 1-13.

Workshop participants felt that 14-m resolution was adequate, but that 10-m resolution was preferred when motion degradation was present.

2.3.2.4 Full-Swath Image Resolution Requirements

The operational resolution investigation was the second part of the resolution study. Participants examined full swath images with reduced pixel resolutions of 10 m, 20 m, and 40 m. Two of the mosaics for this investigation came from the Nov. 12, 1992, test and two came from the Nov. 15, 1992, test. Downsampling was performed by adjacent window averaging, as discussed in Chapter 1. Pixel replication was not performed following adjacent window averaging since the task was to produce a smaller image of the full swath for display on an airborne monitor.

Several significant comments were made by the workshop participants who examined the resolution-degraded full-swath images. Figure 2-19 shows one of the Nov. 12, 1992, images at 20-m and 40-m pixel resolution. Notice that the windrows to the right of Goleta and Coal Oil Points are retained at 20-m resolution, but lost at 40-m pixel resolution. Figure 2-20 shows one of the Nov. 15, 1992, images at 20-m and 40-m pixel resolution. Kelp texture (just below Coal Oil Point) is lost at the 40-m pixel resolution. Narrow fingers of oil in the lower-left corner of the image are also lost at 40-m resolution. The 20-m resolution image clearly shows continuity of small linear features that are lost in the 40-m resolution image.

The consensus that resulted from the operational resolution study was that full swath images with pixel resolutions reduced to between 20-m and 30-m by adjacent window averaging ("boxcar" filtering) was sufficient. Most agreed that 20 m resolution was preferred, but there was an understanding that monitor size and cost constraints might make 30-m pixels a more attractive alternative. One analyst made an important point, however, that should be considered when deciding upon monitor size and pixel resolution for full-swath display. Eye strain becomes a significant issue in an operational scenario. A high-resolution (20-m pixel) display on a small monitor may provide all the necessary information, but fatigue from examining a small monitor will ultimately negate the advantage of the higher resolution. Participants all agreed that 40-m pixel resolution was too coarse for identifying regions needing detailed analysis at full resolution (10 m).

2.4 SAR vs. SLAR: DISCUSSION OF TECHNICAL ISSUES

Section 2.3.2 dealt with the determination of appropriate resolution for a Coast Guard SAR by comparing AIREYE SLAR images with SNL SAR images from the November 1992 Santa Barbara flight tests. The purpose of this section is to discuss technical advantages and disadvantages of SAR vs. SLAR. Portions of the discussion will compare generic strengths of SAR with the current AIREYE SLAR. However, as appropriate, SAR attributes will be compared to those of a more generic SLAR.

2.4.1 Attributes That Need Not Be Used in the Comparison

There are a number of attributes of modern SAR that the AIREYE SLAR does not currently possess but that could be incorporated into a new-design SLAR or into the AIREYE SLAR as an upgrade. It is important to at least list these capabilities; however, it is not proper to use them in a

(This page intentionally left blank.)

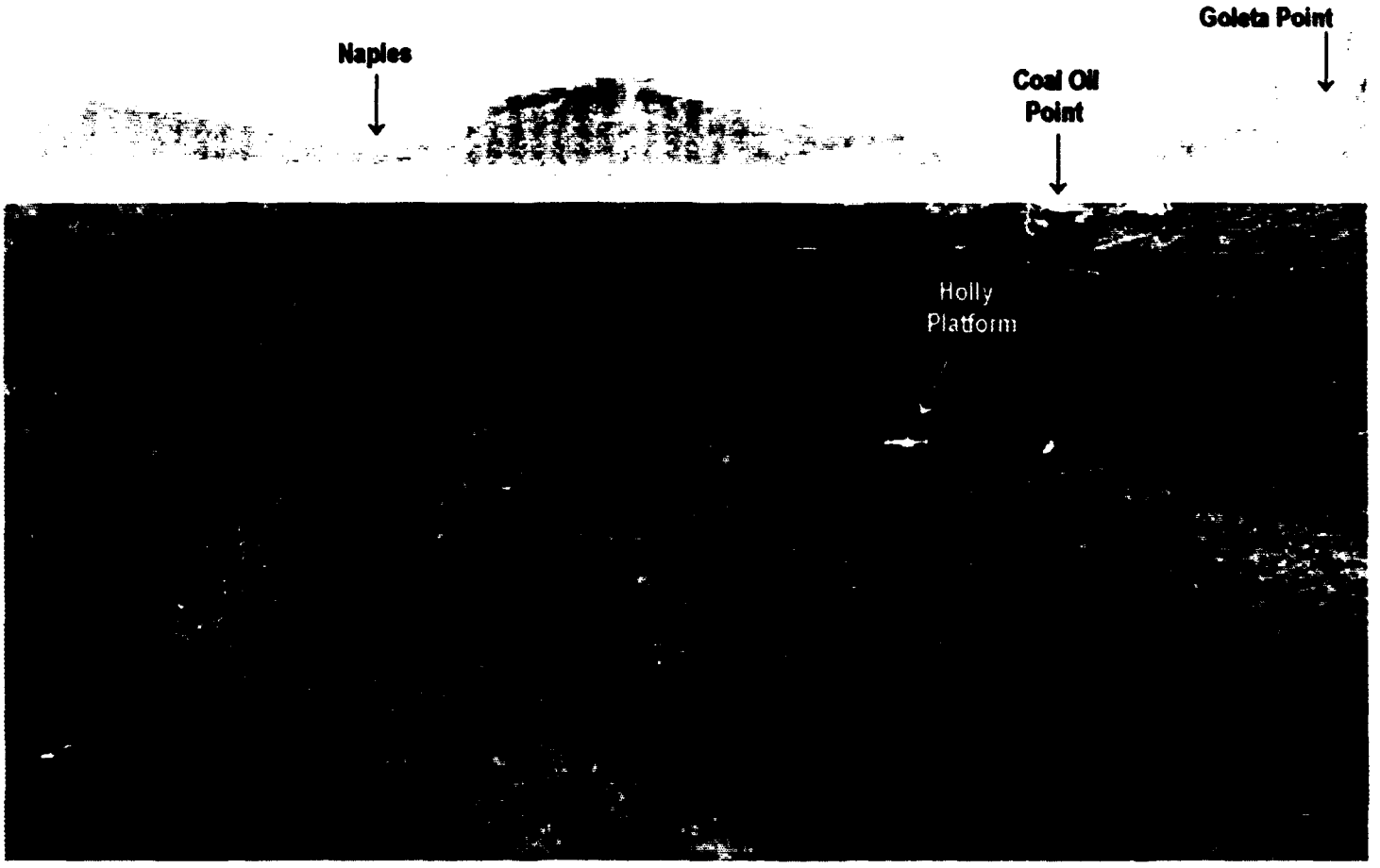

(a)

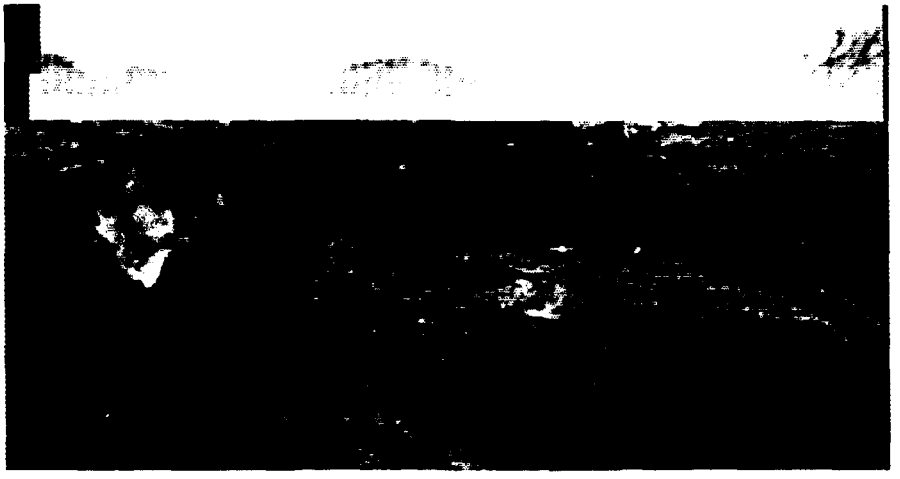

(b)

Figure 2-19. Example of 20-m (a) and 40-m (b) full-swath display images from the Nov. 12, 1992 data set

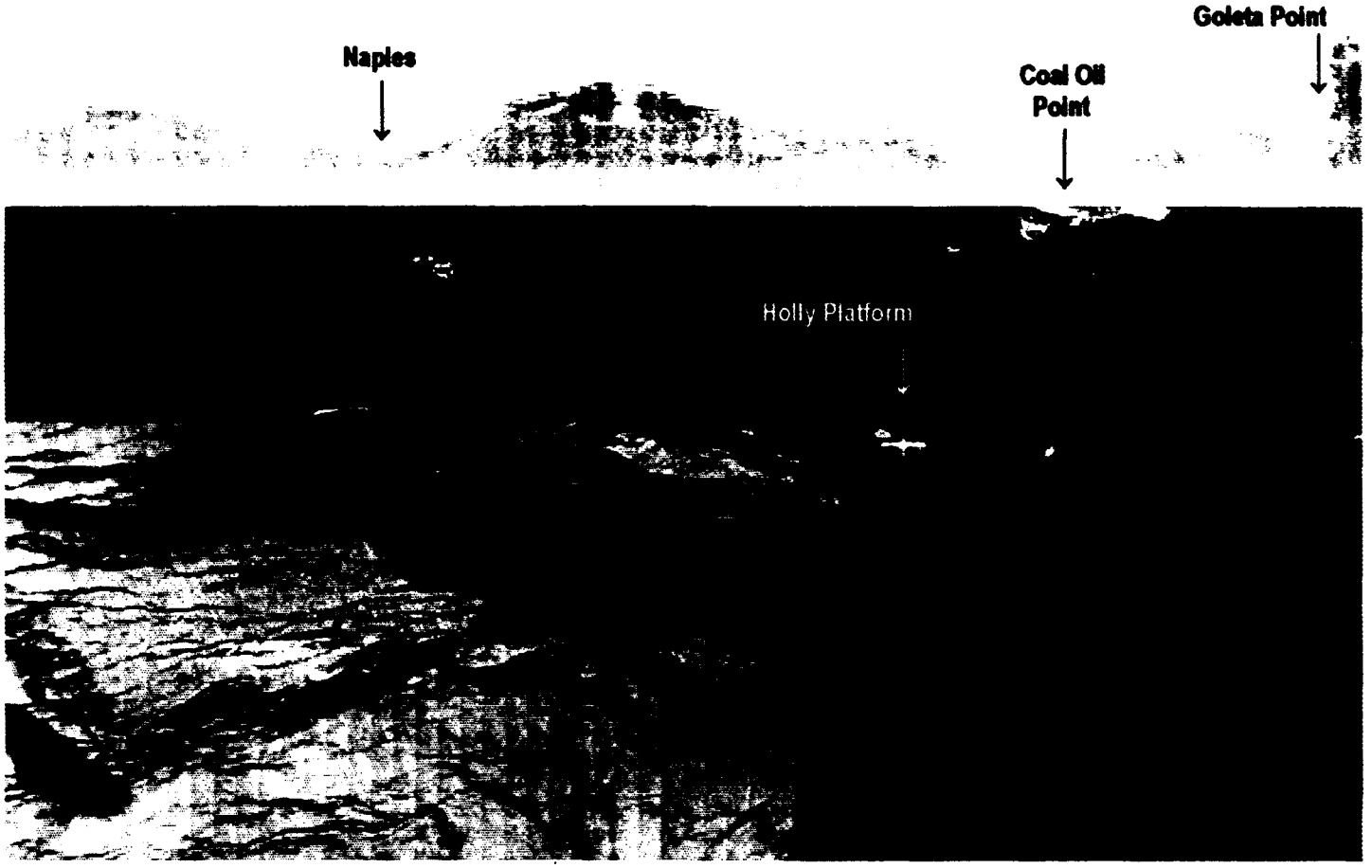

(a)

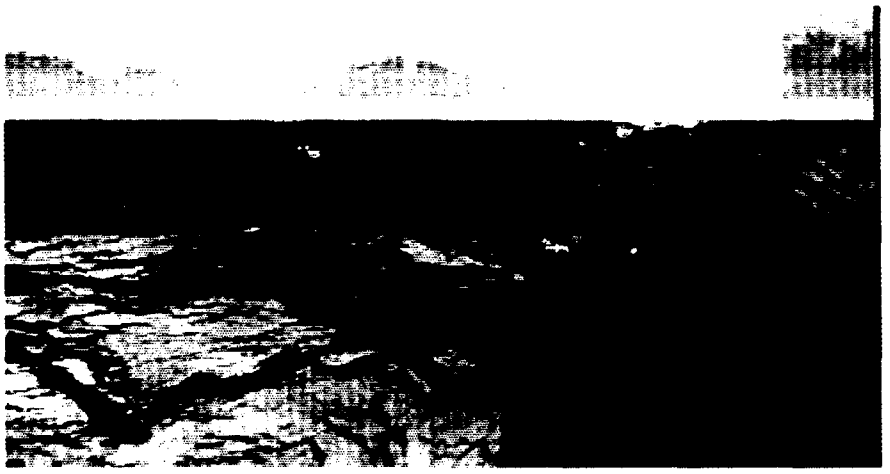

(b)

Figure 2-20. Example of a 20-m (a) and a 40-m (b) full-swath display image from the Nov. 15, 1992 data, set.

SAR/SLAR comparison, because either type of radar could use these features. These attributes are listed below.

Pulse Compression and Range Resolution

The use of pulse compression to trade pulse width for peak transmitter power is not peculiar to SAR. The AIREYE SLAR does not employ pulse compression; however, some SLARs do. Also, ignoring the issue of system sensitivity for the moment, either SAR or SLAR can achieve the same levels of range resolution, since this resolution is determined only by bandwidth of the transmitted pulse.

Digital Representation, Storage, Manipulation, and Display of Strip-Map Data

Modern technologies for acquisition and handling of digital data could be applied in the design of a SLAR as well as that of a SAR. This issue is expected to be addressed as part of the AIREYE system upgrade project recently initiated by the Coast Guard's Aeronautical Engineering Division (G-EAE).

Automatic Registration of Images with Standard Charts

One strong feature of the AIREYE SLAR is its ability to produce hardcopy image products that can be laid-over standard aeronautical charts for the purposes of image interpretation and spill-response planning. An equivalent capability should be incorporated into any new Coast Guard SAR design.

2.4.2 Attributes for Which SAR and SLAR Differ Significantly

There are a number of intrinsic differences between SAR and SLAR that can be compared and contrasted in terms of the advantages and disadvantages they offer. This section describes these basic differences.

Advantage of SAR: Achievable Azimuth Resolution

The principal benefit of SAR is its ability to use a synthetic aperture to synthesize extremely fine beamwidths. This allows the SAR to obtain resolution of the order of 10 m (or better) at 54-km range. SLAR uses a real antenna beam; airborne antennas cannot be made large enough to achieve azimuth resolutions that can be achieved by the SAR technique. In particular, the AIREYE SLAR's 0.8° beamwidth supports azimuth resolution of about 750 m at 54-km range. As explained in Section 1.3.3.1, the SLAR azimuth resolution grows progressively coarser as range from the aircraft increases and the beam spreads. This means that, in the SLAR image, definition of along-track features in the target area is not uniform and can become unusable for oil slick identification at medium to long ranges.

Advantage of SAR: Constant Azimuth Resolution Over the Swath

Because the length of the synthetic aperture can be changed as a function of range, it is possible to keep azimuth resolution reasonably constant over a very wide swath using the SAR technique. As shown in [17] (Appendix D), it is also possible, in the SAR processing, to keep the

number of looks approximately constant across the wide swath. A SLAR's azimuth resolution must degrade in proportion to the target range; therefore, if range increases 6:1 across the swath, resolution will be 6 times as coarse at far range as at near range. For example, the AIREYE SLAR's azimuth resolution degrades from about 120 m at 8.5-km range to about 750 m at 54-km range.

Advantage of SAR: System Sensitivity

When sensitivities of SAR and SLAR are compared in terms of σ^{o}_{min}, the minimum detectable distributed-target cross section that the radar can detect at a stated signal-to-noise ratio (SNR) and range-to-pixel, the resulting SAR and SLAR numbers may be comparable, given that average transmitter power and other critical parameters (particularly antenna beamwidth and range resolution) are similar. For example, estimated AIREYE sensitivity at 54-km range is about -42 dB [7](Appendix A) and, by design, sensitivity of the SAR proposed in Section 2.5 of this report is about -45 dB. However, when sensitivity is viewed in terms of the minimum detectable radar cross section (in m^2) of a single pixel (either of a point target or of a distributed target), SAR sensitivity will normally be much better (other factors being equal). This is because the SAR's clutter-cell area will normally be one or more orders of magnitude smaller than the SLAR's clutter-cell area. The improved sensitivity of the SAR is due to its ability to coherently integrate energy across the aperture, whereas a SLAR only integrates energy noncoherently. This improved sensitivity carries over to the case of imaging moving targets, in the event that the Sequential Doppler-Frequency Translation SAR Moving Target Indicator (SFT/SAR MTI) mode [18] (Appendix E) is implemented.

Advantage of SAR: More Precise Image Registration Knowledge

Although not an attribute exclusive to SAR, The SAR's ability to determine the geographical coordinates of the imaged patch should be better than for SLAR because of the presence of a more accurate navigation system (required for the SAR image-formation process [19]). Further, the better azimuth resolution of the SAR contributes to improved accuracy in determination of relative locations of image features.

Advantage of SAR: Smaller, Steerable Antenna

A SAR can, in principal, use a very small antenna (wide azimuth beamwidth) and still synthesize a very narrow synthetic beam. In practice, it is prudent to limit azimuth beamwidth to keep transmitter power requirements under control. As will be concluded later in this report, it should be possible to make the SAR's antenna of the order of one meter long and maintain transmitter power at a reasonable level. This means that the SAR antenna could be steered so that it always points at a right angle to the desired flight path (no squint). This makes image rectification automatic. In contrast, the current AIREYE SLAR rectifies the image by manipulation of the CRT trace. Further, any image rectification performed in an AIREYE SLAR upgraded for recording of digital data would require additional digital signal processing of image data.

Advantage of SAR: Superior Performance of MTI Mode

As discussed in detail in [18](Appendix E), SLAR's signal-to-clutter performance for point targets (either moving or stationary) against an ocean clutter background is not very good, and any MTI mode added to either SLAR or SAR radars will greatly enhance performance against fast movers. If an SFT/SAR [18] MTI mode is implemented with a SAR, very significant performance increases can be had. For detection of a fast moving point target in ocean clutter, SFT/SAR mode sensitivity is estimated to be about 37 dB better than a simple RAR mode that might be added to an operational SAR and about 42 dB better than AIREYE SLAR performance [18].

Disadvantage of SAR: Azimuth Defocusing Due to Ocean Movement

November 1992 flight test images provided evidence of a shortcoming of SAR in imaging the ocean. Because the SAR image is formed based upon the Doppler frequency of echo from each point in the scene and based upon the assumption that nothing in the scene is moving, movement of elements of the target scene radially toward or away from the radar can cause local distortions in the SAR image. In particular, elements moving toward the SAR will be translated, in the SAR image, along-track, in the direction of motion of the aircraft. Elements moving away will be translated in a direction opposite the motion of the aircraft. This effect only degrades the system's effective azimuth resolution capability; range resolution is not affected.

The west-looking SAR image from November 12, shown in Figure 2-18, shows that motion of the long waves can cause significant rending of cross-track linear features in the image. The effect is most pronounced when the SAR look direction is normal to the wave fronts of the long waves. As the long wave propagates, water molecules on the front of the wave move toward the radar; molecules on the back of the wave move away. Therefore, the front of the wave is moved one way in the image and the back of the wave is moved the opposite way. This defocusing effect caused by motion of the long waves is not strongly dependent on the aperture time and is more determined by wave velocity, aircraft speed (faster is better), and imaging geometry.

The effects of wave motion are obvious upon examination of narrow, linear, cross-track (east-west) features visible in the Figure 2-18 image. Half of the linear features appear to have been combed forward (along-track), the other half backward. Azimuth defocusing of tens of meters is apparent in the subject image.

By contrast, south-looking SAR images of the same test area and on the same day (see, for example, Figure 1-13) show no such effects. This is because for these images, the look direction of the SAR is very nearly along the wave crests, and there is no significant motion of the water radially toward or away from the radar.

The amount of displacement (in the SAR image) of a radially-moving target cell will be proportional to the range from the SAR to the target, so significant defocusing (many tens of meters) must be expected in the worst-case scenario (high wave-front velocities, look direction normal to the wave-fronts, far side of the range swath).

Although not apparent from the flight-test images, some azimuth smearing should be expected due to more-or-less random movement of capillary waves that ride on the long waves. Radial velocities of water molecules due to capillary wave motion appear to be significantly smaller than velocities due to long-wave motion. This effect, were it observable, could be expected to be most pronounced when the SAR looks either down-wind or up-wind. This smearing effect due to capillary-wave movement should also become more pronounced at longer ranges.

One can conclude from the discussion above that minimum azimuth smearing of the SAR image will occur when the SAR looks in a direction normal to the direction of wave propagation and normal to the direction of the wind (wind and wave directions often coincide).

Defocusing of the SAR image due to long-wave motion must be recognized as a fundamental limitation of SAR for oil-spill monitoring. This effect implies that, while the SAR's range resolution capability can be realized in all cases, its azimuth resolution capability will be a strong function of look direction and wind/wave conditions, with optimum performance occurring at a look direction parallel to the long-wave wave-fronts and poorest performance occurring when the SAR looks normal to the wave-fronts. A detailed analysis of this phenomenon is provided in [21] (Appendix H).

Advantage of SLAR: Same Mode for Moving and Stationary Targets

All moving targets appear in the SLAR image, their resolution and crispness depending on their range and speed. The basic SAR mode only images stationary and slowly moving targets (radial velocities less than about 2 knots). Either a real-aperture radar (RAR) or moving-target indicator (MTI) mode would need to be added to an operational SAR to image fast movers (radial velocities between about 2 knots and 40 knots).

Advantage of SLAR: Simplicity

One of the primary advantages of SLAR is its simplicity in relation to SAR. It is important to identify and compare the major components and/or functions for which SAR complexity is significantly greater than for SLAR. Then cost/benefit considerations can concentrate on these areas, and the costs of added complexity of the SAR can be weighed against the primary SAR benefits of finer azimuth resolution and better sensitivity.

- Inertial Measurement Unit (IMU). Motion measurement for SAR must be more precise and support higher update rates than for SLAR. GPS aiding will also be required [19].

- Gimbal Mounting and Control. Under the assumption that it would not be feasible to gimbal-mount an antenna for an oil-spill monitoring SLAR, this item should be identified as an extra expense in a comparison of SAR and SLAR complexity. Note, however, that any SLAR would require some pointing control and movement of the antenna to account for short-term yaw variations, so a proper approach would be to attempt to compare estimated costs of the AIREYE SLAR's antenna- mounting and control system with those for a SAR gimbal implementation.

- rf Circuit Linearity. Phase and amplitude linearity of rf circuits is more important for SAR than SLAR; however, we believe that, because of the relatively narrow bandwidths (less than 15 MHz) of the proposed SAR system, these added requirements do not translate to a significant cost difference.

- IF Processing and Digital Prefiltering. SAR processing requires that matched in-phase and quadrature (I & Q) video channels be created at the output of the final IF mixing stage. Both channels are then digitized and pre-filtered using a dual-channel presummer/high-pass filter combination. SLAR requires only one video channel, this being a magnitude-only channel, followed by an accumulator that is simpler than the SAR pre-filter.

- Image Former. This component is the greatest single contributor to increased complexity in the SAR. For the SLAR, the image comes directly out of the relatively simple accumulator. Image formation for SAR requires that many computations be performed very rapidly in order to "compute" the SAR image. More detail on the image former is provided in Section 2.5.2.

- Operator Training. There will be some increased operator training burden for a SAR sensor system; however, we believe that radar and navigator initialization and operation can be largely automated and that the primary need for increased operator training will be in the area of ROI selection, processing, and disposition. Some of this increased training would also be needed for operators of any new-build SLAR or upgraded AIREYE SLAR having similar data-manipulation capabilities.

- Sensor System Maintenance. The IMU, gimbal, and phase-history collector are likely to require more periodic maintenance and alignment than their counterpart assemblies in the current AIREYE SLAR. Further, the image former will increase the maintenance burden somewhat. This is because the image former is only required for the SAR (as pointed out before, the SLAR's image former is really just an accumulator) and because it is a relatively complex module.

2.5 SAR PARAMETERS ANALYSIS RESULTS

A SAR parameters analysis study conducted by SNL resulted in a detailed set of specifications for a conceptual Coast Guard SAR that would be capable of both oil-spill monitoring and imaging moving vessels at sea. This section summarizes the results of this analysis. Where specific components and architectures are called out, they have been selected based on proven, currently-available technology. Future developments may provide alternative designs and components that are more desireable.

2.5.1 Development of Requirements

Conceptual requirements for a Coast Guard SAR are documented in Reference [15](Appendix B). This section describes the major requirements identified during the study. Other requirements will be evident from Section 2.5.2. Primary requirements are as follows.

- Aircraft Type: Falcon 20 or HC-130; typical velocity 125 m/s.

- Missions: ocean imaging for oil-spill monitoring ice reconnaissance, and imaging of moving ships. Moving-target imaging may require either a RAR or MTI mode.

- Resolution: approximately equal range and azimuth resolution, values to be determined by analysis of flight-test data.
- Technologies: emphasize "off-the-shelf" components.
- Current systems: consider use or modification of existing SARs to meet Coast Guard requirements.
- Data availability: real-time.
- Operators: enlisted Coast Guard airmen.
- Swath: 20-25 nmi minimum.
- System sensitivity: $\sigma^0 < -40$ dB at 6-dB SNR and maximum range.
- Operating frequency: (C-Ku bands), to be determined.
- Polarization: VV.
- Image requirements: magnitude-only, rendered as square pixels in the ground plane.
- Image calibration: no requirement.
- Image annotation: latitude/longitude, date, time, altitude, speed, pitch/yaw/roll, heading, comments, and other mission support symbology.
- Data recording: all real-time imagery, navigation, and auxiliary radar data. Requires "engineering evaluation" capability for recording of phase histories. Media to be of removable type.
- Image display: one display for decimated, full-swath real-time imagery and one for display/processing of regions of interest (ROIs) and for radar control.
- Image processing: capability to select and extract full-resolution regions of interest (ROIs) and process these ROIs (decimation, replication, contrast stretching, preparation for downlinking).
- Telemetry: SAR system must prepare files for downlinking via third-party telemetry (TM) link.
- Printing: must provide capability to print coarse-resolution imagery in-flight.

2.5.2 Calculations and System Specifications

By interpreting requirements identified in [12] and by performing SAR design calculations, SNL engineers arrived at system specifications detailed below.

2.5.2.1 General Description of Recommended Design

The recommended design is a wide-swath, relatively coarse-resolution (10-30 m), SAR operating in the X band. The system could operate from 2.5 - 6 km altitude with little change in performance. The imaged swath would extend from 8.5-km near-range to about 54-km far range (about 25 nmi swath). The SAR employs a relatively long chirped pulse and uses surface-acoustic-wave (SAW) technology for compression of the received echoes. Use of pulse compression allows peak power out of the TWT transmitter to be only about 200 W (for a 10-m resolution system). Motion compensation derived from precise navigation information will be required in order to accurately image the target area. All processing after analog-to-digital (A/D) sampling of compressed pulses is digital.

Sequential, fully-focused, overlapping SAR patches would be formed in a digital signal processor, and combined to form real-time, multi-looked images at the required resolution. Up to nine looks could be obtained within the constraints of the maximum 10-m resolution system defined here. Because of the extremely wide swath, the image-formation processing will need to partition echo pulses into a number of adjacent range channels, and sub-image patches for each channel will be formed, resampled, and multi-looked separately; then multi-look images from the various channels can be merged to assemble the full-swath image. An advantage of this approach is that azimuth resolution-cell size and the number of looks can be kept nearly constant across the entire swath, even though the antenna's azimuth footprint changes by a factor of 6:1 from near-range to far-range.

Because of the relatively coarse resolution of this system, tape recorder requirements are modest; a 4-mm tape unit can meet the requirement. Several approaches to the antenna design are possible: either rigid-mounted or gimbal-mounted (see Section 2.5.3.1 for more information).

The basic SAR design proposed is not capable of imaging ships moving at radial velocities greater than a few knots. Two basic approaches to meet the moving-target requirement are possible.

- **Alternative 1**: A real-aperture radar (RAR) mode could be added to the radar. In this mode, the radar would provide performance slightly better than that of the AIREYE SLAR. Assuming a 10-m SAR system, RAR range resolution would be 10 m, and azimuth resolution would be about the same as the AIREYE SLAR (about 50 m at 2-nmi range). Although the RAR implementation is conceptually simple, it requires added hardware and software to implement. The RAR mode would exhibit performance against moving ships in clutter that is about 5 dB better than that of the AIREYE SLAR. Neither SLAR nor the RAR mode provide any filtering to reduce stationary background clutter, and this clutter usually limits detection performance against discrete targets such as vessels. Reference [20](Appendix F) provides a detailed description of RAR-mode implementation and performance estimates.

- **Alternative 2**: A moving-target-indicator (MTI) mode could be added to the radar. As documented in [18](Appendix E), two candidate MTI modes were analyzed: 1) "High-Pass Filtering with RAR" (HPF/RAR), and 2) "Sequential Doppler-Frequency Translation with SAR" (SFT/SAR). The HPF/RAR approach is more traditional, and although its performance against point targets is much better than RAR or SLAR, its performance is

inferior to that of SFT/SAR. SFT/SAR takes advantage of the SAR's ability to "tune" its receiver to any of a number of Doppler bands; each band corresponding to a different band of target radial velocities. For each tuning setting, a full-resolution patch (or look) can be formed that shows movers as more-or-less focused entities. For all tuning settings except zero Doppler, stationary clutter will be greatly reduced in intensity; this allows smaller discrete targets to be seen. The SAR would image the target swath with overlapping looks. Sequentially, look-by-look, the Doppler tuning setting would be varied to allow a different velocity band to be imaged with each look. The radar can be configured to cover the desired range of velocities (e.g., ±20 knots radial) in the number of looks available. As shown in [18], performance of SFT/SAR against discrete targets would be up to 40 dB better than SLAR. About 20 dB of this improvement is due to clutter-rejection filtering, and the other 20 dB is due to SFT/SAR's smaller clutter-cell area.

SNL's recommendation is that, if a future Coast Guard SAR is produced by modifying an existing SAR, and if that SAR doesn't have the flexibility to easily implement the SFT/SAR approach, then the RAR approach should be implemented to satisfy the requirement of imaging moving vessels. However, if the SAR is a new design, the SFT/SAR approach should be implemented because of its far superior performance for detecting discrete targets in a clutter background.

2.5.2.2 System Specifications

Table 2-3 contains quantitative specifications for the conceptual SAR design resulting from this study. The specifications deal mainly with the radar proper. More description of the image-formation processing and post-formation image processing approaches will be given later. Reference [17](Appendix D) provides more detailed information on how most parameter calculations were performed. Reference [21](Appendix G) gives results of corrected calculations for required peak transmitter power.

As can be seen, in some cases, calculations have been made at several different values of a particular parameter. For example, the effect of resolution on required peak transmitter power is shown, antenna size is estimated at several azimuth beamwidths, and the relationship between azimuth beamwidth and Doppler spectral width is given. Each of these special parameters will be discussed later in the section relating to system trade-off analyses.

It is interesting to note that, in order to keep azimuth resolution and the number of looks constant over the wide swath, the number of azimuth pixels per patch increases from 18 at near-range to 116 at far-range. Likewise, the required length of the synthetic aperture for a single patch increases from 14 m at near-range to 87 m at far-range. This latter increase in aperture length is due to the need to have a narrower synthetic beamwidth at far-range to obtain the same synthetic footprint (the azimuth resolution) as at near-range.

Results show that, even with the reasonably narrow 1° beamwidth, a good number of looks can be obtained if adjacent synthetic apertures for the looks are spaced as closely as possible. Table 2-3 also shows that the number of available looks increases in proportion to the azimuth resolution desired. Although it is not shown in Table 2-3, the number of looks is also approximately proportional to azimuth beamwidth.

Table 2-3. SAR System Specifications

Parameter or Attribute	Units	Value or Description
Agency Name	----	US Coast Guard
System Name	----	SAR for oil-spill response
Prime Usage of System	----	oil-spill imaging
Secondary System Usage	----	imaging of moving targets
Aircraft Platform	----	Falcon 20
platform velocity	m/s	90-124
Radar Supported Modes	----	side-looking strip map
	----	real-time multilook imaging;
	----	either RAR or MTI mode for ships
Real-Time Image Attributes		
real magnitude	----	recorded
complex data	----	available, not recorded
# bits per pixel	----	8 or 16
slant-range resolution ρ_r	m	10/30 (ROI/full-swath display)
azimuth resolution ρ_a (@ 25 nmi)	m	10/30 (ROI/full-swath display)
IPR maximum sidelobes	dB	-30
image slant-range swath	nmi	25
	km	46
# pixels, range dimension	pixels	6950 (25 nmi swath; 10-m ρ_r)
(assuming 1.5 oversampling)	pixels	2315 (25 nmi swath; 30-m ρ_r)
# pixels (per patch), azimuth	pixels	18 near-range; 116 far-range
	----	(1° β_a, 10-m resolution)
pixels per resolution cell	----	1.5 (range and azimuth)
maximum pass length	nmi	200
Geometry		
altitude	kft	8-20
	km	2.5-6
slant range (near range)	km	8.5
slant range (far range)	km	54 (@ 25 nmi swath)
depression angle (near range)	°	17-45
depression angle (far range)	°	2.6-6.4 (ignoring curvature)
squint angle	°	$\pm$90 nominal
near-range az. antenna footprint	m	148 (1° az. beamwidth, β_a)
far-range az. antenna footprint	m	942 (1° β_a)
Typical Aperture Length	m	87 (10-m ρ_a @ 54-km range)
	m	14 (10-m ρ_a @ 8.5-km range)
Typical Aperture Time	s	0.7 (10-m ρ_a @ 54-km range)
	s	0.1 (10-m ρ_a @ 8.5-km range)

Table 2-3. SAR System Specifications, continued ....

Minimum-detectable σ^o Required	dB	-45 (@ 25-nmi., SNR = 6 dB)
Amplitude Calibration	----	pre- or post-mission
mean error	dB	$-3 \leq \mu_e \leq 3$
standard deviation	dB	$\sigma_e \leq 3$
Multilook Processing (real-time)		
temporal, $\Sigma_i \mid V^i_{j,k} \mid /N$	looks	9 @ 10-m resolution
(maximum number of available	looks	21 @ 20-m resolution
looks, assuming $\beta_a = 1°$)	looks	31 @ 30-m resolution
pixel averaging, $\Sigma_{j,k} \mid V^i_{j,k} \mid /N$	pixels	no
Frequency Generator and Transmitter		
operating frequency	GHz	≈ 9.3
operating wavelength, λ	cm	≈ 3.2
transmitter bandwidth	MHz	≈ 15 @ 10-m ρ_r
	MHz	≈ 5 @ 30-m ρ_r
pulse duration	μs	≤ 57 μs (near-range constraint)
waveform intra-pulse modulation	----	LFM chirp
prf	kHz	≤ 2.4 kHz (far-range constraint)
interpulse modulation	----	$0/\pi$ PN phase coding (for ambiguous range abatement)
microwave transmit losses	dB	0.8
peak tx power (at antenna)	W	173 (10-m resolution, $\beta_a = 1°$)
	W	57 (20-m resolution, $\beta_a = 1°$)
	W	31 (30-m resolution, $\beta_a = 1°$)
maximum duty factor	%	13 (based on maximum pulse length and maximum prf)
maximum average tx power	W	[22, 7.4, 4] @ [173, 57, 31 peak]
Antenna		
polarization	----	vertical
elevation pattern	----	$\csc^2(\phi)$; ϕ = depression
(roughly 6° equiv. beamwidth)		angle
azimuth beamwidth, β_a	°	1°, 2°, or 3° (choose one)
length (controls az. pattern)	m	1.83, $\beta_a = 1°$
	m	0.92, $\beta_a = 2°$
	m	0.62, $\beta_a = 3°$
height (controls elev. pattern)	m	0.3 (about 1 foot)

Table 2-3. SAR System Specifications, continued ...

Antenna, continued		
antenna gain (rough estimate)	dB	35 (β_a = 1°; 50% efficiency)
radome losses, two-way	dB	1.5
vertical rotational steering	----	yes
azimuthal steering	----	either gimbaled, wide-angle or
	----	near-rigid, short-term yaw steering
Receiver		
front-end noise figure (& losses)	dB	2
rf bandwidth	MHz	≃15 @ 10-m ρ_r
	MHz	≃5 @ 30-m ρ_r
IF bandwidth	MHz	same as rf bandwidth
sensitivity time control	----	selectable curves
IF pulse compression	----	SAW filter
gain @ 10-m ρ_r	----	855 (29.3 dB)
gain @ 30-m ρ_r	----	285 (24.5 dB)
video bandwidth	----	same as rf bandwidth
A/D converter and presum filter		
# A/D bits	bits	10 (I) + 10 (Q), minimum
A/D Sample Rate	MHz	22.5 @ 10-m ρ_r
(1.5 oversampling)	MHz	7.5 @ 30-m ρ_r
number of video samples	----	≃6900 @ 10-m ρ_r
(25-nmi swath)	----	≃2300 @ 30-m ρ_r
Doppler spectral width	Hz	136 (1° β_a @ 125 m/s)
(assume nominal β_a is 1°)	Hz	273 (2° β_a @ 125 m/s)
	Hz	409 (3° β_a @ 125 m/s)
presum integer (approximate)	pulses	[12, 6, 4] @ [1°, 2°, 3°] beamwidths
(assuming spectral widths above & 2.4-kHz prf)		
antenna oversampling factor	----	1.5
typical azimuth sample rate	Hz	200 (presummer output rate)
Real-Time Image Former		
numerical precision	bits	minimum of 16 (I) + 16 (Q)
algorithm type	----	channelized in range; azimuth FFT with interpolation
estimated floating point op's	Gop/s	0.35
integration gain	----	1650 (32.2 dB)
windowing and other losses	dB	1.2
elevation antenna correction	----	yes
azimuth antenna correction	----	optional

Table 2-3. SAR System Specifications, continued ...

Real-Time Image Former, continued		
ground-plane projection	----	yes (vary A/D rate)
range-law correction	----	yes
sensitivity-time-control correction	----	yes
video filter correction	----	probably not needed
presummer correction	----	optional
auto-focus	----	no
Data Handling		
rate to tape (8-bit images only)	Mbits/s	1.1 @ $\rho_r = \rho_a = 10$ m
	Mbits/s	0.12 @ $\rho_r = \rho_a = 30$ m
number of tape units	----	1
candidate tape-unit data-rate	Mbits/s	1.6 (8-mm cartridge tape)
limits (approximate)	Mbits/s	4-8 (4-mm cartridge tape)
candidate tape-unit capacities	Gbits	40
record-time capacity	hours	5-10 hours (8-bit images)
phase histories	----	for engineering evaluation
radar auxiliary data	----	yes
Image Display		
horizontal display size	pixels	2048
vertical display size	pixels	2048
dynamic range	bits/pixel	8
Navigation Accuracies		
navigator type	----	inertial
attitude accuracy	°	$\leq$ 0.05, all axes
position accuracies @ pass start	m	$\leq$ 30 m, all axes
velocity accuracies	m/s	$\leq$ 1 m/s, 1-σ, all axes
GPS aiding (Y/N)	----	yes
Motion Compensation		
approach	----	real-time
update rate to SAR, Hz	----	200
Mechanical Characteristics		
total power to system	kW	2.3
physical volume of system	m^3	1.4

Range resolution, of course, determines receiver bandwidth; bandwidth requirements decrease as resolution coarsens; this, in-turn, decreases peak transmitter-power requirements. Transmitter power estimates at each resolution were made under the assumption that the maximum available number of looks was used in the processing and that required transmitter power is inversely proportional to the square root of the number of looks combined.

Corrections listed in the "Real-Time Image Former" section of the Table require some explanation. In single-look systems that have patch widths very nearly equal to the antenna's azimuth footprint, the effect of azimuth antenna-pattern shape and presummer transfer function can cause significant amplitude roll-off near the edges of the image patch; therefore, in these systems, corrections are often used to spatially normalize the image across azimuth. In a multi-look system of the type specified here, these effects will be nearly eliminated by the multi-look averaging process. Therefore, these corrections are specified as optional. Corrections applied to the range dimension, however, are very important, even in multi-look systems. Effects of the elevation antenna pattern, range-law fall-off, sensitivity-time-control, and, perhaps, IF-filter/ SAW-device transfer functions should be implemented to spatially normalize the image intensity in the range dimension.

An SNL analysis has shown that auto-focus processing will not be needed for the proposed SAR [19]. For projection of the image from the slant plane into the ground plane, we recommend implementing nonlinearly-spaced A/D sampling. This eliminates a processing step that would otherwise place an additional burden on the image-formation processor.

2.5.2.3 System Block Diagrams and Related Discussion

Figure 2-21 is a high-level block diagram of the SAR system. Block diagram entities are representative of how we recommend the system be partitioned for any new-design Coast Guard SAR. This partitioning is consistent with a modular design approach that SNL will be using on its own future SAR development programs. Major signal paths are shown; however, many interconnecting control and data paths are omitted for clarity. A brief description of the SAR imaging process is given below.

The phase-history collector generates the X-band chirp waveform that is routed to the TWT to be amplified. The TWT output is then routed to the antenna for transmission. Echoes collected by the antenna are amplified by a front-end, low-noise amplifier and routed to the microwave receiver in the phase-history assembly. The phase-history assembly contains all receiving, mixing, digitizing, and prefiltering circuitry. Its output is a stream of in-phase and quadrature (I,Q) digital video samples. If the RAR mode is implemented, the phase-history assembly also outputs RAR magnitude data. The primary output of the phase-history collector is video destined for the image former. Although not indicated by the diagram, the system must be designed so that phase histories can be fed directly to the tape recording for use in system prove-in, engineering evaluation, and trouble-shooting. The image former forms fully-focused, multi-look, strip-map SAR images. Image-former outputs are recorded to magnetic tape and simultaneously routed to a full-resolution image buffer for display processing. The image buffer provides decimated data to a dedicated, full-swath image display. It also provides full-resolution ROI data to the host computer for processing and display.

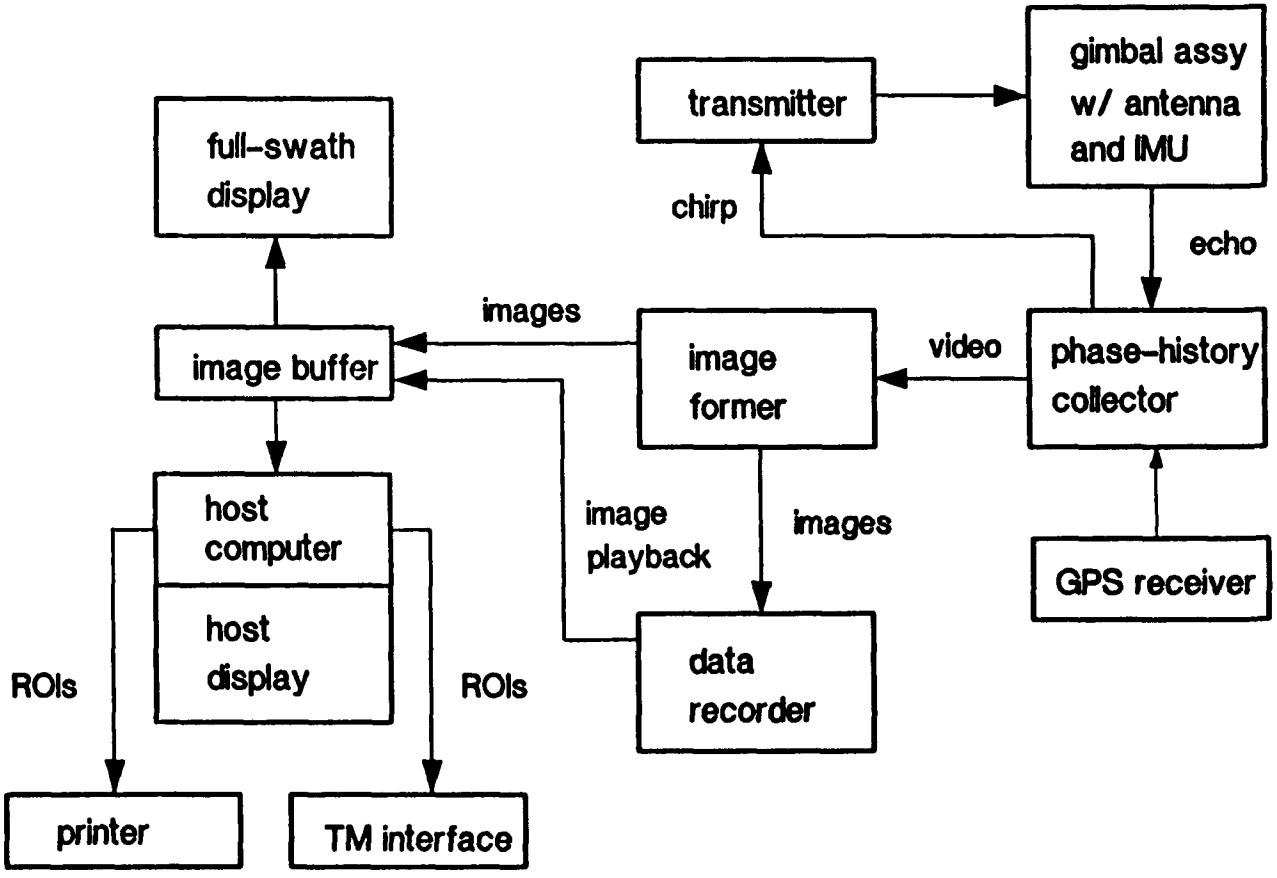

Figure 2-21. High-level block diagram of the SAR system.

The host computer provides low-speed configuration and control for all elements of the radar. It is also the operator's interface to the radar. It provides the ability to manipulate and process ROIs for display, disk storage, printing, and downlinking (via the TM interface). The following sections describe the SAR design in more detail.

Transmitter

The X-band TWT amplifier will have its own power supply and should be mounted as near the antenna as is feasible to reduce transmitter losses.

Antenna, Front End, and IMU

If the smaller antenna option (about 1 m length) is chosen, the antenna can be affixed to a gimbal and steered over a wide range of angles. If the larger antenna option is used, only steering to compensate for short-term yaw variations will be performed. In either case, the radar's rf front-end components will be co-located with the antenna. The front end contains a circulator that routes the transmitter output to the antenna. Ferrite latching switches provide isolation to protect the transmitter and receiver. The front end also contains a low-noise amplifier (LNA), which sets the receiver noise figure. The LNA would be a high-electron-mobility transistor (HEMT) device. Figure 2-22 shows a block diagram of the rf front-end assembly. Also shown are an isolator and waveguide sections that carry high-power rf from the TWT to the front end.

Phase-History Collector

Schematically, the phase-history collector (PHC) is the most complex part of the radar, since it contains much of the rf circuitry as well as a good deal of high-speed logic circuitry. Refer to Figure 2-23 for a block diagram of the PHC. The PHC contains the following major subassemblies.

- Frequency Generator. The frequency generator subassembly generates a stable, high-speed clock (the SNL SAR employs an 800-MHz clock) that is the master clock for the entire SAR. In the event that the transmit chirp is synthesized, this subassembly translates the chirp signal to X- band for input to the TWT and develops the local oscillators used in the two-stage mixing process. In the event that a SAW device is used to generate the chirp, that SAW would reside in the frequency generator subassembly.

- Timing and Control. This subassembly contains logic circuitry that provides all high-speed timing and control for the PHC assembly. In the event that the chirp is synthesized, this subassembly would also perform that synthesis.

- X-band Receiver. The receiver amplifies and filters the echo signal.

- rf/IF Mixer. Here, X-band echo is mixed to an IF.

- Pulse Compressor. rf video (fast-time) pulses are compressed to provide ultimate resolution in the range dimension.

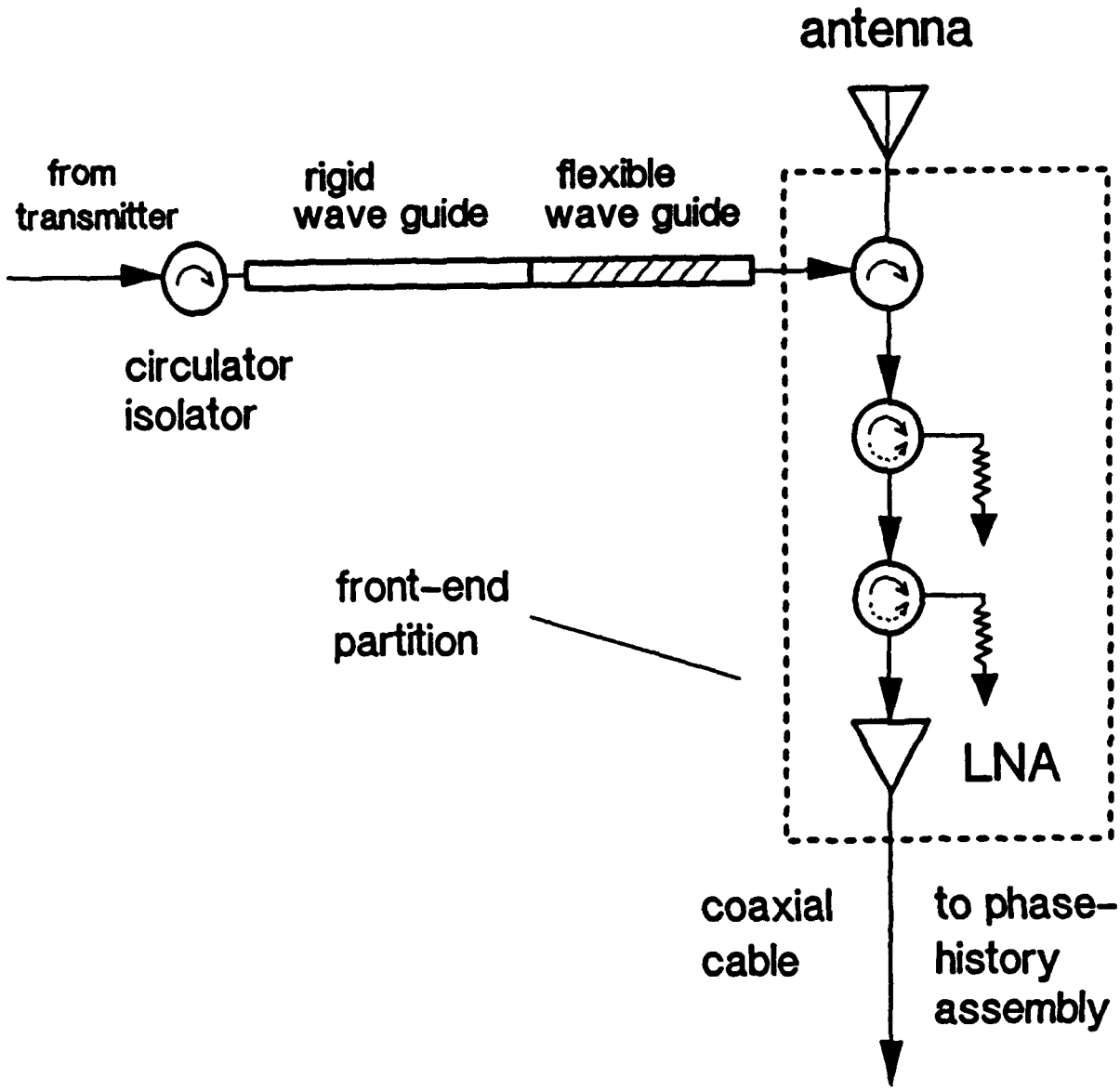

Figure 2-22. Block diagram of the SAR rf front-end assembly.

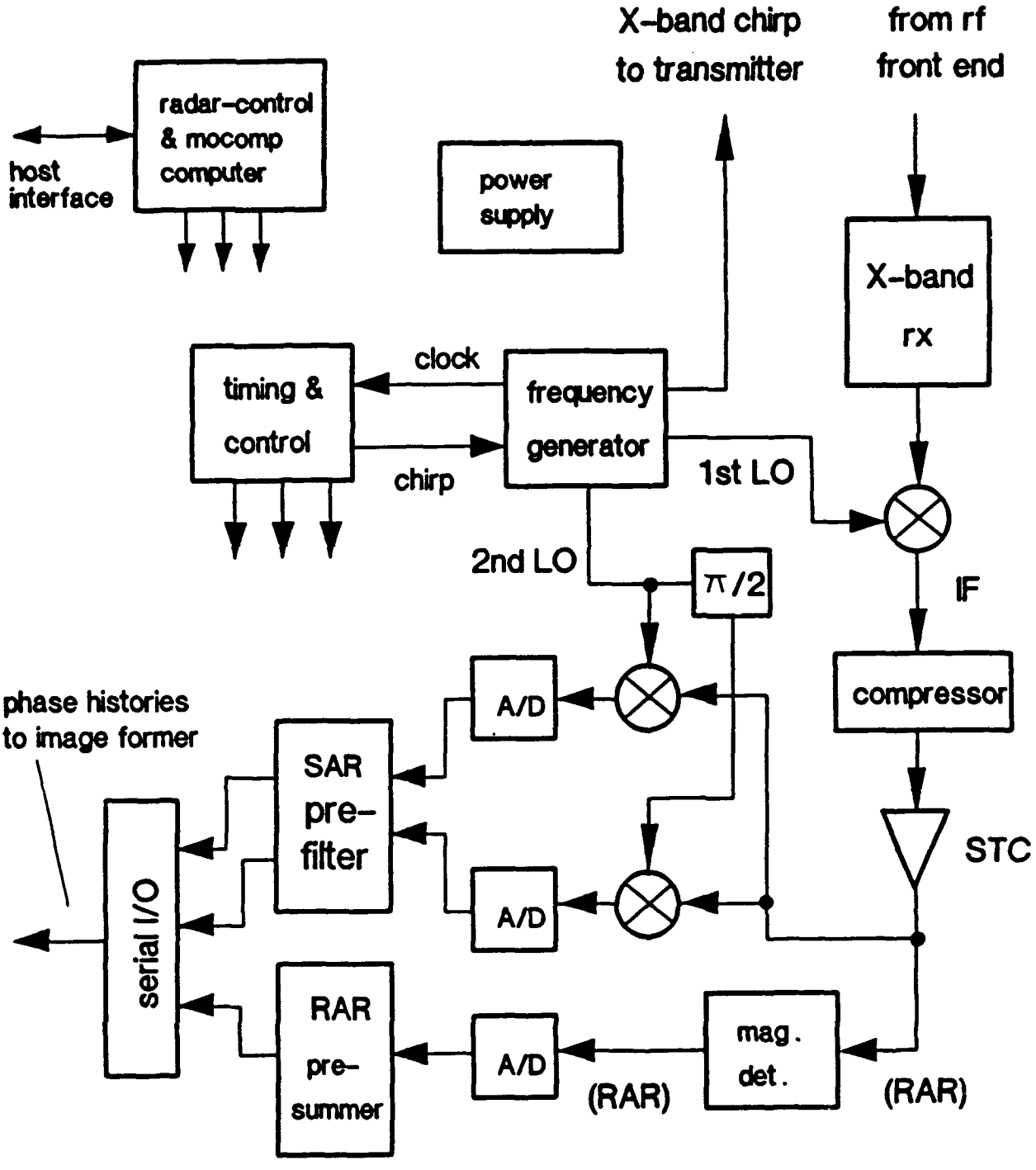

Figure 2-23. Block diagram of the phase history collector.

- Sensitivity Time Control (STC). STC may be required to reduce A/D converter dynamic-range requirements. Depending upon the transmit-pulse length, the STC may either go after the compressor, as shown, or before it.

- IF Amplification and Filtering. (Not shown).

- Quadrature Mixer. A quadrature mixer translates IF video pulses to baseband frequency to create in-phase (I) and quadrature (Q) video channels.

- A/D Converters. Dual 10-bit A/D converters digitize the I and Q channels separately.

- SAR Prefilter. The SAR prefilter module performs two functions: 1) high-pass filtering to remove any long-term dc bias introduced by the A/D converters and 2) presumming to coherently combine (in each separate range bin) a number of adjacent pulses. This latter presumming function is essentially a low-pass Doppler filter, which filters out extraneous Doppler components prior to image formation and significantly reduces the data rate to the image former. The rate at which the prefilter feeds data to the image former is called the "azimuth-sample rate" (equal to the prf divided by the presum integer).

- RAR A/D and Presummer. Blocks required for implementation of the RAR mode are shown. If the SFT/SAR MTI scheme is used, the RAR blocks can just be removed; that is, the block diagram for SAR and SFT/SAR are identical. RAR presummer outputs would be fed to the image former at the same rate as the SAR azimuth sample rate.

- Radar/Mocomp Computer. A microprocessor-based control computer controls the radar, performs motion-compensation (mocomp) computations, and provides pointing data to the gimbal.

- Image-Data I/O. One principal feature of the modular design approach is to maximize use of a standardized, high-speed, serial data link for movement of phase-history and image data. The PHC contains an interface for such a link to pass phase-history data to the image former.

- Power Supply. Consistent with the modular design approach recommended, the PHC would have its own integral power supply.

A number of interconnections within the phase-history collector are not shown explicitly in Figure 2-23. For example, both the radar-control computer and the timing and control subassembly must interface to nearly all logic subassemblies and to a few points in the rf subassemblies.

Image Former

The image former must contain a powerful computational capability in order to form image patches and combine these patches in real-time. Range compression of video pulses at IF and reduction of the data rate by presumming in the SAR prefilter reduce computational requirements of the image former somewhat; however, the image formation task is still fairly formidable.

Using currently available technology, the recommended approach for implementation of the image former is to use an i860-based parallel processing architecture like that shown in Figure 2-24. The i860 arrays are commercially available in VME packaging. The control processor would probably be a 68040-type microprocessor. Complete 68040-based microcomputer cards suitable for this control task are commercially available in VME packaging. Software for the i860s and the control processor would be new-design. Phase histories and associated data originating in the PHC are input to the image former via the high-speed serial link. Commercially-available Fibre-Channel™ I/O cards (VME format) appear to be a good choice for this task. The array of i860 processors performs the bulk of the computations associated with image formation. The control processor controls and steers data to the i860s. The output image is formatted and multiplexed with other radar and mocomp data for transmission to the image buffer and the data recorder. As is the case for the other major assemblies, the image former would have an interface to the host computer as well as its own integral power supply.

If RAR or SFT/SAR modes are implemented, the image former must accommodate these modes as well. Detailed descriptions of implementation of these modes are presented in Reference [18](Appendix E) and are not repeated here.

Data Recorder

The data recorder assembly is shown in Figure 2-25. Image data arrive at this assembly over a high-speed serial link. The modular concept implies that nearly all data to be recorded (including image, mocomp, and radar auxiliary data) be embedded in the high-speed serial link from the image former. Some additional ROI (image) and configuration data can be written to the recorder via the host interface. The basic tape recorder will be a commercial, 4-mm unit. The data recorder assembly would have its own power supply.

The data recorder assembly must also support an image-playback mode, wherein image and other data are communicated either to the image buffer for processing and display or to a ground computer for processing and distribution. In this mode, the data recorder should simulate the image former in providing input images; that is, the interface between the data recorder and the image buffer (both in terms of hardware and software) should look just like the interface between the image former and the image buffer.

Although not shown in the diagram, the data recorder must have an "engineering evaluation" capability to record phase histories and associated data directly from the PHC for purposes of system prove-in and trouble shooting.

Image Buffer

The image buffer (Figure 2-26) receives image data and other information over its high-speed serial interface from the image former (or from the data recorder in image-playback mode). The image buffer must be capable of providing a decimated image to the full-swath display. Mission symbology relating to geographical information, platform motion, date, time, etc., must also appear on the full-swath display. This annotation information should be assembled in the decimated-image buffer. Both the host computer and the high-speed serial link can be sources for the annotation information.

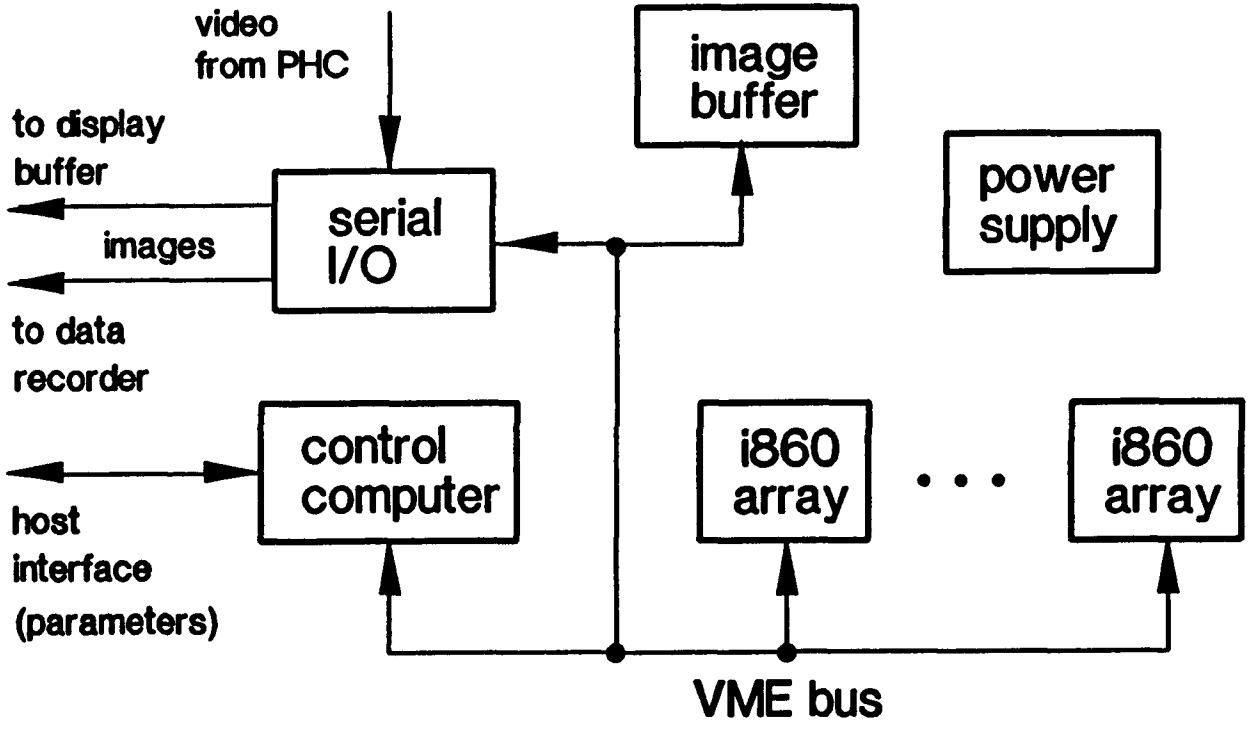

Figure 2-24. Recommended parallel processing architecture for the image former.

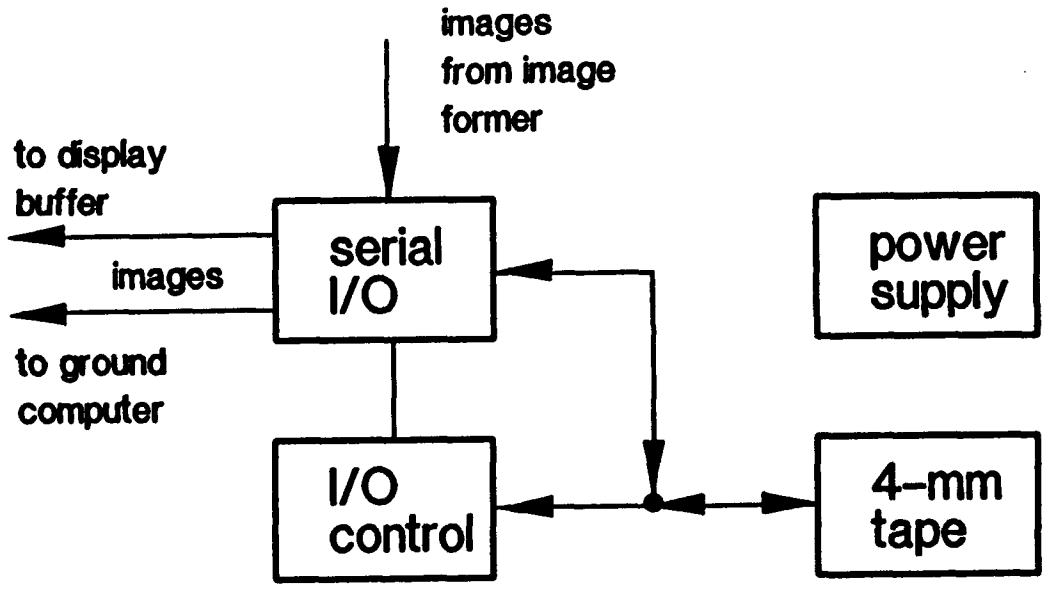

Figure 2-25. Data recorder assembly.

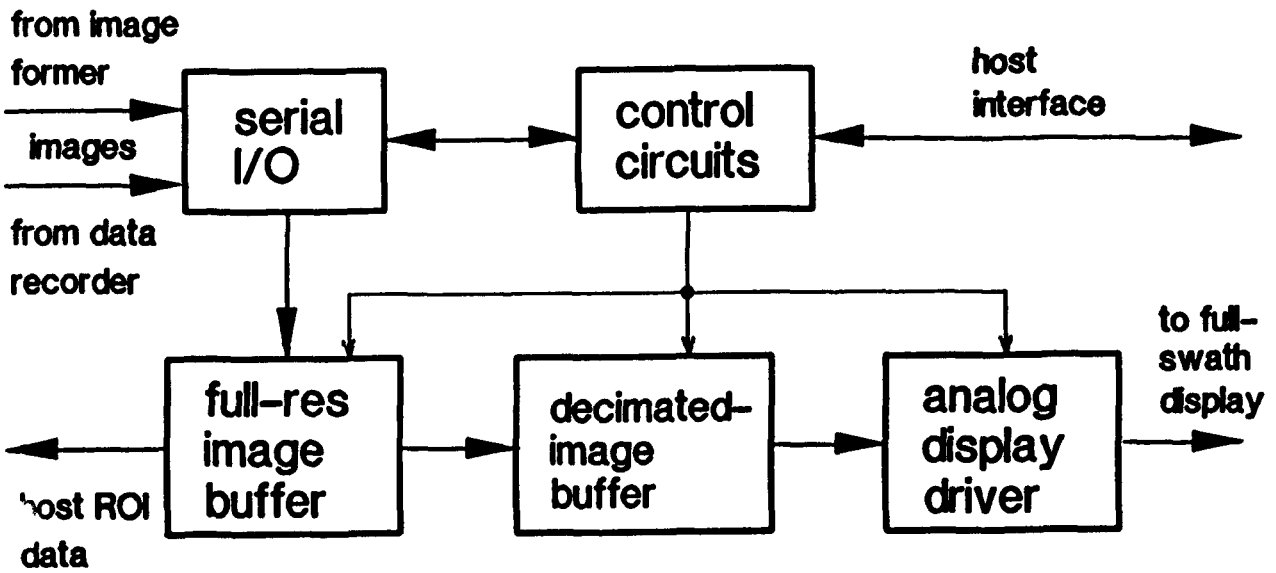

Figure 2-26. Image buffer for holding full-resolution images for ROI extractio operational display of downsampled, full-swath images.

In order to allow the operator to select ROIs on the full-swath display, the operator's mouse must be able to drive a cursor on the that display. Once the operator has indicated an ROI, the host computer will down-load the ROI data from the full-resolution image buffer for further processing, storage, printing, or TM. While the ROI is being selected, the full-swath display must be frozen temporarily. Because of the low image data rates, (only about 10 full-resolution azimuth columns per second), the image buffer should easily be able to support the freeze frame for several seconds and still be able to return to continuous scrolling without any loss of data.

It may be possible that the image buffer assembly could be one or more adapter cards in the host computer chassis.

Full-Swath Display

The full-swath display presents to the operator the decimated, full-swath image. Fine-resolution monitors that can display 2048 pixels vertically and 2560 pixels horizontally are commercially available. For a 10-m system (6.7-m pixel spacing), for example, that requires 6950 pixels to cover the 25-nmi swath (see SAR specifications Table 2-3, given earlier in this chapter), decimation by four (new pixel spacing of about 27 m) would result in about a 1740-pixel swath, which could all be displayed on such a monitor.

Host Computer

The host computer and its associated display are the operator's primary interface to the SAR sensor system. The host computer performs the following functions.

- Creates radar configuration files based on operator inputs and default values of parameters and downloads these configuration files to the appropriate radar assemblies (principally, the phase-history collector, image former and data recorder assemblies).
- Provides high-level, low-speed monitoring and control of the radar.
- If software for microprocessors in major radar assemblies is down-loaded for each mission, this task is performed by the host computer.
- Down-loads ROIs from the image buffer to host RAM for full-resolution ROI inspection and processing.
- Performs processing operations (contrast stretching, decimation, etc.) on selected ROIs.
- Formats ROI files for output to a) host magnetic media, b) the data recorder assembly, c) an on-board printer, and d) a telemetry link.
- Provides the operator with a windowing, mouse-driven environment, within which a number of configuration, processing, and control windows can be displayed simultaneously.

The minimum host computer requirements could be met by a -486 or Pentium™ based personal computer under windows. The following components should be included in the host computer definition.

- monitor: super-VGA, 19", 1024 (vertical) x 1260 (horizontal) pixels
- 64 Mbytes of RAM
- 250-Mbyte removable-cartridge magnetic drive (e.g., Passport™ or MegaDrive™) for system, application, and radar-assembly software.
- 150-Mbyte MicroBernoulli™ for storage of real-time images, radar configuration files, and radar log files.
- parallel printer port
- serial port for I/O to telemetry (TM) link.
- Printer

The printer would be a laser-type printer to be used for printing ROI images and miscellaneous text files.

2.5.3 Trade-Off Studies

A number of trade-off issues were identified and analyzed during the course of the SAR parameters analysis [17](Appendix D) and [21](Appendix G).

2.5.3.1 Squinted Operation Versus Antenna Steering

The present AIREYE SLAR actually operates in squint mode; that is, the antenna doesn't point along a line that is perpendicular to the flight path. The antenna's pointing direction is, instead, 90° away from the aircraft's centerline, averaged over the pass. Because the plane will crab to counter the wind, the antenna actually squints away from 90° by an amount equal to the average drift angle of the aircraft. Short-term yaw variations are electromechanically compensated by moving the antenna as much as ±3° to assure that the antenna always points at the same squint angle with respect to the average drift angle. An alternative would be to use navigator information to drive a gimbal so as to always point the antenna at 90° with respect to the ideal flight path. However, the current SLAR antenna, presumably because of its size (8' long), is not steered in this way. Operating at squint angles away from 90° complicates data processing; however it eliminates the problem of having to steer a large antenna over angles of tens of degrees. Like the SLAR antenna, the antenna for a wide-swath SAR need not be very large in the elevation dimension (height); however, like the SLAR's antenna, it needs to be long in order to form a narrow azimuth beam. Doubling the nominal 1° beamwidth of the proposed Coast Guard SAR would probably make the antenna short enough to mount on a steerable gimbal. This approach also doubles required transmitter power; however, such doubling is feasible without undue expense. This is the recommended approach.

2.5.3.2 Number of Bits Per Image Pixel

Estimated data rates to tape are fairly modest (1.1 Mbits/s) under the assumption of 10-m image resolution, 125 m/s velocity, and 8-bit magnitude image data. Because of the 4-8 Mbit/s

data-rate capability of 4-mm tape, recording of 16-bit image data does not appear to present a burden at these resolutions. This option should be considered.

2.5.3.3 Slant-Range Resolution

Initial SAR design calculations assumed range resolutions of 10 m and 30 m. Improved range resolution directly increases transmitter power as well as image-former input data rates, computational complexity, and output data rates. Discussion given later in this report will shed more light on the transmitter-power issue. The benefits of finer resolution in oil-spill monitoring have been assessed in the joint SNL/Coast-Guard/NOAA data analyses, and results are presented in Section 2.3.2 of this report.

2.5.3.4 Azimuth Resolution

Initial SAR design calculations considered azimuth resolutions of 10 m and 30 m. Improving (reducing) azimuth resolution directly increases image-former input data rates, computational complexity, and output data rates. The relationship between azimuth resolution and required transmitter power is more complicated and depends on whether the target being imaged is a point target or a distributed target (like the ocean). For the latter target type, reducing azimuth resolution increases the aperture time, allowing more pulses to be integrated; however, it also either reduces maximum allowable real antenna gain or the number of looks achievable, or both. The net result is to increase transmitter power for this case. There are several aspects of SAR imaging of the ocean that cause the pursuit of fine azimuth resolution to be imprudent. These aspects are the azimuth defocusing and smearing that can occur due to radial motion of both long waves and capillary waves on the ocean's surface [22](*Appendix H*).

2.5.3.5 Minimum σ^o of Noise Required

Based on data from several sources (see References [3,23]), we have chosen to require the radar to be sensitive enough to develop a 6-dB signal-to-noise ratio for a distributed ocean target area having a scattering coefficient, σ^o, of -45 dB at 54-km range. This should provide measurable signal return under conditions between sea state zero and sea state one.

2.5.3.6 Choice of Operating Frequency

A number of factors affect the choice of operating frequency.

1. Contrast between oil-covered and open ocean varies with frequency. From literature we have reviewed in the course of the Coast Guard study [5,24], it appears that good contrast can be obtained at X and Ku bands; however, data are lacking at Ka band, and contrast is reduced at C and L bands. Contrast at Ku band may be a little better than at X band.

2. Increasing the operating frequency increases transmitter power. At a given resolution, required power increases as λ^{-1}. High-power rf sources are less plentiful and more expensive at Ku band than at X band.

3. Attenuation due to atmospheric absorption becomes significant for broad-swath systems operating at Ka band. Rain attenuation is significant at Ku and Ka bands.

Based on these factors, we recommend an X-band SAR for the Coast Guard.

2.5.3.7 Multi-look Processing

Another important issue is multi-look processing. As explained in Chapter 1, noncoherent averaging of multiple images or "looks" of the same scene reduces the effects of speckle (amplitude variability in a region of the image containing a more-or-less homogeneous assembly of distributed scatterers). Two different multi-look schemes could be applied to a broad-swath, Coast Guard SAR: 1) temporal multi-look, and 2) pixel averaging.

Temporal Multi-Look

In temporal multi-look, a number (N) of looks at a pixel are noncoherently averaged. In this technique, each look is produced by a distinct synthetic aperture, so looks are statistically uncorrelated, both in terms of signal and noise. Normally, pixel amplitudes are averaged to produce the multi-look image. This technique preserves the spatial resolution of the original single-look images. It also provides a modest improvement in image signal-to-noise ratio.

Pixel Averaging

In the pixel-averaging technique, an image patch is formed at a resolution that is finer than that required in the multi-looked output image. Then amplitudes of adjacent pixels are averaged. This averaging reduces speckle and also improves image signal-to-noise ratio. But because adjacent pixels are somewhat correlated (due to the choice of 1.5 oversampling in the azimuth dimension), the effective number of looks, N, is somewhat less than the number of pixels averaged.

Both techniques can be looked at as effective ways of using all available echo energy when the azimuth antenna pattern is wider than it really needs to be to achieve the desired azimuth resolution. The use of temporal multi-look is recommended in any future Coast Guard SAR system.

2.5.3.8 Image-Formation Algorithm/Signal-Processing Approach

In the design implied by Table 2-3, range compression is performed at an IF frequency by an analog device, such as a surface-acoustic-wave (SAW) filter. This is feasible for the Coast Guard SAR because of the relatively coarse range-resolution requirement (ten meters or so). At these range resolutions pulse bandwidth is narrow enough that A/D circuitry can directly digitize the sampled echo, and no special bandwidth-reduction technique (such as stretch processing, which is used on the SNL Ku-band platform) is required.

A detailed algorithm approach has not been worked out; however, the general approach would be to perform patch processing to form single-look patches and then combine the patches using temporal multi-look. Because of the large variations in aperture time and in azimuth antenna footprint from near-range to far-range (about 6:1), the full range swath will need to be divided into overlapped channels, and each channel will be processed somewhat differently.

A detailed analysis documented in Reference [17](Appendix D) showed that azimuth resolution and the number of achievable looks could be kept approximately constant across the entire swath using the channelized approach mentioned above.

Another analysis documented in Reference [19] has addressed motion-compensation issues associated with image formation; therein, the following conclusions are reached.

- For the SAR design proposed here, range and Doppler frequency of the return signal need to be stabilized before an image can be formed.
- A phase shift must be applied to each return pulse before the A/D to keep the Doppler spectrum from the middle of the swath in the presummer passband. Achievable presum integer may be slightly smaller than the number specified in Table 2-3.
- Autofocus is unnecessary because of the coarse azimuth resolution required for this system.

The basic image formation process could be performed as follows.

- An azimuth focus vector will be applied to each azimuth row (corresponding to a particular range bin). The same focus vector can be applied to a TBD number of adjacent range bins.
- Because of the small azimuth patch sizes and the relatively coarse resolution, no range-walk correction will be required.
- An FFT is then performed on each azimuth row. The FFT length will depend upon the range bin number, but the phase history should be channelized so that the FFT length is the same for a TBD number of adjacent rows.
- FTT outputs are then interpolated to provide the desired sample location and sample spacing in each range bin.
- Magnitudes of common pixels in overlapping looks are summed to produce the multi-look image.

A rough estimate of required processing power for this problem is 0.35 Gop/s. This estimate was made under the conservative assumption that Chirp-Z transform processing would be used instead of FFTs followed by image-domain interpolation.

2.5.3.9 Pulse-Compression Issues

The conceptual design given in Table 2-3 recommends pulse compression implemented using a SAW filter. There are a number of issues here.

Peak Transmitter Power

Use of a pulse-compression technique reduces the peak transmitter power requirement by a factor equal to the time-bandwidth product of the uncompressed transmitter-output pulse. For this conceptual design, this factor is about 855 at 10-m resolution and about 285 at 30-m resolution.

Use of a SAW Device for Compression

Using a surface-acoustic-wave (SAW) device for pulse compression appears to be attractive. This technique eliminates computational requirements that would be present if the pulse compression were done digitally. The SAW approach should be more cost-effective when compared to digital compression, and reliability should be better than the digital approach by virtue of the fact the SAW is a passive device.

A/D Dynamic Range Considerations for the SAW Pulse Compression Technique

Use of a SAW device for pulse compression will increase dynamic range requirements at the A/D input. Therefore, it will likely be necessary to use A/Ds having ten bits in each channel (I & Q).

Length of the SAW Filter

The pulse length specified in the conceptual design is fairly long (57 μs). If SAW compression of such a long pulse is problematic, the pulse length may need to be shortened somewhat at the expense of higher peak power. It appears that, even if the pulse length had to be shortened by a factor of 4, peak power would still not be excessive.

2.5.4 SAR Capabilities Survey Results

The SAR Capabilities Survey [16](Appendix C) and conceptual requirements [15](Appendix B) documents were sent to twelve vendors. The purpose of the survey was to obtain information on current capabilities of SAR vendors for use in the Coast Guard study. The survey consisted of two parts: a) a request for specific numerical tabulated data on vendor systems, and b) a request for a more free-form textual discussion of the vendor's capabilities as they might relate to meeting Coast Guard requirements. Survey instructions also stated that existing vendor brochures and specification sheets could serve instead of the requested tabulated data. Seven of twelve vendors responded, each at varying levels of detail. Results of the survey are summarized in this section.

2.5.4.1 Listing of Responding Vendors

Responding vendors are listed in alphabetical order, by agency. In each case, name and mailing address of the agency point of contact are listed. Telephone numbers of responding-vendor points of contact have also been provided to the US Coast Guard.

ERIM
Dale A. Ausherman, Vice President, ERIM Director, Sensor Systems Division
P. O. Box 134001
Ann Arbor, MI 48113-4001

Intera Information Technologies (Canada) Ltd.
Ed Krakowski
Manager, Radar Engineering Support
Suite 1000
645 Seventh Avenue, SW
Calgary, Alberta Canada T2P4G8

LORAL
Bob Dubois
LORAL Defense Systems-Arizona
P. O. Box 85
Litchfield Park, AZ 85340-0085

MacDonald Dettwiler
Paul Ellis
Project Manager, Space and Defence Systems
13800 Commerce Parkway
Richmond, British Columbia, Canada V6V2J3

Norden Systems, Inc. (United Technologies)
Dr. Marshall Greenspan
Director of Technology
10 Norden Place
P. O. Box 5300
Norwalk, CT 06856-5300

Raytheon
Harold J. Geller
Program Manager
180 Hartwell Road
Bedford, MA 01730

Westinghouse Electric Corporation
George Bendor
Manager, Radar Systems Engineering
P. O. Box 746
Mail Stop 550
Baltimore, MD 21203

2.5.4.2 Overview of Vendor-Supplied Materials

Vendor responses varied in amount and level of detail. Only unclassified information was requested from vendors. This section summarizes materials supplied by vendors in response to the survey.

ERIM

- Completed Functional Performance Characteristics (FPC) sheets describing the ERIM/ USAF (Wright Laboratories) (SAR) Data Collection System.
- FPC sheets describing the ERIM/Navy (NAWC) P-3 SAR.
- FPC sheets describing the ARPA/ERIM Interferometric SAR (to be operational July 1994).

Intera

- Completed FPC sheets describing Intera's STAR-1 SAR.
- Completed FPC sheets describing Intera's STAR-2 SAR.
- A 13-page document entitled "Response to Conceptual Requirements for a Synthetic Aperture Radar System for Oil-Spill Response."
- An 18-page brochure entitled "Intera-The Integrated Solution."
- A 10-page brochure entitled "Comprehensive Real-Time Surveillance Services, Airborne Radar: A Key Tool," describing STAR-2 and STAR-VUE, a ground-based receiving/ processing station.
- A one-page flyer entitled "Radar Services and Products."

LORAL

- A letter containing 1) a high-level summary of SAR assets including UPD-8, UPD-6, CAPRE, and ASARS-1 systems; 2) brief tables of characteristics of UPD-6 and UPD-8 systems, and 3) a table, entitled "SAR Parameters", summarizing high-level data on a number of LORAL- developed systems, including those mentioned above.
- A brochure describing the RMW-900 Reconfigurable Modular Workstation, a workstation to be integrated into mobile, real-time systems.

MacDonald Dettwiler

- A four-page brochure entitled "IRIS: Tactical & Strategic Radar Reconnaissance," describing their Integrated Radar Imaging System (IRIS).

- An 86-page brochure entitled "IRIS Reconnaissance Radar". Sections of the brochure are 1) An Introduction to Imaging Radar; 2) Applications of Synthetic Aperture Radar; 3) Features and Advantages of the IRIS; 4) The IRIS Technical Description; 5) IRIS Configurations; and 6) Integrated Logistics Support.

Norden Systems

- A completed FPC sheet for Norden's AN/APG-76 Multimode Radar System (MMRS).
- Cover letter identifying AN/APY-3 Joint STARS radar and AN/AGP-76 MMRS radar as Norden products and recommending that the USCG explore an integrated-mission sensor (one having both coarse-resolution, broad- swath capabilities and fine-resolution, narrow-swath capabilities) to meet Coast Guard requirements.
- A two-page textual addendum addressing the conceptual requirements in [15].
- A 37-page ring-bound hardcopy of Norden presentation materials entitled "Norden SAR and MTI Radar Systems," relating to both the Joint STARS and MMRS radars.
- A >100-page ring-bound hardcopy of Norden presentation materials entitled "Presentation of Norden System Advanced Technology Radar and Research and Development Activities."

Raytheon

- A completed FPC sheet for Raytheon's Millimeter Wave Attack Seeker (MAS).
- A one-page letter and attached two-page textual description of the MAS with suggestions on how the MAS might be used for oil-spill phenomenological data collection.

Westinghouse

- Completed FPC sheets describing the Westinghouse MODAR MR4000 radar system.
- A brief textual description of how the MODAR MR4000 might be modified for oil-spill monitoring.

2.5.4.3 Summary of System Functional Performance Characteristics

As mentioned previously, the amount and level of detail available on the surveyed systems varies from vendor to vendor. In one case, even though significant detail is available, not all of the details could be released publicly. The approach we have taken in summarizing system capabilities is to provide comparative information on only a subset of the performance characteristics and to attempt to do it in such a way that 1) system capabilities are fairly presented, 2) vendor requests for restricting disclosure of full details are honored, and 3) emphasis is placed on potential relevance of the capabilities to the primary oil-spill monitoring mission. Results are summarized in Table 2-4.

Table 2-4. Functional Performance Characteristics

System	Vendor	Prime Usage	Aircraft Platform	Primary Radar Operational Modes
IFSARE II	ERIM	terrain height maps	Learjet 36A	interferometric strip map
P-3/SAR	ERIM	ocean science	P-3A Orion	(X/L/C, full-pol.) strip map, spotlight, dragging spot, circle; (X/C dual-pol.) DPCA
WL-ERIM DCS	ERIM	technology demonstration	CV580	(X/Ku) strip map, spotlight, hopping spot; (X) 3-D interferometric-polarimetric fine-resolution height measurement, DPCA-polarimetric velocity measurement
UPD-8	LORAL	surveillance/ reconnaissance	RF-4C	strip map, SAR MTI
ASARS-1	LORAL	surveillance/ reconnaissance	SR-71 (inactive)	strip map and two spotlight modes
STAR-1	Intera	terrain mapping	Conquest C441	strip map
STAR-2	Intera	ice reconnaissance	Challenger CL60	strip map
IRIS	MacDonald Dettwiler	surveillance/ reconnaissance	exec.-class turbo-prop, -jet	strip map SAR; SAR true-position MTI
MMRS	Norden	air-surface target detection & weapon delivery; air-air fire control	F-4E Phantom; Gulfstream II testbed	real beam; Dopp. beam sharpening; patch SAR; 3-port clutter-suppression interferometry for true-position MTI; (also air-to-air modes)
MAS	Raytheon	air-ground seeker	A-3 (pod)	multi-beam spotlight SAR
MODAR MR4000	Westinghouse	weather detection & avoid.; navigation	Lockheed C-130 Hercules	Doppler beam sharpening; monopulse ground image; BIT/CAL

Table 2-4. Functional Performance Characteristics, continued ....

System	Frequency Band	Real-Time Imaging	Range Resolution m	Azimuth Resolution m	Cross-Track Swath km	Multi-look	Number of Units
IFSARE II	X	no[1]	2.5	0.6	10	no	being developed
P-3/SAR	L, C, X	digital	4.7[2]	4.5-12	4-9.2	no	one
WL-ERIM DCS	X, Ku	digital	2.1	1.5	~ 3	no	one
UPD-8	X	analog (film)	≥ 3	≥ 3	18.5	---	50 built
ASARS-1	---	digital	≤ 3	≤ 3	16	---	16 built
STAR-1	X	digital	8/14	6	23/46	7, pixel averaging	few
STAR-2	X	digital	18/30	18/30	2x63/104	10/15, pixel averaging	few
IRIS	X	digital	3-18	3-18	12/60	---	multiple
MMRS	Ku	digital	3-54	3-54	1.5-26	no	≥ 60 ordered
MAS	Ka	digital	3	3	0.5	no	1 built; production-ready
MODAR MR4000	X	digital	7.5-180	7.5-180	8	1-6, temporal 1-6, pix. ave	180 on order

[1]Ground processing of flight tapes at real-time rates.
[2]Resolutions selectable down to 1.5 m in ground processing.

Table 2-4. Functional Performance Characteristics, continued ....

System	Antenna Polarization	Antenna Gain, dB	Average Transmitter Power, W	Motion Compensation	Other Comments
IFSARE II	H	29	54	ground-based	
P-3/SAR	V & H	L: 16.5 C: 23 X: 27	L: 40 C: 11 X: 12	real-time	
WL-ERIM DCS	V & H	X: 29 Ku: 33	X: 100 Ku: 8	ground-based	four-port antenna
UPD-8	H	30-35	125	real-time analog	early '80s modification of UPD-4; UPD-4 is early '70s vintage
ASARS-1	H	35	1000	real-time hybrid	last unit produced in late '80's
STAR-1	H	30.5	72	real-time analog	
STAR-2	H	31	120	real-time digital	
IRIS	---	---	---	real-time digital	
MMRS	V	28-34.5 4 ports	500	real-time digital	
MAS	tx RHC rx RHC or LHC	---	---	real-time digital	antenna has 25-mrad beamwidth
MODAR MR4000	H	33	15	real-time digital	

2.5.4.4 Interpretation of Data Provided on SAR Systems

The vendor and system capabilities can be compared and contrasted in a number of different ways.

One-of-a-Kind SARs Versus Multi-Unit SAR Production

For the ERIM and Intera SAR data collection systems, only one or perhaps two systems of each type have been built. The other systems surveyed appear to have been designed for multi-unit production. UPD-8 is an early-'80s, second-generation modification of the UPD-4 (early '70s vintage). ASARS-1 production runs were completed in the late '80s. MacDonald Dettwiler literature indicates that the IRIS system is now being adapted to a number of different aircraft. Norden's MMRS and Westinghouse's MODAR MR4000 are being built to fill existing orders. One unit of Raytheon's MAS systems has been completed; however, no current production applications are identified.

Data Collections Versus Production SAR Systems as Products

Both ERIM and Intera routinely perform large data collections. Norden's Gulfstream II has also been used for data collections; however, it appears that Norden's primary (SAR) business is as an integrator and provider of SAR systems. ERIM's platform, being multi-mode, is likely used for a wider variety of different types of experiments and collections than is Intera's.

Intera's platform is more designed for a specific set of mission types, the emphasis being on broad-swath, coarse-resolution imaging of land or ice. Other vendors appear not to be in the data-collection business in any significant way and appear to focus more on the SAR system as the product. Of course more production-oriented vendors do conduct field tests, as is evidenced by Raytheon's mention of a November flight test of MAS along with the suggestion that MAS might be used for phenomenological studies of oil-on-ocean.

Broad-Swath, Narrow-Swath and Multi-Mode Systems

Intera's STAR-1 and STAR-2 systems appear to be configured principally and perhaps solely for broad-swath, coarse-resolution imaging. For example, STAR-2 can map at either 18- or 30-m resolution and can cover up to a 104-km swath. STAR-2 also provides two-sided mapping capability at 63-km swath. By contrast, the MAS and ERIM's WL-ERIM DCS are relatively narrow-swath, fine-resolution systems. Most of the other systems appear to support operation across a range of selectable resolutions and with variable swaths up to 10 or 20 km in most cases. MacDonald Dettwiler's IRIS system, which has selectable resolution from 3-18 m provides a generous 60-km swath.

Real-Time Image Formation

Most of the systems provide real-time imaging; however, the real-time images are not always the primary output product of the system. For example, for ERIM's P-3/SAR system, extensive ground processing capability extends the range of resolutions available (selectable down to 1.5 m), in contrast to more moderate real-time values (4.5-12 m). Number of range pixels processed in real-time varies significantly across the systems, as well. Some systems provide

about 400-500 pixels in range (MODAR MR4000, WL-ERIM DCS, and MMRS), while others provide thousands of range pixels in real time (P-3/SAR, 2023 pixels; STAR-1, 4096 pixels; STAR-2, 2x4096 pixels; and IRIS, estimated from available information to be between 3000 and 4000 pixels).

While the survey did not request information on specific technologies being used for image formation, discussions with several vendors indicate that parallel processing implementations (e.g. i860-based systems) are being pursued.

Systems Having Multiple Modes

A number of the systems stand out because of the number of modes they support. ERIM's P-3/SAR and WL-ERIM DCS employ a variety of cutting-edge modes, including full polarimetrics, spotlight, circle, 3-D interferometry (for height measurement), and DPCA for velocity measurement. MacDonald Dettwiler's IRIS boasts a true-position MTI mode that puts movers in their proper position on the SAR map. IRIS literature explains that this is done using a unique Doppler processing technique that provides an accurate estimate of a moving target's position. It is not stated whether a single antenna phase center or multiple phase centers are used. Norden's MMRS employs a three-phase-center interferometric MTI technique to put the movers back to their true positions. These true-position MTI techniques are certainly relevant to the Coast Guard mission of imaging moving ships.

System Size

Although not tabulated above, numbers on estimated system volume, in m^3, were obtained from five of the seven vendors. The smallest numbers (less than 0.1 $m^{3)}$ were for MAS and the MODAR MR4000; however, these numbers did not include volume for operator control, display, or recording equipment. MMRS is about 0.25 m^3; ASARS-1 is about 1 $m^{3;}$ UPD-8 is about 1.3 m^3; STAR-1 is about 1.5 m^3; STAR-2 is about 2.4 m^3; and ERIM's P-3/SAR and WL-ERIM DCS are estimated to be about 4 m^3 each. These numbers are very rough, but there is a clear trend toward larger volume for systems that either cover larger swaths, possess multiple modes, or are testbed systems as opposed to production systems.

System Input Power Required

Estimates of required input power for some of the systems were also obtained. MAS input power is about 800 W; MODAR MR4000 is 1.2 kW; STAR-1 is 4 kW; UPD-8 is 4.8 kW; ASARS-1 is 5.7 kW; STAR-2 is 9 kW; and MMRS is 7 kW.

System Replication Costs

The survey requested estimates for cost of replicating existing systems, including fabrication, laboratory integration, and testing of radar and motion compensation subsystems, but not including any platform integration. Rough order-of-magnitude estimates varied from as little as $1 M for to as high as $30 M. It is understandable that several of the vendors did not feel they could adequately respond to this question without a more complete statement of system requirements.

System Sensitivity Data

Although the survey requested data on minimum detectable scattering coefficient for the system, evaluation of the information revealed that it would be difficult to compare the systems on this basis.

2.6 DISCUSSION OF COST VS. BENEFIT OF SAR

Any discussion of cost vs. benefit for a SAR system will be based on both quantitative and qualitative information. Specific technical issues such as component cost, benefits of size and weight, and maintenance cost can generally be quantified. Issues such as "image quality" or "image acuity" are based on the judgement of human experts and are much more qualitative. In this section, we strive to assess both qualitative and quantitative costs and benefits. We also summarize issues previously discussed in Section 2.4.2 that are important when comparing and contrasting SAR and SLAR.

2.6.1 Image Quality Benefits, SAR vs. SLAR

The most fundamental question is whether SAR imagery provides benefits to oil-spill image analysts that SLAR imagery cannot. The answer seems to be based primarily on the issue of spatial resolution. Do increased spatial resolution and constant (not a function of range to the scatterer) spatial resolution, help the analyst? The consensus of the workshop participants is that increased spatial resolution, beyond that of the existing SLAR resolution, would be a benefit. If a *finer* spatial resolution, i.e. finer than the best (near-range) SLAR resolution the AIREYE is capable of producing, is perceived as a benefit, then it stands to reason that SAR imagery would be a benefit compared to SLAR imagery. Several comparison SAR and SLAR images have been included to make this point. Figure 2-27 shows a SAR image from the Nov. 12, 1992, experiment with a ROI designated just off Coal Oil Point. The ROI is shown in Figure 2-28 at full resolution. Note the clear definition of wind rows (upper portion of Figure 2-28), the detail in the emulsified oil forming an arc (upper-left portion of Figure 2-28), and the distinct texture of kelp in the same region. Now, examine Figure 2-29 and Figure 2-30. Figure 2-29 shows the SLAR image from which the ROI in Figure 2-30 was extracted. The SLAR image was captured roughly 1 hour before the SAR image[1]. The ROI in Figure 2-30 was also magnified by a factor of 10 (with pixel replication) so that features in the SLAR image have roughly the same size as features in the SAR ROI (Figure 2-28). Note the absence of detail in the wind row region (upper portion of Figure 2-30). The arc of emulsified oil has moved right in the SLAR image so that it is positioned against the left edge of the wind row region. It is barely resolved in the SLAR image. The kelp does not have a texture distinct from the sea returns near shore.

Another SAR/SLAR comparison example is shown in Figure 2-31 through Figure 2-34. Figure 2-31 shows the SAR image from which the ROI in Figure 2-32 was extracted. Note the clear definition of the wishbone-shaped return from emulsified oil (bottom of Figure 2-32). The

1. A better point-by-point comparison of ocean features can be made between this SAR image (Nov. 12, south-looking) and the Nov. 12, west-looking SLAR image. These images differed in time by only 30 min. This comparison was not used here because it portrays an optimal SAR imaging geometry (antenna looking along wave crests) against a suboptimal SLAR imaging geometry (poor azimuth resolution due to far-range imaging) which could unfairly bias the reader in favor of SAR imagery.

(This page intentionally left blank.)

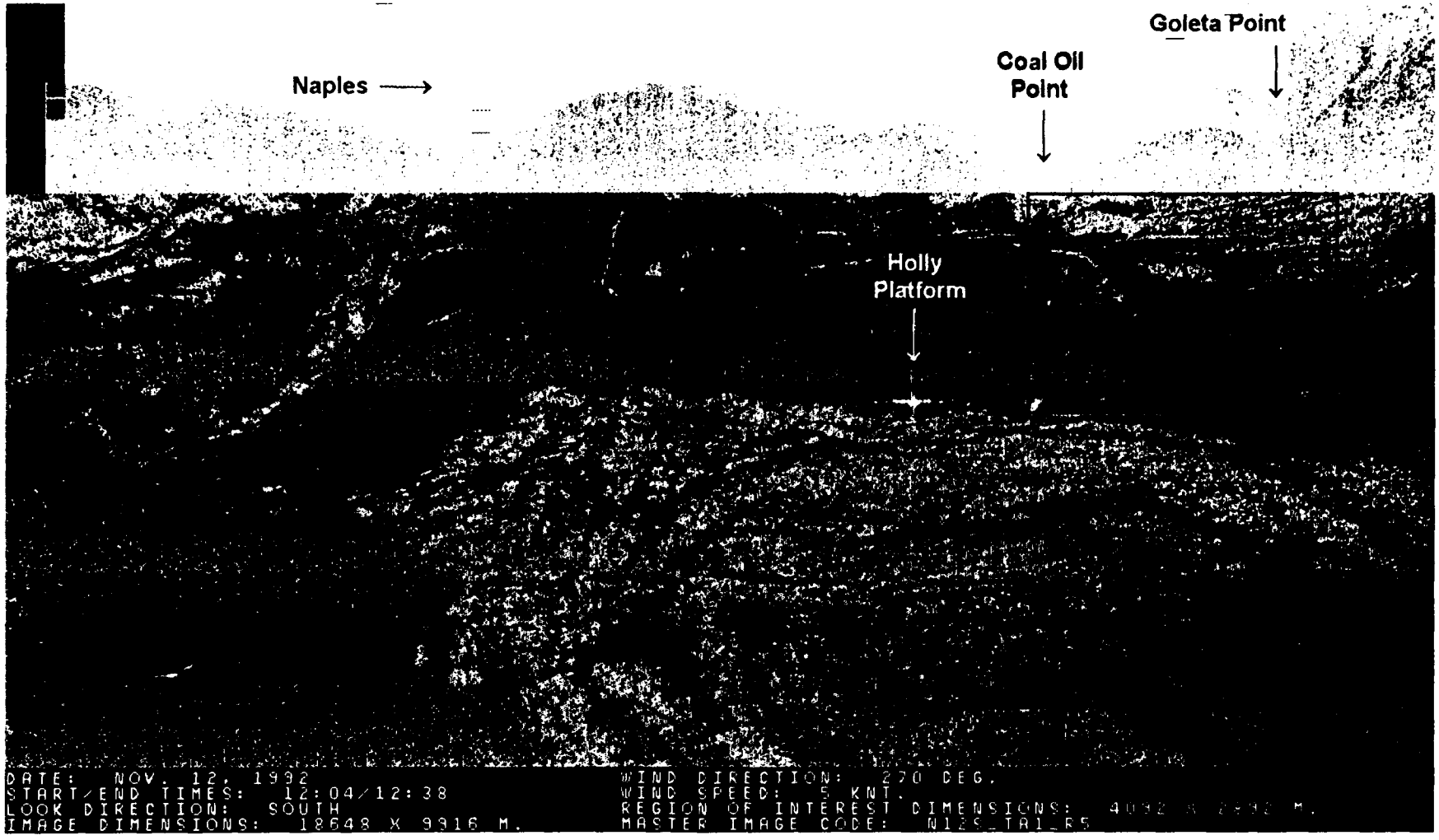

Figure 2-27. Full-swath SAR image from the Nov. 12, 1992, experiment.

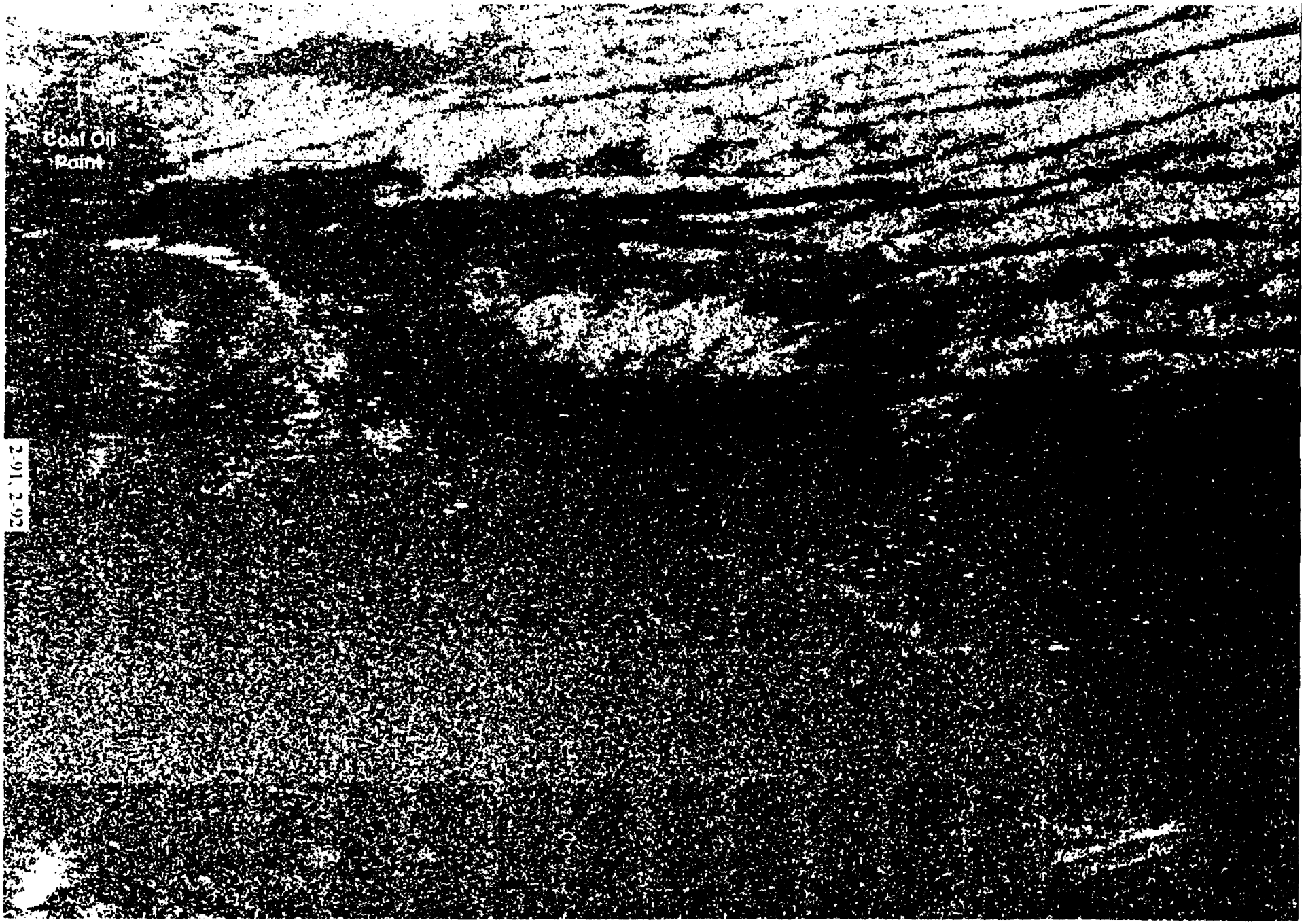

Figure 2-28. ROI extracted from the full-swath SAR image. Compare this ROI image with the SLAR ROI image in Figure 2-30.

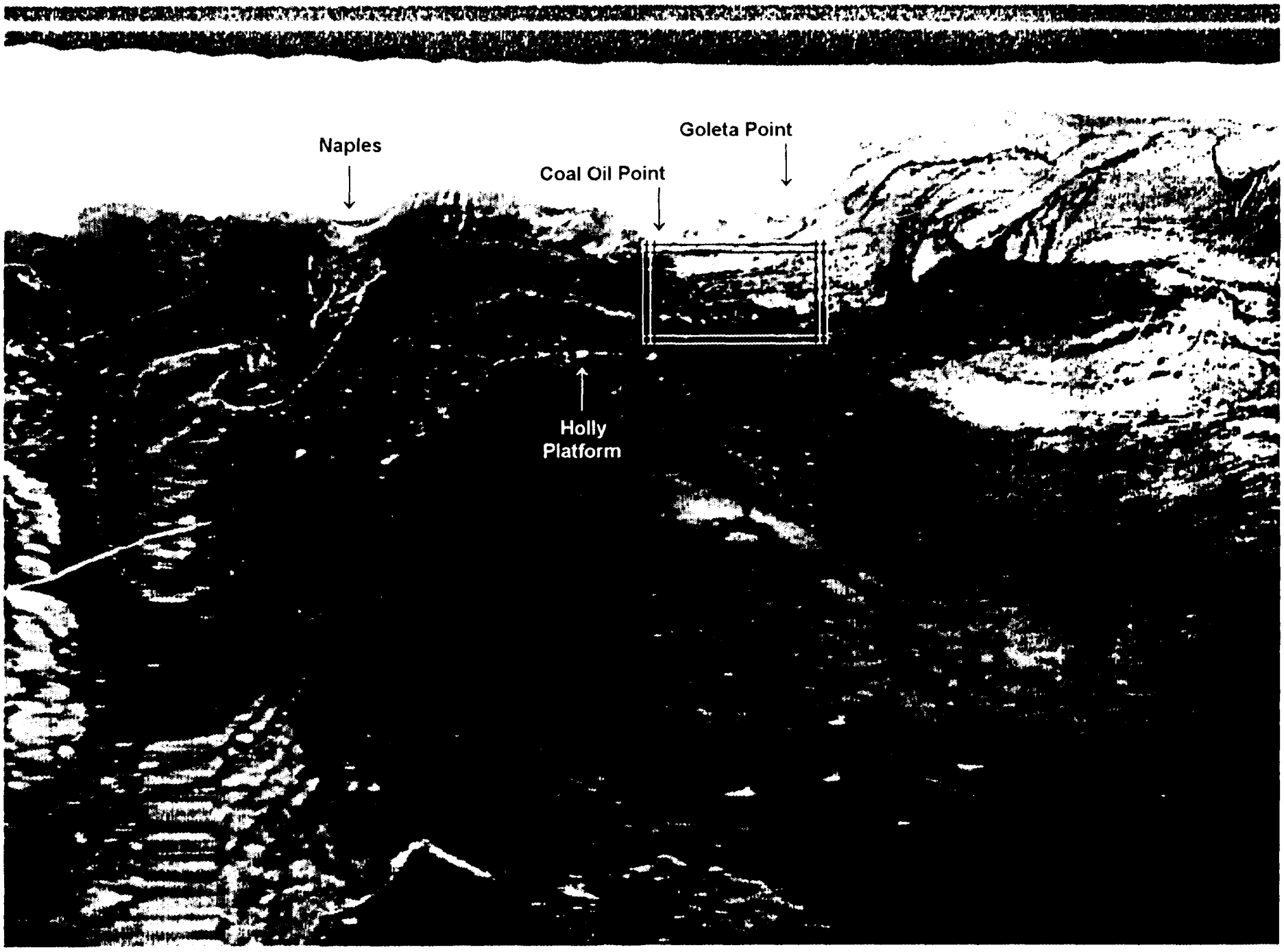

Figure 2-29. Wide-swath SLAR image from the Nov. 12, 1992, experiment.

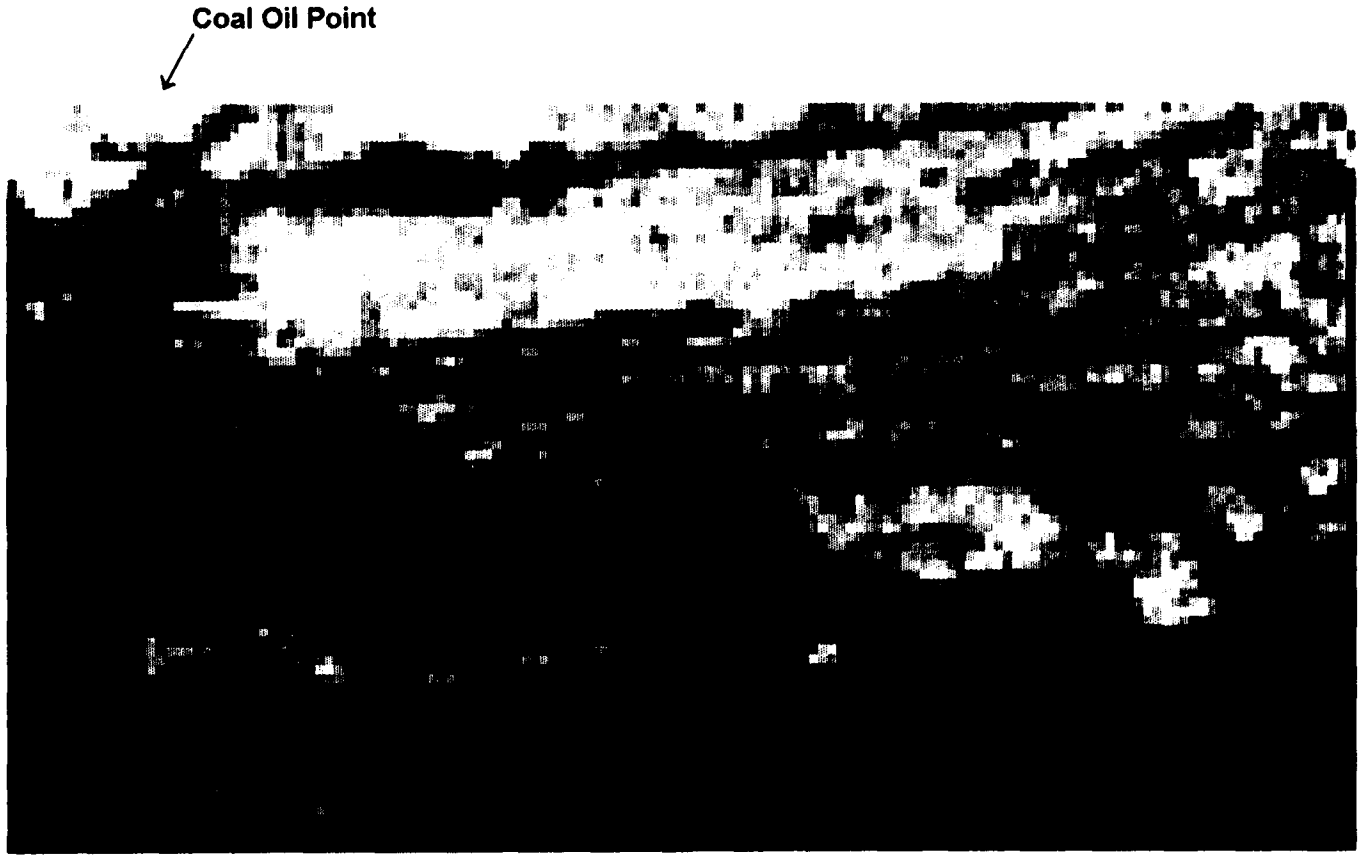

Figure 2-30. ROI extracted from the wide-swath SLAR image. This image has been magnified with pixel replication so that the features have roughly the same size as those in the SAR ROI image in Figure 2-28.

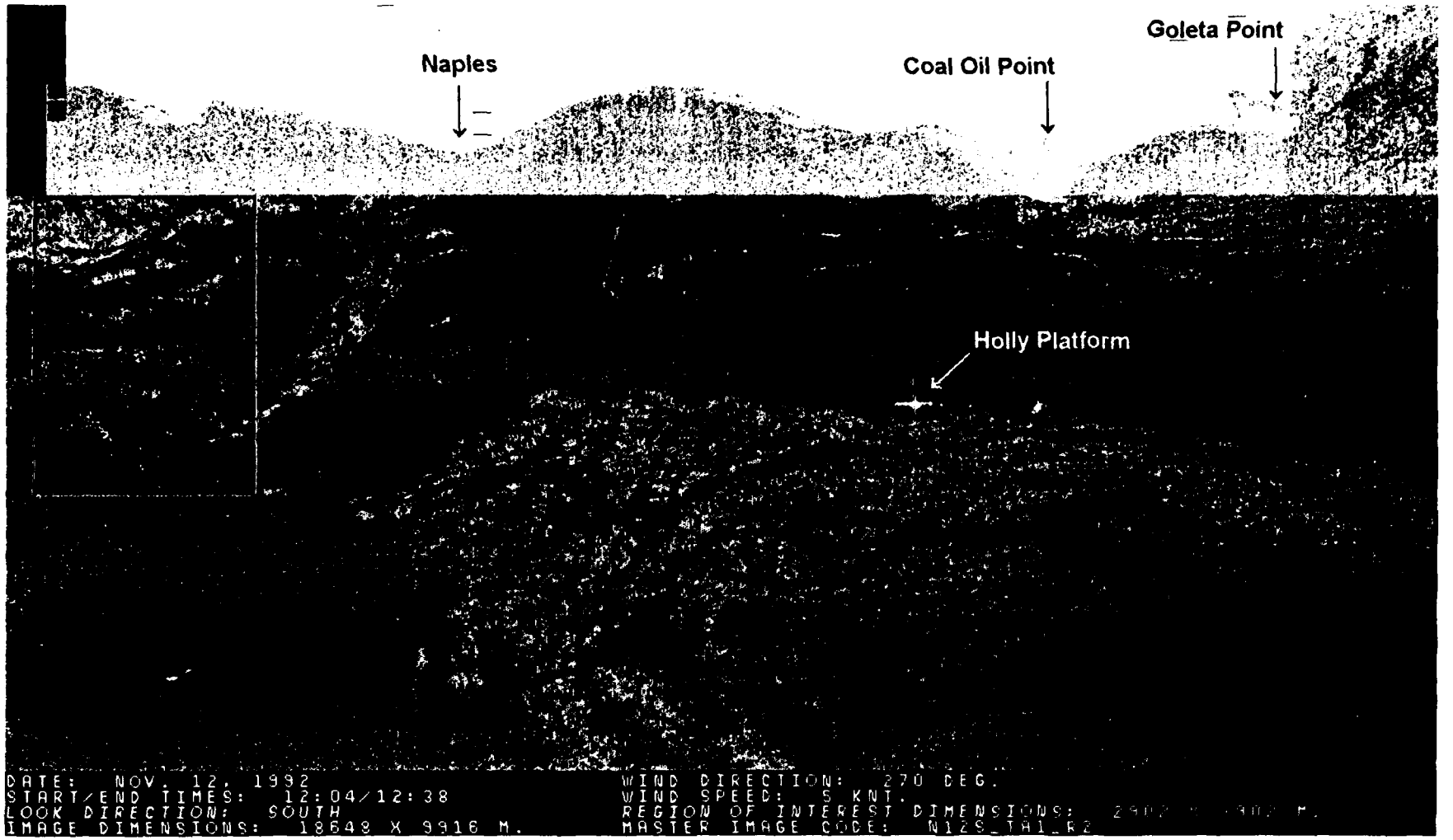

Figure 2-31. Full-swath SAR image from the Nov. 12, 1992, experiment.

Figure 2-32. ROI extracted from the full-swath SAR image.
Compare this ROI image with the SLAR ROI image in Figure 2-34.

same feature is visible in the SLAR ROI. Figure 2-33 shows the full scene from which the SLAR ROI was extracted, and Figure 2-34 shows the ROI magnified (by pixel replication) so that features are roughly the same size in both the SAR and SLAR ROIs. The wishbone-shaped return has changed some in the time between the SAR and SLAR images, but the wishbone is still quite visible in the SLAR ROI. Detail in the wishbone structure and details in the vicinity of the isolated point scatterers near the wishbone are much better defined in the SAR ROI (Figure 2-32) than in the SLAR ROI (Figure 2-34).

The disadvantage of azimuth resolution being a function of range in SLAR images can also be emphasized by looking at two SLAR images from Nov. 12, 1992. Figure 2-35 is a south-looking SLAR image of the test area. Near-range is at the top of the image. Figure 2-36 is a west-looking SLAR image of the same test area. Near-range is on the right edge of the image. In Figure 2-35, one can see 4 bright isolated scatterers (ships) near the bottom of the image, all at roughly the same range. The azimuth side-lobes actually overlap. In Figure 2-36, the same 4 bright scatters are visible on the upper-right edge of the image. Notice that the width in azimuth (measured vertically) of the brightest parts of the 4 scatterers (the main lobes) is greater for the scatterer farthest in range (left-most) than for the scatter nearest in range (right-most). These scatterers are actually about the same size, but the degradation in azimuth resolution as a function of range makes the far-range scatterers appear larger than the near-range scatterers. In Figure 2-35, these 4 scatterers are all at the same range, but they are far away in the range dimension, so they are all 4 poorly resolved in azimuth (measured horizontally).

It is also beneficial to compare the south-looking and west-looking SLAR images globally to assess the impact of azimuth resolution degradation with increased range. These two images were captured within a few minutes of each other, so the ocean features remain essentially the same in both images. Begin with the west-looking SLAR image. Note the detailed sea return on the southeast (lower right) side of this image. Now, compare this with the south-looking SLAR image. All this detail is lost due to spatial resolution degradation with increasing range. This effect does not occur in SAR images. Also, compare the west (left) side of the west-looking SLAR image to the west (left) side of the south-looking SLAR image. Near-range features in the south-looking image are retained, but these same features are absent in the west-looking image.

The benefit in image quality with SAR is clear, but this benefit is bought at a nontrivial cost. Most of the trade-offs have already been mentioned in detail, but to summarize, the SAR costs are a more complex hardware and software system, greater volumes of data to be processed and archived, and artifacts due to motion within the scene during aperture synthesis. The following subsections present a detailed look at those costs and benefits that can be quantified.

2.6.2 Identified Technical Benefits of SAR

A number of technical benefits of SAR have been identified and discussed, in detail, in Section 2.4.2. We list those benefits below

- Improved azimuth resolution (up to a factor of about 75 at 54-km range). It must be noted that, as discussed, in detail, in Section 2.4.2, ocean-wave movement can significantly defocus the SAR image in the azimuth dimension.

(This page intentionally left blank.)

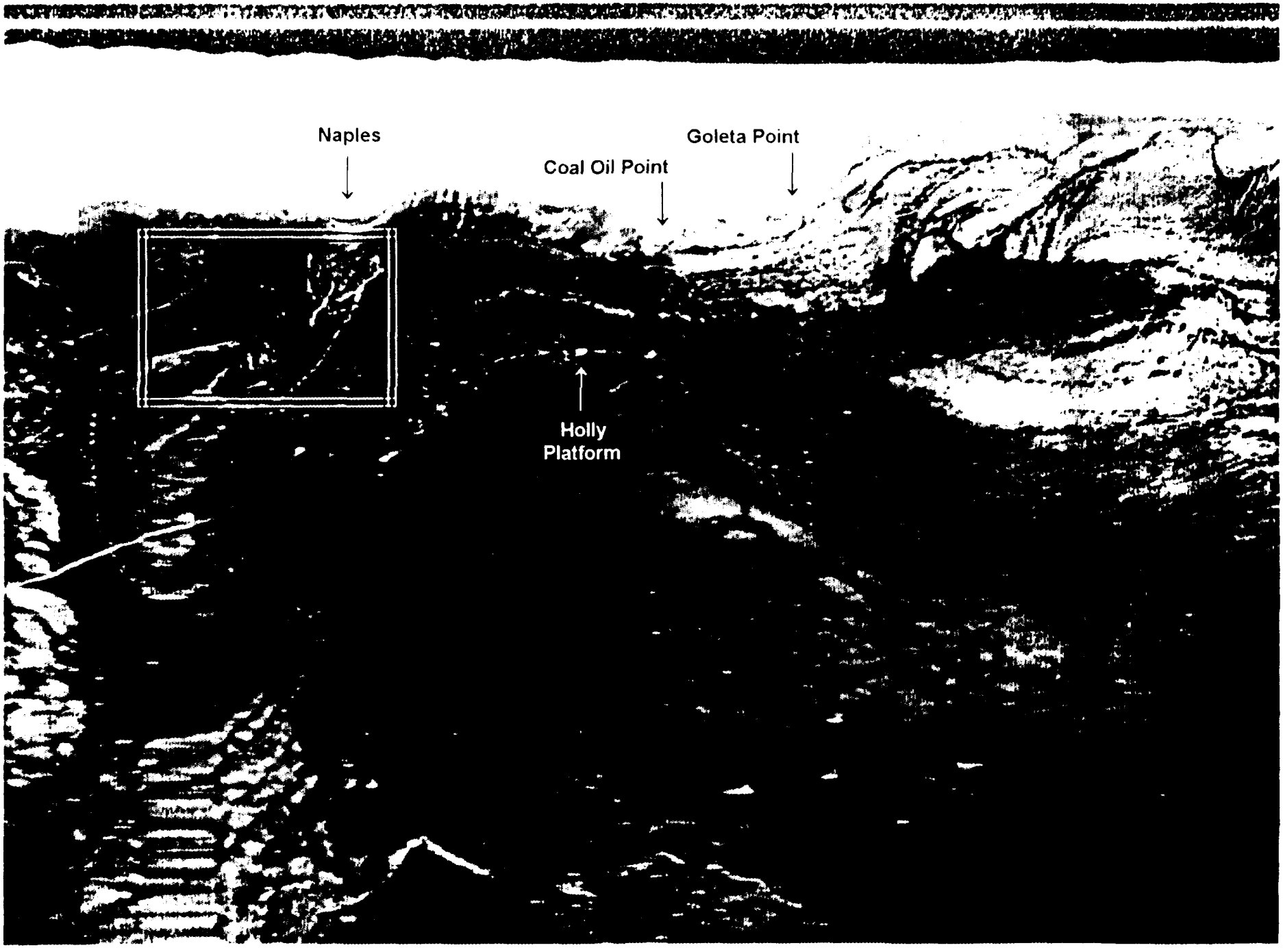

2-103, 2-104

Figure 2-33. Wide-swath SLAR image from the Nov. 12, 1992, experiment.

Figure 2-34. ROI extracted from the wide swath SLAR image. This image has been magnified with pixel replication so that features have roughly the same size as those in the SAR ROI image in Figure 2-32.

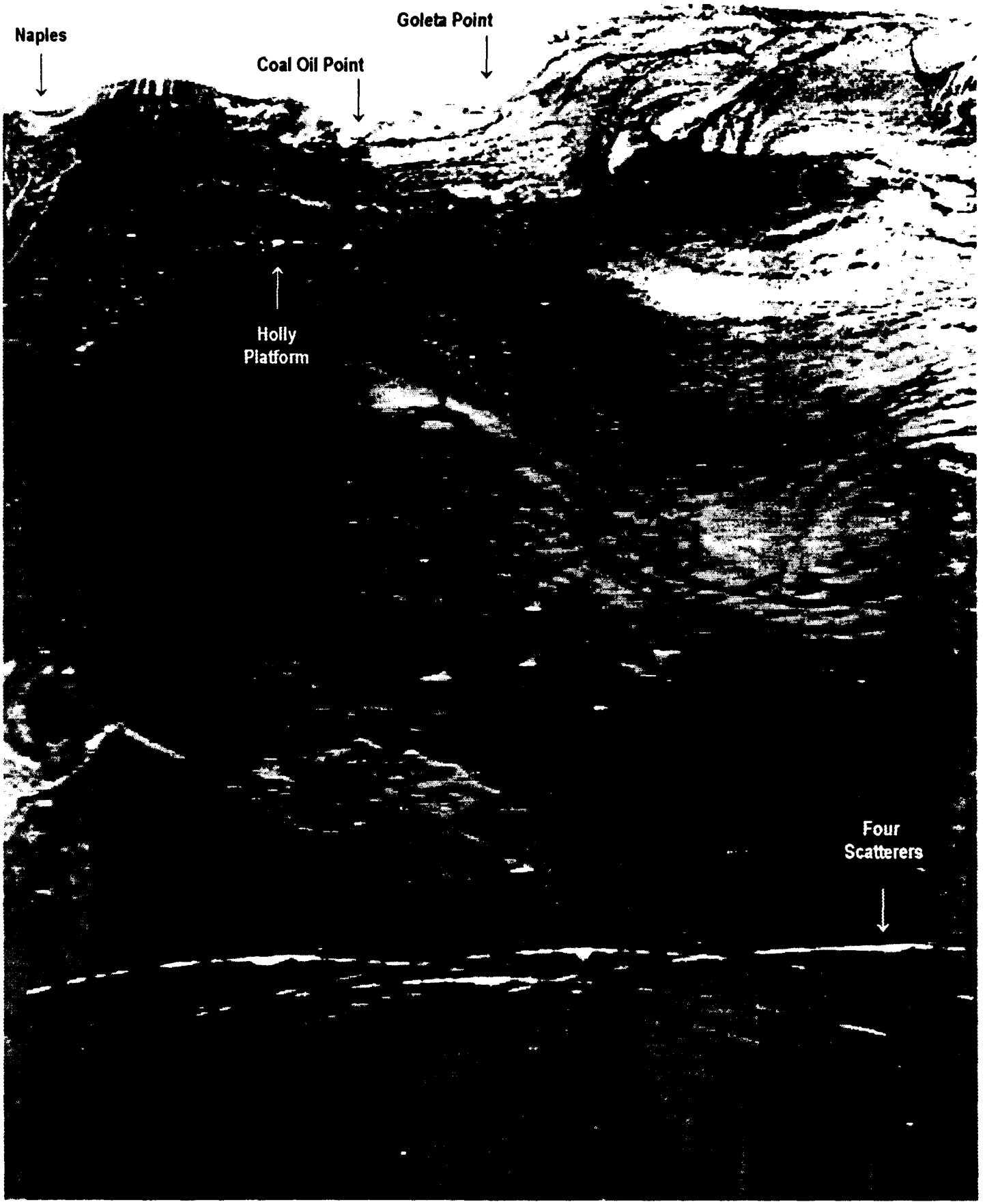

Figure 2-35. South-looking SLAR image from Nov. 12, 1992.

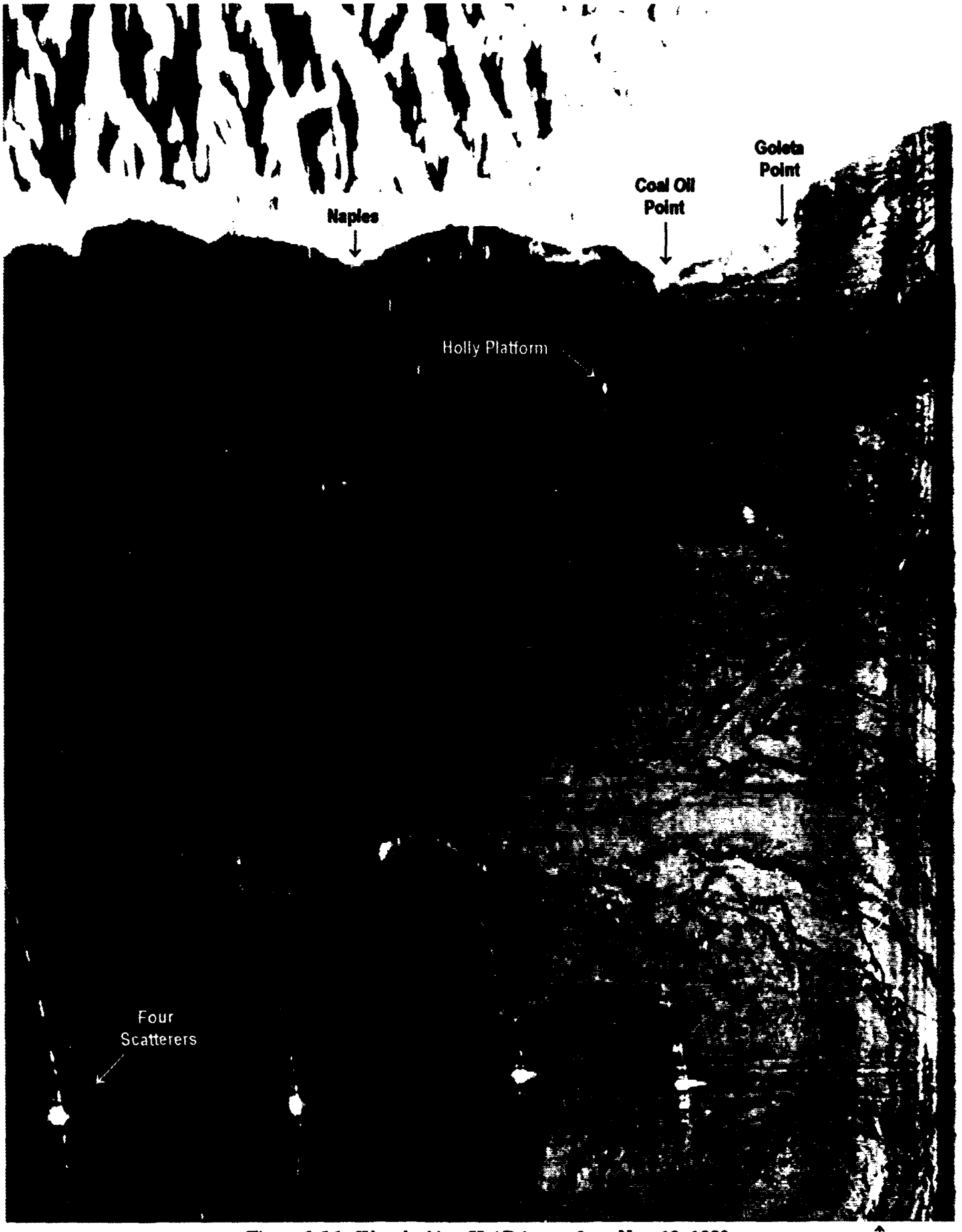

Figure 2-36. West-looking SLAR image from Nov. 12, 1992.

- Constant azimuth resolution achievable over a wide swath (not possible with SLAR), ignoring azimuth defocusing effects due to wave motion.
- Constant number of looks achievable over a wide swath.
- Better sensitivity in terms of minimum-detectable target-cell radar cross section.
- More precise image-registration knowledge.
- Smaller (about 1 m long), steerable antenna is feasible.
- Superior performance, in SAR MTI mode, against moving ships (10's of dB better performance than SLAR).

2.6.3 Rough Estimates of Coast Guard SAR Size, Power, and Cost

Table 2-5 gives rough estimates of physical volume, input power, and development and replication costs for a new-design Coast Guard SAR. Cost estimates are for SAR hardware and software only and do not include costs for aircraft integration, flight testing, ground processing, or data analysis. The estimates have been made under the assumption that significant miniaturization of radar circuitry is not required. The following paragraphs discuss notable information that can be derived from Table 2-5.

Physical Volume

The largest components of the SAR will be the antenna/gimbal/front-end assembly, the image displays, and the image former. Even with modular design, cabling will occupy significant volume. Total estimated system volume, discounting radome volume, is about 1.4 m^3. For this estimate, the antenna is assumed to have 2° azimuth beamwidth (therefore the antenna is only about 1 m long).

Based upon these estimates and the known size of the AIREYE SLAR, the following observations can be made.

1) A new SAR can be economically designed to be about the same size as the AIREYE SLAR.

2) Although portions of the SAR could be further miniaturized (e.g., the phase-history assembly and the image former), many of the larger system components could not be easily miniaturized. Miniaturization of the identified components would increase costs significantly. Therefore, it does not appear to be cost effective to further miniaturize beyond the size estimates given in Table 2-5.

The conclusion is that there is no significant difference, proposed SAR vs. AIREYE SLAR, with regard to physical volume occupied by the radar.

Table 2-5. Rough Estimates for New Coast Guard SAR[1].

Module	Volume m^3	Input Power, W	First-Unit Cost ($k)	Replication Cost ($k)	Commercial Availability
antenna	0.1	---	300	30	may be available
radome	0.25	---	100	10	custom; easy follow-on fabrication
gimbal	0.03	200	250	120	new development
IMU	0.02	15	250	150	available with minor modification
rf front end	0.002	10	170	50	custom
transmitter	0.01	1300	280	150	tube available; design housing, p.s.
ph collector	0.06	200	3000	500	some custom digital; all custom SW
image former	0.1	100	1000	250	custom power supply; other available
data recorder	0.15	100	500	50	custom power supply and software
image buffer	0.003	20	100	15	some custom HW/SW
full-swath display	0.2	100	35	25	available
host computer	0.07	50	100	30	available; some custom boards
host display	0.1	100	15	10	available
host software	---	---	700	---	custom; built on commer. op. sys.
printer	0.07	30	5	5	available
TM interface	0.002	5	50	5	may be available
ext. pwr supplies	0.03	50	50	20	some custom
cables	0.2	0	50	10	some custom
ext. I/O module	0.01	10	50	10	custom
racks, mechanical	---	---	200	35	some custom
built-in test	---	---	700	---	some custom HW; custom SW
lab test equipment	---	---	750	---	some custom; located at vendor
system design	---	---	200	---	
analysis/simulation	---	---	350	---	
documentation	---	---	300	---	
proj. mgmt & admin.	---	---	1000	200	
lab. integration	---	---	1000	250	
30% error allowance	---	---	3500	575	
totals	1.4	2290	15000	2500	

[1]Costs are for SAR hardware and software only and do not include aircraft integration, flight testing, ground processing, or data analysis. We believe development costs shown to be conservative in that they assume a) minimal reuse of existing vendor designs, b) conservative labor rates, and c) the 30% allowance for error explicitly included. We believe replication costs shown to be less conservative.

Required Input Power

Major power dissipation will occur in the transmitter, phase-history collector, image former, and gimbal. Total estimated power dissipation for the system is about 2.3 kW.

Based upon these estimates and inspection of the AIREYE SLAR specifications, it appears that required input power for the proposed SAR would be very similar to that of the AIREYE SLAR.

The conclusion is that there is no significant difference, proposed SAR vs. AIREYE SLAR, with regard to estimated input power requirements.

First-Unit Development Cost

Major contributors to SAR development cost are the phase-history collector ($3M) and the image former ($1M), identified earlier in this report as the most complex portions of the SAR. Other major items include the gimbal, the data recorder, host software, transmitter, antenna, and gimbal. Total estimated first-unit development cost is about $15M

Replication Costs

Replication cost estimates are, in most cases, between 10% and 30% of development costs. For example, the major cost of the image former will be software, which is a non-recurring cost, so replication cost is about 25% of development cost in this case. On the other hand, for the transmitter, the combined replication costs of the TWTA and the power supply by themselves represent a significant fraction of the transmitter's development cost. Therefore, replication cost of the transmitter is a higher percentage of development cost, being about 50%. Total estimated replication cost for the SAR is about $2.5M.

Costs of SAR vs. Costs of SLAR

As pointed out in Section 2.4.2, the SAR brings added complexity (in comparison with the SLAR) is the following modules.

- IMU: higher accuracy required
- Gimbal mounting and control: more degrees of freedom.
- IF processing and digital prefiltering (in PHC).
- Navigational computations for motion compensation and antenna pointing control (not identified previously as an item of added complexity).
- Image former (not required for SLAR).

From the items costed in Table 2-5, it is clear that the additional costs associated with developing a Coast Guard SAR (vs. developing a SLAR) number into the millions of dollars. For example, assuming the costs of the five items listed immediately above are in excess of what would be

required to develop a SLAR, this additional development cost is estimated to be between $2M and $3M.

Also, replication costs for the SAR will be higher. For example, doing the same computation, but this time using corresponding replication costs, leads to the conclusion that replication costs of these "additional" capabilities, which are necessary for SAR, amount to between $400k and $500k per system, or roughly 20% of the replication cost of the complete SAR system.

2.6.4 Discussion of Other Identified Costs of SAR

Additional costs will be incurred in operator training and system maintenance. To minimize training and system maintenance costs, SNL recommends that certain philosophies, discussed below, be embraced in the design and implementation of any new SAR system. The following discussion also presents, where appropriate, estimates of costs (either absolute or relative) associated with training and maintenance.

Design for Operability. The SAR could and should be designed to maximize ease of operation. The number of options available to the operator should be minimized to a small, necessary set. Unlike the case of an R&D SAR system, for which nearly all parameters (resolution, geometry, swath width, etc.) can be varied under the direct control of the operator, a Coast Guard SAR system should be optimized to a point design. Major SAR parameters (resolution, prf, etc.) should be fixed, and necessary changes in parameters due to changes in imaging geometry should be automatically computed by the host computer or the radar-control and mocomp computer in the phase history collector assembly. Reconfiguration and self-test of the radar should be automated to avoid complicating the operator interface. The operator interface for control of the radar and display and processing of ROIs should be windows-driven and built atop a standard commercial operating system.

Operator Training Costs. It is SNL's assessment that the SAR and its operator interface can be designed in such a way that the system can be effectively operated by enlisted Coast Guard airmen who undergo a classroom training program of the order of 2 to 4 weeks followed by in-flight training amounting to the equivalent of about 5 to 10 missions. Periodic (perhaps yearly) abbreviated retraining should be conducted for SAR system operators. Classroom training could include experience with a SAR simulator that could use a number of components of the operational SAR. At a minimum, the simulator should include the full-swath display, host computer, printer, and data recorder. This minimal simulator would allow images to be viewed and ROIs extracted and manipulated. In summary, given that the system is designed properly, ease of operability should not be a weak point of a new Coast Guard capability. Estimates of system development cost presented in Table 2-5 include costs for implementing the above-described system design features that would minimize training costs. Table 2-5 does not include costs of a simulator or costs for training of Coast Guard personnel.

Design for Testability. The SAR should also be designed to include a significant number of self-test and diagnostic functions. It is possible to design the SAR with a built-in test capability that allows radar circuit inputs to be stimulated using internally generated test signals and circuit outputs to be sampled and monitored by the radar control and mocomp computer. Results of

diagnostic testing could be reported to the operator or technician on the host computer screen. Basic built-in test functions could be exercised at the beginning and end of a mission, and more extensive and detailed test functions could be used during trouble-shooting operations when the system is known to be malfunctioning.

It is SNL's assessment that the SAR could be designed so that a large percentage of potential fault conditions could be detected during routine self-test and that trouble-shooting down to the board level could be done using built-in-test hardware and software designed into the system. This built-in functionality would allow troubleshooting operations that otherwise may not have been feasible to be efficiently performed by Coast Guard personnel. Use of the built-in test philosophy should lower long-term maintenance costs by cutting trouble-shooting time and reducing the need for open-setup type diagnostic equipment (scopes, logic analyzers, etc.). This would result in maintenance procedures that are simpler and more automatic than those now used to maintain the AIREYE SLAR.

Design for Maintainability. In addition to incorporating the built-in test features described above, designing for maintainability involves prudent decisions about how modules are designed and built; which components, subassemblies, and assemblies will be spared; and where (e.g., air station, prime SAR contractor, SAR subcontractor, or component vendor) repair and replacement of components will occur.

Maintenance Technician Training Costs. Maintenance personnel should first undergo the 2 to 4 weeks of operator training specified above. SNL estimates that approximately 4 weeks of additional training would be required for a technician to become proficient at installing/de-installing SAR equipment in the airplane; using system diagnostics; disassembling and assembling line replaceable units (in most cases, to the board level); and performing any required manual or open-setup testing at either the system, line-replaceable-unit, or board levels. Periodic (perhaps yearly) abbreviated retraining should also be conducted.

A Suggested Approach to Maintenance Schedules. As stated above, power-up and pre-power-down diagnostics should be designed into the SAR system. A reasonable approach to periodic maintenance would be to have a technician perform detailed, on-plane diagnostic tests once every 20 hours of system operation or at least once every two weeks, whichever comes first. The entire system might be removed from the plane once every six months for visual inspection and ground-based testing at either the system or subsystem level.

Mean Time Between Operational Failures. The proposed periodic diagnostic checks should help reduce the number of failures that occur during a mission. It is difficult at this point to estimate reliability of a new SAR. Certainly, this should be one of the design requirements specified at the time of acquisition of the system.

(This page intentionally left blank.)

CHAPTER 3
CONCLUSIONS AND RECOMMENDATIONS

3.1 CONCLUSIONS

Seven fundamental questions were posed by the U. S. Coast Guard and NOAA HAZMAT at the beginning of this project. The goal of this project has been to answer as many of these questions as possible. Here are the questions and their best answers as a result of this study.

- *Do finer resolutions make it easier for image interpreters to differentiate false positives from oil slicks?*

  Yes. (See Section 2.3.2.)

- *At what resolution is the optimum benefit gained?*

  A spatial resolution of 10 m per pixel is adequate, or slightly better than adequate. This spatial resolution provides a nice trade-off between resolution for detailed feature analysis and full-swath coverage (25 nmi) that can be achieved practically. Full-swath data sets will be large, but manageable with current technology. (See Section 2.3.2.)

- *How well does SAR bring out edge details for the interpreter, relative to SLAR?*

  Edge sensitivity, from the perspective of the scattering cross-section, is slightly higher with the SAR, but for the most part it is comparable to that of the SLAR. Increased resolution in the SAR, however, provides more edge detail. (See Appendix A, Appendix D, and Section 2.3.2.)

- *How is this "acuity" affected by wind speed, look direction, and apparent slick thickness/ oil state?*

  There was not enough variation in wind speed during the experiment to measure the effect of wind speed on acuity. Acuity is degraded somewhat when the SAR images across wave crests (up-wind or down-wind) as opposed to along wave crests (cross-wind), but this degradation can be minimized by using higher aircraft speed and/or flying passes that transmit perpendicular to the dominant wave fronts. This degradation only affects rapidly moving objects such as waves, but can indirectly affect detail at wave/slick boundaries. Acuity does not appear to be a function of oil-slick thickness. Changes in acuity as a function of oil state are similar in SAR and SLAR. For example, emulsified oil creates isolated specular returns when imaged against a calm sea. It can also trap flotsam that returns more energy to the radar antenna. (See Sections 1.3.1 and 2.3.2.3.)

- *How well does the SAR differentiate between ocean clutter and oil slicks?*

  As well, if not better, than SLAR. (See Section 2.4.2, Appendix A, Appendix D, and Appendix G.)

- *How sensitive is the SAR to oil thickness?*

  There appears to be no correlation between oil thickness and SAR returns. The behavior of a SAR is identical to a SLAR regarding oil thickness. Compare SAR and SLAR images in Chapter 2 for confirmation.

- *What are the wind speed cutoffs for the SAR, relative to the SLAR?*

  This question remains unanswered. There was not enough variation in wind speeds during the Santa Barbara experiments. We have no reason to believe that there should be a significant difference in wind speed cutoffs between the SAR and the SLAR.

3.1.1 Benefits and Cost Effectiveness Offered by SAR and SLAR

The benefits and cost effectiveness offered by SAR and SLAR are summarized in Table 3-1. Cells of the table having a "(+)" in them signify a positive attribute while cells having a "(-)" in them signify a negative attribute. Notice that there are two columns for SLAR. The first SLAR column (column 2) identifies attributes that apply to SLAR in general. Some attributes may apply to generic SLAR systems, but are not applicable to the existing AIREYE SLAR. For this reason, the column heading is "Generic SLAR or Modified AIREYE SLAR". The second SLAR column (column 3) identifies attributes applicable to the existing AIREYE SLAR.

3.1.2 Critical SAR Parameters

Our analysis has shown that it is feasible to design and build a SAR using existing component technology that has 10-m resolution and that covers a broad, 25-nmi swath. There appear to be no insurmountable technical barriers; however, some prudent trade-offs are required in order to achieve the desired system characteristics. The following critical SAR parameters were identified during the SAR parameters analysis. For each critical parameter, we summarize the conclusions of the SAR parameters analysis.

Antenna size

The analysis showed that, for a SAR, if the azimuth beamwidth is set at about 2°, the antenna can be made small enough that it can be steered. The advantage of this is that the antenna can always be pointed at 90° squint. Therefore, no geometrical rectification of the image will be required to correct for squint-mode operation.

Transmitter power

With the shorter antenna (azimuth beamwidth of 2°) and with 10-m resolution, required peak transmitter power will be between 300 and 400 W (average power will be between about 40 and 50 W). These power levels are readily achievable and are very close to levels specified for several of the surveyed vendor systems. Attempting to push peak transmitter power above several kW would significantly increase cost of the transmitter and drive up overall power requirements for the system.

Table 3-1. Advantages and Disadvantages of SAR and SLAR

Attribute	SAR	Generic SLAR or Modified AIREYE SLAR	Current AIREYE SLAR
az. resolution	(+) superior (10 m)	(-) inferior (by factor of >50)	(-) inferior (by factor of >50)
az. resolution	(+) constant over swath	(-) coarsens over swath	(-) coarsens over swath
az. defocusing	(-) yes	(+) no	(+) no
sensitivity	(+) superior	(-) inferior to SAR, amount unspecified	(-) inferior; 15-20 dB worse than SAR
registration knowledge	(+) superior	(-) inferior	(-) inferior
steerable antenna	(+) yes	(-) no	(-) no
images movers	(-) MTI mode req'd	(+) yes; SLAR MTI mode possible	(+) yes; but no MTI mode
signal/clutter on movers	(+) SAR/MTI is superior	(-) SLAR MTI inferior to SAR MTI by 15-20 dB	(-) real-beam mode inferior to both SAR MTI & SLAR MTI
complexity	(-) most complex	(+) least complex	(+) least complex
physical size	1.4 m^3	about the same	about the same
input power	several kW	$\geq$ several kW	several kW
development cost up to lab integration	(-) about $15M	(+) about $12M	(++) easy modification to obtain digital data
replication cost up to lab integration	(-) about $2.5M	(+) about $2M	(-) sunset technology

Image Resolution

Desired resolution for a future Coast Guard SAR is 10 m. Coarser resolution hinders the image interpreter's ability to see detail in the image. Refining resolution further increases system cost and/or impacts system sensitivity. For example, asking for the same 25-nmi swath at 3-m resolution would drive required transmitter power to an unacceptably high level. Further, at this refined resolution, data recording requirements would be placed well beyond the capabilities of a commercial 4-mm tape unit.

Operating Frequency

Operation in the X band appears to be best. Oil/open-ocean contrast may be slightly better at Ku band than at X band; however, at Ku band, required transmitter power would be higher, and high-power sources are not generally available at Ku band. Further, atmospheric absorption and rain-attenuation effects are more limiting at Ku band.

Pulse-Compression Technique

Pulse compression using a SAW device is recommended, because this eliminates the need to perform digital compression. If it is not feasible to compress the relatively long transmitted pulse (57 μs), the transmitter pulse can be shortened, and the peak transmitter power can be increased accordingly to maintain system sensitivity while keeping average transmitter power constant.

Image-Formation Algorithm

The general image-formation algorithm approach described in Section 2.5.3.8 varies the size of the synthetic aperture as a function of range in order to allow azimuth resolution to remain approximately constant across the wide swath. Also, Section 2.5.3.7 describes how multi-look processing can be performed while keeping the number of looks approximately constant across the swath. These features appear to be important and desirable, and these general approaches should be applied to any new SAR design for the Coast Guard.

3.1.3 Benefits of Image Processing Techniques

Some of the full-resolution SAR regions-of-interest may benefit from speckle smoothing a small percentage of the time, but, based on the sea state encountered during this experiment, the need is not significant enough to build speckle smoothing into an airborne SAR system. Those few cases where smoothing is needed should be processed on the ground as a post-flight step. There are cases where, even at 10-m resolution, speckle in single-look SAR images can obscure fine detail that is important to an analyst. Multi-look SAR images provide speckle reduction without the resolution degradation effects that result from digital filters for speckle smoothing. These results are discussed in Section 2.3.

Image processing offers benefits for real-time airborne display and manipulation. Fine resolution (10 m) in conjunction with wide swaths (25 nmi) creates very large images. These images are too large to display on a conventional video monitor. Full-resolution images can be loaded into a large buffer memory from which the data can be manipulated for presentation. One option is to provide two standard video displays on the aircraft, one showing the full swath at

reduced pixel resolution (20 m/pixel or 30 m/pixel), and one showing a user-selectable region-of-interest at full resolution (10 m/pixel). The best approach for displaying the full-swath images is to perform adjacent window averaging ("boxcar" filtering) on the data in the buffer memory. Regions-of-interest identified by the operator upon examining the full-swath images can be extracted and, if needed, down-linked to users on the ground or sea surface. Section 2.3 discusses these issues.

3.1.4 Comments on "Off-the-Shelf" SAR Technology

As a result of the SAR parameters analysis and the SAR Capabilities Survey, we have learned the following.

3.1.4.1 New SAR Design

A new-design SAR cannot be constructed by simply and cleanly putting together commercially available modules and software. As pointed out previously in this report, some of the modules will be or may be available. For example, almost all hardware for the image former will be available for purchase. An existing antenna may be compatible with Coast Guard SAR requirements. The IMU could probably be purchased. Host computer requirements can readily be met by a commercial PC. However, a considerable amount of custom hardware will have to be developed. For example, the phase-history collector will contain a number of custom rf and high-speed logic circuits. Further, a large software investment will be required, particularly in the areas of the host computer, the image former, and the phase-history collector.

Having stated this, we must note that the design, development, and production of a SAR meeting the requirements defined in this report appear to be well within the capabilities of a number of existing SAR vendors. So, the technology to develop such a SAR exists; however, the development can't be done simply by piecing together existing hardware and software modules.

3.1.4.2 Existing SARs

Most of the SAR systems surveyed operate in the X band. Some have steerable antennas with characteristics similar to those recommended in the conceptual SAR design of Section 2.5.2. The resolutions and swath widths of some of the systems are also compatible with what is required (about 10-m pixel resolution and 25 nmi swath width). It may be that an existing system could meet or be readily modified to meet Coast Guard requirements.

3.2 RECOMMENDATIONS

3.2.1 If SAR, What SAR

As explained above, two primary approaches for developing a SAR to meet Coast Guard requirements are possible: a) design and build a new SAR, and b) modify an existing SAR.

3.2.1.1 New SAR Design

In the event that a new SAR is developed, we recommend that, as a minimum, it meet the performance specifications detailed in Section 2.5.2. Those specifications are for a 10-m, X-band

system with real-time motion compensation and real-time multi-look image formation, providing an imaged swath of about 25 nmi. Digital image data and auxiliary radar data would be recorded to 4-mm tape as the images are formed. The operator would have two displays on which to view images: one for decimated-image, full-swath viewing; and a second, the host computer display, for viewing of full-resolution regions of interest. The operator would also be able to perform various post-processing operations on regions-of-interest (contrast stretching, resizing, etc.), as well as store regions-of-interest to disk or tape, print hardcopy images of regions, and format region-of-interest image files for output to a telemetry downlink. The conceptual SAR design, described in Section 2.5.2 and detailed in a number of the References, can serve as a starting point for the design of a new system.

We further recommend inclusion in the design of a SAR MTI mode (herein called SFT/SAR), a detailed description of which is given in Reference [12](Appendix E). This mode allows full SAR processing of moving targets over a number of velocity sub-bands (for example, 10-each 5-knot sub-bands over a total velocity band of $\pm$20 knots). In this mode, moving targets would be threshold-detected and displayed as synthetic-video icons over a normal SAR look showing stationary and slow-moving clutter.

Two other enhancements to the conceptual design presented in Section 2.5.2 appear to be desirable.

- Two-sided imaging could be implemented by modifying the antenna, adding rf switching, and enhancing the capabilities of the digital pre-filter, image former, and data handling software. Each side would be illuminated at one-half the one-sided prf rate, so the SAR would be desensitized by 3 dB in this case at any given range. Processing the full swath on both sides would, of course, double requirements for formation, handling, and storage of the image data; however, costs could be controlled by cutting the swath size in two-sided mode.

- As suggested by several vendors who responded to the SAR Capabilities Survey, a dual-mode system could be developed. In one mode, this system would provide broad-swath imaging at coarse resolution to meet requirements for oil-spill monitoring defined in Section 2.5.2. A coarse-resolution, broad-swath SAR/MTI capability would also be required in order to image moving ships. In a second mode, the SAR could provide fine-resolution, narrow-swath images of the target area. Implementation of a dual-mode capability would increase overall cost of the system; however, it appears that performance of the SAR in its primary mode (i.e., broad-swath oil-spill monitoring) would not have to suffer as a result of the dual-mode approach. A distinct disadvantage, however, of a dual-mode system is that a second flight pass at a shorter range would be required for fine-resolution imaging. Conceptual design and costing of a dual-mode SAR for the Coast Guard was beyond the scope of this study.

3.2.1.2 Modification of an Existing SAR

Modification of an existing SAR to meet Coast Guard requirements may be a viable option. As noted above, results of the vendor survey give cause for optimism. A number of existing systems operate in the X band, and some have design parameters that are similar to those desired

for a Coast Guard SAR. It is not the purpose of this study to recommend that a particular vendor's system be modified in the development of a possible future Coast Guard SAR. Instead, we will discuss below what appear to be optimal circumstances under which an existing system could be modified to obtain a SAR compatible with Coast Guard requirements.

A large portion of the expense of the SAR development will be in the antenna/gimbal/rf/IF/ video-processing portion of the SAR. These parts constitute the classical "radar" portion of the system. If it were possible to find an existing system, developed using reasonably current technology (say, ≤ 5 years old), that exhibited appropriate characteristics (with regard to the radar portions identified above) or that could be easily modified to obtain the desired characteristics, a great savings over a new-design development could likely be realized. Even if the antenna had to be redesigned, such a system would still be a good candidate for modification.

It should be noted also that a Ku-band system (or a system operating in another frequency band) could be modified to X band by replacing the transmitter, antenna, and rf front end. The expensive portion of the radar that we refer to as the phase-history collector would not necessarily require extensive modification in order to go from Ku (or another band) to X band.

Given that the system to be modified had the appropriate "front-end" characteristics, or some major subset of those characteristics, major modifications would be limited primarily to the digital portions of the system: the image former, host computer, displays, and data recorder. It is in these digital portions that existing systems are least likely to match up to Coast Guard needs. It is also in these portions that today's technology is making the most rapid advances, so it makes good sense to completely redesign most of these portions.

The ease with which the newly-developed digital portions of the SAR can be interfaced to the existing SAR will depend on the degree of modularity exhibited by the existing SAR. If all portions of the SAR are tightly integrated, it will be difficult to split the design apart to add the new modules. On the other hand, if the existing SAR architecture exhibits modularity, replacing portions of it with upgraded modules is easier.

3.2.2 Image Presentation, Manipulation, and Exploitation Algorithms

We recommend a SAR design that acquires full-resolution images and loads them into a large buffer memory from which full-swath, reduced resolution images can be displayed on one video monitor and from which full-resolution, region-of-interest images can be displayed on a second monitor. The resolution of the full-swath images should be no finer than 20 m/pixel and no coarser than 30 m/pixel. User selectability of this resolution may be advantageous. A mechanism for selecting and displaying regions-of-interest (trackball, mouse, pen, etc.) from the full-swath images is needed. We recommend that some means of archiving and/or down-linking regions-of-interest be provided. Where possible, other pertinent flight or environmental information should be incorporated with this image data.

Some means of viewing and post-processing SAR images on the ground is required. A modern PC-based computer system should be adequate. This system should include software to perform simple image manipulation techniques such as speckle smoothing, region-of-interest extraction, image annotation with symbols and text, data archiving, and data display. This system

should also include a high-quality printer for producing hardcopies of important images. Dedicated hardware for receiving down-linked images and porting them to the PC is also an attractive option.

3.2.3 Recommended Follow-On SAR Testing

Should the Coast Guard decide to actively pursue the acquisition of a SAR system, an informative first step would be a set of test flights with a commercially available SAR whose capabilities most closely match those of the conceptual design specified in this document. A joint experiment with simultaneous imaging of oil-slicks using both the modernized APS-131 SLAR and the commercial SAR would be ideal. Images could then be compared in a similar fashion to the comparisons made between the AIREYE and Twin Otter in this report. A study where the commercial system is contracted for use only during a joint experiment would provide another opportunity to verify that the resolution and swath-width values specified in this report continue to meet Coast Guard requirements. The advantage of such a study is the elimination of any financial risk that would be entailed in designing and acquiring a dedicated SAR system. In the event that a commercial SAR would not have a multi-look capability, the multi-look simulation discussed in Section 1.6.3.1 could be employed to make realistic comparisons.

REFERENCES

1. **Report: U.S. Coast Guard Oil Spill Remote Sensing Workshop**. (Prepared by the Environmental Research Institute of Michigan, Ann Arbor, MI), Report 213259, March 1991. Workshop held January 28-29, 1991, Avery Point, Groton, CT.

2. K. Hasselmann, et al, "Theory of Synthetic Aperture Radar Ocean Imaging: A MARSEN View,"**J. Geophys. Res.**, Vol. 90, C3, May 20, 1985, pp. 4659-4686.

3. Lyle C. Shroeder, et al, "The Relationship Between Wind Vector and Normalized Radar Cross Section Used to Derive SEASAT-A Satellite Scatterometer Winds," **J. Geophys. Res.**, Vol. 87, April 1982, pp. 3318-3336.

4. "Choice of Incidence Angle for November Santa Barbara Tests," SNL memorandum from Robert M. Axline, Org. 2344, to Jeffery D. Bradley, Org. 9134, September 11, 1992.

5. Werner Alpers, et al, "The Damping of Ocean Surface Waves by Monomolecular Sea Slicks Measured by Airborne Multi-frequency Radars During the Saxon-FPN Experiment," in **Proc. IGARS '91**, (Espoo, Finland, June 3-6, 1991), pp. 1987-1990.

6. "Operator's and Unit Maintenance Manual, Radar Surveillance Set AN/APS-131," U.S. Coast Guard Document No. 68-PO3879U, March 15, 1981.

7. "Estimated Sensitivity of AIREYE SLAR for the Case of a Distributed Target," SNL memorandum from Robert M. Axline, Org. 2344, to Distribution, June 24, 1993.

8. "Suggested Flight Scenarios for November Santa Barbara Flights," SNL Memorandum from B. L. Remund, Org. 2345, to Jeffery D. Bradley, Org. 9134, September 17, 1992.

9. H. Johnsen, "Multi-look Versus Single-look Processing of Synthetic Aperture Radar Images With Respect to Ocean Wave Spectra Estimation," **Int'l. J. Remote Sens.**, Vol. 16, No. 9, 1992, pp. 1627-1643.

10. Jeffery Bradley, **Evaluation of Synthetic Aperture Radar for Oil Spill Response, Test Plan**, SNL departmental document, Dept. 9134, Revision 1.0, October 16, 1992.

11. Jeffery Lunsford, "ImView Release II: User's Guide," SNL departmental document, Dept. 2344, Jan. 7, 1992.

12. Azriel Rosenfeld and Avinash Kak. **Digital Picture Processing**. Academic Press, New York, NY, first edition, 1976, pp. 197-200.

13. William Pratt. **Digital Image Processing.** John Wiley and Sons, New York, NY, 1978, pp. 330-332.

14. Thomas R. Crimmins, "Geometric Filter for Reducing Speckle," in **Proc. SPIE Int'l. Conf. Speckle**, Vol. 556, (San Diego, CA, Aug. 1985), pp. 213-222.

15. "Conceptual Requirements for a Synthetic Aperture Radar System for Oil-Spill Response," SNL Coast Guard Project Document, April 28, 1993.

16. "Information Survey Relating to Synthetic Aperture Radar Capabilities", SNL Coast Guard Project Document, April 28, 1993.

17. "Coast Guard SAR Design Calculations and Identification of Key Issues," SNL memorandum from Robert M. Axline, Jr., Org. 2344, to Distribution, June 2, 1993.

18. "MTI Mode for the Coast Guard SAR", SNL memorandum from Robert M. Axline, Jr., Org. 2344, to Distribution, June 21, 1993.

19. "Motion-Compensation Requirements for Coast Guard SAR", SNL memorandum from J. T. Cordaro, Org. 2344, to Robert M. Axline, Jr., July 19, 1993.

20. "RAR Mode for the Coast Guard SAR," SNL memorandum from Robert M. Axline, Jr., Org. 2344, to Distribution, July 17, 1993.

21. "Additional Coast Guard SAR Design Calculations," SNL memorandum from Robert M. Axline, Jr., Org. 2344, to Distribution, June 24, 1993.

22. "Interim Response to Gary Hover's Comments on My Memorandum of March 15, 1993 and Transmittal of SAR Capabilities Survey Information," SNL memorandum from Robert M. Axline, Jr., Org. 2344, to Distribution, May 4, 1993.

23 D. E. Fraser and G. V. Morris, "Performance of Coherent-on-Receive Synthetic Aperture Side Looking Airborne Radar," Report No. CG-D-109-76, Motorola, Inc., prepared for the U.S. Coast Guard and the U. S. Army, October, 1976.

24 T. Kozu, et al, "Observation of Oil Slicks on the Ocean by X-Band SLAR,"in **Proc. IGARSS '87 Symposium**, (Ann Arbor, MI, May 1987), pp. 735-740.

APPENDIX A
SLAR SENSITIVITY

This appendix contains a copy of a memo on AIREYE SLAR sensitivity prepared by Robert M. Axline, Jr., June 24, 1993. It is included here for completeness.

(The remainder of this page intentionally left blank.)

Sandia National Laboratories

Albuquerque, New Mexico 87185

date: June 24, 1993

to: Distribution

from: Robert M. Axline, Jr., Radar Analysis Department, 2344

subject: Estimated Sensitivity of AIREYE SLAR for the Case of a Distributed Target

References

[1] "Operator's and Unit Maintenance Manual, Radar Surveillance Set AN/APS-131," U.S. Coast Guard Document No. 68-PO3879U, March 15, 1981.

[2] "Coast Guard SAR Design Calculations and Identification of Key Issues," SNL memorandum from Robert M. Axline, Jr., 2344, to Distribution, June 2, 1993.

[3] "Additional Coast Guard SAR Design Calculations," SNL memorandum from Robert M. Axline, Jr., 2344, to Distribution, June 24, 1993.

[4] D. E. Fraser and G. V. Morris, "Performance of Coherent-on-Receive Synthetic Aperture Side Looking Airborne Radar," Report No. CG-D-109-76, Motorola, Inc., Government Electronics Division, prepared for the U.S. Coast Guard and the United States Army, October 1976.

[5] "Target Detection Predictions for AN/APS-131 and AN/APS-135 Radar Systems," Peter D. Kennedy, Motorola Inc., Government Electronics Division, prepared for the U.S. Coast Guard, May 19, 1982.

The purpose of this study is to determine the approximate sensitivity of the AIREYE SLAR [1] so that its performance can be compared to performance of a conceptual SAR system described in Reference [2]. Herein, system sensitivity will be measured in terms of estimated minimum distributed-target scattering coefficient, σ^{o}_{min}, that can be detected by the AIREYE SLAR at a range of 54 km (maximum SAR range considered in [2] and [3]). Results show that, at this range, estimated σ^{o}_{min} is about -41.9 dB for this SLAR.

Equation for σ°_{min}

Minimum detectable scattering coefficient can be computed approximately from radar and geometrical parameters using equation (1).

$$\sigma^\circ_{min} = (S/N)_{min}(4\pi R)^3 kT_o BF_n L \cos\phi/[P_t G_e^2 \lambda^2 \Delta\theta \rho_r \sqrt{N_e}]. \quad (1)$$

σ°_{min} has units of m^2/m^2. This quantity is more commonly expressed in decibels; this representation is just $10 \cdot \log_{10}(\sigma^\circ_{min})$. The assumption that minimum scattering coefficient is improved as $1/\sqrt{N_e}$ is a only an approximation. Parameters of (1) are defined in Table 1, below.

Table 1. Radar and geometrical parameters in (1).

Symbol	Units	Value	Definition
$(S/N)_{min}$	W/W	4	minimum detectable signal-to-noise ratio
R	m	5.4 E3	range to target pixel [2]
k	J/K	1.38 E-23	Boltzmann's constant
T_o	°K	288	ambient temperature
B	Hz	6 E6	rf receiver bandwidth [1]
F_n	W/W	6.3	not specified in [1]; value of 7.96 dB inferred from [5] and used here; value of 13 dB maximum specified in COR report [4] probably not representative of AN/APS-131
L	W/W	2.5	all rf and propagation losses; assumes 2.44 dB tx loss and 1.5 dB atmospheric loss; receiver loss included in F_n; radome loss included in G_e
ϕ	°	6	depression angle [5]
P_t	W	200 E3	peak transmitter power [5]
G_e	W/W	2.51 E3	average antenna gain over the beam; taken to 34 dB (35.9 dB from [1], derated by 1.9 dB)
λ	m	0.032	electrical wavelength
$\Delta\theta$	rad	0.014	antenna azimuth beamwidth
ρ_r	m	30	range resolution [1] and [5]
N_e	---	180	number of pulses averaged noncoherently in November '92 digital SLAR implementation (see discussion below)

(Note: Table entry for receiver bandwidth, B, corrected on August 15, 1993.)

Equation (1) optimistically assumes that the antenna is pointed so that peak gain corresponds to the direction from the SLAR to the pixel of interest (at 54-km slant range). In fact, the antenna is normally pointed at a nominal 1° depression angle, and the pattern at the pixel of interest (54-km range and 6° depression) would be down by at least about 3.5 dB from its peak value. The quantity N_e has been estimated using the following equation.

$$N_e = (X_a f_p / V_a). \quad (2)$$

Here, X_a is the along-track distance over which averaging takes place, The assumed value of X_a for these calculations is 30 m (this information came from Colin Odom, Motorola Inc., Government Electronics Division). f_p is the SLAR's prf, taken here to have an average value of 750 pulses per second (the SLAR transmits out just one side of the aircraft). In (2), V_a is aircraft velocity. The value used was 125 m/s. The resulting value of N_e is 180. These computations and estimates of N_e apply only to the digital configuration of the SLAR that was fielded for the November 1992 Santa Barbara tests. Ordinarily, raw (unaveraged) video pulses are fed directly to the SLAR's film recorder and integration occurs on the film. The rate of advance of the film is tied to the instantaneous aircraft velocity, therefore, more integration occurs at lower velocities, less at higher velocities.

The estimated value of σ°_{min} resulting from evaluation of (1) is 0.000064 m^2/m^2, or -41.9 dB. This estimate should probably be looked at as a slightly optimistic bound on σ°_{min} because of the uncertainty of the appropriateness of the use of $1/\sqrt{N_e}$ in equation (1).

Azimuth Resolution Cell Size for the SLAR

The range resolution, ρ_r, of the SLAR is 30 m, independent of range; however, the azimuth resolution, ρ_a, increases with increasing range. ρ_a can be computed as approximately

$$\rho_a \simeq R \bullet \Delta\theta, \quad (3)$$

where R is slant range to the target pixel and $\Delta\theta$ is the antenna's azimuth beamwidth. Table 2 shows the result of evaluating (3) at various ranges.

Table 2. Variation of ρ_s Versus R.

R, km	ρ_s, m
10	139
20	279
30	418
40	559
50	698

Therefore, for the SLAR, the clutter cell is quite wide, and the cross-sectional area it covers is large.

Distribution:

Gary L. Hover
USCG R&D Center, Environmental Safety Branch
1082 Shennecossett Road
Groton, CT 06340-6096

Christopher Allen D/852 MG39
Allied-Signal Aerospace Company
P. O. Box 419159
Kansas City, MO 64141-6159

2344 J. T. Cordaro
2344 J. J. Mason
9134 J. D. Bradley
9134 G. A. Mastin
2344 R. M. Axline, Jr.

(This page intentionally left blank.)

APPENDIX B
SAR CONCEPTUAL REQUIREMENTS

This appendix contains a copy of a project document discussing conceptual requirements for a future synthetic aperture radar system for oil-spill response prepared by Robert M. Axline, Jr., April 28, 1993. It is included here for completeness.

(The remainder of this page intentionally left blank.)

Conceptual Requirements for a Synthetic Aperture Radar System for Oil-Spill Response

Prepared for:

The U.S. Coast Guard R&D Center
1082 Shennecossett Road
Groton, CT 06340-6096

Prepared by:

Sandia National Laboratories
P. O. Box 5800
Albuquerque, NM 87185

April 28, 1993

SNL Points of Contact:

J. D. Bradley, SNL/Coast Guard Project Manager
Remote Sensing Systems Applications Department, 9134
Phone: (505) 844-2441; FAX: (505) 844-5767

Robert M. Axline, Jr., Line Manager,
Radar Analysis Department, 2344
Phone: (505) 844-5064; FAX: (505) 844-1599

Introduction

To fulfill its role in oil-spill response, the Coast Guard currently operates the AIREYE sensor suite, carried aboard a Falcon 20 aircraft. One element of that suite is an X-band side-looking airborne radar (SLAR). While the SLAR provides broad-swath coverage and timely image products, the azimuth resolution of that system degrades to hundreds of meters at a range of 20 miles. The Coast Guard's R&D Center is investigating the possible benefits of employing a synthetic aperture radar (SAR) as one of its next-generation sensors. Achievable improvements in the next-generation radar may include improved azimuth resolution; decreased latency of image products; and increased functionality in viewing, manipulation, geo-registration, and annotation of real-time imagery.

This document contains high-level, conceptual requirements for a synthetic aperture radar (SAR) system for oil-spill response. Sandia and the Coast Guard have developed these requirements in a cooperative effort funded by the Coast Guard. At this time, the Coast Guard has no plans to develop a SAR for oil-spill monitoring. These conceptual requirements have been developed only as a tool for use in the joint Sandia/Coast-Guard study.

Scope of Requirements Description

Although the next-generation Coast Guard platform will likely use multiple sensors, requirements given here deal only with the SAR portion of the system. Some components of the SAR system would be usable by other sensors. For example, a hardcopy printer would be used to print outputs of multiple sensors. In these cases, standard devices and interfaces are desired. Any components required for ground-based processing of SAR data are beyond the scope of this requirements document; however, important characteristics of the SAR sensor that will affect ground-processing requirements are relevant here (e.g., volume of data, any requirements for mosaicing or correction of data, etc.)

Aircraft Platform

These preliminary requirements have been written in a manner that is largely independent of the aircraft platform. Typical velocity of the aircraft should be assumed to be in the range of 90-124 m/sec. It should be assumed that the SAR for oil-spill monitoring would be integrated into a multi-sensor platform owned or leased by the Coast Guard. The current AIREYE aircraft is a Falcon 20. Do not assume that the next-generation platform would have the same constraints on weight, volume, and power as are now placed on the AIREYE SLAR.

Primary SAR Usage and Measurements

The primary usage of the SAR will be for oil-spill detection and monitoring. In this mission, the SAR will create broad-swath images of ocean areas. The imaging mode will be broadside (90° squint) strip-map imaging. Image pixel values will be magnitude-only (see comments relating to image phase, below). Number of quantized data bits is TBD. The possibility of using the SAR for other missions (marine pollution, e.g., against bilge pumpers; or law enforcement, e.g., against smugglers) is of secondary interest. A capability for fine-resolution (meter or sub-meter) spotlight SAR for adverse-weather and standoff identification of vessels is desired for this latter requirement.

"Off-the-Shelf" Technology

For any recommended new SAR development or significant modification to an existing SAR system, hardware/software recommended should be of high reliability, be readily available, and be standard in some sense. The system must be maintainable by enlisted Coast Guard personnel. The Coast Guard is willing to let the system grow in size, weight, and power in order to achieve these goals.

Consideration of Existing Systems

Because of the high cost of development of a new SAR, the feasibility of using existing SAR platforms, or modified versions of those platforms, is of primary interest to the Coast Guard.

Real-Time Data Availability

The real requirement is that full-resolution images be available for viewing within a few minutes after the plane lands. In cases where the aircraft can't land near the spill operations center, some means of high-speed data transfer from the aircraft to the spill site would be required. Real-time image-formation capability must be available on the plane. Real-time imagery must be available for immediate on-board viewing, region-of-interest (ROI) selection, recording, and/or downlinking to a ground station near the spill site.

Operators

The operators will have technical skills equal to those of enlisted Coast Guard sensor-suite operators. Two operators will man the multi-sensor suite. The operators will be physically separated from the aircraft's pilots, and there will be voice communications between the operators and the pilots. The operators will have a duplicate Control Display Unit at their sensor control panel.

Installation Configurations

No specific requirements have been determined. Specifications and information on installation configurations should be limited primarily to issues concerning overall system power, size, and weight, including the antenna. System cooling requirements should also be defined. Specification information collected on existing platforms should include brief descriptions, and possibly sketches of mounting configurations (e.g., internal versus external or (pod) mounting).

Stabilization and Navigation Requirements

The SAR system will not control the aircraft's trajectory; however, the system design may place requirements on allowable deviation of the aircraft from an ideal straight-line trajectory in order to assure proper SAR operation. Accuracy of the SAR's integrated navigation and motion compensation system must be sufficient to allow the system meet its stated requirements relating to impulse-response mainlobe width and sidelobe levels.

Required Swath

The baseline requirement is that the SAR be able to image out of one side of the aircraft. The imaged swath must be more than 10 miles in extent for the system to be useful. The AIREYE SLAR routinely images a 27-mile swath. If the SAR can achieve a 20-25 mile swath, this will best meet the requirement. It is highly desirable that the SAR image both sides of the aircraft simultaneously with a minimum 10-mile swath per side.

Required Resolution (Oil-Spill Monitoring Only)

The required resolution of the SAR system is TBD. Recommendations for desired range and azimuth resolutions will result from an ongoing study being performed jointly by the Coast Guard and Sandia.

Range Resolution. Range resolution of the existing AIREYE SLAR is about 30 m (200 ns real pulse). Improved range resolution may be of interest, depending on the outcome of data analyses and priorities of other uses for the system. For this reason, bounds on slant-range resolution for oil-spill monitoring should be considered to be between 3 and 30 meters.

Azimuth Resolution. Azimuth beamwidth for the AIREYE SLAR antenna is about 1°, which yields an azimuth resolution of about 55 m at a range of 2 statute miles and an azimuth resolution of about 550 m at a range of 20 statute miles. SAR promises to provide significantly better azimuth resolution than that of the AIREYE SLAR. At this time, bounds on azimuth resolution should be considered to be between 3 and 30 meters. Required resolution for the SAR should be specified at the range defining the

maximum swath of the SAR. Azimuth resolution will improve as range decreases in the swath.

System Sensitivity
σ^o of noise will need to be $\leq$ -40 dB.

SAR Operating Frequency
Study of the literature has indicated that contrast between oil and open ocean is achievable across a fairly wide range of frequencies. SARs having frequencies between C and Ku bands, inclusive, are of interest.

SAR Polarization
SAR must be like polarized. Optimum polarization at small depression angles is VV.

Image Requirements
Recorded and displayed images will be in digital, magnitude-only form, with pixels quantized to a TBD number of bits. There is no specific requirement for phase data; however, if an existing platform has the capability to produce complex imagery, this fact will be of interest.

Image Rendering. It is desired that images be projected into the ground plane, so that the image will represent a rectangular map of ocean surface reflectivity. One axis of the map will be parallel to the flight path of the plane, and the other axis will be perpendicular to the flight path and in the plane of the ocean's surface. The desired rendering should result in square pixels (equal azimuth and cross-track dimensions) after projection onto the ocean's surface.

Image Calibration. It is desired that gross radar effects, such as antenna pattern and range-law trends be removed in real-time images available on the aircraft. Relative amplitude variation due to spatial location of a target in the corrected image should be less than $\pm$TBD dB. Absolute amplitude calibration, in terms of radar cross section or scattering coefficient is not required for every mission; however, it is desirable that the system be so designed that it can be calibrated for particular missions, and the system should be required to hold that calibration specification over the duration of the mission. Also, the calibration scaling factor could probably be computed either in real time or post-mission.

Image Annotation Requirements
The system must provide a means of annotating images for display and printing. Annotation should include latitude and longitude reference marks, date, time, altitude, speed, pitch/yaw/roll, heading, operator comments, target symbols, ROI boxes, and other mission support symbology. Ideally, the image annotation would be inserted by reconfigurable software that could be selected according to mission requirements. Geographic ties to the imagery are the key issue here.

Data Recording Requirements

The SAR should provide a capability to continuously record all real-time digital imagery produced by the system. The SAR should also be able to record any navigation and/or radar data required for post-mission geo-registration and image-processing operations. Recording media should be of a removable cartridge type. In addition, the SAR system should provide for recording of raw phase histories or other data for the purpose of occasional diagnostic evaluation or maintenance of the system. Equipment required for phase-history recording need not be on the plane on all missions. A provision should be made to record operator comments during and after a mission.

Image Processing Requirements

A number of different types of image processing operations are possible:

1. Real-time, continuous operations on real-time imagery.

2. On-board processing of selected (captured or retrieved) real-time images (either during an imaging operation, or afterward).

3. Post-mission processing of any or all imagery.

Real-time Image Processing. These functions, which are performed automatically by the radar and its signal processor, will be limited to what can be economically done in real-time hardware. Desired functions should include antenna-pattern and range-law corrections, geo-registration, look-up table and mapping-function application. Other features may include temporal multilook or pixel-averaging for speckle reduction.

On-Board Processing of Selected Images. Operations may include pixel decimation and replication (zoom-out and zoom-in), annotation, file preparation for printing on a hardcopy device, and file preparation for downlinking. It is envisioned that on-board processing capabilities will be a subset of post-mission ground-processing capabilities. All image-processing functions must be operator-friendly and easy to train to. Operators must be able to understand tradeoffs associated with the use of any available image processing tools and understand when and when not to use them.

Post-Mission Processing. Post-mission processing will include all capabilities listed above for on-board processing; however, it will likely include additional image enhancement and filtering techniques. Further, post-mission processing will provide the capability to process any and all image data, not just selected images.

Image Display Requirements

The SAR system should include a high-resolution display capable of displaying all real-time imagery produced during a mission. It may be necessary to decimate the real-time imagery in order to provide a full-swath display to the operators. The operator should be able to either display imagery continuously, as it is formed, or to freeze selected frames of imagery for more detailed and lengthy inspection. The image display should be linked to a workstation capable of performing the on-board processing of freeze-frame or retrieved images, as described above. Therefore, the image display should also be able to display the results of this processing. The image display will almost certainly be required to display multiple sensor outputs, with a windowing capability to display data from more than one sensor simultaneously. The primary use of this display will be real-time sensor and aircraft data monitoring and image/target selection by the operator. The interface to the display must be a standard one (RGB, NTSC, etc.).

Other Operator Display Requirements

An operator control display will be required to allow the operator to interactively process, annotate, and downlink selected images. The Coast Guard currently envisions that this display would be separate from the image display; however, integration of any or all of the control-display functions with the image display would be acceptable.

Telemetry Interface Requirements

The SAR should provide an interface that will allow either a raw or a processed/enhanced image to be passed to either a system-control processor or a data telemetry link for transmission of selected image data to a ground station. Northrop's SeaView software will be the product used to format, compress/decompress, and transmit/receive the image data.

Printed Hardcopy

The SAR system must be capable of being interfaced to an on-board printer for production of image hardcopies. The Coast Guard has suggested that the airborne sensor system be equipped with an HP Deskjet-type printer for this purpose. The printer should be standard to the extent that it can also be used to print image data from other sensors in the suite.

Uses of Printed Images

The Coast Guard and NOAA will use the images to determine where oil is and is not, to locate the boundaries of the slick, and to monitor slick movement over time. The on-scene commander will want to see a ground-plane rendering of the SAR image. Likely, he would want to be able to overlay the SAR image with an existing chart or map of the spill area. Images that can be scaled to match standard NOAA nautical charts would be highly desirable, particularly on the ground station, where transparencies could be printed. In addition, the image data should be formattable for porting to computer-based geographic information systems used by NOAA and the USCG (possible future capability).

APPENDIX C
SAR INFORMATION SURVEY

This appendix contains a copy of the survey of SAR capabilities prepared by Robert M. Axline, Jr., April 28, 1993. It is included here for completeness.

(The remainder of this page intentionally left blank.)

Information Survey Relating to
Synthetic Aperture Radar Capabilities

Requesting Agency:

Sandia National Laboratories
P. O. 5800
Albuquerque, NM 87185

April 28, 1993

Please direct questions and written survey responses to:

Robert M. Axline, Jr., Radar Analysis Department, 2344
Sandia National Laboratories
P. O. Box 5800
Albuquerque, NM 87185
Phone: (505) 844-5064; FAX: (505) 844-1599

Alternate SNL point of contact for this survey:

Jeff Bradley (SNL/Coast Guard Project Manager)
Remote Sensing Systems Applications Department, 9134
Phone: (505) 844-2441; FAX: (505) 844-5767

Introduction

Sandia National Laboratories is a non-profit corporation operated by AT&T under contract to the United States Department of Energy. Sandia's goal is to provide exceptional service in the National interest. In recent years, Sandia has developed capabilities in the area of synthetic aperture radar. We currently operate a state-of-the-art Ku-band strip-mapping SAR and have developed significant capabilities in miniaturized microwave components, high-speed digital processing, precise navigation, image-formation algorithms, and auto-focus techniques.

The Coast Guard's AIREYE multi-sensor suite is the principal U.S. sensor platform for oil-spill response. AIREYE employs an X-band side-looking airborne radar (SLAR). We are currently performing work under contract to the U.S. Coast Guard. The purpose of this work is to assess the potential of SAR (versus SLAR) for use in oil-spill monitoring. Our role in this contract is that of an independent advisor. In November of 1992, Sandia collected Ku-band SAR imagery of naturally occurring oil seeps near Santa Barbara, CA. The AIREYE platform simultaneously collected SLAR data of common test areas. Since that time, Sandia, the Coast Guard, and the National Oceanographic and Atmospheric Administration (NOAA) have been jointly analyzing flight-test images to determine effects of radar resolution, wind speed, wind direction, and other factors on an image interpreter's ability to distinguish oil from open ocean. More recent efforts have been aimed at developing preliminary high-level requirements for a possible future Coast Guard SAR sensor.

Currently the Coast Guard has no plan to develop a SAR sensor for oil-spill monitoring. However, that agency is interested in performing exploratory studies, like the one in which we are engaged, to determine what improvements might be possible with a SAR sensor.

The Information Survey

Purpose of the Survey

One of the objectives of our study is to obtain information from other agencies relating to existing SARs and their capabilities. This information will then allow the Coast Guard to understand the current state-of-the-art and to determine how that state relates to the sensor performance features they desire for oil-spill monitoring. To this end, we have prepared an information survey, which we have included in this package.

Requested Response Date

Please complete the survey and return it in the self-addressed envelope that accompanies this package. All responses are to contain only unclassified information. We ask that your response be mailed by May 20, 1993. If your response is belated, we would still appreciate receiving it, provided you mail it no later than July 1, 1993.

Disclaimer

Consistent with information stated above concerning the purpose of this survey, we emphasize that this survey does not constitute a request for quotation or a formal request for information relating to any planned development activity either on behalf of the Coast Guard or of Sandia National Laboratories.

Participation is on a Voluntary Basis

Your participation in this survey is being requested on a voluntary, no-cost basis. Thank you for your help in this work.

Completing and Returning the Survey

Information sought consists of two types:

1. Please provide functional performance information on system(s) you currently own or operate. The attached "Functional Performance Characteristics" can be used as a template or guideline for this information. Alternatively, available brochures or specification sheets you may have in-hand could serve as well.

2. Please review the document entitled "Conceptual Requirements for a Synthetic Aperture Radar System for Oil-Spill Response," which is included in this package. In a free-form response format, please briefly comment on similarities or differences between your system and the conceptual requirements described in the document. You need only deal here with those aspects of your system that are not evident from the information in item 1. Information on imminent upgrades to your system and on new systems you are now developing is also of interest.

Please return the completed survey in the self-addressed envelope provided with this package. If possible, mail your response by May 20, 1993. An advance FAX copy of your completed survey would be greatly appreciated. Belated survey responses mailed by July 1, 1993 will also be welcomed. Information provided by you will be included, in summary form, in a Sandia report to the Coast Guard. That report will be distributed publicly after approval by Coast Guard Headquarters.

Functional Performance Characteristics

* Agency Name
* System Name
* Prime Usage of System
* Aircraft Platform (specify type)
* platform velocity, m/s
* Supported Radar Modes
* strip map (Y/N)
  other modes (squint, spotlight, interferometry, etc., describe)
* real-time imaging (Y/N)
* Real-time (or Ground Processed) Image Attributes (if both, please list separately)
  real or complex (specify)
* # of bits per pixel
* surface cross-track resolution, m
* azimuth (along-track) resolution, m
  IPR maximum sidelobe levels (cross-track and azimuth), dB
* # of pixels, range dimension
* # of pixels (per patch), azimuth dimension
* maximum pass length, km
  pixels per resolution cell (cross-track and along-track)
* image cross-track swath (on the surface), km
* azimuth patch width, km

Geometry

* altitude, km
* slant range (to scene center-line), km
* antenna pointing angles (depression), °
  squint angles (+90° is right side-looking), °
* Noise-equivalent σ^o at Stated Resolution, dB

Amplitude Calibration

can be calibrated (Y/N)
calibrated in real-time (Y/N)
absolute accuracy, μ and σ, dB

Note: If it is not feasible for you to supply all data, please try to supply information on key parameters highlighted with "*". If parameters vary over a range of values, indicate range limits.

Functional Performance Characteristics, continued, ...

* Multilook Processing (Y/N)
* temporal: # of looks at stated azimuth resolution
* range-dimension: # of looks at stated range resolution
* pixel averaging: effective # of independent samples at stated resolution

Frequency Generator and Transmitter

* operating frequency, GHz
* polarization of antenna(s)

transmitter bandwidth, MHz

* pulse duration, μs
* waveform intra-pulse modulation (chirp, PN code, etc.)
* prf, kHz

interpulse modulation type, if any

* peak transmitter power (at antenna input), W
* maximum duty factor, %

maximum average transmitter (at antenna input) power, W

Antenna

* antenna orthogonal beamwidths (3 dB one-way), °

number of phase centers

length and height, m

* peak antenna gain, dB

Receiver

* front-end noise figure, dB

rf bandwidth, MHz

if bandwidth, MHz

* deramp (stretch) processing (Y/N)

video bandwidth, MHz

A/D Converter and Bandpass Filter

* # of A/D bits

A/D sample rate, MHz

number of video samples

presum integer

azimuth antenna oversampling factor

* typical azimuth sample rate, Hz
* Real-Time or Ground-Based Image Former (specify which)

algorithm type (2-D FFT, polar reformatting, etc.)

* elevation antenna correction (Y/N)

Functional Performance Characteristics, continued, ...

Real-Time or Ground-Based Image Former, continued, ...

* azimuth antenna correction (Y/N)
* ground-plane projection
  range-migration correction (Y/N)
  range-law correction (Y/N)
  presummer correction (Y/N)
  video-filter correction (Y/N)
  auto-focus (Y/N)
  geo-referencing (Y/N)

Data Handling

* maximum data rate to tape (phase history and images), Mbits/s
  maximum data rate per tape unit, Mbits/s
  number of tape units online
* recording capacity per unit (Gbytes)

Image Display

* horizontal display size, pixels
* vertical display size, pixels
* dynamic range, bits/pixel

Navigation Accuracies

* navigator type
  attitude accuracy, °
  position accuracies, m
  velocity accuracies, m/s
  GPS aiding (Y/N)

Motion Compensation

* real-time compensation (Y/N)
  update rate to SAR, Hz

Mechanical Characteristics

total power consumption of SAR, kW
physical volume of SAR hardware, m^3

Rough Order of Magnitude Cost to Replicate System, $k

including fabrication, laboratory integration, and testing, of radar and motion compensation subsystem, but not including any platform integration.

(This page intentionally left blank.)

APPENDIX D
SAR DESIGN CALCULATIONS

This appendix contains a copy of a memo on Coast Guard SAR design calculations prepared by Robert M. Axline, Jr., June 2, 1993. It is included here for completeness.

(The remainder of this page intentionally left blank.)

Sandia National Laboratories

Albuquerque, New Mexico 87185

date: June 2, 1993

to: Distribution

from: Robert M. Axline, Jr., Radar Analysis Department, 2344

subject: Coast Guard SAR Design Calculations and Identification of Key Issues

References

[1] "Conceptual Requirements for a Synthetic Aperture Radar System for Oil-Spill Response," SNL CG-Project Document, April 28, 1993.

[2] "Notes on Motorola Report CG-D-109-76," memorandum from R. M. Axline, Jr., 2344, to Distribution, May 19, 1993.

[3] "Interim Response to Gary Hover's Comments on My Memorandum of March 15, 1993, and Transmittal of SAR Capabilities Survey Information," memorandum from R. M. Axline, Jr., 2344, to Distribution, May 14, 1993.

[4] "Choice of Incidence Angle for November Santa Barbara Tests," memorandum from R. M. Axline, Jr., 2344, to J. D. Bradley, 9134, September 11, 1992.

Introduction

This memorandum documents design calculations and tradeoffs for a Coast Guard SAR for imaging of ocean-borne oil spills. The approach taken was as follows.

1. Gather conceptual requirements (see [1]).

2. Translate conceptual requirements into a "starting-point" table of performance characteristics (Table 1).

3. Identify areas of uncertainty and key issues to be resolved.

4. Analyze tradeoffs on key issues to further refine and quantify information given in Table 1.

Conceptual Requirements Summary and Starting-Point Characteristics

Reference [1] defines conceptual requirements for a Coast Guard SAR for oil-spill response. Those requirements dictate a broad-swath SAR (20 to 25 nautical-mile swath) with real-time image formation capabilities. The prime use of the system is to be oil-spill monitoring. In this memorandum, I consider only this mission. Reference [1] contains discussions relating to required swath, range and azimuth resolution, system sensitivity, operating frequency, image characteristics, annotation, data recording, image processing and display, telemetry, and printing. Via interpretation and computational estimates, I have translated these high-level requirements into the "starting-point" performance characteristics given in Table 1.

Table 1. SAR Characteristics Starting Point

Parameter or Attribute	Units	Value or Description
Agency Name	----	US Coast Guard
System Name	----	SAR for oil-spill response
Prime Usage of System	----	oil-spill imaging
Aircraft Platform	----	Falcon 20
platform velocity	m/s	90-124
Radar Supported Modes	----	strip map; squint angles TBD
	----	real-time multilook imaging
Real-Time Image Attributes		
real magnitude	----	recorded
complex data	----	available, not recorded
# bits per pixel	----	8 or 16 (TBD in analysis)
slant-range resolution ρ_r	m	10-30 (TBD in analysis)
azimuth resolution ρ_a (@ 25 nmi)	m	10-30 (TBD in analysis)
IPR maximum sidelobes	dB	-30
image slant-range swath	nmi	20-25
	km	37-46
# pixels, range dimension	pixels	6950 (25 nmi swath; 10-m ρ_r)
(assuming 1.5 oversampling)	pixels	2315 (25 nmi swath; 30-m ρ_r)
azimuth patch width	km	TBD
# pixels (per patch), azimuth	----	TBD
pixels per resolution cell	----	1.5 (range and azimuth)
maximum pass length	km	TBD
Geometry		
altitude, km	kft	20
	km	6
slant range (near range)	km	8.5
slant range (far range)	km	54 (@ 25 nmi swath)

Table 1. SAR Characteristics Starting Point, continued ....

Geometry, continued		
depression angle (near range)	°	45
depression angle (far range)	°	6.4 (ignoring curvature)
squint angle	°	$\pm 90 \pm$ TBD variation
near-range az. antenna footprint	m	148 (1° az. beamwidth, β_a)
far-range az. antenna footprint	m	942 (1° β_a)
antenna steering	----	approach TBD
Typical Aperture Length	m	87 (10-m ρ_a @ 54 km)
	m	14 (10-m ρ_a @ 8.5 km)
Typical Aperture Time	s	0.7 (10-m ρ_a @ 54 km)
	s	0.1 (10-m ρ_a @ 8.5 km)
Noise-Equivalent σ^o Required	dB	-45 (@ 25-nmi., TBD wind)
Amplitude Calibration	----	pre- or post-mission
mean error	dB	$-2 \leq \mu_e \leq 2$
standard deviation	dB	$\sigma_e \leq 2$
Multilook Processing (real-time)		
temporal, $\Sigma_i \mid V^i_{j,k} \mid /N$	looks	number of looks, N is TBD
pixel averaging, $\Sigma_{j,k} \mid V^i_{j,k} \mid /N$	pixels	# of pixels averaged is TBD
Frequency Generator and Transmitter		
operating frequency	GHz	≃9.3 (see discussion)
operating wavelength, λ	cm	≃3.2
transmitter bandwidth	MHz	≃15 @ 10-m ρ_r
	MHz	≃5 @ 30-m ρ_r
pulse duration	μs	$\leq$ 57 μs (near-range constraint)
waveform intra-pulse modulation	----	chirp or PN code
prf	kHz	$\leq$ 2.4 kHz (far-range constraint)
interpulse modulation	----	0/π PN phase coding (for ambiguous range abatement)
microwave transmit losses	dB	0.8
peak tx power (at antenna)	W	TBD
maximum duty factor	%	13 (based on maximum pulse length and maximum prf)
maximum average tx power	W	TBD
Antenna		
polarization	----	vertical
elevation pattern (roughly 6° equiv. beamwidth)	----	$\csc^2(\phi)$; ϕ = depression angle
azimuth beamwidth, β_a	°	$\geq$0.1°, 10-m ρ_r, one look
	°	$\geq$0.03°, 30-m ρ_r, one look
length (controls az. pattern)	m	1.83, β_a = 1°
	m	0.92, β_a = 2°
	m	0.62, β_a = 3°

Table 1. SAR Characteristics Starting Point, continued ....

Antenna, continued		
height (controls elev. pattern)	m	0.3 (about 1 foot)
antenna gain (rough estimate)	dB	35 (β_a = 1°; 50% efficiency)
radome losses, two-way	dB	1.5
vertical rotational steering	----	yes
azimuthal steering	----	TBD
Receiver		
front-end noise figure (& losses)	dB	2 (rough estimate)
rf bandwidth	MHz	≈15 @ 10-m ρ_r
	MHz	≈5 @ 30-m ρ_r
IF frequency	MHz	TBD
IF bandwidth	MHz	same as rf bandwidth
sensitivity time control	----	selectable curves
IF pulse compression	----	SAW filter (suggested)
gain @ 10-m ρ_r	----	855 (29.3 dB)
gain @ 30-m ρ_r	----	285 (24.5 dB)
video bandwidth	----	same as rf bandwidth
A/D converter and presum filter		
# A/D bits	bits	8 (I) + 8 (Q), minimum
A/D Sample Rate	MHz	22.5 @ 10-m ρ_r
(1.5 oversampling)	MHz	7.5 @ 30-m ρ_r
number of video samples	----	≈6900 @ 10-m ρ_r
(25-nmi swath)	----	≈2300 @ 30-m ρ_r
Doppler spectral width	Hz	54 (0.4° β_a @ 125 m/s)
(assume nominal β_a is 1°)	Hz	136 (1° β_a @ 125 m/s)
	Hz	273 (2° β_a @ 125 m/s)
	Hz	409 (3° β_a @ 125 m/s)
presum integer (approximate)	pulses	30, 12, 6, or 4
(assuming spectral widths above & 2.4-kHz prf)		
antenna oversampling factor	----	1.5
typical azimuth sample rate	Hz	200 (assumptions as above)
Real-Time Image Former		
numerical precision	bits	minimum of 16 (I) + 16 (Q)
algorithm type	----	TBD
integration gain	----	1650 (32.2 dB)
windowing and other losses	dB	1.2
elevation antenna correction	----	yes
azimuth antenna correction	----	yes
ground-plane projection	----	yes (might vary A/D rate)
range-law correction	----	yes
sensitivity-time-control correction	----	yes
presummer correction	----	TBD
auto-focus	----	no

Table 1. SAR Characteristics Starting Point, continued ....

Data Handling		
rate to tape (8-bit images only)	Mbits/s	1.1 @ $\rho_r = \rho_a = 10$ m
	Mbits/s	0.12 @ $\rho_r = \rho_a = 30$ m
number of tape units	----	1
candidate tape-unit data-rate	Mbits/s	1.6 (8-mm cartridge tape)
limits (approximate)	Mbits/s	4-8 (4-mm cartridge tape)
candidate tape-unit capacities	Gbits	40
record-time capacity	hours	5-10 hours (8-bit images)
phase histories	----	for engineering evaluation
radar auxiliary data	----	yes
Image Display		
horizontal display size	pixels	TBD
vertical display size	pixels	TBD
dynamic range	bits/pixel	8
Navigation Accuracies		
navigator type	----	TBD
attitude accuracy	°	TBD
position accuracies	m	TBD
velocity accuracies	m/s	TBD
GPS aiding (Y/N)	----	yes
Motion Compensation		
approach	----	real-time
update rate to SAR, Hz	----	TBD
Mechanical Characteristics		
total power to system	kW	TBD
physical volume of system	m^3	TBD

Identification and Discussion of Key Issues

Squinted Operation vs. Antenna Steering

The present AIREYE SLAR actually operates in squint mode; that is, the antenna doesn't point along a line that is perpendicular to the flight path. The antenna's pointing direction is, instead, 90° away from the aircraft's centerline, averaged over the pass. Because the plane will crab to counter the wind, the antenna actually squints away from 90° by an amount equal to the average drift angle of the aircraft. Short-term yaw variations are electromechanically compensated by moving the antenna as much as $\pm 3°$ to assure that the antenna always points at the same squint angle with respect to the average drift angle. An alternative would be to use navigator information to drive a gimbal so as to always point the antenna at 90° with respect to the ideal flight path. However, the current SLAR antenna, presumably because of its size (8' long), is not

steered in this way. Operating at squint angles away from 90° complicates data processing; however it eliminates the problem of having to steer a large antenna over angles of tens of degrees. Like the SLAR antenna, the antenna for a wide-swath SAR need not be very large in the elevation dimension (height); however, like the SLAR's antenna, it needs to be long in order to form a narrow azimuth beam. The 8-foot SLAR antenna forms a 1° beam. It may be possible to develop a scheme for mechanically steering a physically long antenna (6-8'). Other possible methods of beam steering would be: 1) steering by changing the SAR's center frequency, and 2) steering using an antenna array and phase shifters. These issues need to be looked at further.

Number of Bits Per Image Pixel

Estimated data rates to tape are fairly modest (1.1 Mbits/s) under the assumption of 10-m ρ_r, 10-m ρ_a, 125 m/s velocity, and 8-bit magnitude image data. Because of the 4-8 Mbit/s data-rate capability of 4-mm tape, recording of 16-bit image data does not appear to present a burden at these resolutions.

Slant-Range Resolution, ρ_r

The choice of slant-range resolution is at issue. In this study, I have looked at values of 10 m and 30 m. The ultimate choice for ρ_r will result from cost/benefit considerations. The analysis given here can contribute mainly to the cost data. Improved range resolution directly increases transmitter power as well as image-former input data rates, computational complexity, and output data rates. Calculations given later in this memorandum will shed more light on the transmitter-power issue. The benefit of finer resolution in oil-spill monitoring will be assessed in ongoing joint SNL/Coast-Guard data analyses.

Azimuth Resolution, ρ_a

The choice of azimuth resolution is at issue. In this study, I have considered values of 10 m and 30 m. The choice of ρ_a will also depend on results of ongoing analyses. Improving (reducing) ρ_a directly increases image-former input data rates, computational complexity, and output data rates. The relationship between ρ_a and transmitter power is more complicated and depends on whether the target being imaged is a point target or a distributed target (like the ocean). For the latter target type, reducing ρ_a increases the aperture time, T_a, allowing more pulses to be integrated; however, it also either reduces maximum allowable real antenna gain or the number of looks achievable, or both. The net result is to increase transmitter power for this case. There are several aspects of SAR imaging of the ocean that cause me to believe that seeking extremely fine azimuth resolution is not prudent. These aspects are the azimuth defocusing and smearing that can occur due to radial motion of both long waves and capillary waves on the ocean's surface [3].

Minimum σ^o of Noise Required

I have borrowed data from Motorola's Report CG-D-109-76. These data, which describe scattering coefficient, σ^o, in dB, are given in Table 2, below. I have only included data for VV polarization.

Table 2. Scattering Coefficient of Open Ocean

Depression Angles, °	Sea State Zero	Sea State One	Sea State Two	Sea State Three
1	-60	-50	-44	-39
3	-56	-45	-41	-38
10	-49	-42	-36	-32

Initial calculations for transmitter power will require a 6-dB signal-to-noise ratio for a target area having a σ^o = -45 dB at 54-km range.

System Losses

Assumed system losses are tabulated below in Table 3. Atmospheric loss has been estimated at the 54-km range. The transmitter loss number assumes use of an isolator, 10' of rigid waveguide with a short section of flexible waveguide, and a low-loss circulator. The noise figure number assumes the use of protective, low-loss latching ferrite switches before the low-noise amplifier (LNA) and an LNA noise figure of about 1.5 dB (HEMT technology).

Table 3.

Factor	Loss in dB	Comments
atmosphere	1.5	oxygen absorption, two-way
transmitter	0.8	
radome	1.5	two-way loss
noise figure	2.0	includes rf losses
signal processor	1.2	A/D & windowing

Choice of Operating Frequency

A number of factors affect the choice of operating frequency.

1. Contrast between oil-covered and open ocean varies with frequency. From literature I have reviewed in the course of the Coast Guard study, it appears that good contrast can be obtained at X and Ku bands; however, data are lacking at Ka band, and contrast is reduced at C and L bands. Contrast at Ku band may be a little better than at X band.

2. Increasing the operating frequency increases transmitter power. At a given resolution, required power increases as λ^{-1}. In this case, the decrease in λ^2 is offset by an increase in G^2 (azimuth beamwidth is narrowed); however, T_a is reduced in proportion to λ, therefore increasing P_t in (1,. High-power rf sources are less plentiful and more expensive at Ku band than at X band. Therefore, X band appears to be a good choice.

Peak Transmitter Power Required

The equation for required peak transmitter power, P_t, is

$$P_t = (S/N)(4\pi)^3 R^4 k T_o F_n L / [\sigma^o G^2 \lambda^2 \tau f_p T_a \rho_a \rho_r \sec(\phi) \rfloor N_e]. \quad (1)$$

In (1), (S/N) is signal-to-noise ratio (a value of 4 W/W was used), R is slant range from the radar to the pixel of interest (R = 54 km was used here), k is Boltzmann's constant (1.38 E-21 J/°K), T_o is the temperature (288 °K), F_n is the receiver's front-end noise figure (a value of 1.4 W/W was used; this number includes all receiver losses), L is all combined losses (transmitter, signal-processor, atmosphere, etc.; a value of 3.2 W/W was used), σ^o is scattering coefficient ($10^{-4.5}$ was used), G is peak antenna gain ($10^{3.5}$ was used; 1° β_a was assumed), λ is electrical wavelength (0.032 m) , τ is uncompressed transmit-pulse length ($57 \bullet 10^{-6}$ s), f_p is prf ($2.4 \bullet 10^3$ Hz), T_a is aperture integration time (0.7 s), ϕ is depression angle (6°), and N_e is the effective number of temporal looks at the target cell (values of N_e of {5.7, 13.4, and 19.7} were used for ρ_a values of {10, 20, and 30} m; see related discussion below). Substitution of appropriate values into (1) results in a value of about 15 kW for 10-m ρ_r and ρ_a, about 5 kW for 20-m ρ_r and ρ_a, and about 3 kW for 30-m ρ_r and ρ_a. We believe that an X-band traveling-wave tube (TWT) amplifier having about 10-kW peak output power at about 10% duty ratio could be purchased in today's market.

Elevation Antenna Pattern

The elevation pattern called out in the starting-point specifications of Table 1 is proportional to

(Note: value for Boltzmann's constant above is in error, as are estimates for P_t. See memorandum of June 24, 1993 for revised estimates of P_t. RMA, 8-16-93)

$\csc^2\phi$, where ϕ is the depression angle. The choice of this pattern variation is driven by imaging geometry and by estimated variation of echo power versus slant range, R, to the target pixel. The $\csc^2\phi$ variation removes the R^4 variation (as R is varied) in power received at the radar due to a point scatterer at range R. In the case where a distributed target is imaged, the R^4 term is not the only quantity affecting P_t that varies with R. Two other effects also change P_t: 1) the variations with R of aperture time, T_a, for fixed ρ_a, and 2) the variation of scattering coefficient, σ^o, versus depression angle, ϕ, as R changes.

Variation of T_a With R. Let us assume that ρ_a is fixed and independent of range. Then the required aperture time, T_a, is given approximately by

$$T_a = \lambda R/(\rho_a V_a), \qquad (2)$$

where V_a is aircraft velocity. Therefore, T_a is directly proportional to range. Because (see Table 1) far range is about 54 km and near range is about 8.5 km, required T_a will vary from about 0.7 s at far range to about 0.1 s at near range. Therefore, from (1), the range-law variation obtained after combining R^4 and T_a terms is really only R^3.

Variation of σ^o With ϕ, and Therefore, With R. Table 2 shows data extracted from the Motorola report. Other data reported in [4] indicates that at $\phi = 45°$, σ^o varies from about -35 dB at 5 m/s wind velocity to -20 dB at 15 m/s wind velocity. And at $\phi = 30°$, σ^o varies from about -40 dB at 5 m/s wind velocity to -25 dB at 15 m/s wind velocity. The Motorola data imply that, in the region of small depression angles, σ^o is, to first order, proportional to 1/R at a given wind speed. This would imply that, at least approximately, the effects of T_a and σ^o tend to cancel one another at small depression angles. The data of [4] show a stronger variation of σ^o with R in the region of moderate depression angles (30° and 45°). Taking into account the angular region from 6° to 45° of depression, an increase of the order of 10 to 20 dB should be expected in σ^o as ϕ increases. Since the variation in T_a over this same angular range is only $10 \cdot \log_{10}(54/8.5)$ dB, or about 8 dB, the increase in σ^o at near range will dominate, and with a $\csc^2\phi$ pattern, we can still anticipate significant brightening in the image at near range. This points to the possible need for a sensitivity time control in the SAR to further equalize echo power versus R.

The other issue in relation to the elevation pattern in the following. Because we really only need the $\csc^2\phi$ variation over a depression angle range of 6° to 45°, what is the requirement for the pattern at other angles? The answer is probably that we would like the peak gain of the antenna to occur at maximum range (54 km) and then fall off very rapidly at smaller depression angles. Also, at depression angles larger than 45° and in the rear quadrants of the antenna's pattern, we would ideally want the gain pattern to be zero.

Azimuth Antenna Pattern

The azimuth antenna pattern is driven by a variety of factors, and a number of tradeoffs are possible. There is an advantage to making the azimuth beamwidth β_a as narrow as possible. This increases antenna gain, which reduces P_t. However, reducing β_a also reduces the number of separate looks that can be obtained for each target pixel; therefore, for a system requiring multilook, there exists a lower limit on β_a that cannot be violated. Finally, β_a determines antenna length, L. The relation is, approximately,

$$L = 180\lambda/(\pi \bullet \beta_a), \qquad (3)$$

where L and λ are in like units, and β_a is in degrees. For example, beamwidths of (0.4°, 1°, 2°, and 3°) translate to antenna lengths of (4 m, 1.8 m, 0.9 m, and 0.6 m), which lengths are approximately equivalent to (15', 6', 3', 2'). As mentioned before, if antenna length were small enough, it would be feasible to steer the antenna tens of degrees in azimuth, which would simplify signal processing.

Multilook Processing

Another important issue is multilook processing. Noncoherent averaging of multiple images or "looks" of the same scene reduces the effects of speckle (amplitude variability in a region of the image containing a more-or-less homogeneous assembly of distributed scatterers). Two different multilook schemes could be applied to a broad-swath Coast Guard SAR: 1) temporal multilook, and 2) pixel averaging.

Temporal Multilook. In temporal multilook, a number (N) of looks at a pixel are noncoherently averaged. In this technique, each look is produced by a distinct synthetic aperture, so looks are statistically uncorrelated, both in terms of signal and noise. Normally, pixel amplitudes are averaged to produce the multilook image. This technique preserves the spatial resolutions (ρ_r and ρ_a) of the original single-look images. It also increases image signal-to-noise ratio by approximately $5 \bullet \log(N)$, where N is the number of looks.

Pixel Averaging. In this technique, an image patch is formed at a resolution that is finer than that required in the multilooked output image. Then amplitudes of adjacent pixels are averaged. This averaging reduces speckle and also improves image signal-to-noise ratio. But because adjacent pixels are somewhat correlated (due to the choice of 1.5 oversampling in the azimuth dimension), the effective number of looks, N, is somewhat less than the number of pixels averaged. The applicability of this technique in the Coast Guard SAR design is still being considered.

Image-Formation Algorithm/Signal-Processing Approach

In the design implied by Table 1, range compression is performed at an IF frequency by an analog device such as a surface-acoustic-wave (SAW) filter. This is feasible for the Coast Guard SAR because of the relatively coarse range-resolution requirement (ten meters or so). At these range resolutions pulse bandwidth is narrow enough that A/D circuitry can directly digitize the sampled echo, and no special bandwidth-reduction technique (such as stretch processing, which is used on the SNL Ku-band platform) is required.

A detailed algorithm approach has not been worked out; however, the general approach would be to perform patch processing to form single-look images having resolution $\rho_a \bullet \rho_r$. Single-look images would then be combined noncoherently to form multilook images. This amounts to temporal multilook (discussed above). Because of the large variations in aperture time and in azimuth antenna footprint from near range to far range, the full range swath will need to be divided into overlapped channels, and each channel will be processed somewhat differently. Figure 1 demonstrates the approach.

Suppose we define a particular range channel having near-range equal to R, as shown in Figure 1. Then, the azimuth extent of the illuminated area on the ground at any time is approximately $\beta_a \bullet R$. It is implied, but not shown, that the range channel consists of many range bins, perhaps as many as 1000 bins for the case of 10-m ρ_r. The relative sizes of near-range and far-range for the total swath of the SAR (25 nmi.) are shown approximately to scale; however, the antenna beamwidth shown is exaggerated in comparison to the actual beamwidth (1° nominal in this study). Within the indicated range channel, a focused patch of pixels will be formed using the phase-history aperture shown at left. The length L_a of this aperture is roughly to scale in comparison with the illuminated area at the near-range side of the range channel. After a patch is formed, it is assumed that the image former throws away, or skips, an aperture of pulses having length L_s. With these definitions, we can now write some quantitative expressions relating various quantities to one another. First, the spacing Δ between boundaries of patches coming out of the image former can be expressed as

$$\Delta = L_a + L_s$$

$$= \lambda R/(2 \bullet \rho_a) + L_s. \qquad (4)$$

Further, the number of looks N than can be obtained is approximately

$$N = P_a/\Delta, \qquad (5)$$

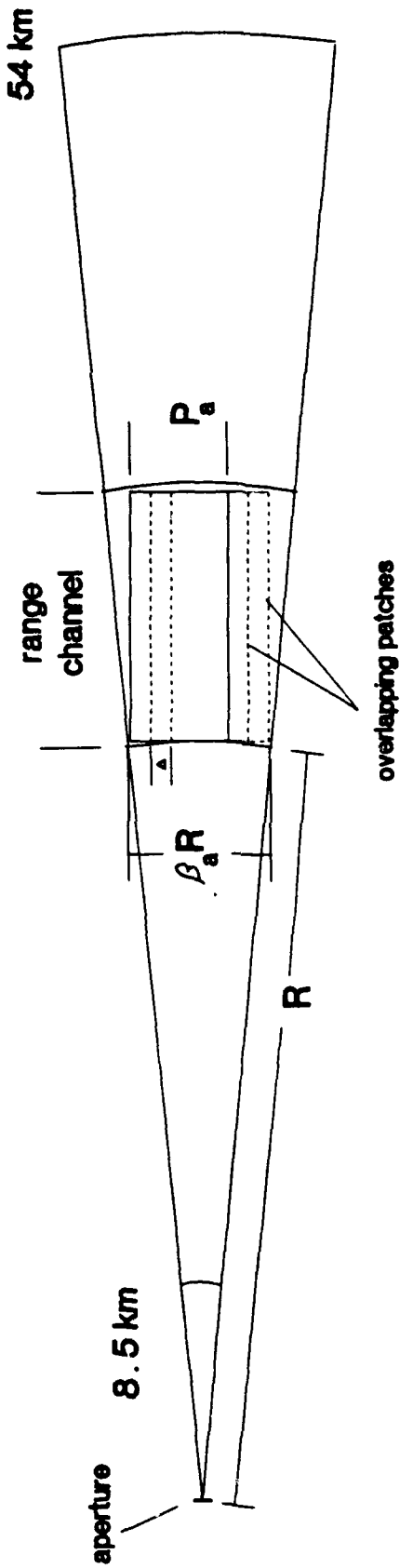

Figure 1. Signal processing considerations.

where the constraint must be met that, for any given patch,

$$P_a \leq \beta_a R - L_a \tag{6}$$

Combining (5) and (6) produces

$$N \leq (\beta_a R - L_a)/\Delta. \tag{7}$$

In the special case that no phase history data are discarded between imaging apertures ($L_a = 0$), Δ just equals L_a, and (4) and (7) can be combined to produce

$$N \leq \beta_a R/\Delta - 1$$

$$= 2\rho_a\beta_a/\lambda - 1. \tag{8}$$

Interestingly, the constraint on N is not a function of R. Table 4 shows the results of evaluating (8) at different values of ρ_a and β_a.

Table 4. Entries are maximum values of N vs. ρ_a and β_a.

ρ_a, m	$\beta_a = 0.4°$	$\beta_a = 1°$	$\beta_a = 2°$	$\beta_a = 3°$
5	1	4	9	15
10	3	9	20	31
20	7	21	42	64
30	12	31	64	97

Notice also from (5) that azimuth patch size, P_a, is just $N\Delta$, or NL_a under the assumptions of Table 4, and because the number of azimuth pixels per patch is just $P_a k_a/\rho_a$, where k_a is the oversampling factor (1.5 assumed), the number of azimuth pixels, N_{az}, is therefore approximately Nk_aL_a/ρ_a, and because

$$L_a = \lambda R/(2\rho_a), \tag{9}$$

then

$$N_{as} \simeq Nk_a\lambda R/(2\rho_a^2). \quad (10)$$

So, for example for the two cases of smallest choices of β_a in Table 4, the following values of N_{as} result at far-range (Table 5) and near-range (Table 6).

Table 5. Entries are the number (N_{as}) of azimuth pixels per patch vs. β_a and ρ_a assuming maximum number of looks and 54-km range.

ρ_a, m	β_a = 0.4°	β_a = 1°
5	51	207
10	38	116
20	22	68
30	17	44

Table 6. Entries are the number (N_{as}) of azimuth pixels per patch vs. β_a and ρ_a assuming maximum number of looks and 8.5-km range.

ρ_a, m	β_a = 0.4°	β_a = 1°
5	8	32
10	6	18
20	4	11
30	3	7

It is important to realize that, due to azimuth roll-off of the antenna's radiation pattern, not all looks at a target pixel will have equal signal strength. This effect makes the "effective" number of looks, denoted here as N_e, somewhat smaller than the actual number of looks, N. Under the assumption that the antenna's two-way pattern has a $\cos^2\theta$ shape (θ being the azimuth angle), the following approximate relationship holds:

$$N_e \simeq 2N/\pi. \quad (11)$$

(Note: "one-way pattern" modified to "two-way pattern" in sentence above on August 16, 1993.)

Pulse-Compression Issues

The conceptual design given in Table 1 recommends a pulse-compression technique implemented using a SAW filter. There are a number of issues here.

Peak Transmitter Power. Use of a pulse-compression technique reduces the peak transmitter power requirement by a factor of $T_{pw} \bullet B_t$, where T_{pw} is the length of the uncompressed transmitter-output pulse and B_t is the transmitter bandwidth. For this conceptual design, this factor is about 855 at 10-m ρ_r and about 285 at 30-m ρ_r.

Use of a SAW Device for Compression. Using a surface-acoustic-wave (SAW) device for pulse compression appears to be attractive. In this approach, the SAR would be used first to generate the transmitted modulation and, upon receive, to compress the echo pulse. This technique eliminates computational requirements that would be present if the pulse compression were done digitally.

Dynamic Range Considerations for a SAW Pulse Compressor. Use of a SAW device for pulse compression will increase dynamic range requirements at the A/D input. Therefore, it will likely be necessary to use A/Ds having ten or more bits in each channel (I & Q).

Navigator Accuracies

TBD

Motion Compensation Requirements

TBD

Mechanical Characteristics

TBD

Distribution: per attached sheet.

APPENDIX E
MOVING-TARGET-INDICATOR MODE

This appendix contains a copy of a memo on moving-target-indicator (MTI) mode for the Coast Guard SAR prepared by Robert M. Axline, Jr., July 21, 1993. It is included here for completeness.

(The remainder of this page intentionally left blank.)

Sandia National Laboratories

Albuquerque, New Mexico 87185

date: July 21, 1993

to: Distribution

from: Robert M. Axline, Jr., Radar Analysis Department, 2344

subject: MTI Mode for the Coast Guard SAR

References

[1] "Coast Guard SAR Design Calculations and Identification of Key Issues," SNL memorandum from Robert M. Axline, Jr., 2344, to Distribution, June 2, 1993.

[2] "Additional Coast Guard SAR Design Calculations," SNL memorandum from Robert M. Axline, Jr., 2344, to Distribution, June 24, 1993.

[3] "Operator's and Unit Maintenance Manual, Radar Surveillance Set AN/APS-131," U.S. Coast Guard Document No. 68-PO3879U, March 15, 1981.

[4] "Estimated Sensitivity of AIREYE SLAR for the Case of a Distributed Target," SNL memorandum from Robert M. Axline, Jr., 2344, to Distribution, June 24, 1993.

[5] "RAR Mode for the Coast Guard SAR," SNL memorandum from Robert M. Axline, Jr., 2344, to Distribution, July 17, 1993.

[6] "Motion Compensation for Coast Guard SAR," SNL memorandum from J. T. Cordaro, 2344, to Distribution, July 16, 1993.

The purpose of this memorandum is to 1) describe two potential moving-target-indicator (MTI) modes that could be implemented in the Coast Guard SAR design [1,2], 2) analyze implementation and performance issues for the two schemes, and 3) compare complexity and performance of these MTI modes to those of RAR [5] and the AIREYE SLAR [3,4]. All calculations are performed under the assumption of a 10-m SAR design.

Summary of Results

- The Coast Guard mission requires radar imaging of sea-borne moving targets. Two potential MTI modes for the Coast Guard SAR are presented: a) "High-Pass Filter with RAR" (HPF/RAR), and b) "Sequential Doppler-Frequency Translation with SAR" (SFT/SAR). Either mode would meet the above-stated requirement. Both MTI modes would yield an image exhibiting reduced clutter (in comparison to RAR or SLAR) and having 10-m range resolution. The HPF/RAR method yields azimuth resolution similar to that of the AIREYE SLAR (140 m @ 8.5-km range and 920 m @ 54-km range). The SFT/SAR method yields 10-m azimuth resolution; however, positioning uncertainty of point targets is much coarser, being equal to the antenna's real azimuth foot-print, $R\Delta\theta$, at a slant range of R m. The proposed SFT/SAR system could image movers over a velocity band of about $\pm$20 kn.

- Implementation of the HPF/RAR MTI approach would require significant additional hardware and software for implementation of the approach given here, regardless of whether concurrent or non-concurrent SAR/MTI functions were desired. Implementation of the SFT/SAR MTI approach would require no additional hardware; however, it would add some to processing and software complexity if thresholding of individual looks were performed in order to detect movers, particularly if synthetic icons were generated and displayed. In the HPF/RAR approach, MTI data could be displayed to the operator separately from or as an overlay (either synthetic icons or actual video) of the normal SAR or RAR image. In the SFT/SAR approach, one of the available looks will be a normal single-look image of the stationary clutter. Synthetic icons from the other looks could be laid over a dim rendition of the single look of stationary clutter. Alternatively, all SFT/SAR clutter-reduced looks could be multilooked in one of a number of ways and displayed, either separately from or as an overlay of the normal SAR single-look of stationary clutter.

- At the maximum 54-km range and low-to-moderate sea states, minimum-detectable point-target radar cross section, σ, for both MTI modes will likely be controlled by thermal noise, as opposed to being controlled by clutter returned from the distributed ocean target surface. Minimum detectable σ for HPF/SAR would be about 0.8 m^2 (-0.8 dBsm). For the 10-m SFT/SAR system, performance would be much better, about 0.008 m^2 (-21 dBsm) under the assumptions that 1) scattering coefficient (σ^o) of the ocean at 6° depression angle does not exceed about -24 dB and 2) clutter reduction for both MTI modes is 20 dB or better. In land-clutter environments, clutter return will likely dominate thermal noise, and minimum-detectable point-target σ will be higher.

Summary of Results, Continued, ...

- Again, assuming 20 dB of clutter rejection, estimated HPF/RAR minimum-detectable point-target cross section against moving targets (for an assumed ocean σ^o of -30 dB) is about 16 dB better than for a 10-m RAR [5] and about 21 dB better than for the AIREYE SLAR [3,4]. Estimated SFT/SAR performance under the same assumptions is about 37 dB better than for a 10-m RAR and about 42 dB better than for the AIREYE SLAR.

- I recommend that the SFT/SAR scheme be implemented, in any newly-developed Coast Guard SAR, as an MTI mode for detection and display of moving targets. If, instead of a new SAR, the Coast Guard chooses to modify an existing SAR, the ease and cost of implementing this MTI mode could very widely, depending on that SAR's capabilities. In this latter case, the RAR mode described in [5] can be viewed as a fall-back position.

The Role of an MTI Mode

As explained in Reference [5], the AIREYE SLAR can image stationary or moving targets on the ocean's surface. However, the conceptual SAR design described in References [1,2] can only image stationary or slowly-moving sea-borne targets. Therefore, an additional mode must be added to the Coast Guard design to allow imaging of more rapidly moving targets ($\geq$ 2 kn radial velocity). A RAR approach to imaging of moving targets was presented in [5]. RAR shows movers but also shows all stationary and slow-moving clutter as well; therefore, it doesn't do a very good job of distinguishing movers for background clutter. As alluded to in [5], several other, perhaps more complex, approaches are possible for imaging moving of targets with SAR. Some of these approaches also provide clutter reduction while providing strong returns from movers. This memorandum describes two such approaches. Both techniques are single-antenna, moving-target-indicator (MTI) schemes. Brief descriptions of the two schemes follow.

Two Possible MTI Approaches

High-Pass Filter with RAR (HPF/RAR)

This scheme adds a digital, high-pass, phase-history filter (running at the prf rate) just after the A/D converters. The high-pass filter output is then magnitude-detected. From this point on, processing is identical to that of the RAR mode [5]. The high-pass filter provides significant rejection of slow-moving and stationary clutter (e.g., land, most ocean waves, and stationary or slowly-moving point targets). Like the RAR, this scheme would provide fine resolution in range (say 10 m), but the azimuth resolution would be determined by the physical beamwidth of the antenna; therefore, azimuth resolution

would be coarse (about 140 m @ 8.5 km, as in RAR mode). The principal advantage of this approach over RAR is its clutter-rejection feature.

Sequential Doppler-Frequency Translation with SAR (SFT/SAR)

Motion compensation for SAR processing will require that the radar employ a low-frequency motion-compensation oscillator at IF to keep the Doppler spectrum of stationary-target echoes within the presummer passband (about 130 Hz) [6]. This same oscillator could be used to shift the Doppler spectrum of the echo to move echo from stationary and slow-moving targets out of the presummer passband and move echo from faster-moving targets into the passband for a particular processed SAR patch. This would allow a number of sequential "looks" to be gotten of the target area, each look at a different oscillator-frequency setting. In this way, the SAR could sweep a fairly wide Doppler band (> 1 kHz) in order to image moving targets. Processing required to form SAR patches in this MTI mode would be identical to processing in normal SAR mode; only the motion-compensation oscillator setting would be changed. Ignoring acceleration effects, moving targets would be reasonably well focused in the patch in which they appeared. Again, range resolution of this system would be the same as for the SAR (say 10 m). Apparent azimuth resolution of the output patches would be equal to the SAR resolution (say 10 m). However, the true position of the moving target would only be known to within an uncertainty interval equal to the RAR azimuth resolution. This is because of an unresolvable ambiguity between the moving target's exact position in the scene and its true radial velocity.

Analysis of Complexity and Performance Issues

Processing Complexity

HPF/RAR. This scheme adds quite a bit of hardware complexity: banks of high-speed, high-pass filters and digital magnitude detectors (one for each range bin) must be added. Additional software complexity required to obtain the MTI image is about equal to that of RAR mode (whatever is required to perform the needed noncoherent integration). If the HPF/RAR MTI image is displayed just like the RAR image, display-function complexity would be the same as for RAR mode. If the MTI image were thresholded to create icons for display as an overlay to the normal SAR or RAR image, some additional complexity would be introduced. As in the case of RAR mode, the image size (if thresholding is not used) need only be about 10% of the size of a normal multilooked SAR image. Use of thresholding would make the output image size much smaller.

SFT/SAR. This scheme adds no hardware complexity to the either the radar analog sections or to the image-formation hardware. Single-look image patches are formed in the same way, regardless of whether the radar is operating in SAR mode or SFT/SAR mode. Some additional computational burden arises if each of the "looks" is to be separately thresholded in order to detect movers on the basis of their strength relative to the total power in the patch. An advantage of this approach, however, is that the amount of image data remaining after the thresholding should be very small; only coordinates of

detections need be stored. Icons from separate looks could be assigned different colors. This would give the operator/interpreter an indication of how fast the target is moving and whether it is approaching or receding. This latter feature is an advantage that the HPF/RAR mode does not exhibit.

If thresholding is not used, another technique must be used to essentially "multilook" the SFT/SAR patches together for display. Each SFT/SAR image patch will have equal resolution in range and azimuth (say 10 m). However, the true position of a moving target in the SFT/SAR image can be determined only to within the azimuth resolution afforded by the physical azimuth beamwidth of the antenna. Therefore, in multilooking the SFT/SAR patches, decimation in the azimuth dimension should be used (e.g., from 10-m to 100-m pixel spacing) to reduce the size of the image. Two possible multilook techniques are:

- Registration and summing of magnitudes (identical to the technique used for normal multilook SAR). This has the disadvantage of reducing signal-to-clutter and signal-to-noise ratios.

- In each patch, choose the largest pixel value in a 10 x 10 submatrix and decimate to a patch 1/100 as large by retaining only this largest value. Combine looks by retaining only the largest value (over all looks) at each common, registered pixel location. This technique retains the largest returns from targets of interest, from noise, and from clutter. It would probably be preferable to summing magnitudes.

I recommend that thresholding be used. This should maintain signal-to-clutter performance and reduce the amount of MTI target data to be displayed.

Performance of MTI Modes Against Point Targets in Thermal Noise (No Clutter)

HPF/RAR. Assuming that processed noise bandwidth for RAR and HPF modes are nearly the same, minimum detectable target radar cross section, σ_{min}, in thermal noise (clutter is neglected in this computation) can be estimated for the HPF/RAR mode by using the minimum-detectable scattering-coefficient-estimate, σ^{o}_{min}, for the 10-m RAR, which, from [5], is about 0.00009 m^2/m^2. The relevant equation for HPF/RAR is

$$\sigma_{min} = \sigma^{o}_{min} \rho_r R \Delta\theta / \cos\phi, \qquad (1)$$

where ρ_r is taken to be 10 m, R is 54 E3 m, $\Delta\theta$ is 0.17 rad, and ϕ is 6°. The result of evaluating (1) is about 0.8 m^2, or about -0.8 dBsm for HPF/RAR mode.

SFT/SAR. In this mode, minimum detectable target radar cross section against thermal noise (no clutter) can be estimated using the minimum-detectable scattering-coefficient-estimate for SAR, which, (by design) from [1], is -45 dB [2]. The governing equation for SFT/SAR is

$$\sigma_{min} = \sigma^{o}_{min}\rho_r\rho_a\sqrt{N_e}/\cos\phi. \quad (2)$$

Here, $\rho_r = \rho_a = 10$ m, and N_e is the effective number of looks for a 10-m system (taken to be 5.73 from [1]). The effect of multiplying by $\sqrt{N_e}$ derates the minimum detectable cross section of SAR by accounting for the fact that in SFT/SAR mode, only one look is obtained of each moving point-like target. The result of evaluating (2) is about 0.0076 m², or about -21 dBsm. This is a very small target!

A few words about the number of available looks are in order. In Table 4, page 13 of [1], I showed that the number of available looks for a system having 10-m ρ_a and 1° azimuth beamwidth is 9 looks, independent of range. For such a system, assuming a 136-Hz presummer bandwidth [1] and assuming that the Doppler-frequency oscillator is tuned to 9 discrete settings spaced 136 Hz apart, the SFT/SAR mode could image movers with radial velocities within the range of about ±20 kn. An SFT/SAR operating at coarser azimuth resolution (say 20 m) could obtain more looks and image a wider velocity band of movers (± 40 kn).

Performance of MTI Modes Against Point Targets in Clutter (No Thermal Noise)
For both MTI modes, their performance against point targets in clutter (the ocean's surface) will depend upon their ability to reject the clutter in favor of faster-moving targets. It is beyond the scope of this memorandum to quantitatively estimate rejection ratios for the two MTI modes described. For the sake of discussion, however, let's assume that the same amount of rejection can be achieved in both HPF/RAR and SFT/SAR modes. In fact, in SFT/SAR mode, rejection will improve as the Doppler frequency offset is increased from zero; this is because of increasing attenuation of stationary and slow-moving clutter due to the presummer's transfer function.

HPF/RAR Performance Against Point Targets in Ocean Clutter. For HPF/RAR imaging of a point target against an ocean background, the minimum detectable target cross section, σ_{min} (in units of m²) can be calculated approximately as

$$\sigma_{min} = A_c(S/C)\sigma^{o}R\Delta\theta\rho_r/\cos\phi, \quad (3)$$

where A_c is the clutter power rejection factor (less than one; typically $10\log_{10}(A_c) \leq -20$ dB or better), (S/C) is the signal-to-clutter ratio required for point-target visibility (assumed here to equal 4), σ^o is the ocean's scattering coefficient, R is target range (taken here to be 54 km), $\Delta\theta$ is the azimuth antenna beamwidth (0.017 rad or 1°), ρ_r is the range resolution (10 m), and ϕ is depression angle (taken here to be 6°). Evaluation of (3) at various assumed values of σ^o and ρ_r and at an assumed value of A_c = 0.01 yields Table 1. These numbers ignore thermal noise, taking into account only the effects of residual stationary and slowly-moving clutter.

Table 1. Clutter-Limited Minimum Detectable HPF/RAR Radar Cross Section (in m²) @ 54 km

Range Resolution ρ_r	Ocean σ^o -30 dB	Ocean σ^o -35 dB	Ocean σ^o -40 dB	Ocean σ^o -45 dB	Ocean σ^o -50 dB
10	0.37	0.12	0.04	0.01	0.004
20	0.74	0.23	0.07	0.02	0.007
30	1.11	0.35	0.11	0.043	0.01

It is interesting to note that in the case of HPF/RAR, 20 dB of clutter rejection is enough to cause thermal noise to control the actual minimum detectable cross section for most examples calculated. That is, the 0.8-m² minimum detectable cross section against thermal noise (from (1)) is larger than every entry in Table 1 except the lower-left entry corresponding to ρ_r = 30 m and σ^o = -30 dB. Of course, at high sea states, σ^o may exceed -30 dB at 6° depression, and clutter would limit system sensitivity.

SFT/SAR Performance Against Point Targets in Ocean Clutter. For SFT/SAR imaging of a point target against an ocean background, the minimum detectable target cross section σ_{min} (in units of m²) can be calculated approximately as

$$\sigma_{min} = A_c(S/C)\sigma^o\rho_r\rho_a/\cos\phi, \quad (4)$$

where A_c, (S/C), and ϕ as defined above for the case of HPF/RAR, and ρ_r and ρ_a are range and azimuth resolution, respectively. Evaluation of (4) at various assumed values of ρ_a, ρ_r, and σ^o and at an assumed value of A_c = 0.01 yields Table 2. These numbers ignore thermal noise, taking into account only the effects of residual stationary and slowly-moving clutter.

Table 2. Clutter-Limited Minimum Detectable SFT/RAR Radar Cross Section (in m²) @ 54 km

Resolutions $\rho_a = \rho_r$	Ocean σ^o -30 dB	Ocean σ^o -35 dB	Ocean σ^o -40 dB
10	0.004	0.001	0.0004
20	0.016	0.005	0.0016
30	0.036	0.011	0.0036

Note that for most cases shown in Table 2, minimum detectable cross section is controlled by thermal noise (0.0076 m², from evaluation of (2) above).

Summary of SLAR, RAR, HPF/RAR and SFT/SLAR Complexity and Performance Comparisons

Table 3 summarizes complexity and performance comparisons for the four modes with regard to moving-target imaging.

Table 3. Comparison of SLAR, RAR, HPF/RAR, and SFT/SAR[1]

Mode	shows slow clutter	shows moving clutter	clutter cell area, m²	relative sensitivity in dB, point target in clutter	added processing complexity wrt SAR design
SLAR	yes	yes	22,600	0	N/A
RAR	yes	yes	9,180	5	moderate (HW & SW)
HPF/RAR	no	yes	9,180	21	high (HW & SW)
SFT/SAR	1 look	yes	100	42	moderate-high (SW only)

[1]Assumes -30 dB ocean σ^o at 6° depression angle.

Distribution:

Gary L. Hover
USCG R&D Center, Environmental Safety Branch
1082 Shennecossett Road
Groton, CT 06340-6096

2344	D. L. Bickel
2344	J. T. Cordaro
2344	W. H. Hensley
2344	J. J. Mason
2344	R. C. Ormesher
2345	B. C. Walker
2345	B. L. Burns
2344	A. W. Doerry
9134	J. D. Bradley
9134	G. A. Mastin
2344	R. M. Axline, Jr.

APPENDIX F
REAL APERTURE RADAR MODE

This appendix contains a copy of a memo on a real aperture radar mode for the Coast Guard SAR prepared by Robert M. Axline, Jr., July 17, 1993. It is included here for completeness.

(The remainder of this page intentionally left blank.)

Sandia National Laboratories

Albuquerque, New Mexico 87185

date: July 17, 1993

to: Distribution

from: Robert M. Axline, Jr., Radar Analysis Department, 2344

subject: RAR Mode for the Coast Guard SAR

References

[1] "Coast Guard SAR Design Calculations and Identification of Key Issues," SNL memorandum from Robert M. Axline, Jr., 2344, to Distribution, June 2, 1993.

[2] "Additional Coast Guard SAR Design Calculations," SNL memorandum from Robert M. Axline, Jr., 2344, to Distribution, June 24, 1993.

[3] "Operator's and Unit Maintenance Manual, Radar Surveillance Set AN/APS-131," U.S. Coast Guard Document No. 68-PO3879U, March 15, 1981.

[4] "Estimated Sensitivity of AIREYE SLAR for the Case of a Distributed Target," SNL memorandum from Robert M. Axline, Jr., 2344, to Distribution, June 24, 1993.

The purpose of this memorandum is to 1) discuss the need for a real-aperture-radar (RAR) mode in the design of a future Coast Guard SAR [1,2], 2) describe how the RAR mode would be implemented, 3) estimate the sensitivity of the radar in RAR mode against distributed- and point-target types, and 4) compare RAR-mode sensitivity to the sensitivity of the AIREYE side-looking airborne radar (SLAR) [3,4].

Summary of Results

- The Coast Guard mission requires radar detection of sea-borne moving targets. A RAR mode in a future Coast Guard SAR would meet this requirement. Such a mode would yield an image having 10-m range resolution and azimuth resolution similar to that of the AIREYE SLAR (140 m @ 8.5-km range and 920 m @ 54-km range).

- Implementation of simultaneous SAR and RAR would require significant additional hardware and software for implementation in the approach given here. Exclusive, or non-concurrent SAR and RAR modes (one mode is selected for a particular pass) would require little additional hardware; however, some additional flexibility in the A/Ds, presummer, and image-formation software would be required. In either case, the RAR should be displayed to the operator as a separate, and perhaps optional, image.

- Sensitivity of a 10-m (ρ_r) RAR to an ocean target is -40.5 dB (σ°_{min}) at 54 km range.

- Sensitivity of the RAR would be similar to that of the AIREYE SLAR. Sensitivity of the 30-m (ρ_r) AIREYE SLAR @ 54 km is about -42 dB, or a little better than the 10-m RAR. A 30-m RAR would, however, have about -50 dB sensitivity, quite a bit better than the SLAR. With an assumed ocean cross section of -40 dB, the 10-m RAR can detect a point target having cross section of about 3.7 m^2 with a signal-to-clutter ratio of 6 dB. At this same range and ocean cross section, the 30-m AIREYE system requires a point target cross section of about 11.1 m^2; therefore, the 10-m RAR would be about 5 dB more sensitive for this function.

The Need for a RAR Mode

The AIREYE SLAR can image stationary or moving targets on the ocean's surface. The conceptual SAR design described in [1,2] can image stationary and slowly-moving sea-borne targets; however, targets having radial velocity greater than about 2 kn would lie (in the Doppler frequency domain) outside the presummer passband; therefore, they would be severely attenuated and likely would not be discernable in the image. Speeds of 10-15 kn for large boats are typical, and speeds of smaller craft could be 25-40 kn. Several fairly complex approaches are possible for imaging moving targets with SAR, including a) use of multiple antennas, receiver, and processing channels, b) use of a single antenna and receiver with multiple Doppler processing channels, c) use of a single antenna and receiver with short-time spectral analysis with averaging, and d) use of a single antenna and receiver with a high-pass filter (for stationary-target removal) and post-detection integration. Although these more complex techniques would provide enhanced system sensitivity, a simpler approach is to implement a RAR mode in the Coast Guard SAR to allow moving targets to appear on the radar display.

Implementation of the RAR Mode

Required Processing

References [1,2] describe a conceptual design for a Coast Guard SAR for broad-swath (25 nmi) oil-spill monitoring. A RAR mode could be implemented in this design in the following way.

- Basic system timing, pulse length, prf, and other key radar parameters are unchanged.
- In RAR mode, coherent presumming is not used. Instead, a magnitude detection of the echo pulse is performed in the IF band (after pulse compression). The detected video is then A/D sampled.
- A number (about 500) of adjacent echo magnitudes in each range cell are added together to achieve noncoherent integration. This was exactly the approach used in the AIREYE SLAR fielded at Santa Barbara in November '92.

Option: Simultaneous SAR and RAR --or-- Either SAR or RAR

The system could be designed to allow both SAR and RAR functions to operate concurrently. In this case, both SAR and RAR information would be available to the operator on any imaging pass. Alternatively, the modes could be exclusive of one another. In this latter case, a pass would either be a SAR pass of a RAR pass.

True simultaneous SAR and RAR requires a third A/D converter and an integrator similar in complexity to the presummer filter. Non-simultaneous implementation of the modes could be achieved using a switchable A/D and a single, more flexible presummer capable of handling either (I,Q) coherent presumming or magnitude non-coherent integration.

If the modes were exclusive of one another, the same image-formation processor could be used to form both SAR and RAR images. In RAR mode, the presummer output could be fed to the image former at the same rate as the (I,Q) samples are fed to it in SAR mode; then the image formation processor could complete the remainder of the required non-coherent integration, a fairly simple task. The RAR image output data rate need only be about 10% of that of the SAR image due to the RAR's much coarser azimuth resolution (about 144-m ρ_a at the 8.5-km minimum range)

Option: Actual or Synthetic RAR Display

In the event that simultaneous SAR/RAR processing were performed, the RAR data could be displayed in either of two ways.

- A separate RAR image could be made available for display. SAR and RAR images could be displayed simultaneously or alternately, at the option of the operator.

- The RAR image could be threshold-detected and coordinates of bright scatterers could be stored. At the option of the operator, icons (synthetic video) at these coordinates could be overlaid upon the SAR image display. This approach is problematic when the imaged swath contains bright return from land; therefore, this approach is not recommended for the RAR display.

RAR Mode Sensitivity

Distributed, or Extended Scattering Target

For an extended scattering target, such as the ocean's surface, the radar competes with thermal noise. In this case, minimum detectable scattering coefficient for RAR mode can be computed approximately from radar and geometrical parameters using equation (1).

$$\sigma^\circ_{min} = (S/N)_{min}(4\pi R)^3 k T_o B F_n L \cos\phi / [P_t N_c G_e^2 \lambda^2 \Delta\theta \rho_r \sqrt{N_i}]. \quad (1)$$

In (1), σ°_{min} has units of m^2/m^2. This quantity is more commonly expressed in decibels; this representation is just $10 \cdot \log_{10}(\sigma^\circ_{min})$. The assumption that minimum scattering coefficient is improved as $1/\sqrt{N_i}$ is a only an approximation. Parameters of (1) are defined in Table 1, below.

Table 1. Radar and geometrical parameters in (1).

Symbol	Units	Value	Definition
$(S/N)_{min}$	W/W	4	minimum detectable signal-to-noise ratio
R	m	5.4 E3	range to target pixel [1]
k	J/K	1.38 E-23	Boltzmann's constant [2]
T_o	°K	288	ambient temperature [1]
B	Hz	15 E6	rf receiver bandwidth [1] (10-m ρ_r)
F_n	W/W	1.58	receiver front-end noise figure [2]
L	W/W	3.2	transmitter, signal-processor, atmospheric, and radome losses [1]
ϕ	°	6	depression angle [1]
P_t	W	173	peak transmitter power [2] for 10-m ρ_r
N_c	---	855	range pulse compression factor [1]
G_e	W/W	2.51 E3	average antenna gain over the beam; taken to 34 dB
λ	m	0.032	electrical wavelength [1]
$\Delta\theta$	rad	0.017	antenna azimuth beamwidth [1]
ρ_r	m	10	range resolution [1]
N_i	---	576	number of pulses averaged noncoherently over 30-m interval @ 125 m/s and 2.4-kHz prf (probably more could be averaged)

The result of evaluating (1) using values from Table 1 is that σ^{o}_{min} for RAR mode is about 0.00009 m^2/m^2, or -40.5 dB. Note that this system has 10-m range resolution, whereas the AIREYE has 30-m range resolution. Reevaluation of [1] for a 30-m resolution system requires use of ρ_r = 30 m and B = 5 MHz. The result is that σ^{o}_{min} is about 0.00001 m^2/m^2, or - 50 dB.

RAR Performance Against Point Targets in Clutter

When the RAR images point targets, point-target echoes must compete with resolution-cell clutter (from the distributed ocean or land target area) in order to be visible in the image. For a RAR (or a SLAR) imaging a point target against an ocean background, the minimum detectable target cross section, σ_{min} (in units of m^2) can be calculated approximately as

$$\sigma_{min} = (S/C)\sigma^{o}R\Delta\theta\rho_r/\cos\phi, \qquad (2)$$

where (S/C) is the signal-to-clutter ratio required for point-target visibility (assumed here to equal 4), σ^{o} is the ocean cross section, R is target range (taken here to be 54 km), $\Delta\theta$ is the azimuth antenna beamwidth, 0.017 rad (1°), ρ_r is the range resolution, and ϕ is depression angle (taken here to be 6°). Evaluation of (2) at various assumed values of σ^{o} and ρ_r yields Table 2.

Table 2. Minimum RAR Detectable Radar Cross Section (in m^2) @ 54 km

Range Resolution ρ_r	Ocean σ^{o} -30 dB	Ocean σ^{o} -35 dB	Ocean σ^{o} -40 dB	Ocean σ^{o} -45 dB	Ocean σ^{o} -50 dB
10	36.9	11.7	3.7	1.2	0.4
20	73.8	23.4	7.4	2.3	0.7
30	110.8	35.0	11.1	3.5	1.1

Comparison of RAR and AIREYE SLAR Sensitivities

Results above show that the RAR and SLAR have similar sensitivities. A 30-m RAR has about -50 dB sensitivity against distributed targets @ 54 km, as opposed to about -42 dB for the AIREYE SLAR [4]. However, a 10-m RAR has about -40.5 dB sensitivity, similar to the SLAR. Table 2 shows that, in terms of detection of point targets in clutter, the 10-m system generally has a factor-of-three (5 dB) advantage over a 30-m system because of the former's smaller clutter-cell area. The conclusion can be drawn that the 10-m RAR system would show improved performance for this function.

Errata for Reference [4]

I made a typographical error in Table 1, page 2 of [4]. The receiver bandwidth, B should be 6•E6 Hz, not 6•E3 Hz. Spreadsheet calculations were made with the correct value of bandwidth, so the error does not affect estimates of AIREYE SLAR sensitivity given in [4].

Distribution:

Gary L. Hover
USCG R&D Center, Environmental Safety Branch
1082 Shennecossett Road
Groton, CT 06340-6096

2344	D. L. Bickel
2344	J. T. Cordaro
2344	W. H. Hensley
2344	J. J. Mason
2344	R. C. Ormesher
2345	B. C. Walker
2345	B. L. Burns
2344	A. W. Doerry
9134	J. D. Bradley
9134	G. A. Mastin
2344	R. M. Axline, Jr.

(This page intentionally left blank.)

APPENDIX G
ADDITIONAL SAR DESIGN CALCULATIONS

This appendix contains a copy of a memo on additional Coast Guard SAR design calculations prepared by Robert M. Axline, Jr., June 24, 1993. It is included here for completeness.

(The remainder of this page intentionally left blank.)

Sandia National Laboratories

Albuquerque, New Mexico 87185

date: June 24, 1993

to: Distribution

from: Robert M. Axline, Jr., Radar Analysis Department, 2344

subject: Additional Coast Guard SAR Design Calculations

References

[1] "Coast Guard SAR Design Calculations and Identification of Key Issues," SNL memorandum from Robert M. Axline, Jr., 2344, to Distribution, June 2, 1993.

[2] "Estimated Sensitivity of AIREYE SLAR for the Case of a Distributed Target," SNL memorandum from Robert M. Axline, Jr., 2344, to Distribution, June 24, 1993.

[3] "Operator's and Unit Maintenance Manual, Radar Surveillance Set AN/APS-131," U.S. Coast Guard Document No. 68-PO3879U, March 15, 1981.

The purpose of this memorandum is to 1) correct an error in a calculation given in [1], 2) to discuss possible SAR system design tradeoffs, and 3) to compare the predicted performance characteristics of the X-band SAR design presented in [1] to the predicted [2] and known [3] characteristics of the AIREYE SLAR.

New Estimates of SAR Required Transmitter Power

On page 8 of [1], I estimated required transmitter power for a conceptual Coast Guard SAR. I used an incorrect value of Boltzmann's constant, k, in that calculation. The correct value is 1.38 E-23. The value of noise figure used was 1.4 W/W. In new calculations, I have increased that value slightly to 1.58 W/W. Other parameter values and assumptions defined in [1] are unchanged. The revised estimates of required transmitter power are much lower than those given in [1]. These estimates are for a minimum detectable scattering coefficient, σ^{o}_{min}, of -45 dB at a slant range of 54 km. The resulting values of P_t versus SAR resolutions are given in Table 1.

Table 1. Required transmitter power for conceptual SAR.

Range Resolution ρ_r, m	Azimuth Resolution ρ_a, m	Required Transmitter Power, W
10	10	173
20	20	57
30	30	31

Discussion in [1] pointed out that a TWT having as much as 10 KW could be procured at X band. More recent discussions with Rick Knudson, Department 2345, have revealed that 600-W units would be quite readily available, that 600-W TWTs and 100-W TWTs would not differ greatly in price, but that the power supply for the 600-W TWT would be somewhat more expensive than the power supply for the 100-W unit.

Possible Tradeoffs for SAR Design

There are a number of directions one could go from the baseline SAR design defined in [1] and refined above.

Configuration A: Low power, nominal sensitivity, large antenna. One could settle for a -45 dB system (at 54 km range) and select the transmitter power from Table 1 corresponding to the desired resolution. The 2-m long antenna (β_a = 1°) may not be steerable.

Configuration B: High power, improved sensitivity, large antenna. One could increase peak transmitter power to, say, the order of 1 kW. If the antenna were not changed, system sensitivity at 54 km would be improved accordingly. The other advantage of this system would be that operating range of the system could be extended somewhat. The increased range would require longer integration time (T_a), and the prf, f_p, would have to be reduced accordingly. The resulting increased range achievable would vary about as the 1/4 power of excess transmitter power. So, for example, for the 20-m system, if we used a 600-W transmitter but only needed 57 W at 54 km for -45 dB system sensitivity, system sensitivity at 54 km would improve to about -55.5 dB, and we could achieve a -45 dB sensitivity at a maximum range of about

$$(600/57)^{1/4} \bullet 54 \text{ km} \approx 97 \text{ km}. \quad (1)$$

However, the integration time T_a would now be about 1.23 s instead of the 0.7 s required at the 54-km range. Again, this system would use the 2-m long antenna.

Configuration C: High power, nominal sensitivity, smaller antenna. One could use a higher transmitter power than that required by Table 1 and use the excess to reduce the antenna size while maintaining a -45 dB system sensitivity. So, for example, let's look at the 20-m system and again select a transmitter power of 600 W. Suppose we wanted to reduce the antenna length to less than one meter by increasing the azimuth beamwidth from 1° to 3°. If we did nothing to try to increase the number of looks obtained, the presum integer would not have to change from the value used at 1° beamwidth (a value of 12 per page 4 of [1]). Because antenna gain G is inversely proportional to the azimuth beamwidth $\Delta\theta$, G^2 would be cut by a factor of about 9, taking up nearly all of the excess transmitter power factor of 600/57 = 10.5. Therefore the resulting system sensitivity would be improved only slightly, about $10\log_{10}(10.5/9) \approx 0.7$ dB.

Configuration D: High power, improved sensitivity, somewhat smaller antenna. One might be able to achieve a steerable antenna design by just cutting the antenna size in half (2° azimuth beamwidth). In this case, peak antenna gain would only be cut by a factor of 4. Therefore, this would leave $10\log_{10}(10.5/4) = 4.2$ dB of excess transmitter power that could be applied to improve system sensitivity from -45 dB to -49.2 dB at 54 km.

Comparison of SLAR and SAR Design Key Performance Parameters

Table 2 summarizes key performance characteristics of SLAR and conceptual SAR systems. This information should be useful in the cost/benefit analysis.

Table 2. Comparison of SLAR and Conceptual SAR

Characteristic	Units	SLAR Performance	SAR Performance
ρ_a	m	100-700, degrades w/ R	10-30, choose one
ρ_r	m	30	10-30, choose one
clutter cell	m^2	3,000-21,000	100-900
σ^o_{min} (54 km)	dB	-41.9	-45 to -55
integration time	s	0.25	6.3 (multilook)
antenna length	m	2	< 1 m possible
antenna steering	--	short-term yaw	20°-30° with short antenna
noise figure	dB	8	2
peak tx power	W	200,000	100-1000, choose one
pulse width	s	200 E-9	57 E-6
prf	Hz	750	2400
duty ratio	s/s	0.00015	0.13
average power	W	30	12-136

APPENDIX H
INTERIM RESPONSE

This appendix contains a copy of a memo responding to comments by Gary Hover, USCG R & D Center, prepared by Robert M. Axline, Jr., May 14, 1993. It is included here for completeness.

(The remainder of this page intentionally left blank.)

Sandia National Laboratories

Albuquerque, New Mexico 87185

date: May 14, 1993

to: Distribution

from: Robert M. Axline, Jr., Manager, Radar Analysis Department, 2344

subject: Interim Response to Gary Hover's Comments on My Memorandum of March 15, 1993 and Transmittal of SAR Capabilities Survey Information

References

[1] "High-Level Requirements for Coast Guard SAR Capability," memorandum from R. M. Axline, Jr., 2344, to Distribution, March 15, 1993.

[2] "CG R&D Center Comments on Bob Axline's Memorandum of 15 March '93," memorandum from Gary Hover, Coast Guard R&D Center, to Bob Axline, April 2, 1993.

[3] "Information Survey Relating to Synthetic Aperture Radar Capabilities," SNL CG-Project Document, April 28, 1993.

[4] "Conceptual Requirements for a Synthetic Aperture Radar System for Oil-Spill Response," SNL CG-Project Document, April 28, 1993.

[5] "A Comparison of Ku-Band Doppler Measurements at 20° Incidence With Predictions from a Time-Dependent Scattering Model," D. R. Thompson, Johns Hopkins University, APL, et al, preprint of journal article that had been submitted for publication in JGR-Oceans circa 1991.

[6] "Doppler Spectra from the Ocean Surface With a Time-Dependent Composite Model," D. R. Thompson, JHU/APL, in Radar Scattering from Modulated Wind Waves, G. J. Komen and W. A. Oost, eds., pp. 27-40, Kluwer Academic Publishers, Dordrecht, Boston, and London (1989).

[7] "Theory of Synthetic Aperture Radar Ocean Imaging: A MARSEN View," K. Hasselmann, et al, Journal of Geophysical Research, vol. 90, no. C3, pp. 4659-4686, May 20, 1985.

Introduction

The purpose of this memorandum is two-fold: 1) to provide interim responses to Gary Hover's recent comments [2] relating to Reference [1]; and 2) to provide the R&D center with a copy of survey documentation we have recently sent to vendors of existing SARs.

Responses to Gary Hover's Comments [2]

Paragraph headings in this section are consistent with Gary's headings in Reference [2].

Scope of Systems Study

I have recently contacted LCDR Bill Paradise to discuss SeaView and obtain a Northrop POC. The POC Bill gave me is Bob Whiteman in Hawthorne, CA, phone: (213) 600-1276. I have since talked by phone with Doug Burger, who works with Mr. Whiteman. Doug described what Northrop is doing for the Coast Guard. I will send Doug a copy of Reference [4] and talk with him further after he has had a chance to study that information.

Aircraft Platform

The velocity range of 90 to 124 m/s has been incorporated into our conceptual requirements document [4].

Primary SAR Usage

Your desire that we consider a fine-resolution spotlight capability is reflected in [4]. I have some comments and questions regarding this desired capability.

- One's ability to positively identify a vessel will, of course, be a function of the SAR's resolution. Positive identification, if feasible, would require extremely fine resolution. I am assuming that classification and/or identification of targets at sea would be performed by human operators or interpreters. Do you (Gary) concur?

- Our experience with the target recognition and ID problem has shown that this is a complex and, perhaps, a costly problem to solve. It may not be feasible, given today's technology, to ID vessels with high confidence.

- However, even if positive ID were not achievable, certain classification information could be obtained. Of course, the SAR image would yield the approximate position of the vessel. Radial motion of the vessel would cause it to be displaced in the image in the along-track dimension. This displacement amounts to about 50 m of displacement per nautical mile/hour for the case of an

aircraft velocity of 100 m/s, and a detection range of 5 nautical miles (a reasonable range for a fine-resolution SAR capability). Further, with resolution of the order of one meter, for example, the approximate length and width of the vessel could be determined from the SAR image. My question is: would this type of characterization of the target be useful to you (Gary)? Please comment.

Off-the-Shelf Technology
The SAR survey [3] is one method we are using to examine this issue. Also, during the cost/benefit study, the results of task 8 will be used, along with our knowledge of commercially available components, to determine feasibility of developing a SAR for oil-spill response using off-the-shelf technology.

Near-Real-Time Data Availability
Gary's comments have been incorporated into Reference [4].

Installation Configuration
Installation configuration tradeoffs and motion compensation issues will be addressed in the final report.

Required Swath
The statement relating to swath has been modified in [4].

Required Resolution
Your desire to have square pixels on the ocean's surface is reflected in Reference [4]. Because range-dimension resolution and cross-track resolution (on the ocean's surface) are nearly equal for shallow depression angles, and because pixels over most of the swath of the SAR will be viewed from these shallow angles, the SAR's baseline resolution requirement will be that range and azimuth resolutions be the same and that the image be sampled in the range dimension in such a way that image pixels will be square on the ocean's surface.

We have not concluded our investigation relating to a possible "practical limit" on image resolution imposed by wave motions produced by wind speeds of 5 to 25 knots. We are now examining one ROI from November 12 (SAR, west-looking) that appears to show azimuth smearing for a SAR look direction along the wind vector. At this point, we can offer the following observations.

Swell Action. We have evidence from the Santa Barbara November 12 west-looking data that long-wavelength swell action can significantly affect the SAR image. These effects occur predominately when the SAR is looking in a direction normal to the wavefront of the long waves. The phenomenon (for a wave approaching the SAR) is that the front edge of the wave moves upward and forward, with a portion of this motion toward the SAR, while the back side moves downward and away from the SAR. This motion is often called orbital

motion of the long waves [5]. The effect is that the front of the wave will be displaced forward (along the flight path) in the image, and the back side will be displaced aft. The amount of displacement D (in the image) of the front side of the wave, for example, will be approximately

$$D = V_f R/V_a. \quad (1)$$

where V_f is the radial velocity of the wavefront material toward the SAR, R is the range from the SAR to the pixel containing the wavefront, and V_a is the aircraft scalar velocity (speed). Aircraft velocity for the SNL SAR at the Santa Barbara test was about 55 m/s. Range to scene center-line was about 6400 m. So, for example, a radial velocity of 0.2 knot (about 0.1 m/s) would produce an azimuthal displacement of about 11.6 m. Larger wavefront radial velocities will cause proportionately larger displacements (e.g., 1 knot causes 58 m of displacement!). Because of the relatively long period of these long waves, the SAR's resolution cell (3 m x 3 m) doesn't contain both the front and back sides of the wave. From study of the November 12th west-looking (approximately along the wind vector and perpendicular to the long-wave wave-fronts) and south-looking (approximately perpendicular to the wind vector and along the long-wave peaks and troughs), it appears that the horizontal (east-west) motion of the long waves is the dominant contributor to the ocean's radial velocity with respect to the SAR. The southlooking pass shows tens of meters of displacement of the wave-fronts, apparently caused by radial motion.

Wind-Induced Capillary-Wave Scatterer Velocities. Significant image smearing (as opposed to a displacement) in the azimuth (along-track) dimension could also result from radial velocity of capillary waves (that is, movement toward and away from the radar) that are induced by local winds. The motion of interest here is the differential motion of the capillaries with respect to a coordinate frame of reference that moves with the orbital motion of the long waves. A given SAR resolution cell can contain capillary waves moving at different velocities, relative the radar. The result of many differently moving scatterers is to produce a "spectrum" of radial velocities within the resolution cell. The width of this spectrum maps directly to an azimuthal width over which the SAR's image will be defocused, or smeared. The effective width, X_a of the smearing will be approximately

$$X_a = V_s R/V_a. \quad (2)$$

where V_a and R are as defined above, and V_s is the two-sided effective width of the radial velocity spectrum of the scattering cell. So, for example, if the velocity spread of the spectrum is 0.2 knot (about 0.1 m/s), the smearing width, X_a, would be about 11.6 m. If the

spectral width were 1 knot (0.5 m/s), X_a would be about 58 m, and so on. Thompson's results reported in [5] imply that at 20-knot wind speeds, 20° incidence, and with a Ku-band radar looking directly into the wind, the estimated effective velocity spread is about 1 knot. Thompson's results would imply that under the same wind conditions and at the same look angle, significant azimuth smearing (58 m of it!) should be evident in 3-m images SAR for either down-wind or up-wind look directions. Examination of the south-looking November 12 pass shows no smearing of the order of 58 m; however, some smaller amount of smearing may well be present. It is most likely that apparent radial velocity spread varies with both depression angle and wind speed.

Another fact that seems apparent is that the principal direction of travel of capillary waves should be along the vector of the local wind. Therefore, the effect of radial scatterer velocities should be most pronounced when the radar is looking either up-wind or down-wind. In cases where the SAR is looking cross-wind, these effects should be minimized. What we are missing at this point is information relating to how the Ku-band Doppler spectrum caused by capillary-wave motion in the resolution cell relates to wind speed and depression angle and how much movement of capillaries occurs in directions that deviate from the direction of the local wind vector. I'm confident that we can quickly obtain more information from literature we have in-hand [6,7]

Bulk Flow Effects. A bulk average velocity of the ocean surface being imaged will cause an azimuthal shift of the entire scene over which the bulk flow applies uniformly. This phenomenon should not be a major concern for oil-spill imaging.

A separate phenomenon, image smearing in the range dimension, can result from a bulk flow or movement of the target-cell material through SAR resolution cells during the time the synthetic aperture is being constructed. The ideal application of this model requires the unrealistic assumption that the surface of the moving material remains rigid as it moves. With this assumption, the dimension X_r of this smearing should be approximately

$$X_r = T_a V_b, \tag{3}$$

where T_a is the aperture time and V_b the bulk target-cell velocity. The aperture time, T_a, for the November 1992 Santa Barbara data collection can be calculated as

$$T_a = \lambda R/(2V_a\rho_a), \tag{4}$$

where λ, R, and V_a are as defined above, and ρ_a is the azimuth resolution (3 m). Combining (3) and (4) produces

$$X_r = \lambda R V_b/(2V_a\rho_a). \quad (5)$$

The aperture time T_a resulting from evaluation of (4) is about 0.4 s. So, from (3) for example, a bulk velocity of the one knot would produce a range smearing of only about 0.2 m. Larger bulk velocities would cause proportionately larger range smearing. This same phenomenon would also result in smearing in the azimuth dimension if the SAR were looking normal to the direction of bulk flow. Although, as in the cases mentioned above, we lack detailed information, at this point, on the physics of the ocean's dynamics, the bulk-flow phenomenon appears to be a minor player in defocusing of the image.

Comments on the Above Observations. One interesting point to note is that equations (1) and (2) are not functions of λ, the electrical wavelength, while (5), which depends on aperture time, is proportional to λ. A common element of equations (1), (2), and (5) is the presence of the characteristic scatterer velocity in the numerator and the aircraft velocity, V_a, in the denominator of the equations. These facts imply that the practical limit of resolution for ocean imaging can be extended somewhat by increasing aircraft velocity. Of course, increasing V_a increases the rate at which data enters the real-time image former; this also increases the rate at which image data must be stored to tape. The available aircraft will also place limits on velocity. Another way to counter the effects of displacement of the long-wave wave-fronts is to image along the peaks and troughs of the long waves. And the potentially significant effects of differential radial motion of capillary waves could probably be reduced by imaging cross-wind. In any event, none of the above discussion implies that range resolution of the SAR is significantly affected by "motion of the ocean".

Image Requirements

Gary had asked that I explain a number of comments I made in the like-titled paragraph of [1]. The comments, which related to the possible need for complex data, were probably confusing, because they do not appear to relate to any of the other requirements. Let me explain. At this time, we see no requirement for complex data to meet the Coast Guard oil-spill response mission. However, the real-time image former will "compute" the image by performing arithmetic operations that produce a complex image (both magnitude and phase data are produced). My intent in the "Image Requirements" paragraph was to say that although we cannot identify a reason now for retaining the phase information, it is a good idea (assuming that the cost is not excessive) to design any new system to retain the phase and provide it as an optional output data stream. If in the future, it is determined that complex data could be exploited in the oil-spill response mission, the SAR could perhaps be modified at reduced cost. Complex image data have been used previously by JPL to map scatterer velocities on the ocean's surface. Complex data are also being used

at Sandia to measure height (topography) of terrain and man-made structures. It may be possible to measure ocean wave heights and vertical size of vessels using the topographic SAR scheme. In any event, these techniques amount to interferometry, which, for ocean imaging, requires multiple antennas and, at a minimum, a separate receiver front end for each antenna. These techniques are beyond the scope of our investigations; however, our experience has shown that it isn't a good idea to design out a phase-data spigot if it is possible that spigot might be useful in the future.

Image Calibration

Most modern SARs are capable of being calibrated to plus or minus 2 or 3 dB, so this capability is not necessarily going to cost a lot. But even if calibration is not required, we should at a minimum require that the noise level in the output image be known. This would give the image interpreter a way to know when he is just seeing noise and not meaningful echo.

Likely, calibration for different missions that require different system sensitivities would amount to adjustment of receiver gain and, possibly, transmitter power. Probably the best operator interface would be one that allowed the operator to specify the class of target to be imaged. Then the SAR would translate this class into the proper SAR control settings.

Likely, fine-resolution imaging would be done at a fixed depression angle, say at 45°, and at shorter range, for example, at a few nautical miles. The imaging altitude may be lower, as well. The ROI in wide-swath mode would have to be identified and designated by an operator. Then the coordinates of the ROI could be used to compute the aircraft's trajectory for a fine-resolution imaging pass. This would probably be the most complicated operation for switching from wide-swath to fine-resolution modes. Other necessary reconfiguration of the SAR could be automatic, including repointing of the antenna, adjustment of transmitter power, receiver gain, and other parameters.

Image Annotation Requirements

Gary's comments on this subject have been incorporated into [4].

Image Processing Requirements

Real-time functions mentioned would be automatically performed by the real-time signal processor and would require no operator actions. Other comments have been incorporated into [4].

Image Display Requirements

Your points regarding two separate displays are well taken and have been incorporated into [4].

Telemetry Interface Requirements

See "Scope of System Study" section, above.

Printed Hardcopies
Please relate more about your experiences with the HP Laserjet III printer in our next telephone conversation.

Use of Printed Images
Gary's comments have been incorporated into [4].

Additional Comments
I want to thank recipients of this memorandum in advance for their comments and inputs.

SAR Capabilities Survey

I have solicited responses from a number of SAR vendors by sending them copies of References [3] and [4]. I am sending Gary Hover a copy of each of these documents. We expect to start getting some responses in late May.

Gary L. Hover (1 FAXed, 1 mailed)
USCG R&D Center, Environmental Safety Branch
1082 Shennecossett Road
Groton, CT 06340-6096
FAX: (203) 441-2792
Note: include copies of References [3] and [4] for Gary.

2344 J. J. Mason
9134 J. D. Bradley
9134 G. A. Mastin
2344 R. M. Axline, Jr.

(This page intentionally left blank.)

APPENDIX I
REGION-OF-INTEREST INFORMATION

This appendix contains a table of regions-of-interest (ROIs) extracted from SAR and SLAR imagery for resolution studies. It is included here for reference should additional data exploitation be necessary.

(The remainder of this page intentionally left blank.)

Table I-1. Regions-of-Interest

Date	Sensor	Region-of-Interest Designator[a]	Coord.[b]	Comments
Nov. 10	SAR	N10W_TA4_R1	(1208,120) (1498,510)	E. of Goleta Point
Nov. 10	SAR	N10W_TA4_R2	(53,320) (440,610)	W. of Holly
Nov. 10	SAR	N10W_TA4_R3	(615,210) (905,600)	S. of Goleta Point
Nov. 10	SAR	N10N_TA4_R1	(1208,120) (1498,510)	E. of Goleta Point
Nov.10	SAR	N10N_TA4_R2	(50,320) (440,610)	W. of Holly, Ship wake
Nov. 10	SAR	N10_TA4_R3	(615,210) (905,600)	S. of Goleta Point
Nov. 11	SAR	N11E_TA4_R1	(472,258) (860,546)	S. of Goleta Point, incl. Holly
Nov. 11	SAR	N11E_TA4_R2	(216,42) (504,430)	NW of Holly
Nov. 11	SAR	N11E_TA4_R3	(1256,54) (1646,344)	E. of Goleta Point, kelp
Nov. 11	SAR	N11E_TA4_R4	(952,256) (1242,646)	S. of Goleta Point
Nov. 11	SAR	N11E_TA4_R5	(1216,316) (1606,606)	SE of Goleta Point
Nov. 11	SAR	N11S_TA4_R2	(8,208) (298,598)	W. of Holly
Nov. 11	SAR	N11S_TA4_R5	(1029,400) (1419,690)	SE of Goleta Point
Nov. 11	SAR	N11S_TA4_R6	(210,545) (600,835)	S. of Holly
Nov. 11	SLAR	HN11N_TA4_R1	(1,2292) (1000,3192)	

Table I-1. Regions-of-Interest

Date	Sensor	Region-of-Interest Designator[a]	Coord.[b]	Comments
Nov. 11	SLAR	HN11E_TA4_R1	(111,1) (1011,1000)	Poor quality
Nov. 11	SLAR	HN11W_TA4_R1	(1953,1) (2853,1000)	
Nov. 11	SLAR	LN11N_TA4_R1	(1,2292) (1000,3192)	
Nov. 11	SLAR	LN11E_TA4_R1	(72,1) (972,1000)	Poor quality
Nov. 11	SLAR	LN11W_TA4_R1	(1990,1) (2890,1000)	
* Nov. 12	SAR	N12W_TA1_R1	(862,425) (1252,715)	SW of Holly, broken patches of oil on water, wave motion effect
Nov. 12	SAR	N12W_TA1_R2	(35,246) (325,639)	SW of Naples
* Nov. 12	SAR	N12W_TA1_R3	(1661,44) (1951,434) *(1400,180) (1809,469)	E. of Goleta Point, oil (and biomass?). The region was expanded left past Goleta point for resolution study
Nov. 12	SAR	N12W_TA1_R4	(40,465) (330,855)	S of N12W_TA1_R2, some overlap
* Nov. 12	SAR	N12S_TA1_R1	(862,425) (1252,715)	SW of Holly, compare w/ N12W_TA1_R1
Nov. 12	SAR	N12S_TA1_R2	(35,246) (325,639)	SW of Naples, compare with N12W_TA1_R2

Table I-1. Regions-of-Interest

Date	Sensor	Region-of-Interest Designator[a]	Coord.[b]	Comments
* Nov. 12	SAR	N12S_TA1_R3	(1558,48) (1848,438) *(1331,246) (1740,535)	E. of Goleta Point, prime study region, excellent example. The region was expanded left past Goleta point for resolution study.
Nov. 12	SAR	N12S_TA1_R4	(40,465) (330,855)	S of N12S_TA1_R2, compare w/ N12W_TA1_R2
Nov. 12	SLAR	HN12S_TA1_R1	(1,330) (1000,1220)	
Nov. 12	SLAR	HN12E_TA1_R1	(15,1) (909,1000)	Poor quality
Nov. 12	SLAR	HN12W_TA1_R1	(1962,1) (2862,1000)	
* Nov. 12	SLAR	LN12S_TA1_R1	(1,330) (1000,1220)	Compare with SAR, N12W_TA1_R3 and area just west to Goleta Point.
Nov 12	SLAR	LN12E_TA1_R1	(15,1) (909,1000)	
*Nov. 12	SLAR	LN12W_TA1_R1	(1962,1) (2862,1000)	Wishbone emulsion outline S. of Naples
Nov. 14	SAR	N14S_TA1_R1	(1300,159) (1590,549)	S. of Goleta Point, incl. gas bubble
Nov. 14	SAR	N14S_TA1_R2	(676,381) (1066,671)	W. of Holly, long diag. emulsion line
Nov. 14	SAR	N14S_TA1_R3	(974,217) (1364,507)	N. or Holly, long diag. emulsion line
Nov. 14	SAR	N14W_TA1_R2	(660,382) (1050,672)	W. of Holly, long diag. emulsion line

Table I-1. Regions-of-Interest

Date	Sensor	Region-of-Interest Designator[a]	Coord.[b]	Comments
Nov. 14	SLAR	HN14S_TA1_R1	(1,260) (1000,1160)	Long diag. emulsion line
Nov. 14	SLAR	HN14E_TA1_R1	((20,1) (920,1000)	
Nov. 14	SLAR	HN14W_TA1_R1	(2000,1) (2900,1000)	
Nov. 14	SLAR	LN14S_TA1_R1	(1,260) (1000,1160)	
Nov. 14	SLAR	LN14E_TA1_R1	(20,1) (920,1000)	
Nov. 14	SLAR	LN14W_TA1_R1	(2000,1) (2900,1000)	
* Nov. 15	SAR	N15E_TA1_R1	(852,334) (1242,624)	W. of Holly
* Nov. 15	SAR	N15E_TA1_R3	(1154,120) (1444,520)	S. of Goleta Point, incl. Holly and gas bubble
Nov. 15	SAR	N15E_TA1_R4	(1456,130) (1746,520)	E. of Goleta Point, kelp
Nov. 15	SAR	N15S_TA1_R1	(798,358) (1188,648)	Holly and W., excellent example
Nov. 15	SAR	N15S_TA1_R2	(11,430) (401,648)	S. of Naples, excellent example
* Nov. 15	SAR	N15S_TA1_R3	(1128,166) (1418,556)	S. of Goleta Point,, incl. Holly and gas bubble, kelp, compare w/ SLAR LN15W_TA1_R1
Nov. 15	SLAR	HN15N_TA1_R1	(1,2300) (1000,3200)	
Nov. 15	SLAR	HN15E_TA1_R1	(1,1) (900,1000)	Poor quality

Table I-1. Regions-of-Interest

Date	Sensor	Region-of-Interest Designator[a]	Coord.[b]	Comments
Nov. 15	SLAR	HN15W_TA1_R1	(2140,1) (3040,1000)	
* Nov. 15	SLAR	LN15N_TA1_R1	(1,2300) (1000,3200)	
Nov. 15	SLAR	LN15E_TA1_R1	(1,1) (900,1000)	
Nov. 15	SLAR	LN15W_TA1_R1	(2140,1) (3040,1000)	Compare w/ SAR N15S_TA1_R3, kelp off Goleta Pt.
Nov. 16	SLAR	HN16S_TA1_R1	(1,320) (1000,1220)	
Nov. 16	SLAR	HN15E_TA1_R1	(57,1) (957,1000)	Poor quality
Nov. 16	SLAR	HN15W_TA1_R1	(1944,1) (2844,1000)	
Nov 16	SLAR	LN15S_TA1_R1	(1,320) (1000,1220)	
Nov. 16	SLAR	LN15E_TA1_R1	(57,1) (957,1000)	
Nov. 16	SLAR	LN15W_TA1_R1	(1990,1) (2890,1000)	

a. SAR image region-of-interest designator interpretation: N15S_TA1_R1 means Nov. 15 (N15), antenna is south-looking (S), experiment test area 1 (TA1), the first region-of-interest extracted from the data set (R1). SLAR image region-of-interest designator interpretation: Same as for SAR, except that the designator is prefixed with H or L. H means high altitude imaging (9500 ft) and L means low altitude imaging (5500 ft). SLAR images are not as large as SAR mosaics, so only 1 region is designated per SLAR pass, all of which can be displayed at one time.

b. Coordinates are specified as they would be entered into the SNL region-of-interest extraction program. In the case of SAR images, these coordinates are the "key image" coordinates which is a subsampled version of the entire mosaic, subsampled by a factor of 5. For SLAR images, these are the actual coordinates of the full resolution image.